Microglia in psychiatric disorders

A search for immune activation

Marjolein Anna Maria Sneeboer

Microglia in psychiatric disorders
A search for immune activation

Microglia in psychiatrische ziekten -
de zoektocht naar immuunactivatie

(met een samenvatting in het Nederlands)

Proefschrift

ter verkrijging van de graad van doctor aan de Universiteit Utrecht op gezag van de rector magnificus, prof.dr. H.R.B.M. Kummeling, ingevolge het besluit van het college voor promoties in het openbaar te verdedigen op dinsdag 12 maart 2019 des middags te 12.45 uur

door

Marjolein Anna Maria Sneeboer
geboren op 19 januari 1989 te Heemstede

ISBN: 978-90-393-7100-8

Author: Marjolein A.M. Sneeboer

Cover: Marjolein A.M. Sneeboer
Layout: Proefschrift-All-in One | www.proefschrift-aio.nl

Promotoren: Prof.dr. R.S. Kahn
Prof.dr. E.M. Hol

Copromotor: Dr. L.D. de Witte

Moed is goed,
doorzettingsvermogen is beter

- Theodoor Fontane-

Table of Contents

Chapter 1	General introduction	9
Chapter 2	Characterizing primary human microglia: a comparative study with myeloid subsets and culture models	35
Chapter 3	Human microglia regional heterogeneity and phenotypes determined by multiplexed single-cell mass cytometry	63
Chapter 4	Exploring translocator 18kDa protein as a marker for measuring microglial immune activation in schizophrenia	101
Chapter 5	Post-mortem analysis of the four hallmarks of neuroinflammation in schizophrenia: microglial activation, lymphocytic infiltrates, and gliosis.	123
Chapter 6	Microglia in post-mortem brain tissue of patients with bipolar disorder are not immune activated	147
Chapter 7	*Ex vivo* profiling of microglia in major depressive disorder	177
Chapter 8	General discussion	209
Appendices	I Nederlandse samenvatting	232
	II List of publications	234
	III Acknowledgements	236

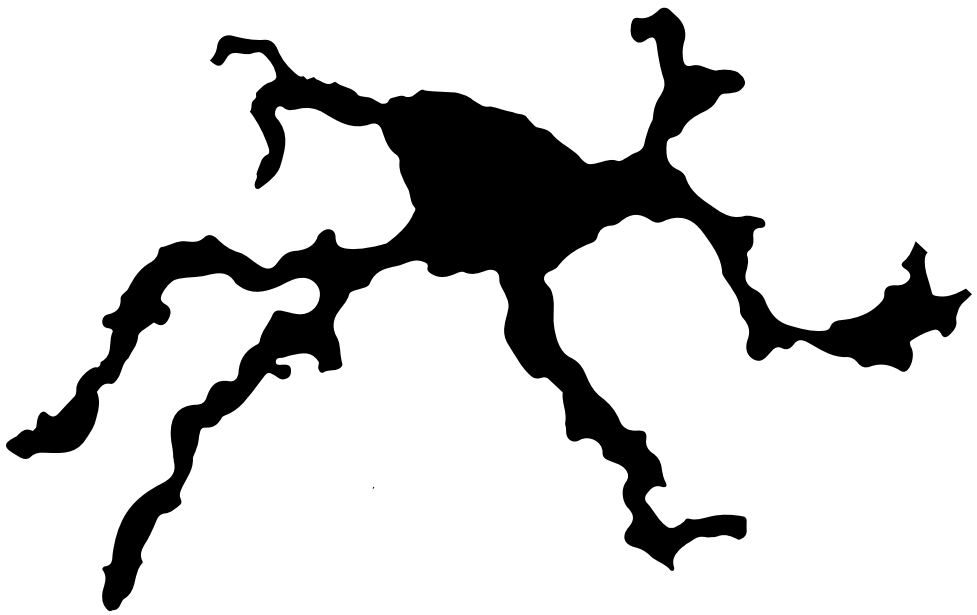

Chapter 1

General introduction

For over a century the immune system is implied to be involved in the aetiology of schizophrenia, bipolar disorder, and major depressive disorder[1,2]. The last years, there is a steep increase in the interest of immunological processes underlying these psychiatric disorders. This is reflected in the substantial raise in the number of published articles with terms as 'immune' and 'psychiatry' (Figure 1; source: pubmed). The start of the substantial growth coincided with the publication of genome wide association study (GWAS) showing involvement of immune related genes in schizophrenia[3].

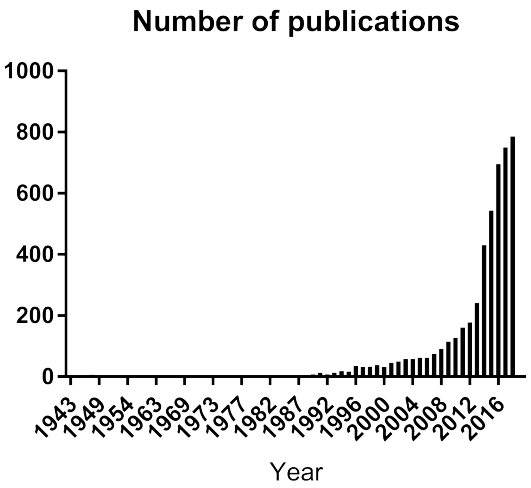

Figure 1: Number of publications with search terms 'immune' and 'psychiatry' from 1946-2018. Number of papers studying the immune system in psychiatry increased substantially in the last decennia. Source: pubmed.

The epidemiological link between immune-related diseases and psychiatric disorders and genetic risk loci for these disorders became also more apparent by larger cohort studies[4–7]. Furthermore, researchers reported elevated levels of circulating cytokines and chemokines in blood and CSF of patients of all three disorders. Although the link between the immune system and schizophrenia, bipolar disorder, and major depressive disorder is proposed, it remains unclear how the immune system plays a role in the pathogenesis of these disorders at a mechanistic level. The development of *in vivo* imaging tools (e.g. functional magnetic resonance imaging (fMRI), positron-emission tomography (PET) imaging) and the increased availability of brain banks and brain material worldwide makes it now possible to study brain alterations of psychiatric patients at a functional and molecular level.

This thesis will focus on the microglia, the immune cells of the central nervous system, and their contribution to schizophrenia, bipolar disorder, and major depressive disorder. As an introduction to this topic, the basic concepts, rationale and current literature on this subject are described. First, the clinical characteristics (**chapter 1.1**), common pathophysiology (**chapter 1.2**), reported brain abnormalities (**chapter 1.3**), and current evidence for a role of the immune system (**chapter 1.4**) are summarized for all three disorders. The next paragraphs introduce microglia (**chapter 1.5**), discuss literature supporting their contribution to the disorders (**chapter 1.6**) and provide an overview of methods to study microglia *in vivo* (**chapter 1.7**) and *in vitro* and *ex vivo* (**chapter 1.8**). Finally, the further outline of the thesis is presented (**chapter 1.9**).

1.1 Clinical features of schizophrenia, bipolar disorder and major depressive disorder

1.1.1 Schizophrenia

Schizophrenia (SCZ) is a chronic psychiatric disorder with a high burden for patients, their families and society. Symptoms of SCZ are categorized in 'positive', 'negative', and 'cognitive' subgroups. Positive symptoms are thoughts and behaviours that are normally not present, such as hallucinations, delusions and disorganized thoughts. The negative symptoms of the disorder are lack of motivation and pleasure, social withdrawal, diminished speech, and flattened affect. Finally, the cognitive symptoms consist of cognitive dysfunctions, such as memory deficits and problems with attention and executive functioning (e.g. understanding, decision making)[8].

Worldwide 21 million people are suffering from SCZ[9]. The onset of the disorder often starts early in life with a decline in social and cognitive functioning. During adolescence or early adulthood, the first psychosis manifests itself, indicating the clinical starting point of the disorder. SCZ is slightly more common and severe in men than women, but the onset of the disorder in women is later compared to men[8]. Psychiatric comorbidities are very common in SCZ, with substance abuse, anxiety, and depression as most prevalent[10]. Although many patients benefit from psychological and pharmaceutical treatment, there is still a substantial population of non-responders. Besides, the medication is only effective for a subset of the symptoms and will not cure the whole symptom spectrum of the disorder. For example, the antipsychotic medication, targeting the dopamine-2 receptor, will only diminish the positive symptoms. For the negative and cognitive symptoms, which have the highest burden for the patients, very few pharmaceutical options are available[8].

1.1.2 Bipolar disorder

Bipolar disorder (BD), previously known as manic-depressive disorder, is characterized by periods of elevated (mania or hypomania) and depressed mood. There is a distinction between bipolar disorder I (BD-I), in which episodes of full-blown mania and depression are present, and bipolar disorder II (BD-II), mainly defined by depressive episodes and hypomania[11].

On average BD affects 1% of the population worldwide[12]. Where men have more tendency to show (hypo)mania, women are more likely to suffer from the depressive side of BD[13]. A diagnosis of BD is most often made in early adulthood after experiencing the first manic or hypomanic episode. There is a high comorbidity with other psychiatric disorders, such as anxiety disorder, major depressive disorder, and attention deficit hyperactivity disorder (ADHD). The course of the disorder is episodic (e.g. fluctuating between manic and depressive episodes) and often accompanied with functional and cognitive impairment and decreased quality of life[14]. Treatment strategies involve medication with mood stabilizers, anti-depressant, and anti-psychotics and psychotherapy.

1.1.3 Major depressive disorder

Major depressive disorder (MDD) is a mood disorder with symptoms of depressed mood, anhedonia, change in sleep patterns (hyper- or insomnia) or weight, increased fatigue, loss of energy, negative thoughts, and suicidality[15]. Additionally, cognitive problems, such as lack of attention and indecisiveness, are often present in MDD. The onset of the disorder is around 25 years of age and the symptoms must be present for at least two weeks before the diagnosis MDD is given. On average, a depressive episode lasts between 13 and 30 weeks and the course of MDD is pleomorphic, meaning variation in remission and chronicity[15].

Worldwide, 6% of the adult population suffers from MDD[15]. MDD is twice more frequent in women compared to men, with more reoccurring episodes in women[16]. MDD is associated with psychiatric and somatic comorbidities, such as heart disease, stroke, and diabetes. Treatment is often a combination of psychotherapy and pharmaceutical interventions. More treatment-resistant patients might benefit from electroconvulsive therapy[15].

1.2 Common pathophysiology of SCZ, BD, and MDD

The pathophysiology of psychiatric disorders is much less understood compared to most somatic disorders, but progression is made in understanding the biology underlying SCZ, BD, and MDD. It is clear that a combination of genetic and environmental factors is causing these disorders. The heritability of SCZ and BD is estimated between 60-80%, whereas genetic factors contribute to MDD for 35%[17]. Additionally, associated risk factors for SCZ, BD, and MDD are environmental factors, such as urbanicity, migration status, drug abuse, low socioeconomic status, and lifestyle factors (smoking, alcohol consumption, traumatic experience). Furthermore, stress is an important factor to trigger a new psychotic, manic, or depressive episode in SCZ, BD, and MDD. For example, increased activation of the hypothalamus-pituitary-adrenal (HPA) axis, the neuroendocrine system important for the regulation of stress and the immune system, is associated with MDD relapse[18].

In SCZ, BD, and MDD there is a dysregulation of several neurotransmitter systems (e.g. serotonin, dopamine, acetylcholine). This is supported by the fact that effective pharmacotherapies for these disorders target the altered neurotransmitter systems[8,11,15]. Also, imaging studies showed that dopamine levels are increased in the midbrain of SCZ patients[8], whereas serotonin levels are decreased in the synaptic cleft of MDD patients[15]. How the combination of genetic and environmental factors ultimately leads to the dysregulation of these neurotransmitter systems is less clear.

1.3 Brain alterations in SCZ, BD and MDD

The exact underlying biological mechanism of SCZ, BD, and MDD is still unclear, despite their genetic overlap, shared environmental risk factors, and neurotransmitter imbalance in the brain. Neuroimaging studies are investigating structural and functional abnormalities in SCZ, BD, and MDD. These studies focus on the detection of volumetric changes, functional alterations, and brain connectomics (e.g. interaction between different brain areas). Researchers use post-mortem brain material of patients and controls to study molecular and cellular changes, whereas PET imaging provides information about brain functionality and metabolism *in vivo*. The next paragraphs describe the structural as well as functional brain changes in SCZ, BD, and MDD.

1.3.1 Schizophrenia

The most pronounced brain abnormalities in SCZ are a decrease in brain volume, enlargement of the ventricles, disruption of the white matter integrity, and changes in gyrification and cortical thickness, especially in the dorsolateral prefrontal cortex (DLPFC) and parahippocampal regions[8,19]. The reductions in brain volume are not limited to grey or white brain matter, although grey matter volume decreases more rapidly over time. Functional imaging and connectomic studies showed increased activation in the midbrain and altered connectivity between several brain regions, especially between the DLPFC, hippocampus and limbic regions[8]. On a cellular level,

the most replicated finding is the excessive loss of dendritic spines in layer 3 of the DLPFC (figure 2)[20,21].

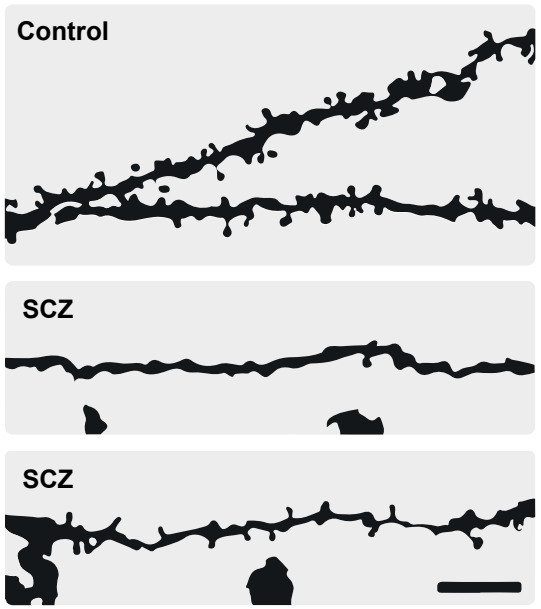

Figure 2: Alterations in spine density in schizophrenia (SCZ).
Upper panel shows dendrite with multiple spines in a healthy control. Spine density is clearly decreased in SCZ (lower 2 panels). Scale bar is 10 µm. Figure adapted from Lewis and González-Burgos[22].

1.3.2 Bipolar disorder

Enlarged lateral ventricles, decreased cortical thickness, and reduced grey matter volume are often reported in patients with BD[23,24]. These changes are most pronounced in brain areas involved in emotion regulation and –processing (e.g. superior PFC, left cingulate, and temporal lobe, including the parahippocampal gyrus and anterior cingulate cortex (ACC))[25] and mainly occur in BD with pediatric or juvenile onset[26–29]. Patients with BD show enlargement of the amygdala, which is consistent with more blood flow and elevated glucose metabolism detected in this region. Hyperintense white matter lesions are observed in patients with BD. The pathogenesis of these lesions is not well understood, but it is thought that they are related to vascular ischemia and aging[28]. Functional MRI studies found under-activation of the frontal cortex and over-activation of the limbic areas, including the amygdala and hippocampus[30]. Similar as in SCZ, reduced spine density and dendritic length is observed in the DLPFC[21]. Furthermore, patient with BD have a consistent downregulation of the number of hippocampal GABAergic interneurons[31].

1.3.3 Major depressive disorder

Research shows decreased volume of the hippocampus, dorsolateral and dorsomedial PFC, left temporal lobe, ACC, amygdala, and basal ganglia in MDD[15,32,33]. Additionally, increased hyperintensity of the white matter tracts are positively correlated with the cognitive decline seen in MDD[34]. On a functional level, increased and decreased activity of the mesolimbic system is reported, depending on the medication used and status of the depressive symptoms.

1.4 Immune system and psychiatry

In the search for the pathophysiology of SCZ, BD, and MDD, the possibility of an 'inflamed brain' was suggested as an underlying mechanism for these disorders. The next paragraphs provide a short recap on the immune system and discuss current literature supporting a role of the immune system in SCZ, BD, and MDD.

1.4.1 General introduction of the immune system

The immune system protects the body against infection and injury. It recognizes, contains and eliminates the source of the infection (e.g. bacterial, viral, fungi) and is able to regulate its own response to avoid an autoimmune reaction. The immune system is often divided in two parts: the innate immune system and the adaptive immune system. The innate immune system is aspecific, meaning that it will protect the body against any pathogen without long-lasting immunity. It consists of several cell types, including monocytes, macrophages, and dendritic cells. These cells engulf the pathogen and secrete cytokines and chemokines, thereby inducing inflammation and activating the adaptive immune system. The adaptive immune system is specialized in such a way that it eliminates specific pathogens. The adaptive system also has a memory function. In case an earlier identified pathogen re-enters the body, the adaptive immune system will be quickly activated to remove the pathogen directly before inducing an infection. B- and T-lymphocytes are part of the adaptive immune system. B-lymphocytes produce specific antibodies, whereas the T-lymphocytes are prone to kill, activate and regulate the immune response[35].

1.4.2 Evidence for a role of the immune system in SCZ, BD, and MDD

Current literature suggests a potential role for the immune system in the pathophysiology of SCZ, BD, and MDD. Evidence comes mainly from epidemiological studies, studies investigating circulating cytokines and chemokines, and genetic association studies.

Clinical indications

Several clinical characteristics suggest that the immune system is involved in SCZ, BD, and MDD. First of all, the onset in adolescence/early adulthood and fluctuating patterns of these disorders resembles the course of autoimmune disorders. In addition, it is known that antidepressants and antipsychotics can alter the immune system[36]. Moreover, autoimmune and infectious disorders, such as systemic lupus erythematosus and autoimmune encephalitis, can cause symptoms resembling a primary psychiatric psychotic, manic, or depressive episode. Finally, common infectious diseases, such as influenza, induce sickness behaviour consisting hallmarks of depressive symptoms (e.g. depressed mood, lack of energy, and anhedonia). Also, it is well-known that the administration of interferon alpha (IFNα) can lead to development of severe depressive and cognitive symptoms[37–39], indicating that peripheral cytokines can induce an depressive episode.

Epidemiological studies

Epidemiological studies have described a relation between psychiatric disorders and immune diseases, including both atopic and autoimmune disorders. This is a dual interaction, in which patients with an immune disorder have an increased risk for developing SCZ, BD, and MDD, and vice versa[4,40–42]. In addition, birth-cohort studies showed that a maternal infection during pregnancy will increase the risk of SCZ and BD in the offspring with two to seven times[43–4]5.

Animal models

Animal models showed that infection and immune activation during pregnancy lead to cognitive and behavioural symptoms and long-lasting neurobiological alterations in the offspring[46]. Inflammation during pregnancy decreases the survival of serotonergic neurons and increases the number of midbrain dopaminergic neurons in the offspring[47]. This has direct implications for the functioning of the neurotransmitter system later in life. Additionally, SCZ related deficiencies in serotonin levels and brain abnormalities (e.g. reduced hippocampal volume, disturbed corticogenesis) were also found in the offspring[48–52].

Immune marker studies

A large number of studies have determined cytokine concentrations in blood and cerebrospinal fluid (CSF) in SCZ, BD, and MDD. Studies show elevated levels of interleukin 1 beta (IL-1β), interleukin 1 receptor (IL-1R), interleukin 2 (IL-2), and TNFα in these disorders[53–58]. Whereas interleukin 6 (IL-6) is increased in SCZ and BD, both higher and lower levels are found in MDD[56,59,60]. Cytokines with more anti-inflammatory functions, such as interleukin 4 (IL-4) and IL-10, are lower expressed in patients with SCZ, BD, and MDD[33,54,61,62]. Cytokine levels can also be related to symptomatology; the levels of IL-2, IL-4, IL-6, and TNFα are increased during a manic episode, whereas decreased levels of IL-6 define depressive[63]. This suggests that manic episodes are possibly related to elevated cytokine expression, both peripherally as well as in the brain.

Besides changes in cytokine levels in blood and CSF, similar alterations are found in post-mortem tissue. Gene expression analysis of post-mortem tissue of patients with BD showed altered mRNA expression and protein levels for *IL1B, IL6*, transmembrane *TNF, IFN,* interleukin 13 (*IL-13*), interleukin 33 (*IL-33*), IL-2, and chemokine (C-C motif) ligand 2 (*CCL2*)[64–67]. Additionally, brain abnormalities correlate with cytokine levels, in which a smaller brain volume is related to increased cytokine levels in patients with SCZ[68]. Thus, research finds aberrant cytokine and chemokine levels in the periphery as well as in the CNS, indicating immune activation in SCZ, BD, and MDD.

Genetic studies

In the past years, multiple genome wide association studies (GWAS) with large sample sizes have been performed for SCZ, BD, and MDD and revealed significant loci associated with the disorders. The strongest genetic association with SCZ is located in the major histocompatibility complex (MHC), a large region on chromosome 6. This locus is an important regulator of the immune response, since many of the human leukocyte antigen (HLA) genes, coding for antigen presenting molecules, are part of the MHC69. Due to the large coverage of this region, it was only recently discovered that patients with SCZ, due to copy number variants, have more expression of complement factor 4A (*C4A*), which is part of the complement system and important for (auto)immunity and tolerance[70].

Risk genes for BD are not directly related to the immune system, but pathway analyses showed associations with immune response pathways[71]. MDD is associated with several polymorphisms in immune genes, including *IL1B, TNF*, and interferon regulatory factor 1 (*IRF1*)[72–75] and many of the genome-wide significant associated loci are related to immunity and the immune response[76].

When looking at the overlapping genetic architecture of SCZ, BD, and MDD, there is solid evidence that the immune system is a contributing factor in all three disorders. A recent study found a shared association for these disorders with immune genes, histone methylation, postsynaptic density, and neuronal signalling across disorders[77].

Furthermore, a substantial part of the polygenic variation found in SCZ, including the MHC, also contributes to the risk of BD[78].

Although previous research supports immune alterations in SCZ, BD, and MDD, less is known about how the immune system is involved in causing brain dysfunction in these disorders. Since microglia are the main immune cells in the CNS, it is hypothesized that these cells could play an important role in causing psychiatric disorders[79].

1.5 Microglia

Microglia were first described by del Rio Hortega in the 20th century and account for 2-10% of the total cell number in the brain[79–81]. They originate from the yolk sac and populate the CNS during embryonic development. Due to their different ontogeny, microglia are distinct from hematopoietic macrophages and circulating monocytes[82,83]. In the human brain, microglia can be detected from 13 weeks of gestation and fully ramified cells are present from 19 weeks onwards. By the end of gestation, all cortical layers contain ramified microglia[84]. An important factor for adequate microglial development is the colony stimulating factor 1 receptor (CSF-1R) signalling. Deficiency of CSF-1R or interleukin-34 (IL-34), the ligand for CSF-1R, will directly diminish microglial density and cell viability[85].

1.5.1 Microglial functions

Microglia are very dynamic cells and fulfil multiple functions in the brain[79,86]. They are most known for their role in the immune system. Microglia are constantly scanning the environment for infiltrating pathogens (e.g. viruses, bacteria) and other danger signals. When detecting a pathogen, microglia respond by secreting inflammatory cytokines, such as IL-1β, IL-6, interferon gamma (IFNγ), and TNFα. These cytokines can induce an inflammatory reaction in the brain, whereby peripheral immune cells (e.g. T- and B-cells) are recruited and pathogens are removed via phagocytosis[87]. Besides, microglia are also able to dampen the immune response via the secretion of anti-inflammatory cytokines (e.g. IL-4, transforming growth factor beta (TGFβ), and IL-10)[87]. Even though cytokines are often categorized as pro- or anti-inflammatory, their functioning in stimulation or dampening the immune response is highly dependent on their concentration in the CNS. For example, TGFβ is known for its pro- and anti-inflammatory properties in the brain[88].

Next to immune control, microglia are important players in shaping neuronal networks in the brain. In homeostatic conditions, microglia are in constant contact with synapses[89]. There are various molecules that are necessary for the close connection between microglia and neurons. For example, neuronal cell surface proteins CD22, CD47, CD200, and CX3CL1 interact with microglial CD45, CD172α, CD200 receptor (CD200R), and CX3CR1, respectively[90,91]. Whereas some interactions will lead to increased microglial activation (e.g. CX3CL1-CX3CR1), others will suppress activation[90]. During CNS development or neuronal distress, microglia reduce the number of synapses by pruning (e.g. removal)[92–94]. This neuronal refinement is necessary for normal brain development[95], but can contribute to brain disorders when induced by neuronal distress. The exact mechanism for synaptic pruning remains to be elucidated, but it is suggested that microglia actively phagocytose or nibble away the synapses[96] or secrete factors that will induce degradation of the synapse. The complement system is highly involved in the removal of synapses, in which complement factors C3 and C1q tag the inappropriate synapses. Microglia recognize C3 via the C3 receptor on their membrane and this induces phagocytosis[97]. Besides eliminating dysfunctional synapses, microglia also promote neurogenesis, axon growth, and neuronal survival. Microglia are a useful source for secreting neurotrophic and growth factors in the CNS (e.g. brain derived neurotrophic factor (BDNF), nerve growth factor (NGF), and TGFβ). For example, microglial secretion of IL-1β and IFNγ can promote neurogenesis in the subventricular zone (SVZ)[98], whereas blocking insulin growth factor 1 (IGF-1) results in more apoptotic neurons in layer V of the neocortex in mice[99].

1.5.2 Microglia morphology

Microglia are highly motile cells and change their morphology and phenotype in relation to their function in the brain. Microglia are not a uniform population, but show heterogeneity in the CNS. Brain regions differ in their cellular and biochemical composition and execute different functions, suggesting that each brain region needs specific support and assistance[100]. While research regarding microglia heterogeneity across brain regions on transcript level is still on-going, morphologically four different phenotypes are identified in both grey and white matter[94]. In homeostatic conditions, microglia have a ramified morphology with a small cell body and multiple processes (Figure 3 a-b). In the case of immune activation, microglia are primed first (larger and more elongated cell body with similar number of processes; Figure 3 c-d). With sustained immune activation and phagocytic functioning, microglia are less complex (Figure 3 e-f), retract their processes, and adopt a so-called amoeboid shape (Figure 3 g-i). Despite their similar morphological phenotypes, microglia do differ between grey and white matter. Microglia in the grey matter have a larger diameter, whereas in the white matter they are smaller and follow the course of the white matter tracts, resulting in more elongated cells. Furthermore, microglial density is thought to be larger in grey matter compared to white matter[91].

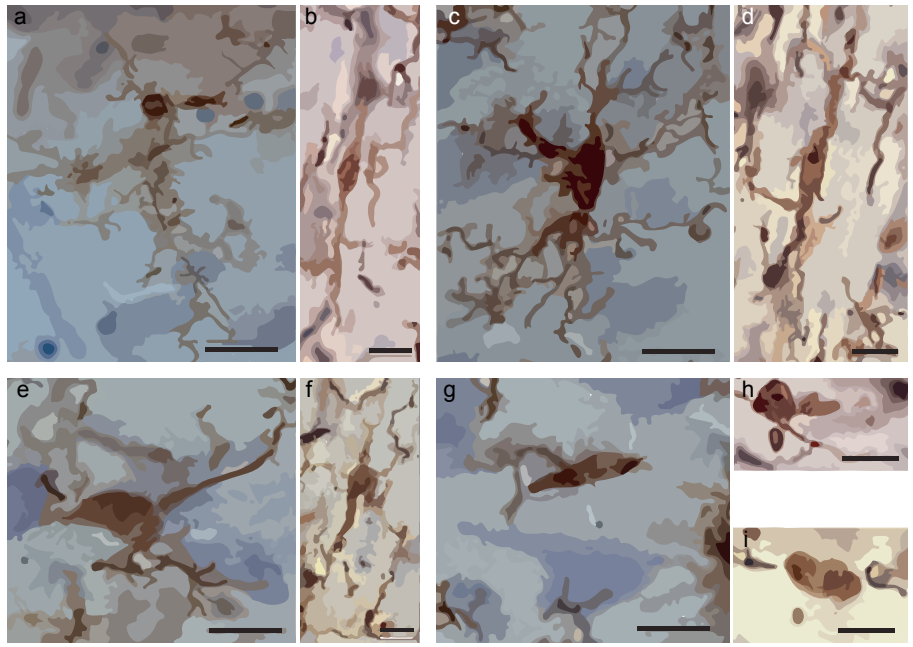

Figure 3: Microglial morphology in grey and white matter of the human brain.
Four different microglial morphological phenotypes are distinguished in grey (a, c, e, g) and white matter (b, d, f, h, i) of the human brain. a-b) Homeostatic microglia with small cell body and multiple processes. c-d) Cell body is elongated and thickened in primed microglia. With sustained immune activation, microglia retract their processes (e-f) and adopt an amoeboid phenotype with few processes (g-i). Scale bar is µm. Figure adapted from Torres-Platas et al.[101].

1.6 Post-mortem studies on microglia in SCZ, BD, and MDD

Microglial changes in psychiatric disorders are most studied in post-mortem brain tissue using immunochemistry, investigating microglial cell numbers and morphology. Several markers are available, such as human leukocyte antigen D Related (HLA-DR), CD11b, CD68, transmembrane protein 119 (TMEM119), and ionized calcium-binding adapter molecule 1 (Iba1). Additionally, mRNA expression of microglial markers and secreted inflammatory cytokines is investigated in total brain tissue.

Most studies have focussed on microglial density and morphological alterations in SCZ. A systematic review reported that of the 22 conducted studies, 11 studies found an increased expression of microglia markers, 8 studies showed no differences, and 3 studies mentioned a decrease[55]. The heterogeneity of the disorder, the different brain regions studied, and the variety of markers used might cause this inconsistency. Specifically in patients with successful suicide attempts signs of microglial activation are found[102,103]. A meta-analysis including 41 studies found an overall effect of

increased microglial density, which is most pronounced in the temporal cortex. Moreover, an increase in gene expression and/or protein levels of pro-inflammatory markers is reported[104]. One remark needs to be made regarding previous described literature. The research reporting the most increase in microglial density in SCZ, which is included in both studies, was retracted.

In BD, a limited number of studies is available investigating microglial density. There is no evidence for increased microglial density, based on immunohistochemistry, in the DLPFC and dorsal raphe nucleus in BD[105,106]. Although mRNA expression of Iba1 in the PFC is similar between BD patients and controls, expression of two other microglial markers (CD11b and CD68) is decreased[107]. Furthermore, another study determined the amount of microglial secreted TNFα in total brain tissue and showed increased levels of transmembrane TNFα in Brodmann's area 24, but less TNF receptor 2 in Brodmann's area 46[66]. Although microglial density itself is not changed in BD, mRNA expression of microglial markers and the immune factors secreted by microglia are different.

For MDD the results are less consistent. In MDD patients, the density of HLA-DR$^+$ microglia is increased in the hippocampus, ACC, DLPFC, and thalamus[102,108]. Also the number of QUIN$^+$, a microglia-specific NMDA receptor agonist, cells is higher in two subregions of the ACC in MDD[109], and more primed microglia are reported in de ACC[110]. Interestingly, the density of Iba1$^+$ cells is more pronounced around the blood vessels in the brain of MDD patients[110,111]. Others could not find a difference in the number of homeostatic or immune activated (amoeboid) microglia[111] and total microglial numbers[106,112]. Even decreased density of HLA-DR$^+$ microglia is found in brain tissue of non-suicidal MDD patients[106]. This suggests a specific role for suicide in microglia immune activation in the disorder.

In summary, post-mortem studies find inconsistent evidence for microglial alterations in SCZ, BD, and MDD. Several reasons are likely to play a role. Microglia have been studied with multiple markers (e.g. HLA-DR, Iba1, CD11b, CD68) and in various brain regions (e.g. PFC, hippocampus, ACC, thalamus). Besides, mostly one technique is applied in a small sample and technical and biological replication is missing. Furthermore, immunohistochemistry has the restriction of only analysing cell numbers and morphological changes. No extensive genetic and protein profiling of microglia is performed in psychiatric disorders so far. It is therefore necessary to study human microglia in a more multi-dimensional approach, incorporating the various functions and heterogeneity of microglia and correlate this to SCZ, BD, and MDD.

1.7 PET studies for microglia *in vivo*

Positron emission tomography (PET) with tracers that bind to the 18kD translocator protein (TSPO) on the membrane of mitochondria is applied to study microglial changes in psychiatric disorders *in vivo*. An increased TSPO signal is thought to reflect an elevated microglia density or elevated microglial activation. Where neuroinflammatory and neurodegenerative disorders, like Alzheimer's disease (AD) [113–115] and multiple sclerosis (MS)[116–118], show increased TSPO expression, PET studies found contradicting results for psychiatric disorders. In SCZ, earlier studies investigating TSPO binding with the [^{11}C]-(*R*)PK11195 tracer found a higher signal in patients compared controls[119–122]. In contrast, more recent studies with larger cohorts and correction methods for TSPO presence on endothelial cells showed equal or decreased TSPO signal in SCZ[123–130]. Not many PET studies with the TSPO ligand are performed in BD and MDD. Decreased TSPO binding is found in BD, but only in a subgroup with comorbidity of post-traumatic stress disorder and adult separation anxiety disorder[131]. TSPO binding in the whole brain is not different between BD patients and controls, although the right hippocampus of BD-I patients showed a small increase in binding[132]. Three PET studies are published for MDD; one study reported no differences[133], whereas the other two showed elevated TSPO binding[134,135]. Interestingly, the latter studies found a positive correlation between TSPO binding and MDD severity of symptoms, but not with the measured neuroinflammatory markers in serum[135]. Also, there is an indication that microglial immune activation in MDD is only related to suicide or suicidal thinking, since elevated TSPO levels are not detected in the non-suicidal patient group[134].

1.8 *In vitro* and *ex vivo* methods to study microglia changes in psychiatric disorders

Since there is a lot of debate about the accuracy of *in vivo* imaging of microglia with PET, other methods have been developed to study microglial phenotype and function. There are several *in vitro* models and cell lines available for human microglia. These include microglial cell lines and monocytes that are differentiated into microglia-like cells *in vitro*[136–142]. These models should be used with care, since the ontogeny of monocytes and microglia is different (e.g. monocytes are bone marrow derived, whereas microglia develop from the yolk sac[143]. Recently several protocols have been published to generate microglia-like cells and brain organoids containing microglia from induced pluripotent stem cells[144–147]. These cell models hold great promise for microglial research, especially for studying the role of genetic background and single genetic risk factors for psychiatric disorders. However, it is still important to realize that these models are different from primary microglia at the phenotypic and functional level. To go beyond the study of microglia in post-mortem brain tissue using immunostaining, an innovative method has been developed to isolate human microglia from fresh post-mortem brain tissue of patients and controls[148–151]. Post-mortem brain tissue is homogenized and separated from the myelin with a density gradient after which microglia are positively selected by flow cytometry (CD11b^{+}/CD45^{dim}) or with commercially available CD11b-coated magnetic beads. This method provides the opportunity for extensive microglial transcriptome profiling, functional experiments and *ex vivo* characterization of the cells in humans, as is already shown for controls and CNS disorders[149,152,153].

1.9 Thesis outline

In summary, despite numerous efforts to unravel the aetiology of SCZ, BD, and MDD, the exact mechanism underlying the disorders is still unknown. Many studies are pointing towards a role of the immune system and it is therefore hypothesized that immune activation of microglia contributes to the pathogenesis of these disorders (Figure 4).

However, the exact involvement of microglia in psychiatric disorders remains to be elucidated. The aim of this thesis is to elucidate the role of microglia, specifically their immune activating properties, in SCZ, BD, and MDD by using a multi-level approach. In **chapter 2** a characterization of our *ex vivo* microglia model is presented. We isolated human microglia from fresh post-mortem brain tissue of controls and showed that these microglia are different from monocytes and monocyte-derived macrophages (mo-MΦ) and maintain their immune functions *in vitro* by responding to inflammatory compounds. Besides, we showed that the *ex vivo* microglia are not comparable to microglia-like cells. **Chapter 3** provides an overview of the proteomic profile of microglia with mass cytometry (CyTOF). We established a cryopreservation protocol, which enables us to profile microglial protein expression from different donors at the same time. We showed that microglia are distinguishable from peripheral blood mononuclear cells (PBMC) and cells in the CSF and that there is microglial diversity across different brain regions. The question whether TSPO is an accurate marker to measure microglial immune activation and plays a role in SCZ is answered in **chapter 4**. *TSPO* mRNA is not elevated in frontal and temporal brain tissue of SCZ patients; neither did immunostainings show more TSPO expression in general or in specific immune activated microglia. Besides, *TSPO* mRNA in *ex vivo* microglia is not increase after inducing an immune response in the cells, suggesting a more complex role for TSPO in microglia immune activation as is thought before. The current debate if SCZ is a neuroinflammatory disorder is highlighted in **chapter 5**. For neuroinflammation, four criteria have to be met: 1) activation of microglia; 2) increased cytokine levels; 3) lymphocyte recruitment and 4) local tissue damage. In this chapter we studied all four hallmarks and emphasize

that SCZ is lacking all criteria for neuroinflammation. **Chapter 6** unravels the role of microglia in BD. Microglia density and morphology as well as gene expression of general microglia and microglia immune activation markers is studied in post-mortem tissue of the frontal lobe. Additionally, the immune response of *ex vivo* microglia isolated from controls and BD patients is investigated after inflammatory stimulation. We found no indications that microglia in BD are immune activated and contribute to the aetiology of the disorder. Finally, we performed a large transcriptomic analysis in combination with protein profiling and *ex vivo* microglia characterization of microglia in MDD (**chapter 7**). Four different brain regions were analysed. We found lower levels of CD14 and CD32 in MDD. *In vitro* immune responsiveness to LPS and dexamethasone was not changed. Transcriptomic analysis showed 194 differentially expressed genes (DEGs), of which 188 genes were downregulated and only six genes upregulated. The top three downregulated genes are involved histone modification and chromatin accessibility. Finally, pathway analyses of all DEGs showed a downregulation in pathways implicated with cell cycle and cell division.

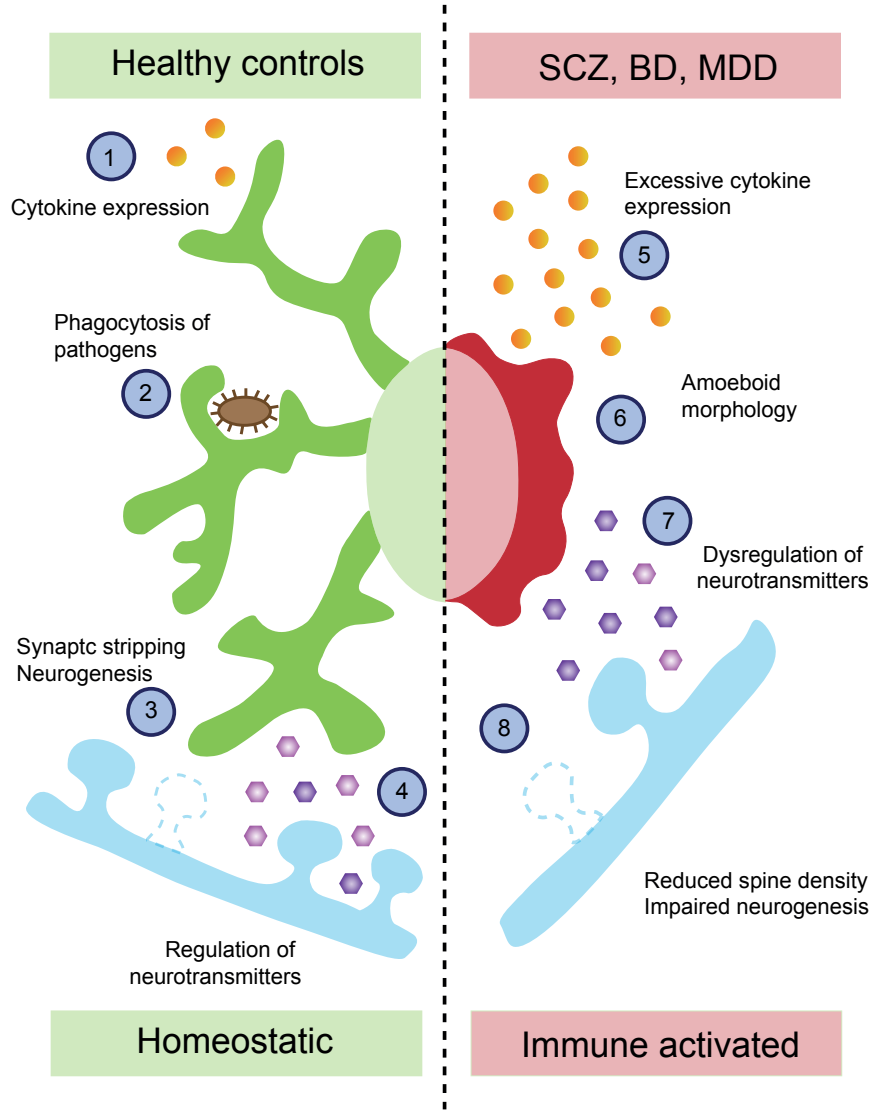

Figure 4: Current hypothesis of microglia in psychiatric disorders.
In healthy controls microglia have a ramified phenotype in steady-state conditions (left). Their functions are regulating immune response, via cytokine expression (1) and the clearance of pathogens (e.g. bacteria) and death cells (2). Additionally, they are involved in synaptic pruning and neurogenesis (3) and the regulation of neurotransmitters (4). In schizophrenia (SCZ), bipolar disorder (BD), and major depressive disorder (MDD) (right), microglia are thought to be immune activated. They express increased levels of inflammatory cytokines (5) and adopt an amoeboid (rounded) shape (6). Immune activation of microglia will result in dysregulation of neurotransmitters in the brain (7). Besides, microglial immune activation may lead to the reduced spine density and impaired neurogenesis (8) as is found in patients with SCZ, BD, and MDD.

References

1. Müller, N., Myint, A.-M. & Schwarz, M. J. Inflammation in schizophrenia. *Adv. Protein Chem. Struct. Biol.* **88,** 49–68 (2012).
2. Suvisaari, J. & Mantere, O. Inflammation theories in psychotic disorders: a critical review. *Infect. Disord. Drug Targets* **13,** 59–70 (2013).
3. Stefansson, H. *et al.* Common variants conferring risk of schizophrenia. *Nature* **460,** 744–7 (2009).
4. Benros, M. E., Mortensen, P. B. & Eaton, W. W. Autoimmune diseases and infections as risk factors for schizophrenia. *Ann. N. Y. Acad. Sci.* **1262,** 56–66 (2012).
5. Benros, M. E. *et al.* Autoimmune diseases and severe infections as risk factors for mood disorders: a nationwide study. *JAMA psychiatry* **70,** 812–20 (2013).
6. Rosenblat, J. D. & McIntyre, R. S. Bipolar Disorder and Immune Dysfunction: Epidemiological Findings, Proposed Pathophysiology and Clinical Implications. *Brain Sci.* **7,** (2017).
7. Rosenblat, J. D., Cha, D. S., Mansur, R. B. & McIntyre, R. S. Inflamed moods: A review of the interactions between inflammation and mood disorders. *Prog. Neuro-Psychopharmacology Biol. Psychiatry* **53,** 23–34 (2014).
8. Kahn, R. S. *et al.* Schizophrenia. *Nat. Rev. Dis. Prim.* **1,** (2015).
9. WHO. Schizophrenia - key facts. (2018). Available at: http://www.who.int/news-room/fact-sheets/detail/schizophrenia.
10. Buckley, P. F., Miller, B. J., Lehrer, D. S. & Castle, D. J. Psychiatric comorbidities and schizophrenia. *Schizophr. Bull.* **35,** 383–402 (2009).
11. Grande, I., Berk, M., Birmaher, B. & Vieta, E. Bipolar disorder. *Lancet* **387,** 1561–1572 (2016).
12. Alonso, J. *et al.* Days out of role due to common physical and mental conditions: results from the WHO World Mental Health surveys. *Mol. Psychiatry* **16,** 1234–46 (2011).
13. Nivoli, A. M. A. *et al.* Gender differences in a cohort study of 604 bipolar patients: The role of predominant polarity. *J. Affect. Disord.* **133,** 443–449 (2011).
14. Rosa, A. *et al.* One-year psychosocial functioning in patients in the early vs. late stage of bipolar disorder. *Acta Psychiatr. Scand.* **125,** 335–341 (2012).
15. Otte, C. *et al.* Major depressive disorder. *Nat. Rev. Dis. Prim.* **2,** 16065 (2016).
16. Seedat, S. *et al.* Cross-National Associations Between Gender and Mental Disorders in the World Health Organization World Mental Health Surveys. *Arch. Gen. Psychiatry* **66,** 785 (2009).
17. Geschwind, D. H. & Flint, J. Genetics and genomics of psychiatric disease. *Science* **349,** 1489–94 (2015).
18. Varghese, F. P. & Brown, E. S. The Hypothalamic-Pituitary-Adrenal Axis in Major Depressive Disorder: A Brief Primer for Primary Care Physicians. *Prim. Care Companion J. Clin. Psychiatry* **3,** 151–155 (2001).
19. Kubicki, M., McCarley, R. W. & Shenton, M. E. Evidence for white matter abnormalities in schizophrenia. *Curr. Opin. Psychiatry* **18,** 121–34 (2005).
20. Glausier, J. R. & Lewis, D. a. Dendritic spine pathology in schizophrenia. *Neuroscience* **251,** 90–107 (2013).
21. Konopaske, G. T., Lange, N., Coyle, J. T. & Benes, F. M. Prefrontal cortical dendritic spine pathology in schizophrenia and bipolar disorder. *JAMA psychiatry* **71,** 1323–31 (2014).
22. Lewis, D. A. & González-Burgos, G. Neuroplasticity of Neocortical Circuits in Schizophrenia. *Neuropsychopharmacology* **33,** 141–165 (2008).
23. Vargas, C., López-Jaramillo, C. & Vieta, E. A systematic literature review of resting state network—functional MRI in bipolar disorder. *J. Affect. Disord.* **150,** 727–735 (2013).
24. Malhi, G. S., Lagopoulos, J., Owen, A. M. & Yatham, L. N. Bipolaroids: functional imaging in bipolar disorder. *Acta Psychiatr. Scand. Suppl.* 46–54 (2004). doi:10.1111/j.1600-0447.2004.00413.x
25. Harrison, P. J., Colbourne, L. & Harrison, C. H. The neuropathology of bipolar disorder: systematic review and meta-analysis. *Mol. Psychiatry* 1 (2018). doi:10.1038/s41380-018-0213-3
26. Konarski, J. Z. *et al.* Volumetric neuroimaging investigations in mood disorders: bipolar disorder versus major depressive disorder. *Bipolar Disord.* **10,** 1–37 (2008).
27. Hoge, E. A., Friedman, L. & Schulz, S. C. Meta-analysis of brain size in bipolar disorder. *Schizophr. Res.* **37,** 177–181 (1999).
28. Emsell, L. & McDonald, C. The structural neuroimaging of bipolar disorder. *Int. Rev. Psychiatry* **21,** 297–313 (2009).
29. Frazier, J. A. *et al.* Magnetic resonance imaging studies in early-onset bipolar disorder: a critical review. *Harv. Rev. Psychiatry* **13,** 125–40 (2005).
30. Chen, C.-H., Suckling, J., Lennox, B. R., Ooi, C. & Bullmore, E. T. A quantitative meta-analysis of fMRI studies in bipolar disorder. *Bipolar Disord.* **13,** 1–15 (2011).
31. Konradi, C. *et al.* Hippocampal Interneurons in Bipolar Disorder. *Arch. Gen. Psychiatry* **68,** 340 (2010).
32. Kempton, M. J. *et al.* Structural Neuroimaging Studies in Major Depressive Disorder. *Arch. Gen. Psychiatry* **68,** 675 (2011).
33. Barbosa, I. G., Machado-Vieira, R., Soares, J. C. & Teixeira, A. L. The immunology of bipolar disorder. *Neuroimmunomodulation* **21,** 117–22 (2014).
34. Tham, M. W., Woon, P. S., Sum, M. Y., Lee, T.-S. & Sim, K. White matter abnormalities in major depression: Evidence from post-mortem, neuroimaging and genetic studies. *J. Affect. Disord.* **132,** 26–36 (2011).
35. Murphy, K., Travers, P. & Walport, M. *Jenaway's Immunobiology*. (Garland Science, 2008).
36. Al-Amin, M. M., Nasir Uddin, M. M. & Mahmud Reza, H. Effects of antipsychotics on the inflammatory response system of patients with schizophrenia in peripheral blood mononuclear cell cultures. *Clin. Psychopharmacol. Neurosci.* **11,** 144–51 (2013).
37. Capuron, L. & Miller, A. H. Cytokines and psychopathology: Lessons from interferon-α. *Biol. Psychiatry* **56,** 819–824 (2004).
38. Malaguarnera, M. *et al.* Interferon Alpha-Induced Depression in Chronic Hepatitis C Patients: Comparison between Different Types of Interferon Alpha. *Neuropsychobiology* **37,** 93–97 (1998).
39. Lotrich, F. E. Major depression during interferon-alpha treatment: vulnerability and prevention. *Dialogues Clin. Neurosci.* **11,** 417–25 (2009).
40. Pedersen, M. S., Benros, M. E., Agerbo, E., Børglum, A. D. & Mortensen, P. B. Schizophrenia in patients with atopic disorders with particular emphasis on asthma: a Danish population-based study. *Schizophr. Res.* **138,** 58–62 (2012).
41. Wang, L.-Y., Chiang, J.-H., Chen, S.-F. & Shen, Y.-C. Systemic autoimmune diseases are associated with an increased risk of bipolar disorder: A nationwide population-based cohort study. *J. Affect. Disord.* **227,** 31–37 (2018).
42. Andersson, N. W. *et al.* Depression and the risk of autoimmune disease: a nationally representative, prospective longitudinal study. *Psychol. Med.* **45,** 3559–69 (2015).
43. Brown, A. S. *et al.* Serologic evidence of prenatal influenza in the etiology of schizophrenia. *Arch. Gen. Psychiatry* **61,** 774–80 (2004).
44. Parboosing, R., Bao, Y., Shen, L., Schaefer, C. A. & Brown, A. S. Gestational influenza and bipolar disorder in adult offspring. *JAMA psychiatry* **70,** 677–85 (2013).
45. Brown, A. S. & Derkits, E. J. Prenatal Infection and Schizophrenia: A Review of Epidemiologic and Translational Studies. *Am. J. Psychiatry* **167,** 261–280 (2010).
46. Cordeiro, C. N., Tsimis, M. & Burd, I. Infections and Brain Development. *Obstet. Gynecol. Surv.* **70,** 644–55 (2015).
47. Boksa, P. Effects of prenatal infection on brain development and behavior: A review of findings from animal models. *Brain. Behav. Immun.* **24,** 881–897 (2010).

48. Fatemi, S. H. *et al.* Human influenza viral infection in utero increases nNOS expression in hippocampi of neonatal mice. *Synapse* **29,** 84–8 (1998).
49. Fatemi, S. H. *et al.* Defective corticogenesis and reduction in Reelin immunoreactivity in cortex and hippocampus of prenatally infected neonatal mice. *Mol. Psychiatry* **4,** 145–54 (1999).
50. Fatemi, S. H. *et al.* Human influenza viral infection in utero alters glial fibrillary acidic protein immunoreactivity in the developing brains of neonatal mice. *Mol. Psychiatry* **7,** 633–640 (2002).
51. Winter, C. *et al.* Dopamine and serotonin levels following prenatal viral infection in mouse--implications for psychiatric disorders such as schizophrenia and autism. *Eur. Neuropsychopharmacol.* **18,** 712–6 (2008).
52. Harrison, P. J. The neuropathology of schizophrenia. *Brain* **122,** 593–624 (1999).
53. Goldsmith, D. R., Rapaport, M. H. & Miller, B. J. A meta-analysis of blood cytokine network alterations in psychiatric patients: comparisons between schizophrenia, bipolar disorder and depression. *Mol. Psychiatry* **21,** 1696–1709 (2016).
54. Pandey, G. N., Rizavi, H. S., Zhang, H. & Ren, X. Abnormal gene and protein expression of inflammatory cytokines in the postmortem brain of schizophrenia patients. *Schizophr. Res.* **192,** 247–254 (2018).
55. Trépanier, M. O., Hopperton, K. E., Mizrahi, R., Mechawar, N. & Bazinet, R. P. Postmortem evidence of cerebral inflammation in schizophrenia: a systematic review. *Mol. Psychiatry* **21,** 1009–1026 (2016).
56. Dowlati, Y. *et al.* A Meta-Analysis of Cytokines in Major Depression. *Biol. Psychiatry* **67,** 446–57 (2010).
57. Young, J. J., Bruno, D. & Pomara, N. A review of the relationship between proinflammatory cytokines and major depressive disorder. *J. Affect. Disord.* **169,** 15–20 (2014).
58. Haarman, B. C. M. (Benno) *et al.* Neuroinflammation in bipolar disorder – A [11C]-(R)-PK11195 positron emission tomography study. *Brain. Behav. Immun.* **40,** 219–225 (2014).
59. Kern, S. *et al.* Lower CSF interleukin-6 predicts future depression in a population-based sample of older women followed for 17 years. *Brain. Behav. Immun.* **32,** 153–158 (2013).
60. Köhler, C. A. *et al.* Peripheral cytokine and chemokine alterations in depression: a meta-analysis of 82 studies. *Acta Psychiatr. Scand.* **135,** 373–387 (2017).
61. Mansur, R. B. *et al.* Cytokines in schizophrenia: Possible role of anti-inflammatory medications in clinical and preclinical stages. *Psychiatry Clin. Neurosci.* **66,** 247–260 (2012).
62. Munkholm, K., Braüner, J. V., Kessing, L. V. & Vinberg, M. Cytokines in bipolar disorder vs. healthy control subjects: A systematic review and meta-analysis. *J. Psychiatr. Res.* **47,** 1119–1133 (2013).
63. Brietzke, E. *et al.* Comparison of cytokine levels in depressed, manic and euthymic patients with bipolar disorder. *J. Affect. Disord.* **116,** 214–7 (2009).
64. Pandey, G. N. Inflammatory and Innate Immune Markers of Neuroprogression in Depressed and Teenage Suicide Brain. in *Modern trends in pharmacopsychiatry* **31,** 79–95 (2017).
65. Clark, S. M. *et al.* Reduced kynurenine pathway metabolism and cytokine expression in the prefrontal cortex of depressed individuals. *J. Psychiatry Neurosci.* **41,** 386–394 (2016).
66. Dean, B. *et al.* Different changes in cortical tumor necrosis factor-α-related pathways in schizophrenia and mood disorders. *Mol. Psychiatry* **18,** 767–773 (2013).
67. Dean, B., Tawadros, N., Scarr, E. & Gibbons, A. S. Regionally-specific changes in levels of tumour necrosis factor in the dorsolateral prefrontal cortex obtained postmortem from subjects with major depressive disorder. *J. Affect. Disord.* **120,** 245–248 (2010).
68. Zhang, Y. *et al.* Cortical grey matter volume reduction in people with schizophrenia is associated with neuro-inflammation. *Transl. Psychiatry* **6,** e982 (2016).
69. Ripke, S. *et al.* Biological insights from 108 schizophrenia-associated genetic loci. *Nature* **511,** 421–427 (2014).
70. Sekar, A. *et al.* Schizophrenia risk from complex variation of complement component 4. *Nature* **530,** 177–183 (2016).

71. Holmans, P. *et al.* Gene Ontology Analysis of GWA Study Data Sets Provides Insights into the Biology of Bipolar Disorder. *Am. J. Hum. Genet.* **85,** 13–24 (2009).
72. Barnes, J., Mondelli, V. & Pariante, C. M. Genetic Contributions of Inflammation to Depression. *Neuropsychopharmacology* **42,** 81–98 (2017).
73. Ripke, S. *et al.* A mega-analysis of genome-wide association studies for major depressive disorder. *Mol. Psychiatry* **18,** 497–511 (2013).
74. Bosker, F. J. *et al.* Poor replication of candidate genes for major depressive disorder using genome-wide association data. *Mol. Psychiatry* **16,** 516–532 (2011).
75. Okbay, A. *et al.* Genetic variants associated with subjective well-being, depressive symptoms and neuroticism identified through genome-wide analyses. *Nat. Genet.* **48,** 624–633 (2016).
76. Song, G. G., Kim, J.-H. & Lee, Y. H. Genome-Wide Pathway Analysis in Major Depressive Disorder. *J. Mol. Neurosci.* **51,** 428–436 (2013).
77. Network and Pathway Analysis Subgroup of Psychiatric Genomics Consortium. Psychiatric genome-wide association study analyses implicate neuronal, immune and histone pathways. *Nat. Neurosci.* **18,** 199–209 (2015).
78. Purcell, S. M. *et al.* Common polygenic variation contributes to risk of schizophrenia and bipolar disorder. *Nature* **460,** 748–52 (2009).
79. Kettenmann, H., Hanisch, U.-K., Noda, M. & Verkhratsky, A. Physiology of microglia. *Physiol. Rev.* **91,** 461–553 (2011).
80. Von Bartheld, C. S., Bahney, J. & Herculano-Houzel, S. The Search for True Numbers of Neurons and Glial Cells in the Human Brain: A Review of 150 Years of Cell Counting. doi:10.1002/cne.24040
81. Haxby, J. V, Hoffman, E. A. & Gobbini, M. I. Human neural systems for face recognition and social communication. *Biol. Psychiatry* **51,** 59–67 (2002).
82. Ginhoux, F. *et al.* Fate mapping analysis reveals that adult microglia derive from primitive macrophages. *Science* **330,** 841–845 (2010).
83. Schulz, C. *et al.* A Lineage of Myeloid Cells Independent of Myb and Hematopoietic Stem Cells. *Science (80-.).* **336,** 86–90 (2012).
84. Menassa, D. A. & Gomez-Nicola, D. Microglial Dynamics During Human Brain Development. *Front. Immunol.* **9,** 1014 (2018).
85. Elmore, M. R. P. *et al.* Colony-stimulating factor 1 receptor signaling is necessary for microglia viability, unmasking a microglia progenitor cell in the adult brain. *Neuron* **82,** 380–97 (2014).
86. Sklar, P. *et al.* Whole-genome association study of bipolar disorder. *Mol. Psychiatry* **13,** 558–69 (2008).
87. Hanisch, U.-K. Microglia as a source and target of cytokines. *Glia* **40,** 140–55 (2002).
88. Sanjabi, S., Zenewicz, L. A., Kamanaka, M. & Flavell, R. A. Anti-inflammatory and pro-inflammatory roles of TGF-β, IL-10, and IL-22 in immunity and autoimmunity. *Curr. Opin. Pharmacol.* **9,** 447–453 (2009).
89. Tremblay, M.-È., Lowery, R. L. & Majewska, A. K. Microglial Interactions with Synapses Are Modulated by Visual Experience. *PLoS Biol.* **8,** e1000527 (2010).
90. Ransohoff, R. M. & Cardona, A. E. The myeloid cells of the central nervous system parenchyma. *Nature* **468,** 253–262 (2010).
91. Lawson, L. J., Perry, V. H., Dri, P. & Gordon, S. Heterogeneity in the distribution and morphology of microglia in the normal adult mouse brain. *Neuroscience* **39,** 151–70 (1990).
92. Kettenmann, H., Kirchhoff, F. & Verkhratsky, A. Microglia: New Roles for the Synaptic Stripper. *Neuron* **77,** 10–18 (2013).
93. Schafer, D. P. & Stevens, B. Microglia Function in Central Nervous System Development and Plasticity. *Cold Spring Harb. Perspect. Biol.* **7,** a020545 (2015).
94. Schafer, D. P. *et al.* Microglia sculpt postnatal neural circuits in an activity and complement-dependent manner. *Neuron* **74,** 691–705 (2012).

95. Paolicelli, R. C. *et al.* Synaptic pruning by microglia is necessary for normal brain development. *Science* **333,** 1456–1458 (2011).
96. Sierra, A. *et al.* Microglia shape adult hippocampal neurogenesis through apoptosis-coupled phagocytosis. *Cell Stem Cell* **7,** 483–95 (2010).
97. Stevens, B. *et al.* The Classical Complement Cascade Mediates CNS Synapse Elimination. *Cell* **131,** 1164–1178 (2007).
98. Sato, K. Effects of Microglia on Neurogenesis. *Glia* **63,** 1394–405 (2015).
99. Casano, A. M. & Peri, F. Microglia: Multitasking Specialists of the Brain. *Dev. Cell* **32,** 469–477 (2015).
100. Hanisch, U.-K. Functional diversity of microglia - how heterogeneous are they to begin with? *Front. Cell. Neurosci.* **7,** 65 (2013).
101. Torres-Platas, S. G. *et al.* Morphometric characterization of microglial phenotypes in human cerebral cortex. *J. Neuroinflammation* **11,** 12 (2014).
102. Steiner, J. *et al.* Immunological aspects in the neurobiology of suicide: Elevated microglial density in schizophrenia and depression is associated with suicide. *J. Psychiatr. Res.* **42,** 151–157 (2008).
103. Steiner, J. *et al.* Distribution of HLA-DR-positive microglia in schizophrenia reflects impaired cerebral lateralization. *Acta Neuropathol.* **112,** 305–316 (2006).
104. van Kesteren, C. F. M. G. *et al.* Immune involvement in the pathogenesis of schizophrenia: a meta-analysis on postmortem brain studies. *Transl. Psychiatry* **7,** e1075 (2017).
105. Hercher, C., Chopra, V. & Beasley, C. L. Evidence for morphological alterations in prefrontal white matter glia in schizophrenia and bipolar disorder. *J. Psychiatry Neurosci.* **39,** 376–385 (2014).
106. Brisch, R. *et al.* Microglia in the dorsal raphe nucleus plays a potential role in both suicide facilitation and prevention in affective disorders. *Eur. Arch. Psychiatry Clin. Neurosci.* **267,** 403–415 (2017).
107. Seredenina, T. *et al.* Decreased NOX2 expression in the brain of patients with bipolar disorder: association with valproic acid prescription and substance abuse. *Transl. Psychiatry* **7,** e1206 (2017).
108. Bayer, T. A., Buslei, R., Havas, L. & Falkai, P. Evidence for activation of microglia in patients with psychiatric illnesses. *Neurosci. Lett.* **271,** 126–8 (1999).
109. Steiner, J. *et al.* Severe depression is associated with increased microglial quinolinic acid in subregions of the anterior cingulate gyrus: evidence for an immune-modulated glutamatergic neurotransmission? *J. Neuroinflammation* **8,** 94 (2011).
110. Torres-Platas, S. G., Cruceanu, C., Chen, G. G., Turecki, G. & Mechawar, N. Evidence for increased microglial priming and macrophage recruitment in the dorsal anterior cingulate white matter of depressed suicides. *Brain. Behav. Immun.* **42,** 50–9 (2014).
111. Schnieder, T. P. *et al.* Microglia of prefrontal white matter in suicide. *J. Neuropathol. Exp. Neurol.* **73,** 880–90 (2014).
112. Hamidi, M., Drevets, W. C. & Price, J. L. Glial reduction in amygdala in major depressive disorder is due to oligodendrocytes. *Biol. Psychiatry* **55,** 563–569 (2004).
113. Cagnin, A. *et al.* In-vivo measurement of activated microglia in dementia. *Lancet (London, England)* **358,** 461–7 (2001).
114. Kreisl, W. C. *et al.* In vivo radioligand binding to translocator protein correlates with severity of Alzheimer's disease. *Brain* **136,** 2228–38 (2013).
115. Gulyás, B. *et al.* A comparative autoradiography study in post mortem whole hemisphere human brain slices taken from Alzheimer patients and age-matched controls using two radiolabelled DAA1106 analogues with high affinity to the peripheral benzodiazepine receptor (PBR) syst. *Neurochem. Int.* **54,** 28–36 (2009).
116. Colasanti, A. *et al.* Hippocampal Neuroinflammation, Functional Connectivity, and Depressive Symptoms in Multiple Sclerosis. *Biol. Psychiatry* **80,** 62–72 (2016).

117. Herranz, E. *et al.* Neuroinflammatory component of gray matter pathology in multiple sclerosis. *Ann. Neurol.* **80,** 776–790 (2016).
118. Banati, R. B. *et al.* The peripheral benzodiazepine binding site in the brain in multiple sclerosis: quantitative in vivo imaging of microglia as a measure of disease activity. *Brain* **123 (Pt 1,** 2321–37 (2000).
119. Doorduin, J. *et al.* Neuroinflammation in schizophrenia-related psychosis: a PET study. *J. Nucl. Med.* **50,** 1801–7 (2009).
120. van Berckel, B. N. *et al.* Microglia Activation in Recent-Onset Schizophrenia: A Quantitative (R)-[11C]PK11195 Positron Emission Tomography Study. *Biol. Psychiatry* **64,** 820–822 (2008).
121. Bloomfield, P. S. *et al.* Microglial Activity in People at Ultra High Risk of Psychosis and in Schizophrenia: An [11 C]PBR28 PET Brain Imaging Study. *Am. J. Psychiatry* **173,** 44–52 (2016).
122. Holmes, S. E. *et al.* In vivo imaging of brain microglial activity in antipsychotic-free and medicated schizophrenia: A [11C](R)-PK11195 positron emission tomography study. *Mol. Psychiatry* **21,** 1672–1679 (2016).
123. Ripke, S. *et al.* Biological insights from 108 schizophrenia-associated genetic loci. *Nature* **511,** 421–427 (2014).
124. Owen, D. R. J. & Matthews, P. M. Imaging Brain Microglial Activation Using Positron Emission Tomography and Translocator Protein-Specific Radioligands. in 19–39 (2011). doi:10.1016/B978-0-12-387718-5.00002-X
125. Szymanski, S. *et al.* Gadolinium-DTPA Enhanced Gradient Echo Magnetic Resonance Scans in First Episode of Psychosis and Chronic Schizophrenic Patients. *Psychiatry Res. Neuroimaging* 203–207 (1991).
126. York, E. M., Bernier, L.-P. & MacVicar, B. A. Microglial modulation of neuronal activity in the healthy brain. *Dev. Neurobiol.* (2017). doi:10.1002/dneu.22571
127. Zhao, Y.-Y. *et al.* TSPO-specific ligand vinpocetine exerts a neuroprotective effect by suppressing microglial inflammation. *Neuron Glia Biol.* **7,** 187–97 (2011).
128. Yang, Y. *et al.* Inflammation leads to distinct populations of extracellular vesicles from microglia. *J. Neuroinflammation* **15,** 168 (2018).
129. Zrzavy, T. *et al.* Pro-inflammatory activation of microglia in the brain of patients with sepsis. *Neuropathol. Appl. Neurobiol.* (2018). doi:10.1111/nan.12502
130. Takano, A. *et al.* Peripheral benzodiazepine receptors in patients with chronic schizophrenia: a PET study with [11C]DAA1106. *Int. J. Neuropsychopharmacol.* **13,** 943–950 (2010).
131. Abelli, M. *et al.* Reductions in Platelet 18-kDa Translocator Protein Density Are Associated with Adult Separation Anxiety in Patients with Bipolar Disorder. *Neuropsychobiology* **62,** 98–103 (2010).
132. Haarman, B. C. M. (Benno) *et al.* Neuroinflammation in bipolar disorder – A [11C]-(R)-PK11195 positron emission tomography study. *Brain. Behav. Immun.* **40,** 219–225 (2014).
133. Hannestad, J. *et al.* The neuroinflammation marker translocator protein is not elevated in individuals with mild-to-moderate depression: A [11C]PBR28 PET study. *Brain. Behav. Immun.* **33,** 131–138 (2013).
134. Holmes, S. E. *et al.* Elevated Translocator Protein in Anterior Cingulate in Major Depression and a Role for Inflammation in Suicidal Thinking: A Positron Emission Tomography Study. *Biol. Psychiatry* **83,** 61–69 (2018).
135. Setiawan, E. *et al.* Role of translocator protein density, a marker of neuroinflammation, in the brain during major depressive episodes. *JAMA psychiatry* **72,** 268–75 (2015).
136. Nagai, A. *et al.* Generation and Characterization of Immortalized Human Microglial Cell Lines: Expression of Cytokines and Chemokines. *Neurobiol. Dis.* **8,** 1057–1068 (2001).
137. Janabi, N., Peudenier, S., Héron, B., Ng, K. H. & Tardieu, M. Establishment of human microglial cell lines after transfection of primary cultures of embryonic microglial cells with the SV40 large T antigen. *Neurosci. Lett.* **195,** 105–108 (1995).

138. Ohgidani, M. *et al.* Direct induction of ramified microglia-like cells from human monocytes: Dynamic microglial dysfunction in Nasu-Hakola disease. *Sci. Rep.* **4,** 4957 (2014).
139. Ohgidani, M., Kato, T. & Kanba, S. Introducing directly induced microglia-like (iMG) cells from fresh human monocytes: a novel translational research tool for psychiatric disorders. *Front. Cell. Neurosci.* **9,** 1–5 (2015).
140. Leone, C. *et al.* Characterization of human monocyte-derived microglia-like cells. *Glia* **54,** 183–192 (2006).
141. Etemad, S., Zamin, R., Ruitenberg, M. & Filgueira, L. A novel in vitro human microglia model: Characterization of human monocyte-derived microglia. *J. Neurosci. Methods* **209,** 79–89 (2012).
142. Ormel, P. R. *et al.* Characterization of macrophages from schizophrenia patients. *npj Schizophr.* **3,** 41 (2017).
143. Hettinger, J. *et al.* Origin of monocytes and macrophages in a committed progenitor. *Nat. Immunol.* **14,** 821–830 (2013).
144. Abud, E. M. *et al.* iPSC-Derived Human Microglia-like Cells to Study Neurological Diseases. *Neuron* **94,** 278–293.e9 (2017).
145. Muffat, J. *et al.* Efficient derivation of microglia-like cells from human pluripotent stem cells. *Nat. Med.* **22,** 1358–1367 (2016).
146. Douvaras, P. *et al.* Directed Differentiation of Human Pluripotent Stem Cells to Microglia. *Stem Cell Reports* **8,** 1516–1524 (2017).
147. Ormel, P. R. *et al.* Microglia innately develop within cerebral organoids. *Nat. Commun.* **9,** 4167 (2018).
148. Olah, M. *et al.* An optimized protocol for the acute isolation of human microglia from autopsy brain samples. *Glia* **60,** 96–111 (2012).
149. Galatro, T. F. *et al.* Transcriptomic analysis of purified human cortical microglia reveals age-associated changes. *Nat. Neurosci.* **20,** 1162–1171 (2017).
150. Mizee, M. R. *et al.* Isolation of primary microglia from the human post-mortem brain: effects of ante- and post-mortem variables. *Acta Neuropathol. Commun.* **5,** 16 (2017).
151. Melief, J. *et al.* Characterizing primary human microglia: a comparative study with myeloid subsets and culture models. *Glia* 1–12 (2016). doi:10.1002/glia.23023
152. Melief, J. *et al.* Phenotyping primary human microglia: Tight regulation of LPS responsiveness. *Glia* **60,** 1506–1517 (2012).
153. Melief, J. *et al.* Microglia in normal appearing white matter of multiple sclerosis are alerted but immunosuppressed. *Glia* **61,** 1848–1861 (2013).

Chapter 2

Characterizing primary human microglia: a comparative study with myeloid subsets and culture models

J. Melief[1*#], M.A.M. Sneeboer[1,2*], M. Litjens[1,2], P.R. Ormel[1,2], S.J.M.C. Palmen[2], I. Huitinga[3], R.S. Kahn[1], E.M. Hol[2,3,4] and L.D. de Witte[1,2]

* these authors contributed equally

[1] Department of Psychiatry, Brain Center Rudolf Magnus, University Medical Center Utrecht (BCRM-UMCU), 3584 CG Utrecht The Netherlands

[2] Department of Translational Neuroscience, BCRM-UMCU, 3584 CG Utrecht, The Netherlands

[3] Netherlands Institute for Neuroscience, An institute of the royal academy of arts and sciences, 1105 BA, Amsterdam, The Netherlands

[4] Swammerdam Institute for life sciences, Center for Neuroscience, University of Amsterdam, 1098 XH Amsterdam, The Netherlands

[#] current address: Department of Oncology-Pathology, Karolinska Institute, Stockholm, Sweden

Accepted in *Glia*. 64(11): 1857-68 (2016)

Abstract

The biology of microglia has become subject to intense study as they are widely recognized as crucial determinants of normal and pathologic brain functioning. While they are well studied in animal models, it is still strongly debated what specifies most accurately the phenotype and functioning of microglia in the human brain. In this study, we therefore isolated microglia from post-mortem human brain tissue of corpus callosum and frontal cortex. The cells were phenotyped for a panel of typical microglia markers and genes involved in myeloid cell biology. Furthermore, the response to pro- and anti-inflammatory stimuli was assessed. The microglia were compared to key human myeloid cell subsets, including monocytes, monocyte-derived macrophages and monocyte-derived dendritic cells, and several commonly used microglial cell models. Protein and mRNA expression profiles partly differed between microglia isolated from corpus callosum and frontal cortex and were clearly distinct from other myeloid subsets. Microglia responded to both pro- (LPS or poly I:C) and anti-inflammatory (IL-4 or dexamethasone) stimuli. Interestingly, pro-inflammatory responses differed between microglia and monocyte-derived macrophages, as the former responded more strongly to poly I:C and the latter more strongly to LPS. Furthermore, we defined a large phenotypic discrepancy between primary human microglia and currently used microglial cell models and cell lines. In conclusion, we further delineated the unique and specific features that discriminate human microglia from other myeloid subsets, and we show that currently used cellular models only partly reflect the phenotype of primary human microglia.

Introduction

Microglia are considered the key immunocompetent cells of the central nervous system (CNS). They are highly motile cells that rapidly respond to any type of damage, inflammation or infection in the CNS by migrating towards the site of injury where they clear cellular debris, limit further damage and promote recovery[1,2]. More recently, it has been established that microglia are not only involved in these typical damage induced processes, but also play a crucial role in neurodevelopment and physiological neuronal functioning in adulthood[3]. Microglia form an essential part in the neurogenic niche, thereby promoting neurogenesis, mediating synaptic pruning and modulating neurotransmission[1,2]. This knowledge has boosted the already growing interest for microglia as critical determinants of CNS functioning in health and disease.

Apart from microglia, the brain parenchyma contains several other types of myeloid cells, including perivascular macrophages and, especially during pathology, infiltrating monocyte-derived macrophages (mo-MΦ). Microglia were long thought to originate from the same hematopoietic progenitor as the other myeloid immune cells. In contrast to other myeloid cells, which derive from definitive hematopoiesis, it was recently discovered that microglia emerge from $Tie2^{+}$ expressing erythromyeloid progenitors from the embryonic yolk sac that populate the CNS during early development[4–7]. Therefore, primary microglia are now seen as distinct from monocytes and monocyte-derived macrophages. How microglia differ from these other cells at the phenotypical and functional level and which markers can distinguish between the different subsets is at present still unclear.

Recently, three studies described the mRNA expression profile of murine microglia[8–10]. Highly specific microglia markers were identified in mice, some of which were also strongly or even uniquely expressed in human microglia[8]. However, it is still intensely debated how human microglia are most accurately specified, both phenotypically and functionally, and how these cells differ from other human myeloid subsets. This knowledge regarding human microglia is needed since clear species differences have been described for microglia[11]. In addition, tools to study human microglia, including knowledge of microglia-specific markers and functional characteristics, are crucial for unraveling the role of microglia in complex neuropsychiatric diseases, such as schizophrenia and autism spectrum disorder, as these 'human-specific' diseases can never be fully mimicked in animal models.

So far, the role of microglia in human CNS disorders has been commonly studied by *in situ* stainings of post-mortem human brain sections. This approach has revealed that microglia display clear changes in cell density and morphology in most neurologic and psychiatric diseases[12–14]. However, the nature of the observed microglial alterations and their exact contribution to disease development is still unknown. To answer these questions it is essential to go beyond the assessment of microglia morphology and density and investigate microglia at the functional level. In this study, we therefore set out to define the specific phenotypic and functional characteristics of human microglia in more detail. This knowledge is crucial for assessing the exact role of microglia in various stages and types of CNS pathology.

Recently, we and others established new methods to acutely isolate pure populations of microglia from freshly dissected post-mortem human brain tissue[15,16]. We used the method of Melief et al. for a detailed study of the specific phenotypic and functional characteristics of human microglia. As microglia can display brain region-dependent differences, we compared microglia isolated from the corpus callosum (CC) and medial frontal cortex (CTX) with other myeloid subsets, with the aim to create a suitable reference dataset of microglia-specific markers[17]. Finally, we compared the isolated primary microglia with currently used human microglia cell models to assess how accurately these cell models recapitulate microglial biology *in vivo*.

Materials and Methods

Isolation and culture of primary human microglia

Primary human microglia were isolated as described before[15]. For *in vitro* culture experiments, the isolation procedure was slightly altered compared to the earlier published protocol to increase the number of isolated cells. For the *in vitro* experiments we excluded the enzymatic dissociation buffer and erythrocyte lysis step. Post-mortem brain tissue of non-demented healthy controls was provided by the Netherlands Brain Bank (www.hersenbank.nl). Informed consent was obtained for brain autopsy and the use of tissue and clinical information for research purposes (see supplementary Table 1 for clinicopathological information). Isolation procedures were started within 2 to 24 h after autopsy. In summary, after removal of visible veins, tissue was meshed through a stainless steel sieve in a glucose- potassium-sodium buffer (GKN-BSA; 8g/L NaCl, 0.4 g/L KCl, 1.77 g/L $Na_2HPO_4.2H_2O$, 0.69 g/L $NaH_2PO_4.H_2O$, 2 g/L D-(1)- glucose, pH 7.4) with 0.3% bovine serum albumin (BSA), followed by enzymatic dissociation in 4 mL enzyme buffer (4 g/L $MgCl_2$, 2.55 g/L $CaCl_2$, 3.73 g/L KCl, and 8.95 g/L NaCl), with 3700 units/mL collagenase Type I (Worthington, Lakewood, NJ, USA) and 200 µg/mL DNase I (Roche Diagnostics GmbH) for 1 h at 37ºC while shaking. Cells were resuspended in 20 mL Percoll (Amersham, GE Healthcare) of $\rho = 1.03$, underlain with 10 mL Percoll of $\rho = 1.095$, overlain with 5 mL GKN-BSA buffer and centrifuged for 30 minutes at 4000 rpm and 4ºC with slow acceleration and no break. The top myelin layer was discarded, after which cells enriched for microglia were collected from the interface between the myelin and Percoll layer and transferred to a polypropylene coated 50-mL tube. Positive selection of microglia was performed by magnetic-activated cell sorting (MACS) according to the manufacturer's protocol with CD11b-conjugated magnetic microbeads (Miltenyi Biotec GmbH, Bergisch Gladbach, Germany), leading to microglia isolates of around 99% purity. Importantly, both in our study and in a previous published paper, it was shown that expression of CD14 on CD11b+ cells isolated with our method is absent or marginal, compared to CD11b+ cells isolated from the choroid plexus or blood (Melief et al., 2012). This indicates that by the majority of CD11b+ cells we isolated from post-mortem brain tissue represents microglia, and that any substantial contamination with non-microglial myeloid cells (e.g. perivascular macrophages, blood monocytes) is minimal. The microglia were subsequently used for flow cytometric analysis, *in vitro* experiments, or lysed in TRIzol reagent (Invitrogen, Carlsbad, CA, USA) and frozen at -80ºC. For culture experiments, 1.0 x 10^5 microglia were plated in a 96-wells flat-bottom plate (Greiner Bio-One) in a total volume of 200 µl Rosswell-Park-Memorial-Institute medium (RPMI; (Gibco Life technologies, Massachusetts)) with 10% heat-inactivated fetal calf serum (FCS; (Gibco Life technologies, Massachusetts)), 2 mM L-glutamine (Gibco Life technologies, Massachusetts) and 1% penicillin-streptomycin (p/s; 100 units/mL /100 µg/mL; (Gibco Life technologies, Massachusetts)). Microglia were cultured overnight before stimulation with pro- or anti-inflammatory stimuli.

Isolation and culture of other myeloid cell subsets and microglia cell models

Peripheral blood mononuclear cells (PBMCs) were isolated from buffy coats (Sanquin, the Netherlands) of healthy donors by density gradient separation using Ficoll (Ficoll Paque plus, GE Healthcare). Monocytes were isolated from PBMCs by magnetic separation using CD14 microbeads (Miltenyi Biotech, Bergisch Gladbach, Germany), according to the manufacturer's protocol. To generate mo-MΦ, monocytes were plated at a density of 1.0 x 10^5 cells per well in a 48-wells flat bottom plate (Corning, New York, NY) in RPMI and supplemented with 1% p/s, 2 mM L-glutamine and 10% human AB serum (Sanquin, the Netherlands) for 7 days. mo-DC were generated by culturing monocytes (48-wells flat bottom plate; density 1.0 x 10^5 cells per well) in presence of 1% p/s, 2 mM L-glutamine, 100 ng/ml recombinant human granulocyte-monocyte colony stimulating factor (GM-CSF; Miltenyi Biotec) and 100 ng/ml

recombinant human interleukin-4 (IL-4; Miltenyi Biotec) for 3 days. Three culture models for monocyte-derived microglia were selected from the literature and slightly adapted to increase cell viability[18–20]. These three models are referred to as mo-MG-A, -B and –C. Monocytes for these models were obtained as described above. Mo-MG-A were generated according to the protocol of Leone et al. (2006) by culturing monocytes in a 6-wells flat bottom plate with 25% astrocyte-conditioned medium (ACM; Sanbio), 1 ng/ml GM-CSF and 10 ng/ml macrophage-colony stimulating factor (M-CSF; Miltenyi Biotec) for 12 days. To obtain mo-MG-B microglia based on the protocol of Etemad et al. (2012), monocytes were cultured in DMEM with 1% p/s, 10 ng/mL M-CSF, 10ng/mL GM-CSF, 10ng/mL nerve growth factor (NGF)-β (Miltenyi Biotec), 100 ng/mL chemokine (C-C motif) ligand 2 (CCL2; Miltenyi Biotec) and 25% ACM for 14 days. For the final model (mo-MG-C, adapted from Ohgidani et al., 2014) monocytes were cultured in RPMI glutamax with 1% p/s, 10 ng/mL GM-CSF and 100 ng/mL interleukin-34 (IL-34) for 14 days. The SV40 human immortalized microglia cell line, originally derived from microglia isolated from embryonic spinal cord and cortex immortalized with SV-40 virus, was obtained from Applied Biological Materials (ABM) Inc. (Janabi et al., 1995). The CHME-5 cell line was obtained from human foetal microglia transfected with SV-40 virus, and was a kind gift of Dr. Pierre Talbot (INRS-Institut Armand-Frappier, Université du Québec, Canada)[21].

Response to pro- and anti-inflammatory stimuli

Primary microglia and mo-MΦ were stimulated with 100 ng/mL lipopolysaccharide (LPS) from Escherichia coli 0111:B4 (Sigma-Aldrich, The Netherlands) or 100 µg/ml poly I:C (Bio-connect, The Netherlands) for 6h, or with 40 ng/mL IL-4 (Peprotech, London, UK) or 1 µM dexamethasone (Sigma Aldrich, Zwijndrecht, The Netherlands) for 72h. Cells were harvested, lysed with 500 µl TRIzol and stored at -80^{0}C for future analyses of mRNA expression.

Flow Cytometry

Stainings for flow cytometry were performed in v-bottom 96-wells plates (Greiner Bio-One). In short, 0.7 to 1.5 x 10^5 cells were incubated on ice in the dark in 20 µl GKN-BSA with 5% human pooled serum (HPS) for 30 minutes, continued with staining in 25 µl with specific monoclonal or isotype control antibodies. Antibodies with the following specificities were used: from eBioscience (San Diego, CA, USA): anti-human CD11b (clone ICRF44, PE labeled), CD11c (clone 3.9, FITC labeled), CD14 (clone 61D3, APC labeled), CD45 (clone 2D1, FITC labeled), CD83 (clone HB15e, PE labeled), CD163 (clone GHI/61, PE labeled), CD172α (clone 15-414, PerCP-eFluor710 labeled), CD200R (clone OX108, PE labeled), CX3CR1 (clone eB149/10H5, APC labeled), HLA-DR (clone LN3, APC labeled). From BD biosciences: anti-human CD206 (clone 19.2, APC labeled).

From Biolegend (San Diego, CA): CD40 (clone 5C3, PerCP-eFluor710 labeled). To determine aspecific staining, the following isotype control antibodies were used from eBioscience: mouse IgG1 FITC, eFluor710 and APC, mouse IgG2a eFluor710, rat IgG2b-APC. Other isotype control antibodies were from Biolegend: mouse IgG1, and mouse IgG2b PE and APC. As a viability dye, 7-amino-actinomycin D (7AAD; BD Biosciences) was added to each sample in a dilution of 1:40 for 15 minutes before flow cytometric analysis. Phenotyping of primary human microglia, monocytes, mo-MΦ and mo-DC was done on a FACSCanto machine (BD Biosciences). All data were analyzed with FlowJo software version 9.8.5. (Treestar, Ashland, OR). The relative geometric mean fluorescence intensity (geoMFI) was calculated by subtracting the geoMFI of the corresponding isotype control from the geoMFI of the antigen staining.

Gene expression analysis

For gene expression analysis, RNA was isolated using TRIzol reagent, followed by addition of 100 µl chloroform and centrifugation at 12000 rcf at 7^{o}C for 15 minutes. Subsequently, RNA was precipitated from 100 to 200 µl of the aqueous top phase by mixing with an equal volume of isopropanol, using 1 µl glycogen as a carrier, and stored overnight at -20^{o}C. The next day, samples were centrifuged at maximum speed at 4^{o}C for 60 minutes. The pellet was washed twice with 75% ETOH, air-dried and dissolved in 8ul Milli-Q water. Concentrations of extracted RNAs were measured using a nanodrop (ND-1000; NanoDrop Technologies, Rockland, DE). RNA was reversed transcribed using a Quantitect Reverse Transcription kit (QIAGEN, Hilden, Germany) according to manufacturer's protocol. The maximum amount of RNA, supplemented with Milli-Q to a volume of 6 µl, was added to 1 µl gDNA Wipe-Out buffer and incubated at 42°C for 2 minutes. After addition of the master mix containing 2 µl Reverse-Transcriptase buffer, 0.5 µl Reverse-Transcriptase enzyme and 0.5 µl RT random hexamers primer mix, samples were incubated at 42^{o}C for 30 minutes, followed by 95^{o}C for 3 minutes. Samples were subsequently stored at -20^{o}C until further use. Quantitative real-time polymerase chain reaction (qPCR) was done with a 7900 Real Time PCR System (Applied Biosystems) and a QuantStudio™ 6 Flex Real-Time PCR System (Life Technologies Corporation, NY, USA) with the following cycle conditions: 50^{o}C for 2 minutes, 95^{o}C for 10 minutes, 40 cycles at 95^{o}C of 15 seconds and 60^{o}C for 60 seconds. The amount of cDNA used per reaction was based on an input of 5 ng RNA in a final volume of 10 µL. Per reaction, 5 µL SYBRgreen PCR Master Mix (Roche; Life Technologies Corporation, Grand Island, NY, USA), and 1 µL primer mix (2 pmol/mL; see supplementary Table 2) was added. Absolute expression was calculated with the ΔΔCT method. Expression of selected genes was normalized to references genes 18S and GAPDH or to GAPDH solely for the stimulation experiments. The response to inflammatory stimuli was calculated as fold change by dividing

the normalized gene expression of the stimulated sample by the normalized gene expression of the unstimulated sample. Primers were intron-spanning and designed with the online primer designed tool of NCBI or Primer Express. To visualize mRNA expression of all the cell subsets included in the study, heatmaps were generated using Rstudio (RStudio, Boston). Normalized mRNA values were scaled and clustered according to their expression level.

Statistical Analysis

Statistical analysis was performed with GraphPad Prism software (version 5). A Kruskall-Wallis test was used to geoMFI values between microglia and other cell types, whereas a Wilcoxon-signed rank test was used to compare mRNA expression levels between unstimulated myeloid cells and myeloid cells cultured with pro- and anti-inflammatory compounds. To study cytokine responsiveness between microglia and other myeloid subsets a Kruskall-Wallis test was performed. For all analyses, multiple comparison correction was applied and a P-value <0.05 was considered statistically significant.

Results

Primary human microglia display a distinct phenotype from other myeloid cell subsets

In order to further characterize the *ex vivo* phenotype of microglia, we first determined the expression of a panel of markers that are classically used to identify microglia: CD11b, CD14, CD40, CD45, CX3CR1 and HLA-DR. Fig. 1A depicts mRNA and Fig. 1B protein expression. Expression levels were compared between primary microglia isolated from frontal cortex (CTX), corpus callosum (CC, mRNA expression only), monocytes, mo-MΦ and mo-DC. Primary microglia express all classical microglia markers at the mRNA and protein level. Although none of these markers are specifically expressed by microglia, we found differences in expression levels when comparing *ex vivo* microglia and the other myeloid subtypes. Expression of CX3CR1 was higher in microglia compared to the other three myeloid subtypes, although the difference did not reach significance for all comparisons. Protein, but not mRNA, expression of CD11b and CD14 was low on microglia compared to monocytes. Protein expression of HLA-DR was unexpectedly high in three out of four donors. Additional, flow cytometric data of CC microglia are shown in supplementary figure 1, as only a limited number of samples was available for analysis. Note that CX3CR1 expression was not studied for CC microglia and protein expression of several markers was based on a single sample. Next, we analyzed mRNA expression of a panel of genes that have

recently been described to be highly enriched in murine as well as fetal and adult human microglia: PROS1, GAS6, MERTK, GPR34 and P2Ry12[8]. All of these markers were clearly enriched in both CC and CTX microglia in comparison to monocytes with the largest difference in expression for P2Ry12 (Fig. 1C). The expression was also higher compared to mo-MΦ and mo-DC, but these differences did not reach significance for all of the markers.

To further investigate the phenotype of microglia in different brain regions and compare this with other myeloid cell subtypes, we analyzed mRNA expression of a panel of genes that are central to myeloid cell biology. A cluster analysis confirmed grouping of molecules in line with their described function (Fig. 2A and sup. Table 3). We found a distinct expression profile between microglia isolated from CC and CTX (Fig. 2A and B). CC microglia expressed higher levels of the cannabinoid receptors (CB1; CB2), and of molecules involved in pathogen binding (CD16, CD32a), antigen presentation (CD86) and ATP signaling (P2X7). On the other hand, CTX microglia displayed higher gene expression of TLR4. We also found differences in mRNA expression level of this panel of genes between microglia and the other myeloid cell types. Microglia from CC and CTX displayed low expression of CD80, CD206, CD200R, CD209, CD274 and CHRNA4 (Fig. 2A). For six of the genes in the mRNA expression panel, we determined protein expression levels by flow cytometry. Protein expression of most markers was in line with their expression found by qPCR analysis. The expression for CD200R, CD11c and CD206 was low or absent (Fig. 2B). However, similar to Fig. 1, some striking differences between mRNA and protein expression were detected, for instance the expression of CD206 and CD11c on mo-MΦ and mo-DC.

Primary microglia respond to pro- and anti-inflammatory stimuli

Subsequently, we determined how human *ex vivo* isolated microglia respond to pro- and anti-inflammatory compounds. The response was compared with monocytes, mo-MΦ and mo-DC. As read-out we used markers that are known to be upregulated in mo-MΦ after stimulation with pro- and anti-inflammatory compounds[22,23]. Fig. 3 and sup. Fig. 2 depicts the response to stimulation with LPS and poly I:C. After six hours of stimulation mRNA levels of TNFα, IL-1β and IL-6 were induced by LPS and poly I:C in microglia of most donors, although the response differed between donors (sup. Fig. 2). While responsiveness to LPS was similar between CC and CTX microglia, CC microglia showed a stronger response to poly I:C than CTX microglia. The response to LPS treatment of microglia was less pronounced than in monocytes, mo-MΦ and mo-DC (Fig. 3A). In contrast, microglia, especially from CC, responded more strongly to poly I:C than the other myeloid cell types (Fig. 3B). In Fig. 4 and supplementary Fig. 2 the response to stimulation with the anti-inflammatory compounds dexamethasone and

Figure 1

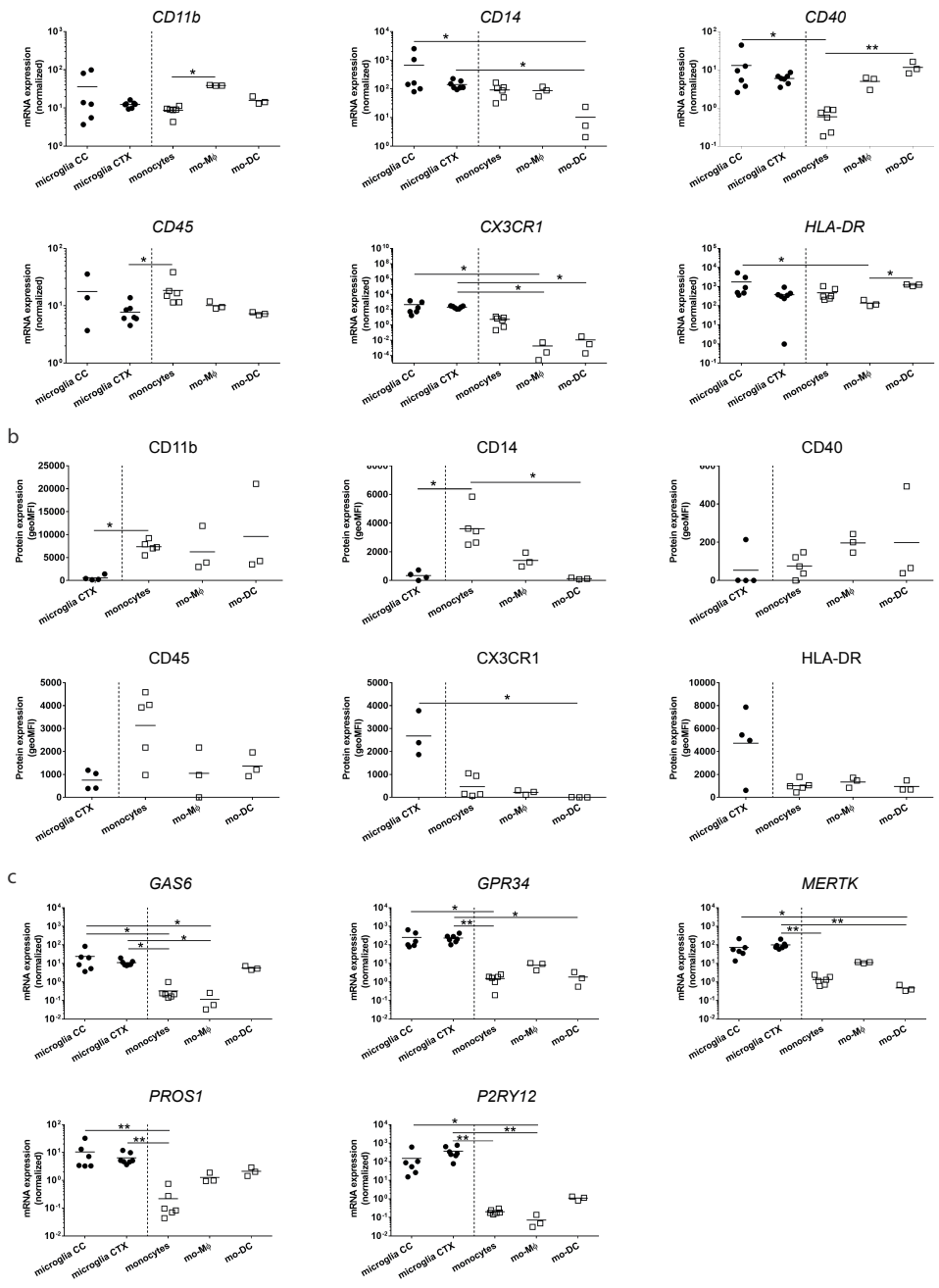

< Figure 1: Expression of commonly used and novel microglia markers in primary human microglia and other myeloid cell subsets. (a) mRNA expression of commonly used microglia markers in primary microglia (CC (N=6) and CTX (N=7)) monocytes (N=6), mo-MΦ (N=3) and mo-DC (N=3) as determined by qPCR. (b) Protein expression of commonly used microglia markers in primary microglia (CTX; N=4) compared to monocytes (N=6), mo-MΦ (N=3) and mo-DC (N=3) as determined by flow cytometry. (C) mRNA expression of novel (c) microglia markers in primary microglia (CC (N=6) and CTX (N=7)) monocytes (N=6), mo-MΦ (N=3) and mo-DC (N=3) as determined by qPCR. The qPCR was performed with a single run for each reaction and mRNA expression was calculated with the ΔΔCT by using 18S and GAPDH as reference genes. For analysis of flow cytometry data, the relative geometric mean fluorescence intensity (geoMFI) was calculated by subtracting the geoMFI of the corresponding isotype control from the geoMFI of the antigen staining. *p<0.05; **p<0.01.

IL-4 is described. As shown before, CD163 was upregulated in both microglia and mo-MΦ after stimulation with dexamethasone. Surprisingly, dexamethasone also induced the expression of CD206 and CD200R, which are considered to be typically induced by IL-4, as shown in Fig. 4B. CC and CTX microglia did not significantly differ from each other or from mo-MΦ in the strength of their response to anti-inflammatory stimuli.

Large phenotypic discrepancy between primary human microglia and currently used microglial cell models and cell lines

Finally, we compared the phenotype of primary microglia with several human microglia cell models that are often used to study microglia biology. We determined gene expression of the same sets of genes that were used in Fig. 1 and 2 in two commonly used microglia cell lines (SV40 and CHME) and three monocyte-derived microglia models (mo-MG-A[18], mo-MG-B[19], and mo-MG-C[20]) (Fig. 5). Genes that were shown in Fig. 1 to be enriched in primary microglia compared to other myeloid cell types (CX3CR1, P2Ry12, MERTK, GAS6, PROS1, GPR34) were expressed at very low or undetectable levels in the microglia cell lines SV40 and CHME. Genes that are involved in immune activation and antigen recognition (e.g. HLA-DR, CD200R, CD163) were expressed at comparable levels in primary microglia and the two cell lines, but expression of the other genes in the panel was highly dissimilar. The mo-MG models showed some more similarities with the primary microglia (e.g. expression of CD45 and CD11c), but still differed substantially. Concerning the microglia specific markers, PROS1 and GAS6, but not MERTK, GPR34, P2Ry12 and CX3CR1, were expressed at levels in the range of the primary microglia in mo-MG-A and mo-MG-B. Instead, mo-MG-C was more comparable in expression of markers such as HLA-DR and CD200R.

Figure 2

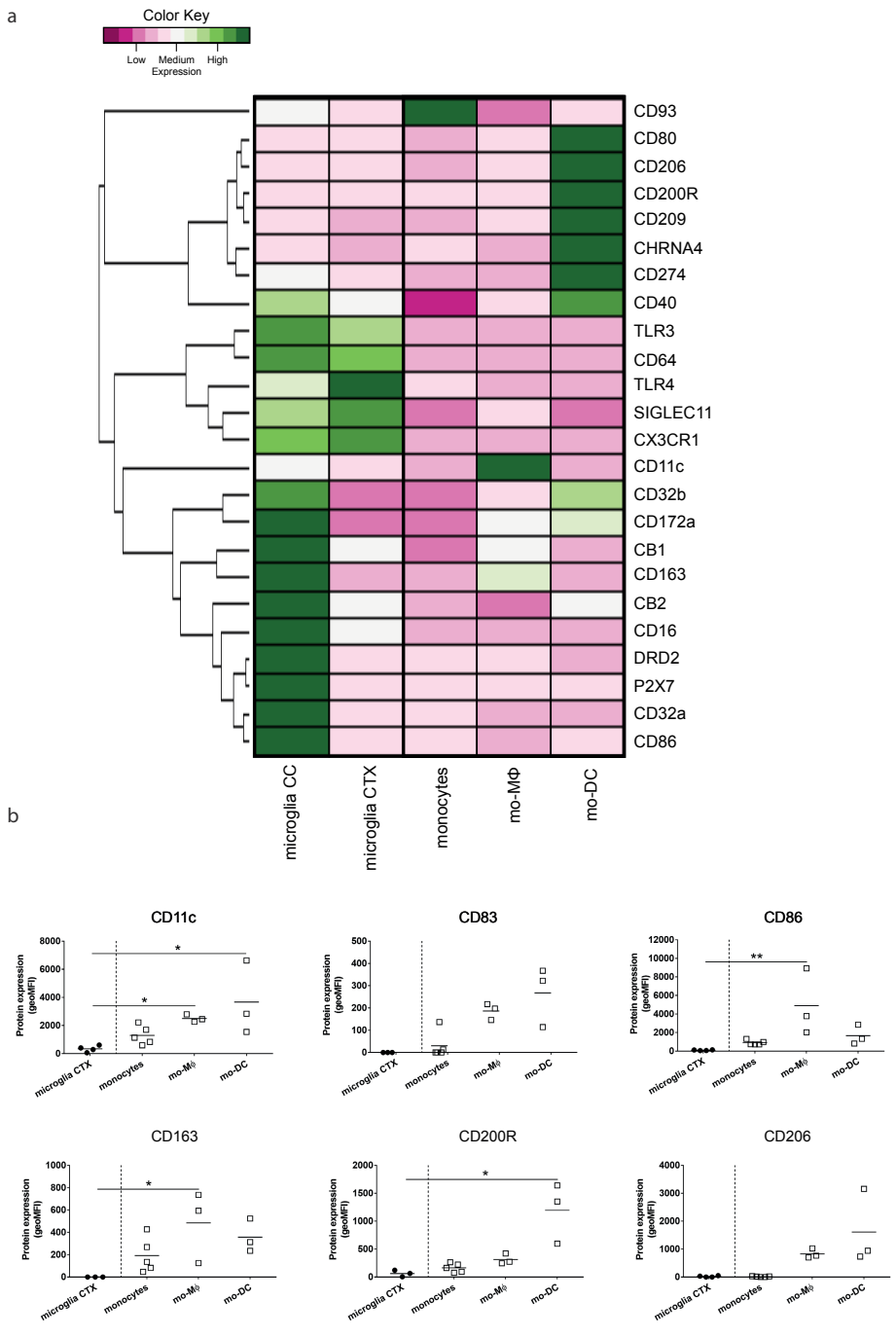

< Figure 2: Expression of a panel of genes involved in myeloid cell biology in primary microglia and other myeloid cell subsets.

(a) mRNA expression, determined by qPCR, in primary microglia and other myeloid cells. Microglia (CC (N=6); CTX (N=7)), monocytes (N=6), mo-MΦ (N=3), mo-DC (N=3). The qPCR was performed with a single run for each reaction and mRNA expression was calculated with the ΔΔCT by using 18S and GAPDH as reference genes, scaled and clustered according to their expression level. (b) Protein expression in primary microglia (CTX; N=4), monocytes (N=6), mo-MΦ (N=3) and mo-DC (N=3) as determined by flow cytometry. The relative geometric mean fluorescence intensity (geoMFI) was calculate by subtracting the geoMFI of the corresponding isotype control from the geoMFI of the antigen staining.

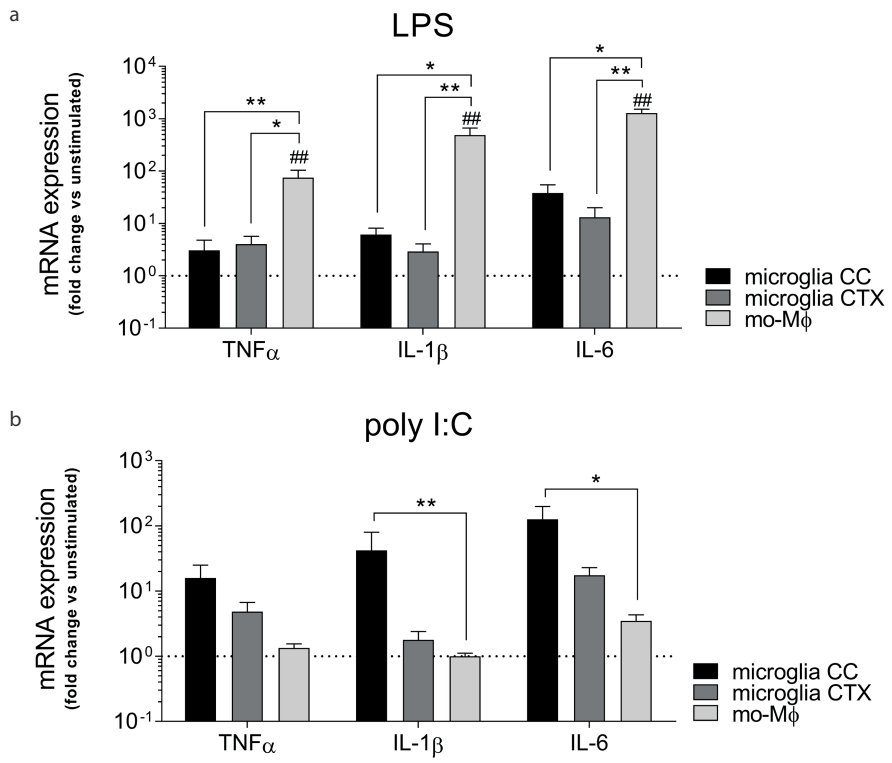

Figure 3: Response to the pro-inflammatory stimuli LPS and poly I:C.

Primary microglia (CC (N=5) and CTX (N=4)), monocytes (N=4), mo-MΦ (N=10) and mo-DC (N=4) were stimulated with pro-inflammatory compounds for 6 hours. (a) mRNA expression of TNFα, IL-1β and IL-6 after LPS stimulation. (b) mRNA expression of TNFα, IL-1β and IL-6 after poly I:C stimulation. Gene expression was determined by qPCR with a single run for each reaction. IL-6 mRNA levels of poly I:C stimulated monocytes were not detectable (ND). Normalized fold changes were calculated by dividing the relative mRNA expression, determined with the ΔΔCT by using GAPDH as reference gene, by the relative expression of the unstimulated control. Dotted line represents mRNA levels of unstimulated cells. Significantly different from unstimulated cells: $^{\#}p<0.05$; $^{\#\#}p<0.01$; $^{\#\#\#}p<0.001$. Significantly different from other cell types: $^{*}p<0.05$; $^{**}p<0.01$.

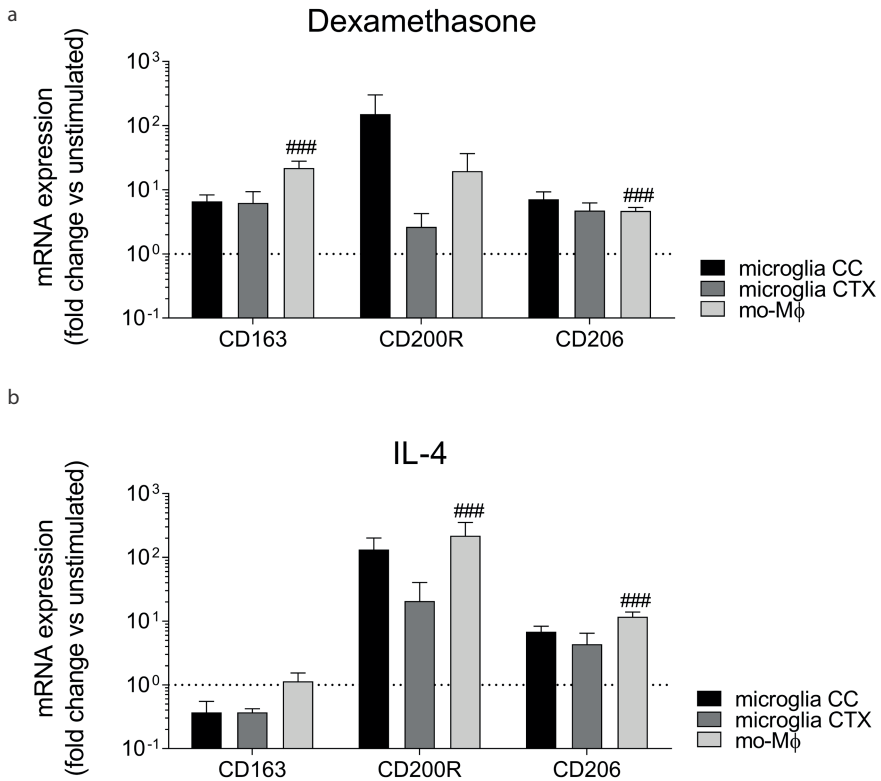

Figure 4: Response to the anti-inflammatory stimuli dexamethasone and IL-4.
Primary microglia CC (N=4), primary microglia CTX (N=5)) mo-MΦ (N=11) were stimulated with anti-inflammatory compounds for 72 hours. (a) mRNA expression of CD163, CD200R and CD206 after dexamethasone stimulation. (b) mRNA expression of CD163, CD200R and CD206 after IL-4 stimulation. Gene expression was determined by qPCR with a single run for each reaction. Normalized fold changes were calculated by dividing the relative mRNA expression, determined with the ΔΔCT by using GAPDH as reference gene, by the relative expression of the unstimulated control. Dotted line represents mRNA levels of unstimulated cells. Significantly different from unstimulated cells: $^{\#}p<0.05$; $^{\#\#}p<0.01$; $^{\#\#\#}p<0.001$.

Discussion

In this study, we applied a procedure for rapid isolation of highly enriched human microglia from post-mortem human brain for a comparative study with common myeloid cell subsets. Primary human microglia from corpus callosum and frontal cortex displayed clearly enriched expression of the classical microglia marker CX3CR1 and a panel of recently proposed microglia markers, of which P2Ry12 was the most

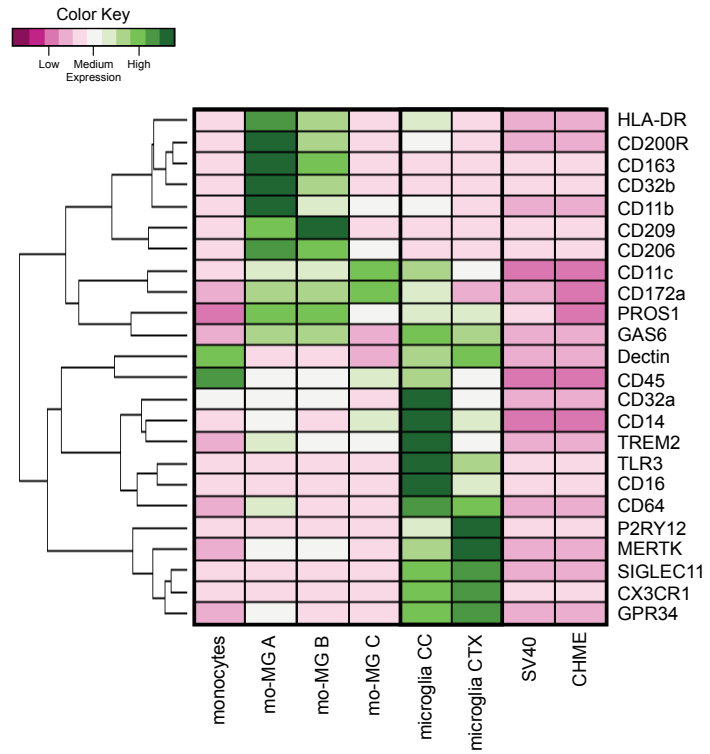

Figure 5: Expression of microglia and myeloid cell markers in microglia cell models.
mRNA expression of a panel of microglia markers and genes involved in myeloid cell biology was determined by qPCR in monocytes (N=6); monocyte-derived microglia models: mo-MG A (N=2); mo-MG B (N=2); mo-MG C (N=2); microglia CC (N=6); microglia CTX (N=7); and the microglia cell lines SV40 (N=1) and CHME (N=1). mRNA values were calculated with the ΔΔCT by using 18S and GAPDH as reference genes, scaled and clustered according to their expression level.

prominent one. Expression of a panel of genes relevant to myeloid cell biology partly differed between microglia isolated from CC and CTX and was clearly distinct from other myeloid subsets. As shown before, microglia responded to both pro- (LPS or poly I:C) and anti-inflammatory (IL-4 or dexamethasone) stimulation *ex vivo*. Our data are in line with previous reports on primary human microglia, where LPS responsiveness was also observed after 18 to 24 hour in culture, but not when stimulated immediately after isolation[15]. Interestingly, microglia differed from monocytes, mo-MΦ and mo-DC in either the strength or type of response to LPS and poly I:C. Finally, we defined a clear phenotypic discrepancy between primary human microglia and currently used microglial cell lines.

Our results show that all commonly used microglia markers are expressed on microglia *ex vivo*, but that only CX3CR1 was expressed at higher levels than other myeloid cells. CX3CR1 is a membrane-bound molecule that is strongly involved in limiting neurotoxicity and plays an important role in neurogenesis and synaptic pruning[24,25]. Moreover, CX3CR1 signaling is implicated in pathogenesis and progression of various neurological disorders[26]. It is important to note that CX3CR1 expression rapidly decreases when primary microglia are cultured (data not shown). A recent paper described specific expression of a subset of genes (PROS1, GAS6, MERTK, GPR34 and P2Ry12) in murine and human microglia[8]. The authors used microglia isolated from fetal human brain tissue as well as brain tissue of adult patients undergoing surgery. In this study, we established the enriched expression of these markers on human microglia isolated from post-mortem tissue compared to primary monocytes, mo-MΦ and mo-DC, the latter two being well-established culture models that recapitulate key features of their in vivo counterparts[27,28], Thus, the enriched expression of proteins on microglia in this study may very well serve as suitable markers to distinguish them from other myeloid cell types. However, it remains unclear whether the differential expression of these markers is preserved under inflammatory and pathological conditions, especially since the other myeloid subsets still express these proteins at low levels. To separate microglia from monocyte-derived macrophages, expression levels of CD45 are often used. Microglia are typically described as $CD11b^{+}CD45^{dim}$, whereas monocyte and macrophages as $CD11b^{+}CD45^{high}$ [29]. In our study we did not find a clear distinction of CD45 expression between microglia, monocytes and mo-MΦ. This is in contrast with original reports that described microglia as $CD11b^{+}CD45^{dim}$ under non-inflammatory conditions, but supported by more recently published data[15,29].

A panel of genes involved in myeloid cell biology was used to further profile the microglia cells. For some of the genes we also determined protein expression levels using flow cytometry. Part of the differences in mRNA expression between microglia and the other myeloid cell subtypes were also detected at the protein level. However, other markers, such as CD11b, CD14, CD40 and HLA-DR, showed a different protein expression profile when comparing the various cell subsets. This is not surprising, since protein expression is a result of several steps in the synthesis and degradation of the proteins, with multiple post-transcriptional mechanisms influencing final protein levels[30]. Because the expression of mRNA is just one of the steps, this does therefore not automatically reflect protein expression. Other reasons, which are related to the isolation procedure and subsequent experiments, may also explain the observed differences. For example, lower mRNA than protein expression, such as seen for CD14 and CD40, might be a result of the quick upregulation of genes during or directly after

the isolation procedure[15,31]. The low expression of CD11b protein may be explained by the fact that we used CD11b-antibody coupled beads to isolate microglia, which might have hindered the binding of the CD11b antibody that is used for staining the cells for flow cytometry. The high expression of HLA-DR protein compared to the other subsets in three out of four donors was surprising, since in *in situ* studies, HLA-DR is often considered to be a marker of 'activated' microglia and to be low or absent on resting microglia[32]. Our results could imply that the microglia were activated, because of *in situ* events in the brain post-mortem or during the isolation procedure. However, additional increased expression of HLA-DR mRNA would be expected, but this was not the case.

Responsiveness to inflammatory stimuli is a key feature of myeloid cells, including microglia, and aberrant inflammatory responsiveness of microglia is hypothesized to be involved in the pathogenesis of neurodegenerative disorders[12–14]. Important insights might therefore be gained from detailed studies of microglia treated with pro- and anti-inflammatory stimuli immediately *ex vivo*. The response of microglia to the key pro-inflammatory stimulus LPS varied between donors, but was overall significantly weaker than in monocytes, mo-MΦ and mo-DC. Earlier findings even showed unresponsiveness of primary human microglia to LPS, but this was immediately after isolation and not after one day in culture as was the case in our study[15]. Low responsiveness to LPS could be due to absent or marginal expression of the receptors for LPS, toll-like receptor (TLR) 4 and CD14, or to differences in downstream signaling pathways[33,34]. Indeed, at the protein level CD14 is expressed at higher levels on mo-MΦ than on microglia, while the CD14 mRNA expression was similar to mo-MΦ. Since CD14 is known to be rapidly upregulated, increased mRNA levels could be an early sign of activation of the cells during isolation[35]. Unexpectedly, mRNA levels of TLR4 were higher on microglia than on mo-MΦ. TLR4 expression levels are therefore unlikely to explain the lower response of microglia to LPS as compared to mo-MΦ. To further study pro-inflammatory responsiveness, we also stimulated microglia with poly I:C, a synthetic analogue of double-stranded RNA, which is present in some viruses. The induction of pro-inflammatory cytokines in microglia in response to poly I:C was stronger than in monocytes, mo-MΦ and mo-DC. Similar to TLR4, expression of TLR3 was higher in microglia than other myeloid cells, which may be a reason for the higher response to poly I:C.

While mouse studies indicate brain region-dependent phenotypical differences in microglia, for example in expression of CD40, CD80 and CD86, this is less studied in humans[36,37]. When comparing CC and CTX microglia, we found similar expression profiles for various genes, but clear differences in other markers. For example, CC

microglia showed enhanced mRNA expression of genes involved in pathogen binding, antigen presentation and ATP signaling. This is in line with the findings that white matter microglia display a more activated phenotype under physiological conditions[38]. Stimulation with pro-inflammatory compounds induced a similar gene expression profile in gray and white matter microglia. Interestingly, CC microglia had an enhanced response to poly I:C. The mRNA expression of TLR3 was higher on CC microglia and may therefore explain these distinct responses. These differences in responsiveness to pro-inflammatory stimuli in combination with the differences in expression of several markers strengthens the idea that microglia are not a uniform population in the brain and may vary between gray and white matter.

Monocyte-derived microglia and microglial cell lines are often used as an alternative to study human microglia. These models are thought to resemble primary microglia as they express Iba1, respond to inflammatory cytokines, and mediate phagocytosis. It is important to realize that these microglia models have never been directly compared to primary human microglia in order to validate their microglial phenotype. Unexpectedly, we found an aberrant mRNA expression profile for primary human microglia in comparison with two human microglia cell models, and to a lesser extent with the three types of monocyte-derived microglia. Earlier described microglia specific genes, which are confirmed in our study in Fig. 1, were expressed relatively low or not at all in the microglia cell lines. Especially the cell lines SV40 and CHME, which are widely used to study microglia biology *in vitro,* showed large differences in the expression of the genes tested in this study. Similar results were shown for murine microglia cell lines[8]. These studies raise questions about the validity to use these models and supports validation studies using primary microglia cells.

Here, we indicate the importance of using primary human microglia to characterize their immediate *ex vivo* phenotype and functionality for comparison with other myeloid cell subsets. Unfortunately, the study is hindered by the small sample size and the fact that we could not use microglia from both selected brain regions for all experiments. This is due to the relatively limited availability of fresh post-mortem brain tissue and the fact that the numbers of viable primary cells isolated per gram tissue is restricted. We have chosen to test for statistical differences in the experiments using standard statistics guidelines. However, the use of several cell populations, relatively small sample sizes, non-parametric tests and correction for multiple testing may lead to an underestimation of true biological differences when only evaluating the statistically different results. In addition, it is important to keep in mind that the microglia cells are likely to be activated to a certain extent during the isolation procedure[39,40] and that the phenotype determined *ex vivo* may therefore not fully reflect the microglia phenotype *in situ*. Studies using laser dissection isolation of RNA from microglia *in situ*, which have their own difficulties and weaknesses, could add important information on the phenotype of microglia *in situ* and how this may differ from isolated microglia.

In summary, the present study provides an overview of a panel of key phenotypical and functional characteristics of isolated primary human microglia from post-mortem brain tissue. It highlights unique features of microglia in comparison with other myeloid cells and differences between brain regions. This description of the specific phenotypic and functional features of human microglia may serve as a suitable reference for future studies on the role of microglia in health and disease. In addition, this study reveals large phenotypical differences between primary microglia and microglial cell models, emphasizing the importance of studying microglia directly isolated from the brain.

Acknowledgements

This project is partly supported by a 2014 NARSAD Young Investigator Grant from the Brain & Behavior Research Foundation. The study was further financially supported by the Virgo Consortium, funded by the Dutch government project number FES0908. The authors thank the team of the Netherlands Brain Bank for their excellent services (www.hersenbank.nl), E. van Bodegraven from the Utrecht University for support with the cluster analysis, Prof. S. Bahn from the University of Cambridge for sharing the SV40 cell line and Dr. J. Hamann for providing valuable advice.

References

1. Tambuyzer, B. R., Ponsaerts, P. & Nouwen, E. J. Microglia: gatekeepers of central nervous system immunology. *J. Leukoc. Biol.* **85,** 352–370 (2009).
2. Kettenmann, H., Hanisch, U.-K., Noda, M. & Verkhratsky, A. Physiology of microglia. *Physiol. Rev.* **91,** 461–553 (2011).
3. Kettenmann, H., Kirchhoff, F. & Verkhratsky, A. Microglia: New Roles for the Synaptic Stripper. *Neuron* **77,** 10–18 (2013).
4. Ginhoux, F. *et al.* Fate mapping analysis reveals that adult microglia derive from primitive macrophages. *Science* **330,** 841–845 (2010).
5. Gomez Perdiguero, E. *et al.* Tissue-resident macrophages originate from yolk-sac-derived erythro-myeloid progenitors. *Nature* **518,** 547–551 (2014).
6. Kierdorf, K. *et al.* Microglia emerge from erythromyeloid precursors via Pu.1- and Irf8-dependent pathways. *Nat. Neurosci.* **16,** 273–80 (2013).
7. Schulz, C. *et al.* A Lineage of Myeloid Cells Independent of Myb and Hematopoietic Stem Cells. *Science (80-.).* **336,** 86–90 (2012).
8. Butovsky, O. *et al.* Identification of a unique TGF-β-dependent molecular and functional signature in microglia. *Nat. Neurosci.* **17,** 131–43 (2014).
9. Gautier, E. L. *et al.* Gene-expression profiles and transcriptional regulatory pathways that underlie the identity and diversity of mouse tissue macrophages. *Nat. Immunol.* **13,** 1118–28 (2012).
10. Hickman, S. *et al.* The microglial sensome revealed by direct RNA sequencing. *Nat. Neurosci.* **16,** 1896–905 (2013).
11. Peterson, P. K., Hu, S., Anderson, W. R. & Chao, C. C. Nitric oxide production and neurotoxicity mediated by activated microglia from human versus mouse brain. *J. Infect. Dis.* **170,** 457–60 (1994).
12. Heneka, M. *et al.* Neuroinflammation in Alzheimer's disease. *Lancet Neurol.* **14,** 388–405 (2015).
13. Radewicz, K., Garey, L. J., Gentleman, S. M. & Reynolds, R. Increase in HLA-DR immunoreactive microglia in frontal and temporal cortex of chronic schizophrenics. *J. Neuropathol. Exp. Neurol.* **59,** 137–50 (2000).
14. Steiner, J. *et al.* Distribution of HLA-DR-positive microglia in schizophrenia reflects impaired cerebral lateralization. *Acta Neuropathol.* **112,** 305–316 (2006).
15. Melief, J. *et al.* Phenotyping primary human microglia: Tight regulation of LPS responsiveness. *Glia* **60,** 1506–1517 (2012).
16. Olah, M. *et al.* An optimized protocol for the acute isolation of human microglia from autopsy brain samples. *Glia* **60,** 96–111 (2012).
17. de Haas, A. H., Boddeke, H. W. G. M., Brouwer, N. & Biber, K. Optimized isolation enables ex vivo analysis of microglia from various central nervous system regions. *Glia* **55,** 1374–84 (2007).
18. Leone, C. *et al.* Characterization of human monocyte-derived microglia-like cells. *Glia* **54,** 183–192 (2006).
19. Etemad, S., Zamin, R., Ruitenberg, M. & Filgueira, L. A novel in vitro human microglia model: Characterization of human monocyte-derived microglia. *J. Neurosci. Methods* **209,** 79–89 (2012).
20. Ohgidani, M. *et al.* Direct induction of ramified microglia-like cells from human monocytes: Dynamic microglial dysfunction in Nasu-Hakola disease. *Sci. Rep.* **4,** 4957 (2014).
21. Janabi, N., Peudenier, S., Héron, B., Ng, K. H. & Tardieu, M. Establishment of human microglial cell lines after transfection of primary cultures of embryonic microglial cells with the SV40 large T antigen. *Neurosci. Lett.* **195,** 105–108 (1995).
22. Ambarus, C. A. *et al.* Systematic validation of specific phenotypic markers for in vitro polarized human macrophages. *J. Immunol. Methods* **375,** 196–206 (2012).
23. Mosser, D. M. & Edwards, J. P. Exploring the full spectrum of macrophage activation. *Nat. Rev. Immunol.* **8,** 958–69 (2008).
24. Cardona, A. E. *et al.* Control of microglial neurotoxicity by the fractalkine receptor. *Nat. Neurosci.* **9,** 917–924 (2006).
25. Rogers, J. T. J. T. *et al.* CX3CR1 deficiency leads to impairment of hippocampal cognitive function and synaptic plasticity. *J. Neurosci.* **31,** 16241–50 (2011).
26. Fuhrmann, M. *et al.* Microglial Cx3cr1 knockout prevents neuron loss in a mouse model of Alzheimer's disease. *Nat. Neurosci.* **13,** 411–3 (2010).
27. Eligini, S. *et al.* Human monocyte-derived macrophages are heterogenous: Proteomic profile of different phenotypes. *J. Proteomics* **124,** 112–23 (2015).
28. Sallusto, F. & Lanzavecchia, A. Efficient presentation of soluble antigen by cultured human dendritic cells is maintained by granulocyte/macrophage colony-stimulating factor plus interleukin 4 and downregulated by tumor necrosis factor alpha. *J. Exp. Med.* **179,** 1109–18 (1994).
29. Dick, A. D., Pell, M., Brew, B. J., Foulcher, E. & Sedgwick, J. D. Direct ex vivo flow cytometric analysis of human microglial cell CD4 expression: examination of central nervous system biopsy specimens from HIV-seropositive patients and patients with other neurological disease. *AIDS* **11,** 1699–708 (1997).
30. Maier, T., Güell, M. & Serrano, L. Correlation of mRNA and protein in complex biological samples. *FEBS letters* **583,** 3966–73 (2009).
31. Vogel, C. *et al.* Sequence signatures and mRNA concentration can explain two-thirds of protein abundance variation in a human cell line. *Mol. Syst. Biol.* **6,** 400 (2010).
32. Mattiace, L. a, Davies, P. & Dickson, D. W. Detection of HLA-DR on microglia in the human brain is a function of both clinical and technical factors. *Am. J. Pathol.* **136,** 1101–1114 (1990).
33. Becher, B. & Antel, J. P. Comparison of phenotypic and functional properties of immediately ex vivo and cultured human adult microglia. *Glia* **18,** 1–10 (1996).
34. Becher, B., Fedorowicz, V. & Antel, J. P. Regulation of CD14 expression on human adult central nervous system-derived microglia. *J. Neurosci. Res.* **45,** 375–81 (1996).
35. Landmann, R. *et al.* Human monocyte CD14 is upregulated by lipopolysaccharide. *Infect. Immun.* **64,** 1762–9 (1996).
36. Lawson, L. J., Perry, V. H., Dri, P. & Gordon, S. Heterogeneity in the distribution and morphology of microglia in the normal adult mouse brain. *Neuroscience* **39,** 151–70 (1990).
37. Mittelbronn, M., Dietz, K., Schluesener, H. J. & Meyermann, R. Local distribution of microglia in the normal adult human central nervous system differs by up to one order of magnitude. *Acta Neuropathol.* **101,** 249–255 (2001).
38. Carson, M. *et al.* A rose by any other name? The potential consequences of microglial heterogeneity during CNS health and disease. *Neurotherapeutics* **4,** 571–9 (2007).
39. de Groot, C. J., Hulshof, S., Hoozemans, J. J. & Veerhuis, R. Establishment of microglial cell cultures derived from postmortem human adult brain tissue: immunophenotypical and functional characterization. *Microsc. Res. Tech.* **54,** 34–39 (2001).
40. Schuenke, K. & Gelman, B. Human microglial cell isolation from adult autopsy brain: brain pH, regional variation, and infection with human immunodeficiency virus type 1. *J. Neurovirol.* **9,** 346–357 (2003).

Supplementary table 1: Clinicopathological information of Donors Included in the Study

NBB no.	Sex	Diagnosis	Age	PMD	pH	Death cause	Used for	PI	HAL	GC
012-101	M	CON	80	04:25	6.59	Patient requested euthanasia* (due to cholangiocarcinoma)	1	no	no	no
2012-104	M	CON	79	06:30	6.71	Patient requested euthanasia* (due to terminal heart failure)	1	no	no	no
2013-010	F	CON	89	06:35	6.73	Heart failure and dehydration	1,2	no	yes	no
2013-011	F	CON	92	04:25	6.65	Patient requested euthanasia* (due general deterioration)	1,2	no	no	no
2013-016	M	CON	83	05:15	6.60	Myocardial infarction and palliative sedation	1,2	no	no	no
2013-022	F	CON	92	04:40	6.70	Palliative sedation and respiratory failure	1,2	no	no	no
2013-056	M	CON	95	07:15	6.56	Heart failure	1,2,3	no	no	no
2013-077	M	PD	86	04:10	6.91	Patient requested euthanasia*	3	no	no	no
2014-029	F	CON	78	07:10	6.32	Patient requested euthanasia* (with multiple myeloma)	1,3	no	no	no
2014-046	F	CON	85	08:00	6.28	Cachexia and dehydration	1,3	no	yes	no
2014-048	F	CON	111	08:40	5.96	Old age	1,3	no	no	no
2014-051	M	CON	92	07:45	6.55	Liver cirrhosis ascites and anuria	3	no	no	no
2014-055	M	CON	84	03:30	6.35	Cachexia	3	no	no	no
2014-069	M	OTHER	73	04:25	7.00	Pneumonia	1,3	yes	yes	no
2015-074	F	CON	89	13:00	6.39	Suicide	3	n/a	n/a	n/a
2015-087	F	CON	75	09:10	6.57	Patient requested euthanasia*	1,3	n/a	n/a	n/a
2015-089	F	CON	92	07:45	6.71	Suicide	1,3	n/a	n/a	n/a

CON = Neurologic and psychiatric control; PD = Parkinson's disease); PI = peripheral inflammation at time of death; HAL = Haloperidol used last 3 days; GC = Glucocorticoids use 3 months prior to death; 1 = Phenotyping by qPCR; 2= Phenotyping by flow cytometry; 3=*In vitro* stimulation. *euthanasia is legal according to Dutch law.

Supplementary table 2: Primer Sequence qPCR Analysis

Primer	Forward sequence	Reverse sequence
18S	TAGTCGCCGTGCCTACCAT	CCTGCTGCCTTCCTTGGA
CB1	TCGTTCTAGCGGACAACCAGCC	TCCAAACGCAACTCTGCCAGGTC
CB2	AGCCCTCATACCTGTTCATTGG	GTGAAGGTCATAGTCACGCTG
CD11b	TGCTTCCTGTTTGGATCCAACCTA	AGAAGGCAATGTCACTATCCTCTTGA
CD11c	GCTCCCGGTGAAGTATGCTG	CCACATGGCTTTCCTTCTCCT
CD14	ACAGGGCGTTCTTGGCTCGC	CGGGAAGGCGCGAACCTGTT
CD16	GACAGCGGCTCCTACTTCT	ATGGTTGACACTGCCAAACCT
CD32a	GTGGTCATTGCGACTGCTGTA	AGCCTTCACAGGATCAGTGGAA
CD32b	CCACTAATCCTGATGAGGCTGACA	TCATCAGGCTCTTCCAGAGCAT
CD40	ACTGAAACGGAATGCCTTCCT	CCTCACTCGTACAGTGCCA
CD45	GCAGCTAGCAAGTGGTTTGTTC	AAACAGCATGCGTCCTTTCTC
CD64	AGGTGTCATGCGTGGAAGGATAA	TGGTGAGGTTAGAATTCCAGTGGAA
CD80	TGCTGGCTGGTCTTTCTCAC	TGCCAGTAGATGCGAGTTTGT
CD86	CTGCTCATCTATACACGGTTACC	GGAAACGTCGTACAGTTCTGTG
CD93	TGCCTGGACCCTAGTCTGC	GCTTGGAGATGCACGAGTTC
CD163	TTTGTCAACTTGAGTCCCTTCAC	TCCCGCTACACTTGTTTTCAC
CD172a	GGCCTCAACCGTTACAGAGAA	GTTCCGTTCATTAGATCCAGTGT
CD200R1	GAGCAATGGCACAGTGACTGTT	GTGGCAGGTCACGGTAGACA
CD206	TGCAGAAGCAAACCAAACCTGTAA	CAGGCCTTAAGCCAACGAAACT
CD209	GATTCCGACAGACTCGAGGA	CCTGACTTATGGAGCTGGGG
CD274	CCTACTGGCATTTGCTGAACG	TCCAGATGACTTCGGCCTTG
CHRNA4	ATGGAACAGGTGGGCCTT	GAGAATGTCACCTCCATCCG
CX3CR1	TTGGCCTGGTGGGAAATTTGT	AGGAGGTAAATGTCGGTGACACT
Dectin	GGAAGCAACACATTGGAGAATGG	CTTTGGTAGGAGTCACACTGTC
DRD2	CAACGGGTCAGACGGGAAG	GAATTTCCACTCACCTACCACC
GAPDH	TGCACCACCAACTGCTTAGC	GGCATGGACTGTGGTCATGA
HLA-DRA	CCCAGGGAAGACCACCTTT	CACCCTGCAGTCGTAAACGT
P2X7	TCTTCCGAGAAACAGGCGAT	CCAACGGTCTAGGTTGCAGT
TLR3	CAAACACAAGCATTCGGAATCTG	AAGGAATCGTTACCAACCACATT
TLR4	AGTTGATCTACCAAGCCTTGAGT	GCTGGTTGTCCCAAAATCACTTT

Supplementary table 3: Geomean and STD of Normalized mRNA Expression

	Microglia CC (N=6)		Microglia CTX (N=7)		Monocytes (N=6)		mo-MΦ (N=3)		mo-DC (N=3)	
Gene	**Geomean**	**STD**	**Geomean**	**STD**	**Geomean**	**STD**	**Geomean**	**STD**	**Geomean**	**STD**
CD206	12.18	32.82	13.96	6.837	0.139	0.067	36.75	16.63	214.6	24.46
CD163	111.1	649.1	8.511	10.37	18.88	18.40	60.23	14.39	8.709	6.211
CD11c	147.5	378.1	79.93	35.27	41.69	13.95	359.1	66.94	74.00	15.41
CD209	0.127	0.309	0.013	0.014	0.014	0.022	0.954	0.304	12.82	1.826
CD16	349.6	621.7	127.2	34.49	16.72	12.91	27.30	3.578	9.500	8.878
CD32a	247.1	499.0	58.65	16.05	45.77	30.30	14.53	3.664	33.12	31.76
CD32b	5.853	9.941	0.153	0.187	0.453	0.650	1.751	0.286	4.412	5.265
CD64	160.3	322.1	132.7	19.82	9.627	9.133	10.77	1.325	0.028	0.014
CX3CR1	151.9	549.0	198.5	73.44	2.619	4.207	0.000	0.002	0.003	0.013
CD200R1	0.434	5.534	0.083	0.148	0.305	0.483	0.379	0.133	33.39	4.077
TLR3	20.12	37.88	12.64	4.499	0.024	0.045	0.237	0.004	0.339	0.071
TLR4	24.25	49.84	36.83	16.62	16.89	2.960	13.72	2.760	14.83	4.473
P2X7	41.47	259.0	0.002	9.150	0.339	3.295	0.000	0.000	0.000	0.000
DRD2	0.052	0.377	0.002	0.019	0.001	0.023	0.003	0.007	0.000	0.000
CHRNA4	0.004	0.029	0.000	0.000	0.001	0.001	0.000	0.000	0.028	0.018
CD80	0.777	0.968	0.622	0.315	0.085	0.117	0.865	0.130	6.827	2.324
CD86	85.81	74.89	31.89	21.04	25.14	27.51	19.10	4.075	26.17	6.975
CD40	7.991	14.34	5.692	1.532	0.493	0.295	4.713	1.413	11.07	3.410
CD274	0.933	1.286	0.496	0.427	0.009	0.007	0.250	0.320	3.733	0.164
CD172a	90.77	147.0	22.94	14.94	18.87	17.03	49.83	10.08	56.74	32.65
CB1	0.374	3.878	0.112	0.109	0.009	0.010	0.138	0.131	0.028	0.349
CB2	0.315	3.984	0.107	0.052	0.008	0.031	0.001	0.028	0.110	0.145
CD93	2.662	4.425	1.831	0.729	6.506	3.505	0.516	0.118	2.301	0.548
SIGLEC11	7.982	23.06	10.28	3.243	0.556	0.637	3.680	1.297	0.028	0.003

Geomean = geometric mean; STD = standard deviation

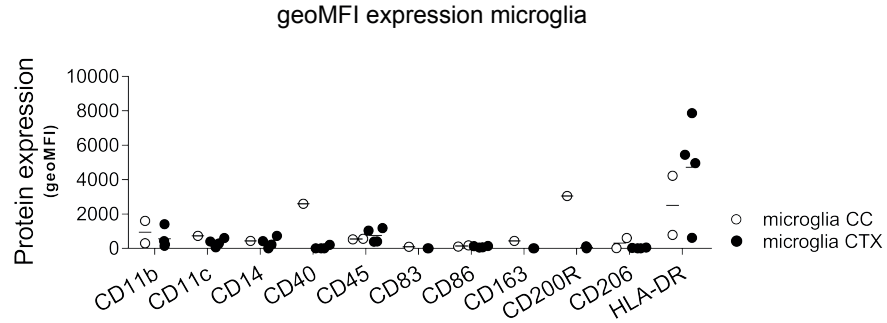

Supplementary figure 1: geoMFI expression of CC and CTX microglia.
Protein expression in primary CC (N=2) and CTX microglia (N=4) as determined by flow cytometry. The relative geometric mean fluorescence intensity (geoMFI) was calculate by subtracting the geoMFI of the corresponding isotype.

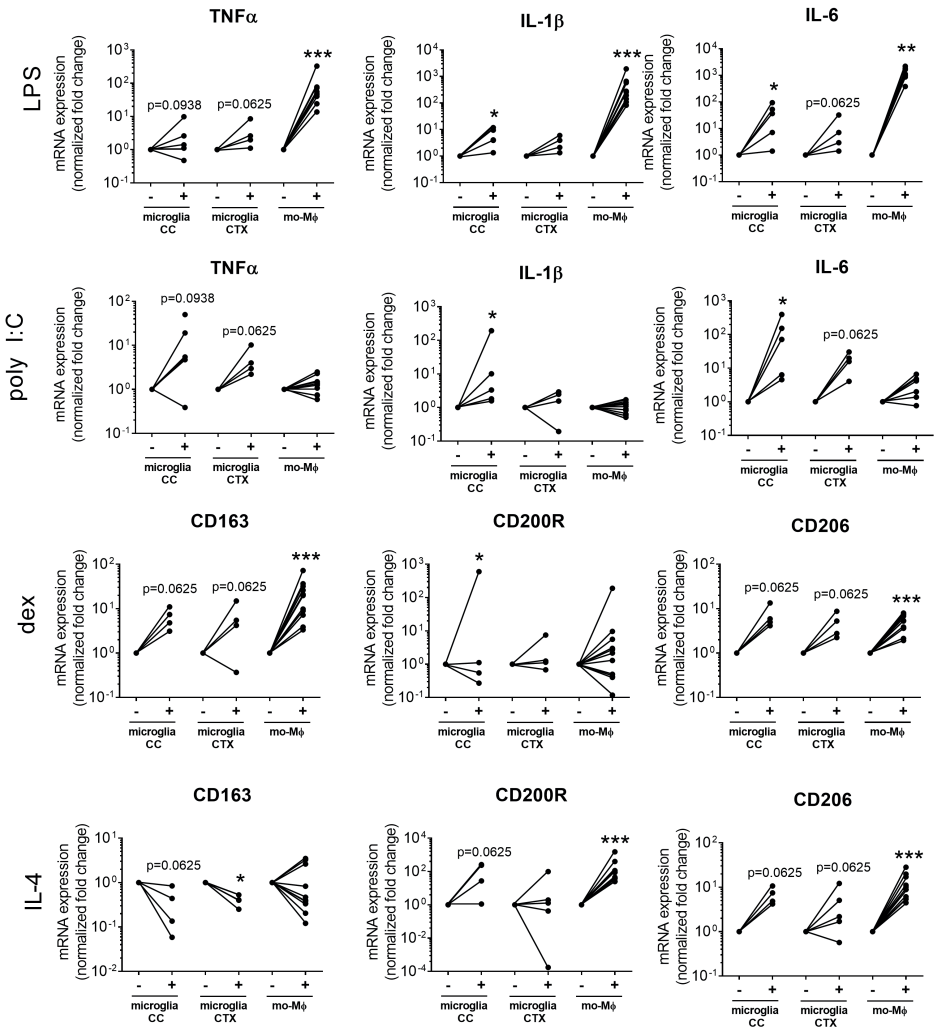

Supplementary figure 2: Individual fold change of mRNA expression levels of primary isolated microglia, monocytes, mo-MΦ and mo-DC without (-) and with (+) pro- and anti-inflammatory stimuli.

Pro-inflammatory stimuli: microglia CC (N=5), microglia CTX (N=4), monocytes (N=3), mo-MΦ (N=10) and mo-DC (N=4); anti-inflammatory stimuli: microglia CC (N=4), microglia CTX (N=5) and mo-MΦ (N=11). IL-6 mRNA levels of monocytes were not detectable (ND). Normalized fold changes were calculated by dividing the relative mRNA expression, determined with the ΔΔCT and normalization to the expression of GAPDH, by the relative expression of the unstimulated control. *p<0.05; **p<0.01; ***p<0.001.

Chapter 3

Human microglia regional heterogeneity and phenotypes determined by multiplexed single-cell mass cytometry

Chotima Böttcher[1*], Stephan Schlickeiser[2*], Marjolein A M Sneeboer[3*], Desiree Kunkel[2], Anniki Knop[1], Evdokia Paza[1], Pawel Fidzinski[5], Larissa Kraus[5,6], Gijsje J L Snijders[3], René S Kahn[4], Axel R Schulz[7], Henrik E Mei[7], NBB-Psy[8], Elly M Hol[3,9], Britta Siegmund[10], Rainer Glauben[10], Eike J Spruth[1,11], Lot D de Witte[3,4#], Josef Priller[1,6,11,12,13#]

* These authors jointly directed this work

# These authors contributed equally to this work.

[1]Department of Neuropsychiatry and Laboratory of Molecular Psychiatry, Charité – Universitätsmedizin Berlin, Berlin, Germany. [2]Berlin-Brandenburg Center for Regenerative Therapies (BCRT), Berlin, Germany. [3]Department of Psychiatry, Brain Center Rudolf Magnus, University Medical Center Utrecht (BCRM-UMCU), Utrecht, The Netherlands. [4]Department of Psychiatry, Icahn School of Medicine at Mount Sinai, New York, USA. [5]Epilepsy-Center Berlin-Brandenburg, Department of Neurology, Charité – Universitätsmedizin Berlin, Berlin, Germany. [6] Berlin Institute of Health, Berlin, Germany. [7]German Rheumatism Research Center (DRFZ), Berlin, Germany. [8]https://www.brainbank.nl/about-us/nbb-psy/. [9]Departement of Neuroimmunology, The Netherlands Institute for Neuroscience, An Institute of the Royal Academy of Arts and Sciences, Amsterdam, The Netherlands. [10]Medical Department for Gastroenterology, Division of Gastroenterology, Infectiology and Rheumatology, Charité – Universitätsmedizin Berlin, Berlin, Germany. [11]DZNE and [12]Cluster of Excellence NeuroCure , Berlin, Germany. [13]University of Edinburgh and UK Dementia Research Institute, Edinburgh, UK.

Accepted in *Nat. Neurosci.* **22**, 78–90 (2019)

Abstract

Microglia, the specialized innate immune cells of the CNS, play crucial roles in neural development and function. Different phenotypes and functions have been ascribed to rodent microglia, but little is known about human microglia (huMG) heterogeneity. Difficulties in procuring huMG and their susceptibility to cryopreservation damage have limited large-scale studies. Here, we applied multiplexed mass cytometry for a comprehensive characterization of post-mortem huMG (10^3 – 10^4 cells). We determined expression levels of 57 markers on huMG isolated from up to five different brain regions of nine donors. We identified core signature of huMG, which was distinct from peripheral myeloid cells but was comparable to fresh huMG. We detected microglia regional heterogeneity using a hybrid workflow combining Cytobank and R/Bioconductor for multidimensional data analysis. Together, these methodologies permit for the first time to perform high-dimensional, large-scale immunophenotyping of huMG at the single-cell level, which facilitate their unambiguous profiling in health and disease.

Introduction

Microglia are resident innate immune cells of the CNS, and have an important role in maintaining CNS integrity and function[1]. They are involved in removing apoptotic neurons, refining synaptic connectivity, and providing trophic support for memory and motor learning[2,3]. In addition, microglia play a role in the development and progression of neurological and psychiatric disorders, including Alzheimer's disease (AD), amyotrophic lateral sclerosis, schizophrenic psychoses and mood disorders[4-7]. Thus, the identification of mechanisms that regulate microglial homeostasis and function may provide the means to manipulate these cells for therapeutic purposes. Over the last two decades, microglial ontogeny, phenotypic heterogeneity and responses to CNS pathology have been extensively studied in rodents[8-15]. However, much less is known about human microglia (huMG). Comparative studies of the transcriptional network revealed overall similarity in the transcriptomic landscapes of human and mouse microglia[16,17]. Nonetheless, these studies also demonstrated species-specific patterns of gene expression, and differences in the responses of human and murine microglia to ageing[16,17]. The heterogeneity of microglia that has been described for the mouse brain[7,14] has so far not been replicated in humans. It is also unclear how human and mouse microglia compare on a phenotypic level.

To date, the phenotypic characterization of huMG has mainly relied on immunohistochemical analysis of post-mortem brain tissue, fluorescence-flow cytometric analysis of isolated microglial cells or *in vitro* cultures of huMG[18-21]. Among the limitations of these approaches are the phenotypic changes induced by cell culture[16,19], the high autofluorescent background of post-mortem tissue and the restrictions in the number of markers that can be simultaneously investigated in one measurement (commonly less than 20). In addition, due to the lack of a validated protocol for cryopreservation, flow cytometric analysis of huMG has been restricted to immediate measurements of acutely isolated cells, which can result in batch effects and contribute to erroneous interpretations of data.

In this study, we developed a novel method to deep profile the immune phenotype of small samples of huMG at the single-cell level. The protocol allows for simultaneous measurement of multiple samples from different donors and brain regions, and at the same time for comparison with cells from other compartments (e.g. cerebrospinal fluid (CSF) and peripheral blood). We isolated huMG from different regions of post-mortem brain tissues and from fresh brain biopsies following an established protocol. Peripheral immune cells were freshly isolated from blood and CSF. The isolated cells (both huMG and peripheral immune cells) were fixed and stored using a novel protocol

for long-term cryopreservation. Subsequently, cryopreserved huMG and peripheral immune cells were simultaneously profiled by multiplexed mass cytometry (CyTOF) using barcoding technology. These powerful methodologies allowed for accurate and unbiased analysis of an unprecedented number of markers at the single-cell level. Our results reveal a unique phenotypic signature of huMG that distinguishes them from other mononuclear cells in the CSF and peripheral blood. Using a hybrid Cytobank- and R/Bioconductor-based data processing and analysis workflow, we provide evidence for the heterogeneity of microglia in the human brain.

Methods

Human blood and CSF samples

Venous blood and lumbar cerebrospinal fluid (CSF) samples were obtained from four individuals (Supplementary Table 1). The study was registered and approved by the Ethics Commission of Charité–Universitätsmedizin Berlin (Ethikkommission der Charité–Universitätsmedizin Berlin; registration number EA1/244/12), Berlin, Germany. All study participants provided informed consent before any study-related procedures were undertaken.

Human brain autopsy

Human brain tissue was obtained through the Netherlands Brain Bank (www.brainbank.nl). The Netherlands Brain Bank received permission to perform autopsies and to use tissue and medical records from the Ethical Committee of the VU University medical center (VUmc, Amsterdam, The Netherlands). All donors have given informed consent for autopsy and use of their brain tissue for research purposes. Generally, the autopsies of five brain regions, which were subventricular zone (SVZ), thalamus (THA), cerebellum (CER), temporal lobe (*Gyrus temporalis superior*, GTS) and frontal lobe (*Gyrus frontalis medius*, GFM), were performed within 10h after death. Brain tissue collected for this study was from the donors whose post-mortem CSF was between pH 6.5 and 7.2. An overview of the donor information and post-mortem variables is summarized in Supplementary Table 1 and 4.

Human brain biopsies

Brain tissue (temporal lobe) was resected for treatment of epilepsy in three patients (Supplementary Table 4) with mesial temporal lobe epilepsy (mTLE). The resected tissue used in this study was in excess of that was needed for pathological diagnosis, and was separated from the epileptic focus with strong epileptogenic activity. Experimental protocol was approved by the Ethics Committee of Charité – Universitätsmedizin Berlin (EA2/111/14) and is in agreement with the Declaration of Helsinki. All Patients gave written consent prior to the surgery. Specimens were collected in the operation room, transported and processed in cold carbogenated NMDG-aCSF (95% O2, 5% CO2) containing (in mM): NMDG (93), KCl (2.5), NaH2PO4 (1.2), NaHCO3 (30), MgSO4 (10), CaCl2 (0.5), HEPES (20), glucose (25), Na-L-ascorbate (5), thiourea (2), Na-pyruvate (3).

Human microglia isolation

Microglia was isolated according to the previously published protocol[19]. Briefly, the isolation was started within 2 to 25 hours after autopsy. Approximately, 2-10 grams tissue was first mechanically dissociated through a metal sieve in a glucose-potassium-sodium buffer (GKN-BSA; 8g/l NaCl, 0.4g/l KCl, 1.77g/l $Na_2HPO_4.2H_2O$, 0.69 g/l $NaH_2PO_4.H_2O$, 2 g/l D-(1)- glucose, 0.3% bovine serum albumin (BSA, Sigma-Aldrich); pH 7.4). For THA (n = 8), CER (n = 5), GTS (n = 18) & GFM (n = 16) tissue mixture, the samples were then supplemented with collagenase Type I (3700 units/ml; Worthington, Lakewood, NJ, USA) and DNase I (200 µg/ml; Roche Diagnostics GmbH) for 1 h at 37°C while shaking. For the SVZ (n = 18) samples, the tissue mixture was subsequently incubated in 2.5% trypsin (Invitrogen) for 20 min at 37°C. Cell suspension (from all brain regions) was put over a 100µM cell strainer and washed with GKN-BSA buffer before the pallet was re-suspended in 20ml GKN-BSA buffer. Next, 10ml of Percoll (Amersham, GE Healthcare) was added dropwise and tissue was centrifuged at 4000 rpm for 30 minutes (4°C). Three different layers appeared: upper layer containing myelin, a lower erythrocyte layer and the middle layer containing all cell types including microglia. The middle layer was carefully taken out without disturbing the myelin layer and washed first with GKN-BSA buffer, followed by magnetic-activated cell sorting (MACS) buffer (PBS, 1% heat-inactivated fetal calf serum (FCS, Gibco Life technologies, Massachusetts), 2mM EDTA). Microglia were positively selected with CD11b conjugated magnetic microbeads (Miltenyi Biotec GmbH) according to manufacturer's protocol, which resulted in a 99% pure microglia population.

MACS-sorted $CD11b^+$ ($0.5 – 1x10^5$) cells were transferred to a 1.5ml low binding Eppendorf (Sigma-Aldrich, the Netherlands) and centrifuged at room temperature (RT) for 5 minutes. Cell pallet was then fixed with fixation/stabilization buffer[22] (SmartTube) and frozen at –80°C until analysis by mass cytometry.

Flow cytometry

Cryopreserved microglia (10 GTS; 9 GFM & 10 SVZ; Supplementary Table 4) were thawed and washed twice in staining buffer (PBS containing 0.5% bovine serum albumin and 2mM EDTA). Then, cells were stained for CD45 (HI30), CD64 (10.1), CD206 (15-2) and HLA-DR (L-243) in the staining buffer. For intracellular staining, the stained (non-stimulated) cells were then incubated in fixation/permeabilization buffer (Fix/Perm Buffer, eBioscience) for 30 min at 4°C. Cells were then wash twice with permeabilization buffer (eBioscience). The samples were then stained with anti-CD68 (Y1/82A) antibody permeabilization buffer for 30 min at 4°C. Cells were subsequently washed once with permeabilization buffer Forward- and side-scatter parameters were used for exclusion of doublets from analysis. Cellular fluorescence was assessed with CantoII (BD FACSDiva Software 6.1.3; BD Biosciences), and data were analyzed with FlowJo software 10.4.2 (TreeStar) and Cytobank.

Barcoding

For live cell barcoding**, i**ndividual CSF samples (0.5 – 1x10^4 cells) were pelleted and stained with ^{89}Y-CD45 (Fluidigm) for 30 min at 4°C. Cells were then washed and pooled with PBMCs from the same individual. After fixation and cryopreservation, sorted microglia and CSF-PBMC-pooled samples were thawed and subsequently stained with premade combinations of six different palladium isotopes: ^{102}Pd, ^{104}Pd, ^{105}Pd, ^{106}Pd, ^{108}Pd & ^{110}Pd (Cell-ID 20-plex Pd Barcoding Kit, Fluidigm). This multiplexing kit applies a 6-choose-3 barcoding scheme that results in 20 different combinations of three Pd isotopes. After 30 min staining (at RT), individual samples were washed twice with cell staining buffer (0.5% bovine serum albumin in PBS, containing 2mM EDTA). Total of up to 20 samples (e.g. 18 microglia & 2 CSF-PBMC pooled samples), were pooled together, washed and further stained with antibodies. In total of two multiplexed samples (36 microglia & 4 CSF-PBMC pooled samples) were analysed for microglial regional heterogeneity. For a comparative characterization, two multiplexed samples of 19 post-mortem-huMG (GTS- and GFM-huMG) and 3 fresh-biopsy-huMG) were analysed.

Antibodies

Anti-human antibodies (Supplementary Table 2 & 3) were purchased either preconjugated to metal isotopes (Fluidigm) or from commercial suppliers in purified form and conjugated in house using the MaxPar X8 kit (Fluidigm) according to the manufacturer's protocol.

Surface and intracellular staining

After cell barcoding, washing and pelleting, the combined samples were re-suspended in 100 µl of antibody cocktail against surface markers (Supplementary Table 2 & 3) and incubated for 30 min at 4°C. Then, cells were washed twice with cell staining buffer. For intracellular staining, the stained (non-stimulated) cells were then incubated in fixation/permeabilization buffer (Fix/Perm Buffer, eBioscience) for 60 min at 4°C. Cells were then wash twice with permeabilization buffer (eBioscience). The samples were then stained with antibody cocktails against intracellular molecules (Supplementary Table 2 & 3) in permeabilization buffer for 1 h at 4°C. Cells were subsequently washed twice with permeabilization buffer and incubated overnight in 2% methanol-free formaldehyde solution (FA). Fixed cells were then washed and re-suspended in 1 ml iridium intercalator solution (Fluidigm) for 1 h at RT. Next, the samples were washed twice with cell staining buffer and then twice with ddH_2O (Fluidigm). Cells were pelleted and kept at 4°C until CyTOF measurement.

CyTOF Measurement

Cells were analysed using a CyTOF2 upgraded to Helios specifications, with software version 6.5.236. The instrument was tuned according to the manufactures instructions with tuning solution (Fluidigm) and measurement of EQ four element calibration beads (Fluidigm) containing 140/142Ce, 151/153Eu, 165Ho, and 175/176Lu served as a quality control for sensitivity and recovery. Directly prior to analysis cells were re-suspended in ddH_2O, filtered (20 µm Celltrix, Sysmex), counted and adjusted to 3–5x10^5 cells/ml. EQ four element calibration beads were added at a final concentration of 1:10 of the sample volume to be able to normalize the data to compensate for signal drift and day-to-day changes in instrument sensitivity.

Samples were acquired with a flow rate of 300-400 events/second. Lower convolution threshold was set to 400, with noise reduction mode on and cell definition parameters set at event duration of 10-150. The resulting flow cytometry standard (FCS) files were normalized and randomized using the CyTOF software's internal FCS-Processing module on the non-randomized ('original') data. Settings were used according to the default settings in the software with time interval normalization (100 seconds/ minimum of 50 beads) and passport version 2. Intervals with less than 50 beads per 100 seconds were excluded from the resulting fcs-file.

Mass cytometry data processing and analysis

Cytobank was used for initial manual gating on live single cells, boolean gating for debarcoding and viSNE to generate t-SNE maps[51-53]. FCS files containing the t-SNE embedding as additional two parameters were exported from Cytobank for

downstream exploratory and statistical analyses using R[54]. The International Society for the Advancement of Cytometry's data standard (Gating-ML 2.0) was used to replicate manual gating within the CytoML/openCyto framework and to update/upload auto-generated gates into Cytobank[55-57]. All FCS files were transformed with Cytobank default arcsinh transformation (scale factor 5). Nucleated single viable cells were manually gated by DNA intercalators ^{191}Ir/^{193}Ir and event length. For debarcoding, Boolean gating was used to deconvolute individual sample according to the barcode combination. For gated circulating cell populations and huMG from different brain regions expression levels of each marker were assessed and visualized in heatmaps. Spearman correlation distance matrices of expression means served as input for Wards agglomerative hierarchical clustering[58]. Microglia immune phenotypes were visualized using two- dimensional t-SNE maps generated from $P2Y_{12}^{+}$ (*Panel A*) or TMEM119^{+} (*Panel B*) pre-gated huMG cells. The following 32 markers of *Panel A* were selected for t-SNE embedding: CCL2, CD115, CD11b, CD11c, CD124, CD16, CD163, CD192, CD195, CD206, CD33, CD37, CD40, CD45, CD56, CD62L, CD64, CD68, CD86, CX3CR1, Cyclin A, Cyclin B1, EMR1, HLA-DR, IL-10, IRF4, IRF8, Ki-67, $P2Y_{12}$, TGF-b, TNF-α, TREM-2; and 35 markers in *Panel B*: Arginase-1, c-kit, CCL2, CD103, CD116, CD11c, CD135, CD172a, CD18, CD192, CD197, CD206, CD274, CD279, CD32, CD33, CD34, CD36, CD37, CD40, CD44, CD54, CD83, CD86, CD91, C/EBPa, CX3CR1, GM-CSF, HLA-DR, IL-10, IL-6, PU.1, TMEM119, TNF-a, TREM-2. All pre-gated events were used without prior downsampling from 36 samples for each panel (218986 *Panel A*, 140550 *Panel B*) for embedding using Cytobank's default hyperparameters (perplexity=30, theta=0.5, and 1000 iterations). We found that results were robust in multiple runs as well as to changes of the input parameters, e.g. increasing perplexity and number of iterations or removal of some of the markers.

Statistical t-SNE maps and automated gating of differentially abundant huMG subsets

As most of the markers exhibited dim or unimodal expression representing in a continuum of different phenotypes in the tSNE maps rather than a number of distinctly segregating clusters of cells, existing methods that rely on clustering techniques[59-61] to first identify a number of subpopulations and then test for e.g. differential abundance could not meaningfully be applied. Therefore, we used a strategy that quantifies and visualizes differences at the level of cellular distribution over t-SNE space[58]. To this end, we generated 2D-histograms of the t-SNE maps using the probability binning algorithm available through the R flowFP package[62-64]. Dependent on the total number of cells available, a single binning model was created on collapsed data from all samples, by recursively splitting the events at the median values along the two t-SNE dimensions. We chose a grid of 512 bins to have on average at least 10 cells per bin in each sample for statistical accuracy. Global differences between samples' cellular density distributions were quantified using the earth mover's distance (EMD), a histogram similarity metric that also takes the relative location of each bin in the t-SNE map into account. EMD scores were computed (using emdist R package) between each pair of 2D-histograms and similarities were visualized by hierarchical clustering in heatmap representation. Regional differences were tested for by permutational analysis of variance using distance matrices[65] as implemented in the function adonis in R package vegan[66] and setting donor as strata to account for inter-subject variability. In order to identify local features, we performed bin-wise statistical testing for differences in cell frequencies between t-SNE maps from different groups, i.e. brain regions[67,68]. We chose the nonparametric Skillings-Mack[69] (SM), a general Friedman-type statistic to account for the non-normality of cell frequency data and inter-subject variability with an incomplete block or repeated measures design (i.e. samples from all five brain regions were not available for every donor). Because of the small sample size in this study and many ties (as there usually is a sample-dependent fraction of bins which will not contain any cell), Monte-Carlo simulation was used (10,000 permutations) to estimate the null distribution and obtain appropriate SM statistics over the grid of bins. Significant differences are visualized in a statistical tSNE map where bins are coloured on a sliding scale corresponding to their –log2 *P*-values, allowing for identification of relevant subsets by spotting areas of connected significant bins[58]. As a complementary approach, we utilized the R cydar package[70] to detect differentially abundant subsets in original multidimensional marker space. Here, cells are counted into overlapping hyperspheres with a given radius centred at each cell and testing is then performed with the quasi-likelihood method in edgeR[71] and negative binomial generalized linear models to account for overdispersion in the count data. For hypersphere counting on the same markers used for tSNE embedding we used the default parametrization for the radius, with downsampled data to 20 percent of total event numbers and a minimum of 5 cells required to report a hypersphere. Likewise, the result of group-level analysis is visualized on the same composite tSNE plot for interpreting and exploring significant hyperspheres by colouring their centre cells according to –log2 *P*-values.

In order to aid characterization of differentially abundant subsets, compact areas of significant bins (or hyperspheres) are identified using a kernel density-based automated gating algorithm. We used an in-house R implementation which builds upon heuristics described by Shekhar *et al*.[59] for partitioning of tSNE maps (ACCENSE), adopts methodologies for automated gating of highest density regions in cytometry data[72,73] and utilizes functionalities provided in the R ks package[74,75] for kernel smoothing (source code and description are available in the Supplementary

Software or at https://github.com/steschlick). A kernel-bandwidth, i.e. the degree of smoothing, was first chosen to find an estimate of the 2D probability density from the binned data which accurately represented the morphology of the t-SNE map. The –log2 *P*-values from bin-wise statistical testing were then integrated as threshold-centred weights into subsequent kernel density estimation after correcting for multiple comparisons by controlling the false discovery rate (FDR) at 5%[76]. This yielded a smoothed profile of the statistical tSNE map. Local maxima representing differentially abundant phenotypes were detected by a 2D peak-finding algorithm[59]. Using a standard contouring function, polygons enclosing at least 6 bins (corresponding to an average cell frequency of 1%) to be reported were grown from each of these peaks to a desired level of significance (SM α=0.005) as tested on the aggregated bins inside a contour. Of note, we also allowed for merging of multiple peaks (or small contours) into a larger single region, as long as these were phenotypically indistinguishable by robust comparison of marker expression profiles as described in the next section.

Phenotypic characterization and automated annotation of significant subsets

Identified cellular subsets were automatically labelled with phenotypes according to their distribution of marker expression levels. In order to describe a subset phenotype, values of a specified pth upper and lower expression quantile of a given marker were compared with up to three user-defined or data-driven cutoffs for marker-positivity. This gave 3, 6, or 10 phenotypic categories for a single, two, or three cutoffs, respectively. For example, a subset is classified to be positive ("+") or negative ("–") for a given marker, if more than 84 % of cells have expression levels above or below a single cutoff value, respectively. Otherwise this marker is non-informative ("0") and will be excluded from the phenotype. Two cutoffs allow phenotypic labelling of subsets e.g. defined by a low/dim ("+–") or high ("++") marker expression. To further facilitate interpretation of subset phenotypes we quantified differential marker expression between each pair of identified subsets as well as the exclusion of all subset gates (cells–subsets) as an additional reference. Conceptually similar to the marker enrichment modelling described by Diggins *et al.*[77], we used a robust effect size, denoted here as Δ, that scales the Hodges-Lehmann estimate[78] of the difference in marker expression between two subsets by a robust measure of marker expression variability which we defined as the median absolute deviation about the Hodges-Lehmann estimator[79]. Since manually defined cutoffs might not capture those features which accounted for the spatial localization of identified subsets in the statistical t-SNE map, computed Δ scores were also used to assess the importance of a given marker in order to algorithmically include only the most relevant markers into

data-driven phenotypes that could distinguish the identified huMG subsets. In short, we first filtered out all markers that did not allow to discriminate at least one subset from any other based on a threshold for Δ and for the amount of expression overlap, i.e. the difference between the pth lower expression quantile of a subset and upper expression quantile of another subset must be non-negative. For each comparison for which the latter holds, we computed cutoffs discriminating respective subsets and assigned phenotypes accordingly. We set p to 0.16, corresponding to a 2-sigma difference between two standard normal distributions. This ultimately yields a number of cutoffs per informative marker, ranging for k subsets from 1 to k-1.

In order to reduce redundancy in the phenotype definitions, we used the R lpsolve package to find a combination of at least 8 markers that maximized the sum of effective differences Δ between any two subsets with one cutoff per marker. This allowed to fed the *flowType/RchyOptimyx pipeline*[80,81] with binary gating-cutoffs as input to feasibly partition the data into all possible phenotypes and score them by SM test.

Statistical analysis

No randomization strategy was used in this study. Data collection and analysis were not performed blind to the conditions of the experiments. However, data processing and analysis were carried out in an unsupervised manner, to exclude the possibility of biased results. CyTOF data are from two multiplexed samples, in which each contains two individual PBMC, two individual CSF cell samples, and eighteen human brain microglia samples (from up to five brain regions of 4- 5 individual donors). No priori statistical methods were used to predetermine sample sizes due to sample accessibility and insufficient previous data. However, sample sizes were chosen based on estimates of anticipated variability through previous studies of mRNA transcriptomic analysis[16,17]. Quantitative data were shown as independent data points with mean, and analyzed using one-way ANOVA with Bonferroni correction for post-hoc Turkey multiple comparison testing. Data distribution was assumed to be normal but this was not formally tested. Statistical tests were performed either using GraphPad Prism 6 (GraphPad Software Inc.) or computational analysis using Skilling-Mack nonparametric one-way repeated measures statistic and FDR-adjustment for multiple hypothesis testing as described above (*Statistical t-SNE maps and automated gating of differentially abundant huMG subsets and Phenotypic characterization and automated annotation of significant subsets*). A single GFM-sample (from donor #12) has to be excluded from statistical analyses as the Skilling-Mack testing requires at least two observations (i.e. regions) per block.

Data availability

Source data associated with Fig. 4-7 can be accessed at https://flowrepository.org/id/FR-FCM-ZYM6.

Code availability

The codes used for the data analyses in this study are available in *Supplementary Software* or at https://github.com/steschlick.

Results

Mass cytometric analysis of cryopreserved human post-mortem brain microglia

To compare the different phenotypes of CNS-resident microglia and peripheral immune cells, we simultaneously profiled peripheral blood mononuclear cells (PBMCs), immune cells from the CSF and huMG in the same run. The experiment is outlined in Fig. 1a. In summary, huMG were isolated from post-mortem brain tissue of different brain regions as described before[23]. Isolated huMG were then cryopreserved at -80°C using paraformaldehyde-containing stabilizing buffer[22]. Of note, classical cryopreservation using DMSO failed to cryopreserve the isolated huMG. Up to $3x10^4$ live CSF-derived cells were CD45-barcoded with ^{89}Y-CD45 antibody (CD45-$^{89}Y^+$)[23] and subsequently pooled with PBMCs (CD45-$^{89}Y^-$) from the same individual. The CSF-PBMC pooled samples were then cryopreserved using the same protocol that was applied to the huMG. In order to minimize the run-to-run variation and to facilitate the comparison of cellular phenotypes from different compartments and individuals, we thawed huMG and CSF-PBMC samples and performed intracellular mass-tag barcoding using palladium (Pd) isotopes. Each sample pool consisted of two CSF-PBMC sample pairs (two individuals with CSF and PBMC each) and 18 huMG samples (from up to 5 brain regions of 4-5 donors) (Supplementary Table 1). The pooled samples were equally split and stained with two different antibody panels (35 antibodies/panel) (Supplementary Tables 2 & 3). *Panel A* was designed to encompass the major circulating immune cell subsets (i.e. T & B cells, monocytes, natural killer (NK) cells) and microglia using proliferation markers, activity-related markers, chemokine receptors and cell subset markers, including $P2Y_{12}$, IRF4, IRF8, CD45, CD3, CD62L, CD19, HLA-DR, CD56, Cyclin A & B1, Ki67. *Panel B* was designed to analyse the phenotypes of huMG and the innate immune cell subsets using 35 antibodies including TMEM119, CD172a, CD279 (PD-1), CD274 (PD-L1), Arginase-1, CCR7, CD44, CD18, CD32. Finally, barcoded and pooled samples were simultaneously acquired on a CyTOF instrument.

To capture and visualize all mononuclear cell subpopulations in a single two-dimensional (2D) map, we first performed an unsupervised high-dimensional data analysis using the t-distributed stochastic linear embedding (t-SNE) algorithm[24,25] on the commercially available analysis platform Cytobank (www.cytobank.org) (Fig. 1b). The t-SNE maps showed a unique and distinct cluster of the huMG samples (Fig. 1b, green gate). This cluster expressed for the microglial marker, $P2Y_{12}$, and based on previous work[12,20] was used to identify human microglia (huMG). Notably, $P2Y_{12}$-negative cells detected in the brain samples (Fig. 1b) showed similar t-SNE coordination in clusters that overlapped with circulating immune cells in the peripheral blood and CSF (Fig. 1b). A unique and distinct cluster of huMG was also identified without the markers traditionally used to identify microglia (e.g. CD11b and CD45) when TMEM119 antibody was used as a huMG marker (*Panel B*, Supplementary Fig. 1a). Importantly, virtually all (> 99.9 %) of $P2Y_{12}^+$ cells expressed TMEM119, and > 99.4 % of TMEM119$^+$ cells expressed $P2Y_{12}$ in the FACS analysis (Supplementary Figs. 1b &c). To extend the phenotypic comparison between PBMCs, CSF cells and huMG, we manually gated CSF and blood mononuclear cells (i.e. monocytes, CD19$^+$ B cells, DCs, CD56$^{dim/+}$ NK cells, CD3$^+$ T cells) and huMG ($P2Y_{12}^+$ or TMEM119$^+$) clusters on the t-SNE map. Based on the mean signal intensity of all 57 markers analyzed (*Panel A* + *Panel B*), huMG clustered distinctly from all cell subsets in blood and CSF (Fig. 1c). Specifically, huMG expressed higher mean levels of $P2Y_{12}$, TMEM119, EMR1 (F4/80), CD64 and TREM2, whereas expression levels of CD44, CCR2, CD45, CD14 and CD16 were much lower in huMG compared to the PBMCs and CSF cells (Fig. 1d). In one huMG sample (out of 36 samples), we could detect an expression of CD19 or CD135 (Figure 1c). However, these cells were positive for markers used to identify microglia such as $P2Y_{12}$, TMEM119, EMR1, CX3CR1, CD11c and CD115. But they were negative for all classical B-cell markers such as CCR7, CD62L, CD37 and CD40, as well as CD44, a general marker for peripheral immune cells. Therefore, a contamination of B cells or peripheral immune cells in this particular sample is unlikely. Nevertheless, this rare expression of CD19 and CD135 deserves further investigation, which require additional markers. CSF cells expressed comparatively high levels of the cytokines IL-6 and TNF-α (Supplementary Figs. 2 & 3). Interestingly, in all cell subsets, peripheral blood cells clustered separately from CSF cells (Fig. 1c). In sum, the unsupervised, t-SNE-based dimensionality reduction effectively demonstrated phenotypic segregation of huMG from circulating immune cells with or without the use of classical cell lineage markers, such as CD45, CD11b, CD3, CD19 and CD56 (*Panel B*, Supplementary Fig. 1). The novel tools allow for the large-scale collection and simultaneous immune profiling of huMG and circulating immune cells.

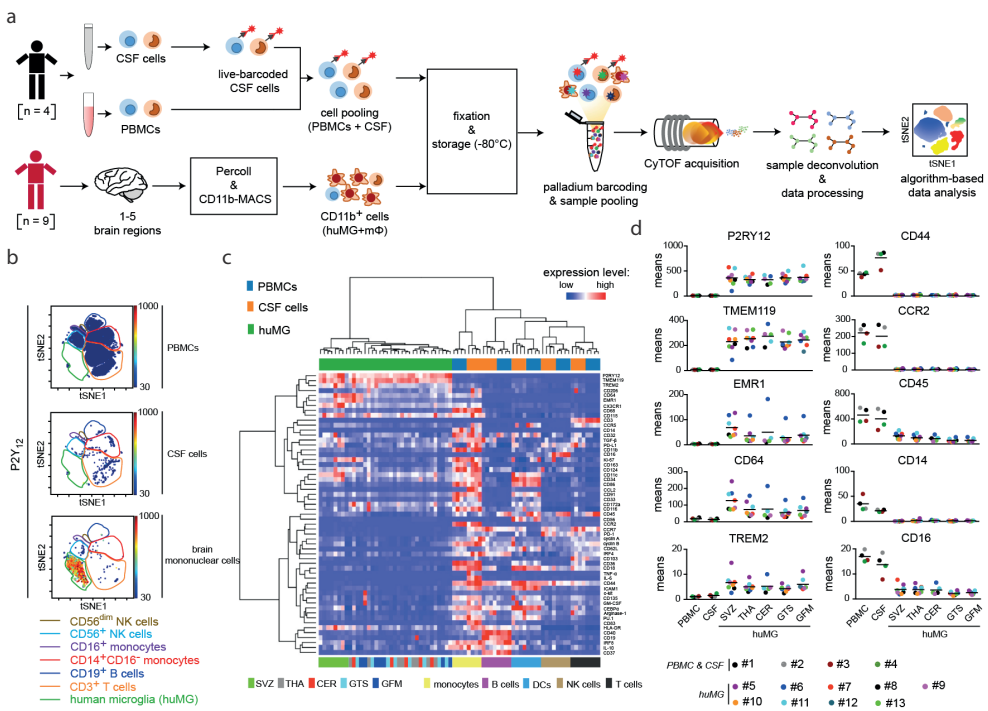

Figure 1: Simultaneous high-dimensional immune phenotyping of human microglia, and mononuclear cells from blood and CSF.

(a) Schematic representation of sample processing and CyTOF measurement. Blood and cerebrospinal fluid (CSF) were collected from the same individuals. Human microglia (huMG) were isolated from subventricular zone (SVZ); thalamus (THA); cerebellum (CER); temporal lobe (GTS) and frontal lobe (GFM) from nine biologically independent donors. One final barcoded and pooled sample consists of 18 huMG samples and 2 PBMC-CSF sample pools. Mixed samples were equally divided and stained with two panels of metal-conjugated antibodies and acquired on the CyTOF instrument. (b) Representative two-dimensional projections of single cell data generated by t-SNE of biologically independent samples: PBMCs (n =4), CSF cells (n = 4) and brain mononuclear cells (n = 36). Each dot represents one cell. The color spectrum represents expression of $P2Y_{12}$ (red denotes high expression, blue denotes no expression). $P2Y_{12}^{+}$ cells were gated as huMG (green) and $P2Y_{12}^{-}$ cells were gated as different circulating immune cells. (c) Heat map and cluster analysis of all samples based on the mean expression of 57 markers (*Panel A* + *Panel B*). Similarities between PBMCs (blue), CSF cells (orange) and huMG (green), as well as the similarities between huMG from different brain regions (SVZ (bright green) = subventricular zone; THA (grey) = thalamus; CER (red) = cerebellum; temporal lobe (GTS, bright blue); frontal lobe (GFM, dark blue) samples and expression levels are indicated by dendrograms. Heat colours of expression levels have been scaled for each marker individually (to the 1st and 5th quintiles), while red denotes high and blue low expression. (d) Mean signal intensity levels of $P2Y_{12}$, TMEM119, EMR1 (F4/80), CD64, TREM2, CD44, CCR2, CD45, CD14 and CD16 staining in PBMCs, CSF cells and huMG from different brain regions (black lines show mean values of the data sets).

Differential immunophenotypes of circulating myeloid cells and huMG

Murine tissue-resident macrophages, including microglia, and circulating monocytes have distinct transcriptomic and enhancer landscapes that are regulated by the local microenvironment[26]. At the protein expression level, murine microglia can be separated from circulating monocytes and other tissue-resident macrophages by clustering[27]. Here, we observed that all $P2Y_{12}$- or TMEM119-expressing huMG also co-expressed HLA-DR and CD11c (Supplementary Figs. 4a & b). We therefore performed a comprehensive t-SNE analysis of HLA-$DR^{+}CD11c^{+}$ huMG and circulating myeloid cells (HLA-$DR^{+}CD11c^{+}$) from blood and CSF. The results shown in Fig. 2a indicate that huMG have a phenotype that distinguishes them from circulating myeloid cells in blood and CSF. We then further analyzed these clusters at the level of marker expression on a donor-by-donor, compartment-by-compartment and brain region-by-region basis (Figs. 2b & c and Supplementary Figs. 2 & 3). Based on the expression levels of 55 investigated markers (*Panel A + Panel B,* excluding CD3 and CD19), the heat map visualization in Fig. 2b revealed a distinct phenotypic signature of huMG, as well as significant phenotypic differences between the myeloid cell populations in blood and CSF from the same donors. $P2Y_{12}$ and TMEM119 expression was highly enriched in huMG and was absent from myeloid cells in blood and CSF (Figs. 2b & c).

Next, we compared the immunophenotypic signatures of post-mortem huMG with microglia isolated from temporal lobe biopsies (fresh huMG) (Supplementary Table 4). The biopsies were obtained from three patients during the resection of brain tissue for the treatment of epilepsy, in analogy to the procedure recently described for transcriptomic and epigenetic profiling of huMG[16]. The epileptic focus with the strongest epileptogenic activity was removed before the surrounding tissue was used for microglia isolation. On the t-SNE map, post-mortem huMG clustered together with fresh huMG and displayed a comparable immunophenotypic signature (Fig. 3a), underscoring the validity of using post-mortem huMG for immunophenotypic profiling in health and disease. However, we did observe differences in the levels of signal intensity, in particular for IRF8 and $P2Y_{12}$, and to a lesser degree also for CD11b, CD68 and HLA-DR (Figs. 3b & c and Supplementary Fig. 5a & c). The expression levels of TMEM119 were not different between post-mortem huMG and fresh huMG (Fig. 3c). Interestingly, we detected $IRF8^{hi}P2Y_{12}^{+}$ cells (G1, Figs. 3a & b) at higher frequencies in fresh huMG than in post-mortem huMG (Fig. 3c). Removing IRF8 and $P2Y_{12}$ from embedding parameters resulted in decreased phenotypic differences between post-mortem huMG and fresh huMG (Figs. 3d & e and Supplementary Fig. 5b), suggesting that IRF8 and $P2Y_{12}$ are key markers that determine the difference between the two sources of huMG. Of note, these differences may result from post-mortem changes and/or effects of epilepsy on the tissue.

Figure 2

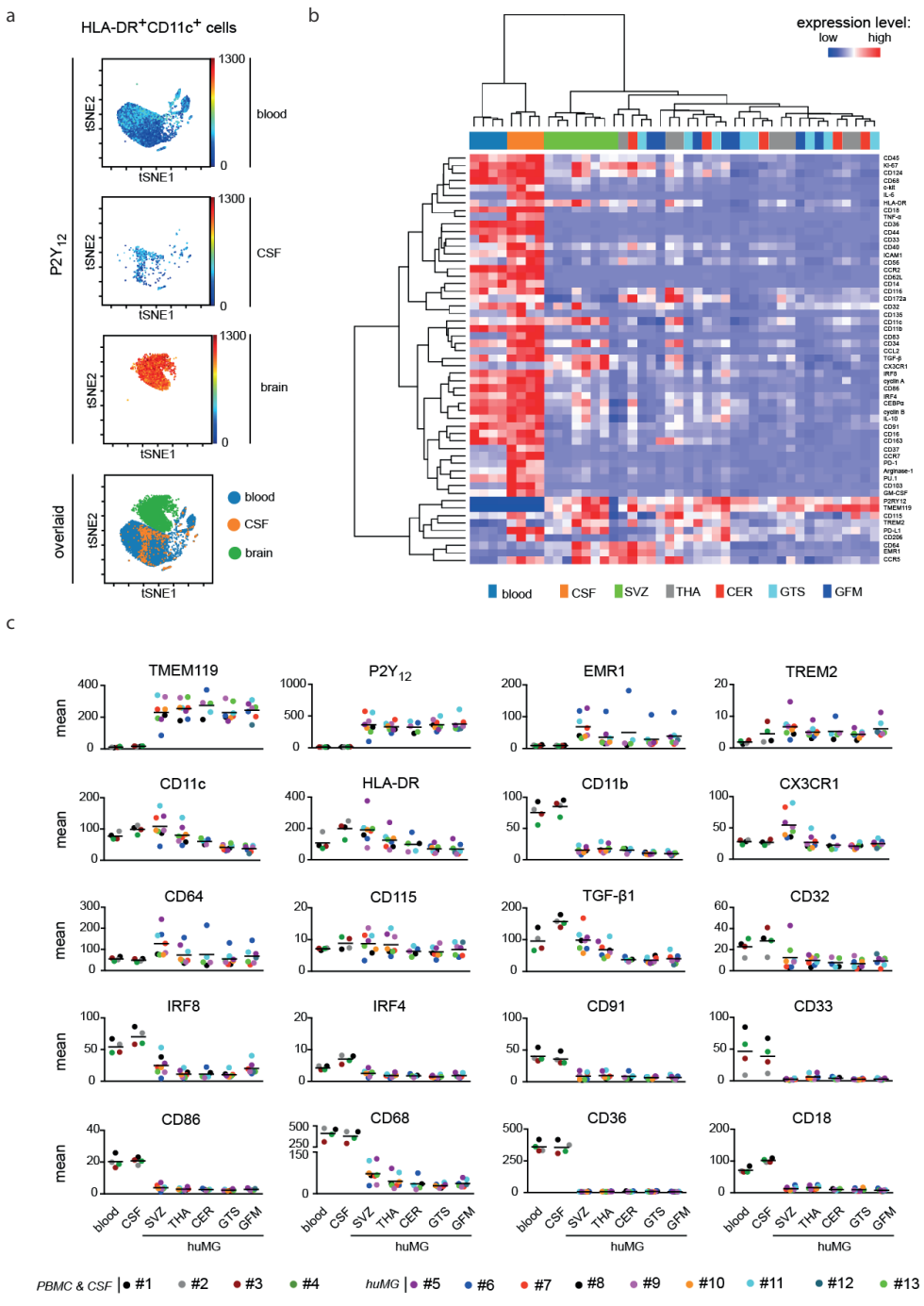

< Figure 2: Comparatively phenotypic analysis of huMG and peripheral myeloid cells.
(a) Representative t-SNE projection of multi-dimensional single cell phenotypes of HLA-DR^{+}CD11c^{+} myeloid cells detected in blood (PBMCs, n = 4 biologically independent samples), CSF (n = 4 biologically independent samples) and brain (huMG, n = 36 biologically independent samples). The colour spectrum represents an expression level of P2Y$_{12}$ (red = high; dark blue = no expression). The bottom image showed overlaid t-SNE plot of all cells from all three compartments (blue = blood, orange = CSF and green = brain huMG). (b) Heat map cluster demonstrates the mean expression of all 55 markers (*Panel A* + *Panel B*) and relationships between blood (blue), CSF (orange) and brain myeloid cells (SVZ = bright green; THA = grey; CER = red; GTS = bright blue; GFM = dark blue). Heat colours have been scaled per marker (red denotes high and blue denotes low expression). (c) Mean expression levels of selected markers in blood, CSF and brain myeloid cells (black lines show mean values of the data sets).

Expression of mannose receptor C-type 1 (CD206) in huMG

We observed variation in the expression of mannose receptor C-type 1 (MRC1 or CD206) in P2Y$_{12}^{+}$ cells across different brain regions (Figs. 4a & b). CD206 was previously suggested as a marker for M2-macrophages and perivascular macrophages in the human CNS[28]. However, recent data obtained from bulk RNA-sequencing showed that huMG also express low levels of CD206 mRNA[17,18]. Moreover, activated murine microglia express CD206 after spinal cord injury[29]. In humans, it is unclear whether the expression of CD206 is confined to a subpopulation of microglia, and what the expression levels of CD206 are at the single-cell level. The low-dimensional t-SNE map of P2Y$_{12}^{+}$ cells derived from up to five brain regions from nine different donors showed a small cluster of CD206^{high}CD163^{+}CD14^{+} cells (G3), which highly expressed HLA-DR, CD68 and CD11b (Figs. 4c & d), suggestive of perivascular macrophages (pmΦ). Interestingly, we observed low expression of P2Y$_{12}$ on this population (Figs. 4c & d and Supplementary Fig. 6a), which has not been reported before[12,20]. However, the expression levels of P2Y$_{12}$ were much lower than for huMG (Supplementary Fig. 6a). The cluster of pmΦ could not be detected when antibodies against CD163, CD14, CD68 and CD11b were not included in the staining panel (*Panel B*: Supplementary Fig. 7a). Interestingly, we also detected other clusters of CD206^{low}CD163^{-}CD14^{-}P2Y$_{12}^{high}$ cells (G2 & G3; Figs. 4c & d). The CD206^{low} huMG did not express CD163, and showed lower expression levels of HLA-DR, CD68, CD33, CD11b and CD45 compared to pmΦ (Figs. 4c & d). However, CD206^{low} huMG showed a higher expression level of CX3CR1 than pmΦ (Fig. 4d). In the *Panel B*, the clusters of CD206^{low} huMG were also identified (Supplementary Figs. 7a & b). Interestingly, we observed regional heterogeneity in the distribution of CD206^{low} huMG. Quantification of the manually gated populations G1–G3 on the t-SNE display revealed that CD206^{low} huMG were more frequent in temporal lobe (*Gyrus temporalis superior*, GTS) and frontal lobe (*Gyrus frontalis medius*, GFM) compared to other brain regions, whereas CD206^{high}

Figure 3

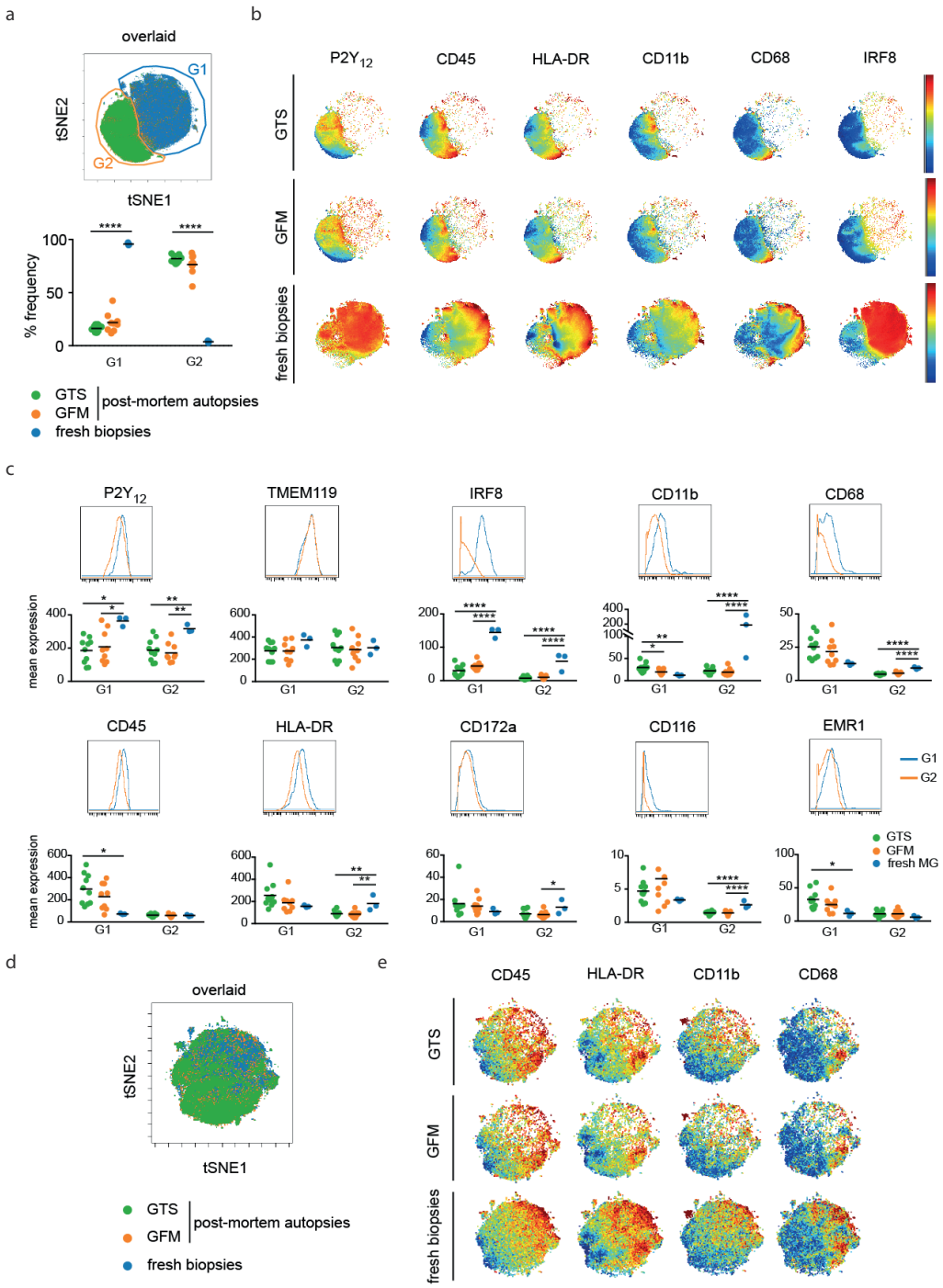

< Figure 3: Comparative immune profiling of post-mortem huMG and fresh huMG.
(a) An overlaid t-SNE plot of all cells from all samples (green = post-mortem GTS-huMG; n = 10 biologically independent samples; orange = post-mortem GFM-huMG, n = 9 biologically independent samples and blue = huMG from fresh biopsies, n = 3 biologically independent samples). Two main clusters, G1 (blue) and G2 (orange), are detected. The graph below shows the quantitative frequencies of G1 and G2 populations in each samples (black lines show mean values of the data sets). ****P <0.0001, one-way ANOVA with Bonferroni correction. (b) Representative reduced-dimensional single cell t-SNE illustrations of $P2Y_{12}^+$ huMG from biologically independent samples of GTS (n = 10), GFM (n = 9) and fresh biopsies (n = 3). The colour spectrum represents an expression level (red = high; dark blue = low expression). (c) Mean expression levels of selected markers showing differential marker expressions between the two gates (G1 & G2 in a) in huMG from biologically independent samples of GTS (green, n = 10), GFM (orange, n = 9) and fresh biopsies (blue, n = 3). *P < 0.05, **P < 0.01, ***P < 0.001, ****P <0.0001, one-way ANOVA with Bonferroni correction. (d) An overlaid high-dimensional plot (embedding without $P2Y_{12}$ and IRF8) of all cells from all biologically independent samples (green = GTS, n = 10; orange = GFM, n = 9 and blue = fresh biopsies, n = 3). No distinct cluster was detected, thus minute differences between samples. (e) Representative reduced-dimensional single cell t-SNE illustrations of $P2Y_{12}^+$ huMG from biologically independent samples of GTS (n = 10), GFM (n = 9) and fresh biopsies (n = 3). The colour spectrum represents an expression level of CD45, HLA-DR, CD11b and CD68 (red = high; dark blue = low expression).

pmΦ were equally distributed across the human brain (Fig. 4e). High proportions of $CD206^{low}$ huMG in temporal and frontal lobes were confirmed using *Panel B* (Supplementary Fig. 7b). Of note, such low expression of CD206 on $P2Y_{12}$-expressing cells was failed to be detected by flow cytometry due to the high autofluorescent background of post-mortem huMG (Supplementary Fig. 6b). The results underscore the power of the multidimensionality of mass cytometry in the attempt to identify microglia subpopulations in the human brain.

Heterogeneity of human post-mortem brain microglia

Recently, region-dependent microglial diversity was detected in the mouse brain based on transcriptional profiling using microarrays[14]. Here, we studied the phenotypic signatures of huMG at the single-cell level, and addressed the issue of regional heterogeneity of human brain microglia by mass cytometry. Our initial results suggested that huMG from the SVZ display a phenotype that is distinct from huMG in other brain regions (Figs. 1c & 2b). To extend these observations, we performed a comprehensive cluster analysis using the t-SNE embedding of the entire dataset, including all brain regions and all donors (36 samples; Figs. 5a - c). In order to quantify phenotypic differences and to fully harness the multi-dimensional nature of the mass cytometry data, we combined the t-SNE algorithm with probability binning[30]. The binning model is created on collapsed data from all samples (i.e. concatenated FCS file) by recursively splitting the events at the median values along the two t-SNE dimensions to yield 512 microgates (binning grids) at sufficiently high resolution (Figs. 5d & e).

Figure 4

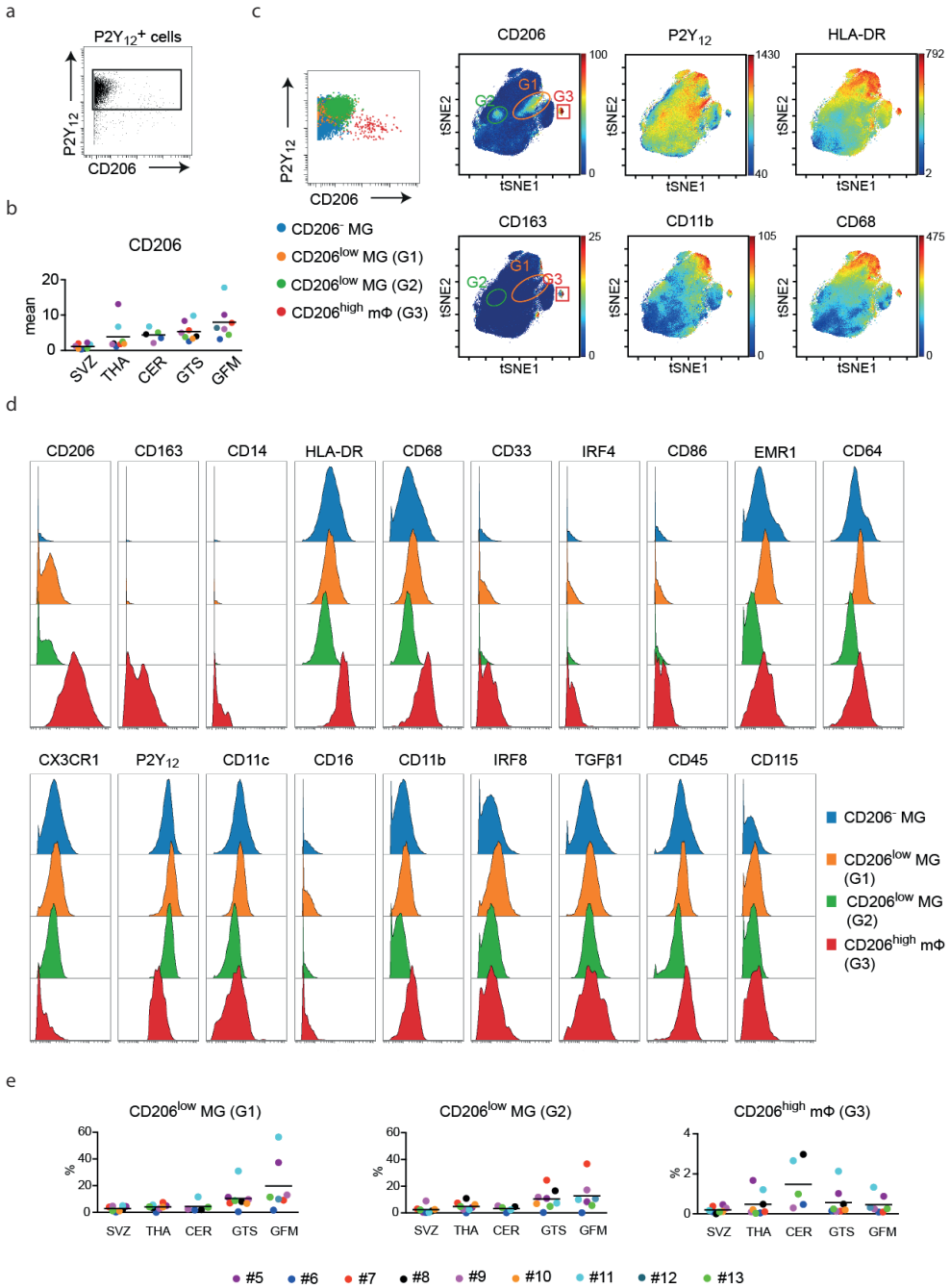

< Figure 4: CD206-expressing huMG and perivascular macrophages in the CNS mononuclear cell fraction.

(a) Representative two-dimensional dot plot of brain mononuclear cell fraction (two independently repeated experiments with similar results; n = 36 biologically independent samples) showing cell population co-expressing $P2Y_{12}$ and CD206. (b) Mean expression level of CD206 in $P2Y_{12}^{+}$ cells gated in Fig. 1a (biologically independent samples of SVZ (n = 8); THA (n = 8); CER (n = 5); GTS (n = 8) and GFM (n = 7)). Black lines show the mean of data sets. (c) High-dimensional t-SNE plots of concatenated FCS file (all 36 huMG samples). Each dot represents one cell. The color spectrum represents an expression level of CD206, $P2Y_{12}$, HLA-DR, CD163, CD11b and CD68. Red colour denotes high expression, blue colour denotes no expression. $CD206^{high}$ perivascular mΦ is gated as "G3" (red square), and $CD206^{low}$ cell population is gated as "G1" (orange circle) and "G2" (green circle). (d) Histogram plots show an expression of selected markers in CD206-negative (blue), $CD206^{low}$ (G1, orange & G2, green) huMG and $CD206^{high}$ perivascular mΦ (G3, red). (e) Frequencies of each CD206-expressing population in different brain regions. The values of an individual donor were plotted in the same color. The black lines represents the mean value.

We used the Earth Mover's Distance (EMD) metric[31] to quantify cell-distributional differences between huMG of samples from different donors and brain regions (Fig. 5f). The EMD score between most of the huMG in the SVZ (6 of 8 investigated donors) was very low, suggesting strong similarity between the SVZ samples (brain region) rather than donor-specific huMG phenotype (see also Supplementary Table 5). Using this methodology, huMG in the SVZ were confirmed to be phenotypically distinct from huMG in other brain regions (Fig. 5f). However, we also observed donor-dependent phenotypic variability (Fig. 5a and Supplementary Figs. 8a – c). In particular, donor #6 revealed a distinct cluster of huMG that we further characterized as a $CD64^{hi}EMR1^{hi}$ population (Supplementary Figs. 8b & c). Removing this donor or the outlier markers (CD64 and EMR1) prior to t-SNE embedding did not change our results regarding the regional heterogeneity of huMG (Supplementary Figs. 8d & e). We therefore included the outlier donor (#6) and the outlier markers (CD64 and EMR1) in all further analyses so as to embrace the biological variability of huMG.

In order to determine and visualize frequencies of differential phenotypes between brain regions, we performed bin-wise, intra-subject, mass univariate statistical testing[32] using the Skillings-Mack (SM) Friedman-type nonparametric one-way repeated measures statistic[33] to account for the non-normality of cell frequency data, the incomplete block design (i.e. unequal number of brain regions between investigated donors) and the small sample sizes. The results of the group-level analysis are presented as a single statistical t-SNE map (Figs. 6a & b and Supplementary Figs. 8f & g), in which areas of connected bins exceeding a given significance threshold are automatically gated to reveal cellular phenotypes accounting for the detected differences. Using this analysis, we identified four huMG subsets that showed differential abundance in

Figure 5

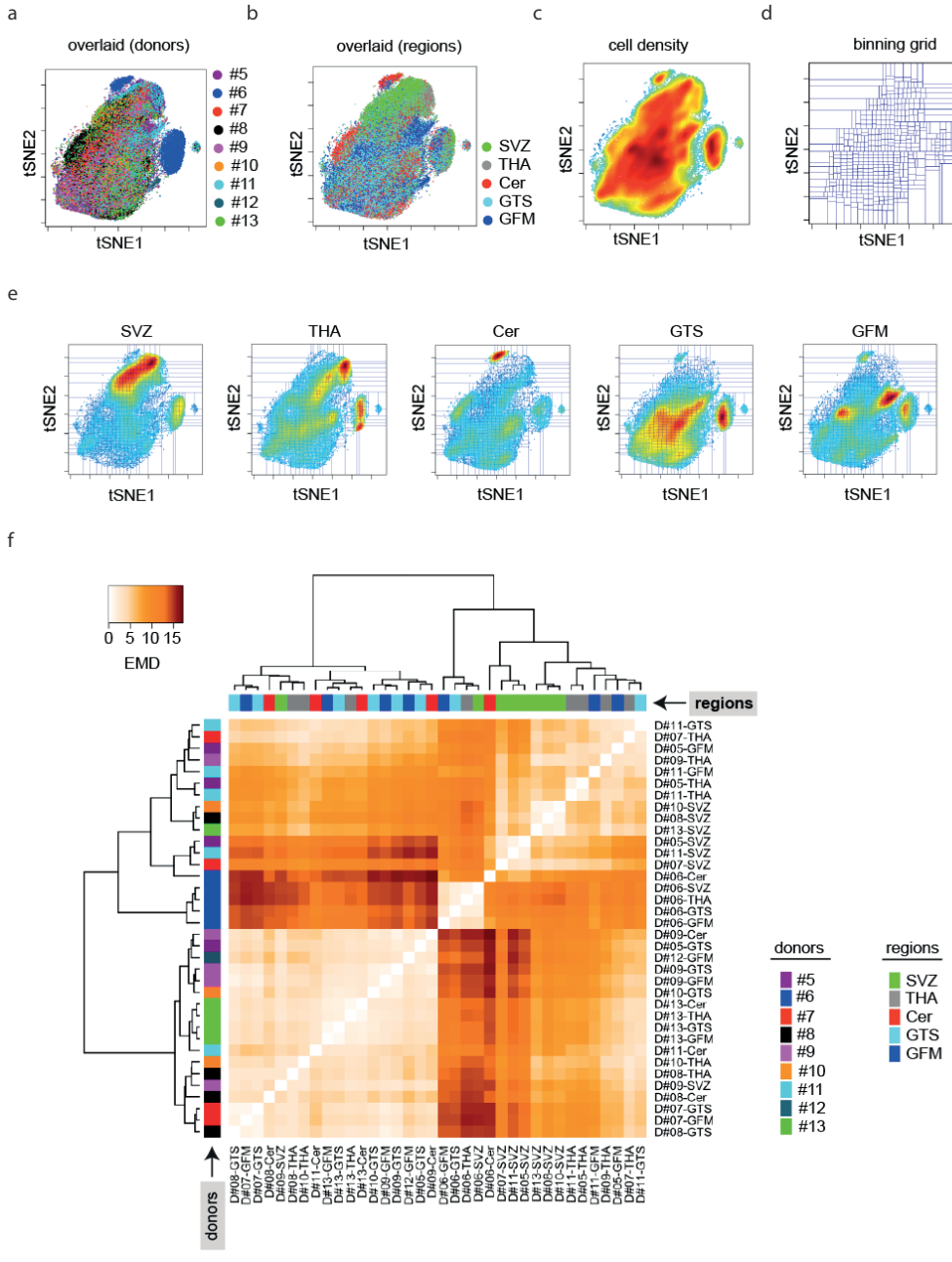

< Figure 5: Assessment of regional differences in huMG phenotypes by probability binning. The top panel shows the same t-SNE plot of concatenated FCS files from 36 huMG samples. The coloring indicates (a) nine donors, (b) five brain regions, or (c) overall cellular density of the concatenated files (spectrum from blue (low density) to red (high density)). (d) From the concatenated files a single binning grid is established, comprising 512 "micro-gates" in which cell frequencies are enumerated. Superimposing the binning grid on individual samples' t-SNE landscapes allows comparative analysis of huMG profiles at sample-to-sample basis across all five regions. (e) t-SNE plots of concatenated FCS files of each brain region. (f) Heatmap representing the pairwise earth mover's distances (EMD) between cellular density distributions over the t-SNE-space among all huMG samples. Hierarchical clustering highlights samples that have a highly similar phenotype, as indicated by low EMD values. The values of EMD range from 0 to 17, as shown by the color bar (top left).

different brain regions (subset 1, 2 & 3: $P < 0.0001$; subset 4: $P = 0.0014$, SM-test with controlled false discovery rate (FDR)) (Figs. 6c - e). We observed that SVZ and thalamus (THA) contain similar huMG phenotypes (subset 1), which are virtually absent from the other brain regions (Figs. 6e - g and Supplementary Figs. 8f & g). Temporal lobe (GTS) and frontal lobe (GFM) are enriched in different huMG phenotypes (subsets 2-4). Interestingly, subset 4 appears to be more abundant in temporal lobe than in frontal lobe (Figs. 6e - g). The profile of huMG in the cerebellum (Cer) was distinct from the other brain regions and revealed low abundance of all subsets (Figs. 6e - g). Similar regional differences were also detected when antibody *Panel B* was applied to the samples (Supplementary Figs. 9 & 10). Finally, we confirmed our findings using the Differential Abundance (DA)-hypersphere analysis in original multi-parameter space with the *cydar/edgeR* framework[34] (Supplementary Figs. 8h & 9c).

Region-dependent phenotypic signatures of huMG

Next, we further characterized the phenotypic signatures of the huMG regional subsets identified in Fig. 6. The four subsets were automatically gated and profiled for marker expression. The phenotypic signature of each subset was extracted (Fig. 7a and Supplementary Fig. 10). Subset 1, which was observed in higher proportions in the SVZ and THA, showed higher expression of CD11c, CD195 (CCR5), CD45, CD64, CD68, CX3CR1, EMR1 and HLA-DR compared to the other subsets (Figs. 7a & b and Supplementary Figs. 10b & d). Moreover, subset 1 of huMG expressed higher levels of the proliferation markers Cyclin A, Cyclin B1 and Ki67 (Supplementary Fig. 8i). These features suggest a more activated state of microglial cells in the SVZ and thalamus. Subsets 2 and 3, which were more abundant in GTS and GFM, expressed higher levels of CD206 compared to the other subsets (Figs. 7a & b and Supplementary Figs. 10b & d). Although the two subsets were generally very similar, subsets 2 and 3 differed in their expression of CD64 and EMR1 (Figs. 7a & b). Interestingly, we observed a positive correlation between donor age and the expression of CD11b, CD68, CD64,

Figure 6

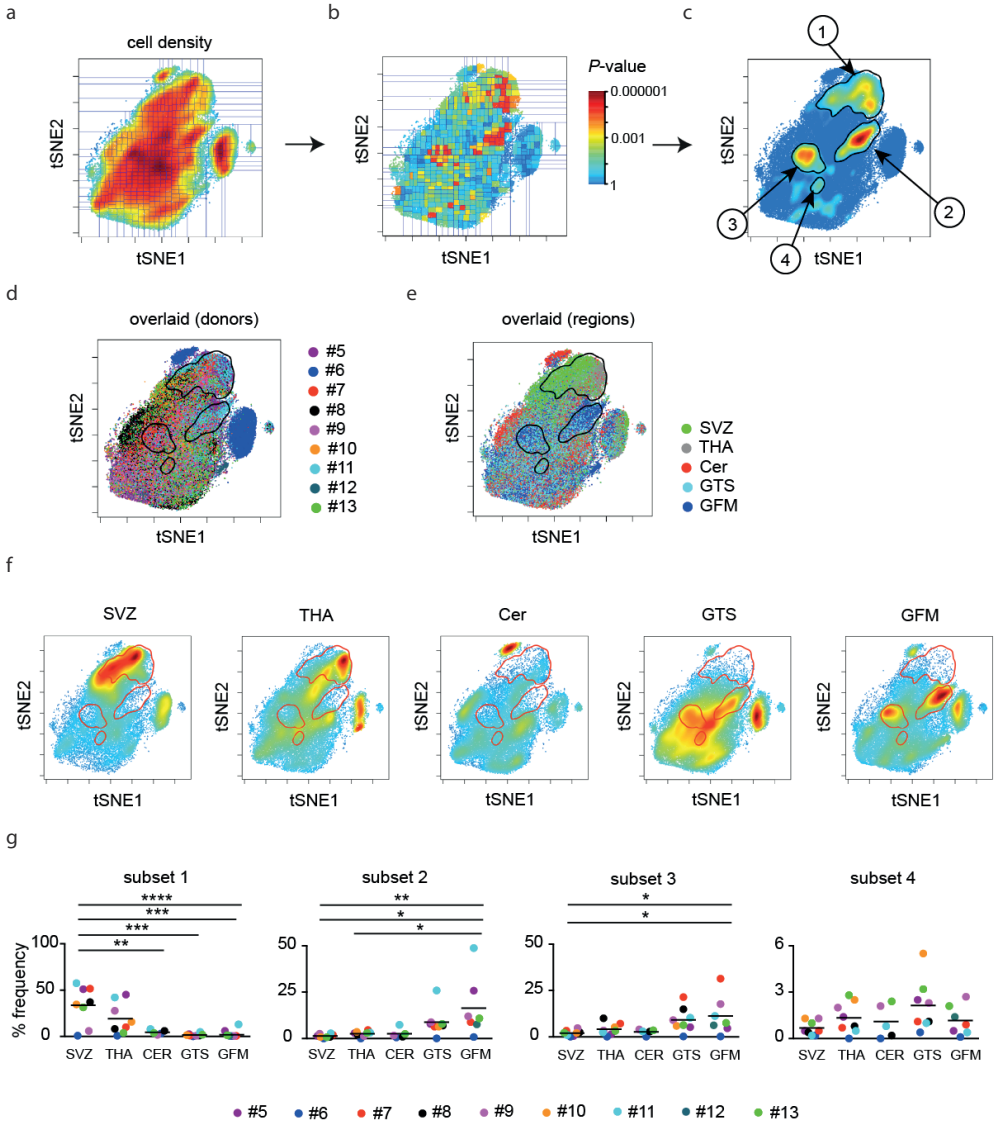

< Figure 6: Region-dependent huMG-subpopulations.
(a) Binning grid superimposed on concatenated t-SNE map (n = 36 biologically independent samples) and (b) statistical t-SNE map resulting from bin-wise testing for frequency differences between huMG samples (n = 35 biologically independent samples) from five brain regions (SVZ (n = 8); THA (n = 8); CER (n = 5); GTS (n = 8) and GFM (n = 6)) using the nonparametric Skillings-Mack statistic for unbalanced two-way block designs. The colour spectrum corresponds to unadjusted *P*-values, ranging from <0.000001 (red) to 1 (blue). (c) Smoothed representation of statistical t-SNE map (Fig. 6b) after FDR-adjustment for multiple comparisons and thresholding to 0.05 FDR-adjusted *P*-values (blue). Areas throughout the t-SNE map comprising significant bins (green to red spectrum) are indicative of differentially abundant subsets with distinct phenotypes and detected using a density-based automated gating approach (black contour lines). Gates of four detected subsets (black lines) are shown in concatenated t-SNE maps, color-encoded to indicate (d) nine donors, (e) five brain regions, and (f) in concatenated cellular density plots for each of the five investigated brain regions, individually. (g) The graphs show frequencies (%) of all four differentially abundant subsets across five brain regions (biologically independent samples of SVZ, n = 8; THA, n = 8; CER, n = 5; GTS, n = 8 and GFM, n = 7). Black lines show mean of the data set. **P* < 0.05, ***P* < 0.01, ****P* < 0.001, *****P* <0.0001, one-way ANOVA with Bonferroni correction.

HLA-DR and TREM2 in huMG from different brain regions, although the results need to be interpreted with caution given the small sample size (Supplementary Fig. 11). Importantly, we identified CD11c, CD206, CD45, CD64, CD68, CX3CR1, HLA-DR and IRF8 as key markers for the detection of huMG regional heterogeneity (Fig. 7b). To test the feasibility of using these 8 molecules in a reduced binary panel and conventional gating, we applied sequential, i.e. Boolean gating strategies to identify the four putative subsets based on the expression of only these 8 markers (Fig. 7c). Then, we compared the outcome frequencies of each Boolean-gated subset with the frequencies obtained by the gates in the t-SNE plot shown in Fig. 6. The frequencies of subsets 1, 2 and 3 were comparable between the two approaches (rho/r^2: subset 1 = 0.87/0.91; subset 2 = 0.85/0.78; subset 3 = 0.87/0.77, Fig. 7d), whereas the frequencies of the lower-abundant subset 4 were slightly different between the two types of analysis (rho/r^2: subset 4 = 0.72/0.34, Fig. 7d). We confirmed the suitability of these eight markers to identify huMG subsets 1, 2 and 3, whereas the detection of the rare subset 4 remained challenging. Next, we tested the robustness of the eight defined markers for identifying regional huMG heterogeneity using the *flowType/RchyOptimyx* pipeline[35] (Fig. 7e). Highly significant scores highlight CD206, CD45, CD64, CD68 and HLA-DR as the most important markers to target region-specific huMG phenotypes in a manual gating strategy.

Figure 7

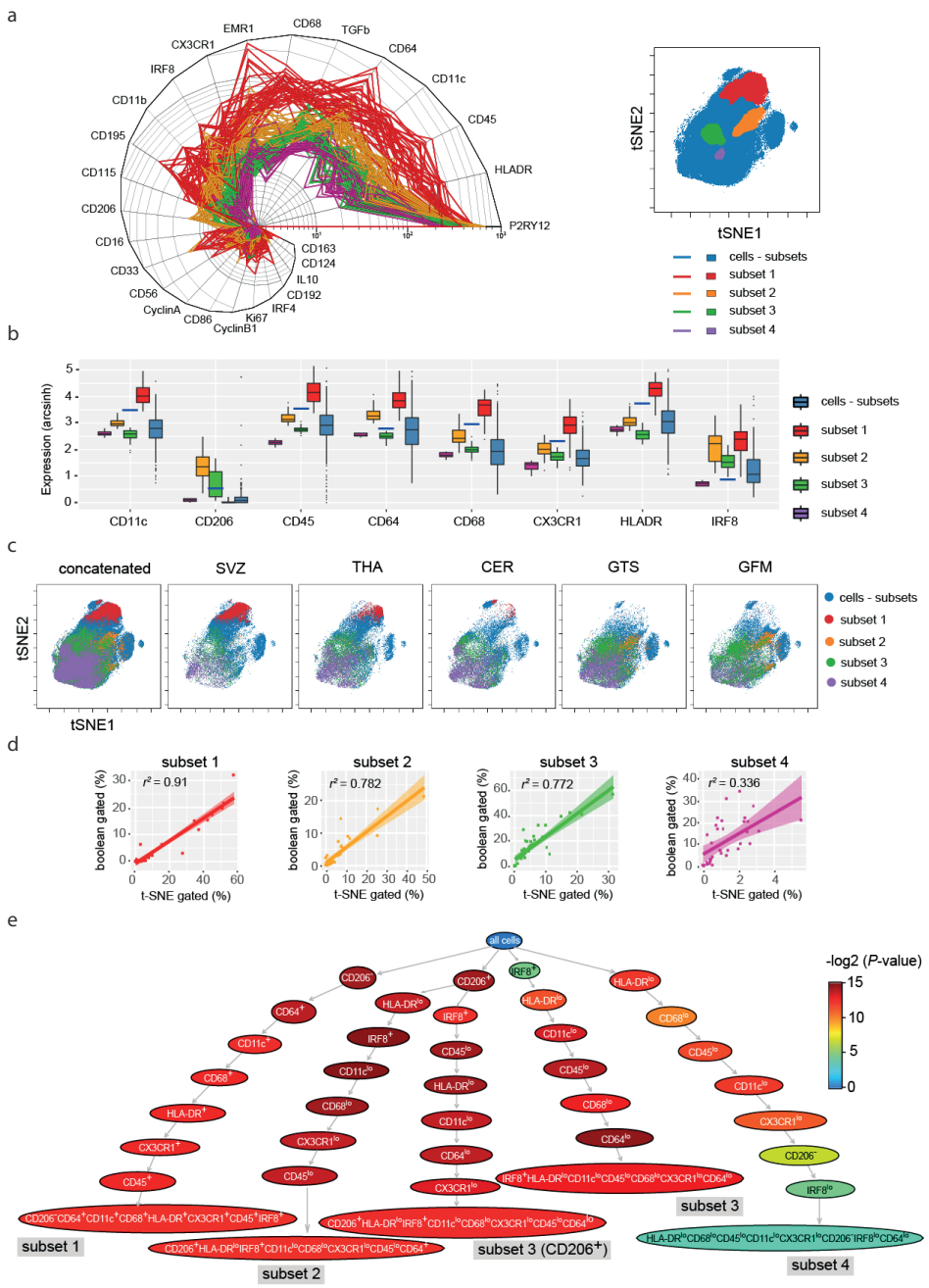

< Figure 7: Region-dependent huMG phenotypes.

(a) Radar chart (or snail plot) shows marker expression levels of each huMG subset (subset 1 = red; 2 = orange; 3 = green and 4 = purple). The snail shell represents transversal (perpendicular) axis mapping marker expression levels on exponential scale. Each line denotes each sample (n = 36 biologically independent samples). The right image demonstrates the automated subset gating on t-SNE map (subset 1 = red; 2 = orange; 3 = green; 4 = purple; remaining cells (cells – subsets) = all blue dots). (b) Selection of eight markers defining huMG subsets (n = 36 biologically independent samples). Median bin-expression levels are shown for each subset and marker in boxplot representation (subset 1 = red box (n = 66 bins); 2 = orange box plot (n = 32 bins); 3 = green box (n = 33 bins); 4 = purple box (n = 7 bins); remaining cells (cells – subsets) = blue box (n = 374 bins)). Blue lines indicate phenotype-defining cutoffs, used to identify the subsets by conventional (multivariate or hierarchical) gating. Box center and limits represent median, upper and lower quartiles; whiskers define the 1.5x interquartile range; points show outliers. (c) t-SNE plots of concatenated FCS files (from left to right: biologically independent samples of all, n = 36; SVZ, n = 8; THA, n = 8; CER, n = 5; GTS, n = 8 and GFM, n = 7) are overlaid with the four subsets identified by multivariate gating using a (Boolean) combination of 1D-gates set according to cutoffs and markers shown in (b). (d) Scatter plots showing correlation between subset frequencies detected by Boolean gating and by automated t-SNE gating in n = 36 biologically independent samples. Shaded areas indicate 0.95 confidence intervals of the linear regression, r^2 denotes respective coefficients of determination. (e) Marker importance analysis using the *flowType/RchyOptimyx* pipeline. The graph shows optimized gating hierarchies of the subsets starting from ungated cells (top node) to the eight-marker phenotypes (bottom nodes) as defined by cutoffs in (b). The color of the nodes shows significance scores of brain region-dependent differential abundance as the negated log-p-value of the Skillings-Mack test conducted on the same n = 35 independent huMG samples (SVZ, n = 8; THA, n = 8; CER, n = 5; GTS, n = 8 and GFM, n = 6) from 8 individual donors for each preferential addition of a subset-defining marker (node labels) which contributes at most to an increase in the significance score. The $CD206^+$ subset 3 phenotype has been included to also target the fraction of cells with CD206-expression above cutoff.

Finally, we performed FACS analysis to test the feasibility of identifying regional heterogeneity of huMG (Supplementary Table 4) by a more widely available technology. We were able to detect phenotypic differences of huMG between regions (SVZ *vs.* GTS & GFM) based on the FACS analysis of CD45, CD64, CD68 and HLA-DR expression (Fig. 8a). Furthermore, we detected a cluster analogous to CyTOF subset 1 (Figs. 6 & 7) of huMG (Fig. 8b, red gate). Importantly, the frequency of this SVZ-enriched subset was comparable between FACS analysis using 4 markers (CD45, CD64, CD68 and HLA-DR) and the CyTOF measurement (Fig. 8c).

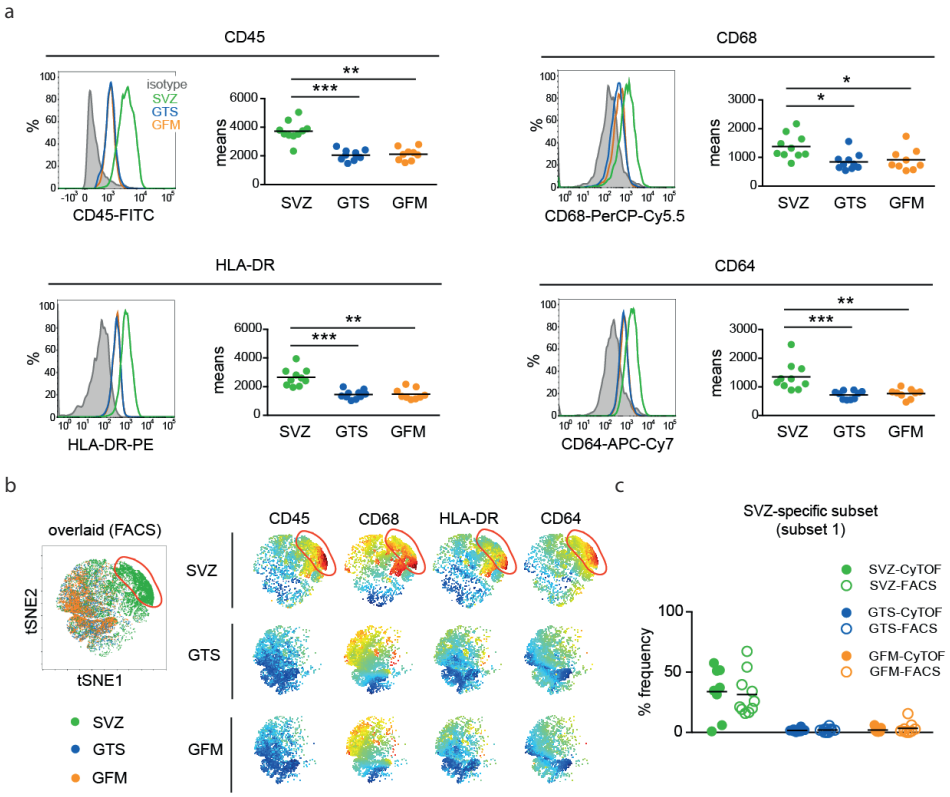

Figure 8: Identification of huMG heterogeneity by flow cytometry.
(a) HuMG isolated from SVZ (n = 10; green dots/lines) express higher levels of CD45, CD68, HLA-DR and CD64 that the ones isolated from GTS (n = 10; blue dots/lines) and GFM (n = 9; orange dots/lines). Data show mean, independent samples, each from an individual donor (total of 10 donors). **P* < 0.05, ***P* < 0.01, ****P* < 0.001, *****P* <0.0001, one-way ANOVA with Bonferroni correction. (b) Representative multi-dimensional single cell t-SNE projections of huMG from biologically independent samples of SVZ (n = 10), GTS (n = 10) and GFM (n = 9). The colour spectrum represents an expression levels of CD45, CD68, HLA-DR and CD64 (red = high; dark blue = low expression). The left image shows overlaid multi-dimensional plot of all cells from all three brain regions (green = SVZ, blue = GTS and orange = GFM). (c) Quantification of the frequency of defined SVZ-specific subset (G1 and red gate in b) obtained by FACS compared with the frequency of subset 1 quantified by CyTOF (as shown in Fig. 6g). *CyTOF*: SVZ (n = 8), GTS (n = 8) and GFM (n = 7; *FACS*: SVZ (n = 10), GTS (n = 10) and GFM (n = 9). No significant differences were found between the two technique (Multiple unpaired *t-test*, two-sided, corrected for multiple comparison using the Sidak-Bonferroni method). *P* = 0.7906 (SVZ); 0.7471 (GTS) and 0.4767 (GFM). Black lines show the mean of data sets.

Discussion

Microglia are resident innate immune cells in the human CNS that are involved in neural development and function, as well as responses to diseases. Although rodent microglia are often used to investigate microglial function, the emerging differences between human and rodent microglia call into question the clinical relevance of some of the research findings obtained in laboratory animals[36,37]. Several research groups have established a firm basis for the use of huMG in neuroscience and neuroimmunology and have provided invaluable transcriptomic information on these cells[18,19,38-45]. However, phenotypic profiling of huMG based on a comprehensive array of marker proteins has remained technically challenging. This is particularly true at the single-cell level, which is required to identify microglia subpopulations.

Here, we have for the first time applied massive single-cell immune profiling of huMG from different brain regions by multiplexed mass cytometry, allowing for a detailed phenotypic characterization of huMG. Our findings support the notion of microglial heterogeneity in the human brain, which is in line with recent data obtained from mouse microglia[14]. Our results substantiate previously published data on mRNA[16-18,44] and protein[18-20,44-46] expression of huMG. The development of a new cell fixation and cryopreservation technique combined with barcoding (multiplexing), mass cytometry and novel algorithms for data analysis enabled us to identify a phenotypical signature of huMG that distinguishes them from other innate immune cells (e.g. cells from blood and CSF).

In this study, we combined t-SNE and probability binning for both of their strengths to detect changes in subset that are defined by dim or unimodal marker (co-) expression or subtle shifts in expression levels (and thus difficult to enumerate by clustering techniques). This approach revealed microglial subsets that differ in their abundance across different regions of the human brain, indicating phenotypic heterogeneity among huMG. Notably, we extracted a panel of 8 (out of 57) phenotypical markers that allow to distinguish major huMG subsets. We confirmed the key transcriptomic signature of huMG[16,17] at the protein level, namely, the expression of $P2Y_{12}$ and TMEM119, the high expression of CD64, CX3CR1, TGF-β1, TREM2, CD115, CCR5, CD32, CD172a, CD91, and the low to absent expression of CD44, CCR2, CD45, CD206, CD163, and CD274 (PD-L1). The results are in line with recent mass cytometry data on immune cells in the mouse brain, which reveal that CD44 is expressed only on infiltrating cells and not on resident myeloid cells[47]. These core immunophenotypes of post-mortem huMG are apparently comparable to fresh huMG, albeit differences of signal intensities for some markers. Likewise, Szulzewsky et al.[48] observed similar

transcriptomic profiles between huMG from epilepsy and post-mortem tissues. Interestingly, we detected the expression of EGF-like module containing mucin-like hormone receptor (EMR)1, the human orthologue of F4/80, in huMG, whereas circulating monocytes and myeloid dendritic cells in the blood and CSF lacked EMR1 expression. This is a surprising finding given that EMR1 has been suggested to be a highly specific marker for eosinophils in human and absent on mononuclear phagocytic cells including monocytes, macrophages and dendritic cell subsets[49].

The combination of antibody panel design, single-cell mass cytometry and computational unsupervised data analysis separated cells with characteristics of perivascular macrophages ($CD11b^{+}CD206^{high}CD163^{+}$) from huMG ($CD11b^{+}CD206^{low/-}CD163^{-}$). Furthermore, we identified two novel microglial subsets that express CD206, but not CD163, particularly in the frontal and temporal lobe. The findings are in line with the recent studies, which showed low expression of CD206 mRNA in human microglia[17,18]. Notably, microglia were found to express CD206 after spinal cord injury in mice[29], suggesting that CD206 expression may reflect the functional responses of huMG.

A recent study demonstrated that microglia in mice and humans are short lived and quickly renewed at the individual cell level[50]. At the population level, CNS microglia are maintained by the balanced regulation between proliferation and apoptosis[50]. In agreement with these observations[50], we were able to detect proliferating huMG at different phases of the cell cycle across five brain regions. Of note, we observed slightly higher expression of Ki-67 (G_1, S & G_2 phase, mitosis), Cyclin A (S & G_2 phase, mitosis) and Cyclin B (mitosis) on huMG subsets in the SVZ and thalamus compared with other brain regions. Whether this increased proliferation mirrors region-specific phenotype and/or function of huMG remains to be investigated.

One important conclusion drawn from this study is that huMG have multiple phenotypic signatures that appear to depend on the brain region they reside in, whereas the core immunophenotype that distinguishes them from circulating and/or infiltrating myeloid cells is retained post-mortemly across the five investigated regions of human brain. The results are in line with previous findings in mouse and man[14,18,19]. We detected comparatively higher expression of markers involved in microglial activation, such as CD68, CD86, CD45, CX3CR1, CD11c, CD64, ERM1 and HLA-DR in the SVZ and thalamus compared to other brain regions. Interestingly, huMG subpopulations in the temporal and frontal lobe expressed the mannose receptor CD206, which is a marker of M2-polarized macrophages. Whether this phenotype implies a region-specific function remains to be investigated. The extent to which the isolation protocol could influence the observed differences in regional expression profile is unclear, although the finding that huMG in the THA and SVZ have similar phenotypic profiles despite differences in the isolation protocol suggests this may not be a major determinant.

In conclusion, this study demonstrates the power of combining multiplexed mass cytometry with bioinformatics to reveal region-dependent signatures of huMG, even for small sample size and/or when the differences between groups are very small. We believe that an appropriate protocol for sample preparation is one of the key success factors for immune profiling of human post-mortem microglia. Our findings of microglial heterogeneity in the human brain may help to reveal region-specific functions of these cells in health and disease, and instruct the development of more selective pharmacological interventions targeting microglia in humans.

Online content

Any methods, supplementary information, additional references, Life Sciences Reporting Summary, source data, statements of data availability and associated accession codes are available at the online version of the paper.

Accession codes

The codes used for the data analyses in this study is available in *Supplementary Software* or at https://github.com/steschlick.

Acknowledgments

We thank Christian Böttcher for excellent technical assistance with FACS analysis. We would also like to acknowledge the assistance of the BCRT Flow Cytometry Lab (Charité – Universitätsmedizin Berlin, Germany). C.B. and J.P. were supported by the German Research Foundation (SFB TRR167, B05 & B07). J.P. received additional funding from the Berlin Institute of Health (CRG2aSP6) and the UK DRI (Momentum Award). S.S. was funded by the EU-H2020 project PACE (grant agreement number 733006). A.K. and E.P. were supported by stipends from the NeuroMac School (SFB TRR167, IRTG). A.K. received additional funding from the Cluster of Excellence NeuroCure. H.E.M. and A.R.S. were supported through grant Me3644/5-1. B.S. was supported by the German Research Foundation (SI 749/9-1, 749/10-1, CRC-TRR 241). B.S. and R.G. was supported by the Deutsche Krebhilfe (70112011). M.A.M.S. was supported by a 2014 NARSAD Young Investigator Grant from the Brain & Behavior Research Foundation and L.d.W. by the Virgo Consortium, funded by the Dutch government project number FES0908. The psychiatric donor program of the Netherlands Brain Bank (NBB-Psy) is financially supported by the Netherlands Organization for Scientific Research (NWO). We acknowledge the Leibniz Science Campus for Chronic Inflammation for general support.

Author contributions

C.B. and J.P. conceived and designed the project. C.B., S.S., D.K., B.S. and R.G. designed the antibody panels for mass cytometry. M.A.M.S., G.J.L.S., E.M.H., R.S.K. and L.D.W. established and performed the isolation of post-mortem huMG. P.F. and L.K. provided biopsy tissues from temporal lobe resections. A.R.S. and H.E.M. set up the fixation approach for cryostorage of human leucocytes and provided guidance in using the system. C.B. established the protocol for cryopreservation of isolated huMG. A.K. and E.P. performed barcoding and antibody staining for CyTOF. A.K. conducted FACS analysis of post-mortem huMG. D.K. performed CyTOF measurements. E.J.S. and J.P. provided peripheral blood and cerebrospinal fluid samples. C.B. and S.S. analyzed the data. C.B., S.S., L.D.W. and J.P. wrote the manuscript.

Competing financial interests

The authors declare no competing financial interests.

References

1. Prinz, M. & Priller, J. Microglia and brain macrophages in the molecular age: from origin to neuropsychiatric disease. *Nat. Rev. Neurosci.* **15,** 300–312 (2014).
2. Sierra, A. *et al.* Microglia shape adult hippocampal neurogenesis through apoptosis-coupled phagocytosis. *Cell Stem Cell.* **7**, 483–495 (2010).
3. Parkhurst, C.N. et al. Microglia promote learning-dependent synapse formation through brain-derived neurotrophic factor. *Cell.* **155**, 1596–1609 (2013).
4. Prinz, M. & Priller, J. The role of peripheral immune cells in the CNS in steady state and disease. *Nat. Neurosci.* **20,** 136–144 (2017).
5. Perry, V.H. & Holmes, C. Microglial priming in neurodegenerative disease. *Nat. Rev. Neurol.* **10,** 217–224 (2014).
6. Colonna, M. & Butovsky, O. Microglia function in the central nervous system during health and neurodegeneration. *Annu. Rev. Immunol.* **35,** 441–468 (2017).
7. Keren-Shaul, H. *et al.* A unique microglia type associated with restricting development of Alzheimer's disease. *Cell* **169,** 1–15 (2017).
8. Ginhoux, F. *et al.* Fate mapping analysis reveals that adult microglia derive from primitive macrophages. *Science* **330,** 841–845 (2010).
9. Kierdorf, K. *et al.* Microglia emerge from erythromyeloid precursors via Pu.1- and Irf8-dependent pathways. *Nat. Neurosci.* **16,** 273–280 (2013).
10. Elmore, M.R. *et al.* Colony-stimulating factor 1 receptor signaling is necessary for microglia viability, unmasking a microglia progenitor cell in the adult brain. *Neuron* **82,** 380–397 (2014).
11. Bruttger, J. *et al.* Genetic Cell Ablation Reveals Clusters of Local Self-Renewing Microglia in the Mammalian Central Nervous System. *Immunity* **43,** 92–106 (2015).
12. Butovsky, O. *et al.* Identification of a unique TGF-β-dependent molecular and functional signature in microglia. Nat. Neurosci. 17, 131–143 (2014).
13. Orre, M. *et al.* Acute isolation and transcriptome characterization of cortical astrocytes and microglia from young and aged mice. *Neurobiol. Aging.* **35,** 1–14 (2014).
14. Grabert, K. *et al.* Microglial brain region–dependent diversity and selective regional sensitivities to aging. Nat. Neurosci. 19, 504–516 (2016).
15. Orre, M. *et al.* Isolation of glia from Alzheimer's mice reveals inflammation and dysfunction. *Neurobiol. Aging.* **35,** 2746–2760 (2014).
16. Gosselin, D. *et al.* An environment-dependent transcriptional network specifies human microglia identity. *Science.* **356,** eaal3222 (2017).
17. Galatro, T.F. *et al.* Transcriptomic analysis of purified human cortical microglia reveals age-associated changes. *Nat. Neurosci.* **20,** 1162–1171 (2017).
18. Melief, J. *et al.* Characterizing primary human microglia: a comparative study with myeloid subsets and culture models. *Glia* **64,** 1857–1868 (2016).
19. Mizee, M.R. *et al.* Isolation of primary microglia from the human post-mortem brain: effects of ante- and post-mortem variables. *Acta Neuropathol. Commun.* **5,** 16 (2017).
20. Mildner, A., Huang, H., Radke, J., Stenzel, W. & Priller, J. P2Y12 receptor is expressed on human microglia under physiological conditions throughout development and is sensitive to neuroinflammatory diseases. *Glia* **65,** 375–387 (2017).
21. Moore, C.S. *et al.* P2Y12 expression and function in alternatively activated human microglia. *Neurol. Neuroimmunol. Neuroinflamm.* **2,** e80 (2015)
22. Gaudilliere, B. *et al.* Coordinated surgical immune signatures contain correlates of clinical recovery. *Sci. Transl. Med.* **6**, 255ra131 (2014).
23. Mei, H.E. *et al.* Barcoding of live human peripheral blood mononuclear cells for multiplexed mass cytometry. *J. Immunol.* **194,** 2022–2031 (2015).

24. Amir, E.A. *et al.* viSNE enables visualization of high dimensional single-cell data and reveals phenotypic heterogeneity of leukemia. *Nat. Biotechnol.* **31**, 545–552 (2013).
25. Van der Maaten, L. & Hinton, G. Visualizing high-dimensional data using tSNE. *J. Mach. Learn. Res.* **9**, 2579–2605 (2008).
26. Lavin, Y. *et al.* Tissue-resident macrophage enhancer landscapes are shaped by the local microenvironment. *Cell* **159**, 1312–1326 (2014).
27. Becher, B. *et al.* High-dimensional analysis of the murine myeloid cell system. *Nat. Immunol.* **15**, 1181–1189 (2014).
28. Holder, G.E. *et al.* Expression of the mannose receptor CD206 in HIV and SIV encephalitis: a phenotypic switch of brain perivascular macrophages with virus infection. *J. Neuroimmune Pharmacol.* **9,** 716–726 (2014).
29. Cohen, M. *et al.* Newly formed endothelial cells regulate myeloid cell activity following spinal cord injury via expression of CD200 ligand. *J. Neurosci.* **37,** 972–985 (2017).
30. Roederer, M. *et al.* Probability binning comparison: a metric for quantitating univariate distribution differences. *Cytometry*. **45,** 37–46 (2001).
31. Orlova, D.Y. *et al.* Earth mover's distance (EMD): a true metric for comparing biomarker expression levels in cell populations. *Plos One* **11**: e0151859 (2016).
32. Nichols, T. & Hayasaka, S. Controlling the familywise error rate in functional neuroimaging: a comparative review. *Stat. Methods Med. Res.* **12,** 419–46 (2003).
33. Chatfield, M. & Mander, A. The Skillings-Mack Test (Friedman test when there are missing data). *Stata J.* **9**, 299–305 (2009).
34. Lun, A.T.L., Richard, A.C. & Marioni, J.C. Testing for differential abundance in mass cytometry data. *Nat. Methods.* **14**, 707-709 (2017).
35. O'Neill, K., Jalali, A., Aghaeepour, N., Hoos, H. & Brinkman, R.R. Enhanced flowType/RchyOptimyx: a BioConductor pipeline for discovery in high-dimensional cytometry data. *Bioinformatics.* 30, 1329–1330 (2014).
36. Smith, A.M. & Dragunow, M. The human side of microglia. *Trends Neurosci.* **37,** 125–135 (2014).
37. Schughart, K. *et al.* Controlling complexity: the clinical relevance of mouse complex genetics. *Eur. J. Hum. Genet.* **21,** 1191–1196 (2013).
38. Durafourt, B.A., Moore, C.S., Blain, M. & Antel, J.P. Isolating, culturing, and polarizing primary human adult and fetal microglia. *Methods Mol. Biol.* **1041,** 199–211 (2013).
39. Rustenhoven, J. *et al.* Isolation of highly enriched primary human microglia for functional studies. *Sci. Rep.* **6,** 19371 (2016).
40. Melief, J. *et al.* Microglia in normal appearing white matter of multiple sclerosis are alerted but immunosuppressed. *Glia* **61,** 1848–1861 (2013).
41. Olah, M. et al. An optimized protocol for the acute isolation of human microglia from autopsy brain samples. *Glia* **60,** 96–111 (2012).
42. Lambert, C. *et al.* Distinct migratory and cytokine responses of human microglia and macrophages to ATP. *Brain Behav. Immun.* **24,** 1241–1248 (2010).
43. Klegeris, A. *et al.* Modulation of human microglia and THP-1 cell toxicity by cytokines endogenous to the nervous system. *Neurobiol. Aging* **26,** 673–682 (2005).
44. Butovsky, O. *et al.* Identification of a unique TGF-β-dependent molecular and functional signature in microglia. *Nat. Neurosci.* **17,** 131–143 (2014).
45. Bennett, M.L. *et al.* New tools for studying microglia in the mouse and human CNS. *Proc. Natl. Acad. Sci. USA* **113**, E1738–1746 (2016).
46. Bianchin, M.M. *et al.* Nasu-Hakola disease (polycystic lipomembranous osteodysplasia with sclerosing leukoencephalopathy--PLOSL): a dementia associated with bone cystic lesions. From clinical to genetic and molecular aspects. *Cell Mol. Neurobiol.* **24,** 1–24 (2004).
47. Korin, B., *et al.* High-dimensional, single-cell characterization of the brain's immune compartment. *Nat. Neurosci.* **20**, 1300–1309 (2017).

48. Szulzewsky, F., et al. Human glioblastoma-associated microglia/monocytes express a distinct RNA profile compared to human control and murine samples. *Glia*. **64**, 1416–1437 (2016).
49. Hamann, J. *et al.* EMR1, the human homolog of F4/80, is an eosinophil-specific receptor. *Eur. J. Immunol.* **37,** 2797–2802 (2007).
50. Askew, K. et al. Coupled proliferation and apoptosis maintain the rapid turnover of microglia in the adult brain. Cell Rep. 18, 391–405 (2017).
51. Kotecha, N., Krutzik, P.O. & Irish, J.M. Web-based analysis and publication of flow cytometry experiments. *Curr. Protoc. Cytom.* **53**, 10.17.1–10.17.24 (2010).
52. Amir el, A.D., *et al.* viSNE enables visualization of high dimensional single-cell data and reveals phenotypic heterogeneity of leukemia. *Nat. biotech.* **31**, 545–552 (2013).
53. van der Maaten, L.J.P. & Hinton, G.E. Visualizing High-Dimensional Data Using t-SNE. *J. Mach. Learn. Res.* **9**, 2579–2605 (2008).
54. R_Core_Team *R: A language and environment for statistical computing.* R Foundation for Statistical Computing, Vienna, Austria. URL http://www.r-project.org/ (2014).
55. Finak, G. *et al.* OpenCyto: an open source infrastructure for scalable, robust, reproducible, and automated, end-to-end flow cytometry data analysis. *PLoS Comput. Biol.* **10**, e1003806 (2014).
56. Jiang, M. *CytoML: GatingML interface for openCyto.* R package version 1.0.1 (2016).
57. Spidlen, J. et al. Gating-ML: XML-based gating descriptions in flow cytometry. *Cytometry A.* **73A**, 1151–1157 (2008).
58. van Dongen, S. & A.J. Enright. *Metric distances derived from cosine similarity and Pearson and Spearman correlations.* CoRR, arXiv:1208.3145 [stat.ME] (2012).
59. Shekhar, K., Brodin, P., Davis, M.M. & Chakraborty, A.K. Automatic Classification of Cellular Expression by Nonlinear Stochastic Embedding (ACCENSE). *Proc. Nat. Acad. Sci. USA.* **111**, 202–207 (2014).
60. Chen, H. *et al*. Cytofkit: A Bioconductor Package for an Integrated Mass Cytometry Data Analysis Pipeline. *PLoS Comput. Biol.* **12**, e1005112 (2016).
61. Samusik, N., Good, Z., Spitzer, M.H., Davis, K.L. & Nolan, G.P. Automated mapping of phenotype space with single-cell data. *Nat. Methods* **13**, 493–496 (2016).
62. Rogers, W.T. & Holyst, H.A. FlowFP: A Bioconductor Package for Fingerprinting Flow Cytometric Data. *Adv. Bioinformatics.* 193947 (2009).
63. Roederer, M. *et al.* Probability binning comparison: a metric for quantitating univariate distribution differences. *Cytometry*. **45,** 37–46 (2001).
64. Japp, A.S., *et al.* Wild immunology assessed by multidimensional mass cytometry. Cytometry A. 91, 85–95 (2017).
65. Anderson, M.J. A new method for non-parametric multivariate analysis of variance. Austral Ecology 26, 32–46 (2001).
66. Oksanen, J., *et al.* Vegan: *Community Ecology Package.* (2008).
67. Nichols, T. & Hayasaka, S. Controlling the familywise error rate in functional neuroimaging: a comparative review. *Stat. Methods Med. Res.* **12,** 419 – 446 (2003).
68. Nichols, T.E. & Holmes, A.P. Nonparametric permutation tests for functional neuroimaging: a primer with examples. Hum. Brain Mapp. 15, 1 – 25 (2002).
69. Chatfield, M. & Mander, A. The Skillings-Mack test (Friedman test when there are missing data). *Stata J.* **9**, 299–305 (2009).
70. Lun, A.T.L., Richard, A.C. & Marioni, J.C. Testing for differential abundance in mass cytometry data. *Nat. Methods.* **14**, 707–709 (2017).
71. Robinson, M.D., McCarthy, D.J. & Smyth, G.K. edgeR: a Bioconductor package for differential expression analysis of digital gene expression data. *Bioinformatics* **26**, 139–140 (2010).
72. Naumann, U., Luta, G. & Wand, M.P. The curvHDR method for gating flow cytometry samples. *BMC Bioinformatics* **11**, 44 (2010).

73. Hahne, F., *et al.* flowCore: a Bioconductor package for high throughput flow cytometry. *BMC Bioinformatics* **10**, 106 (2009).
74. Duong, T. ks: Kernel Density Estimation and Kernel Discriminant Analysis for Multivariate Data in R. *J. Stat. Softw.* **21,** 1–16 (2007).
75. Duong, T., Goud, B. & Schauer, K. Closed-form density-based framework for automatic detection of cellular morphology changes. *Proc. Natl. Acad. Sci. USA.* **109,** 8382–8387 (2012).
76. Benjamini, Y. & Hochberg, Y. Controlling the False Discovery Rate: A Practical and Powerful Approach to Multiple Testing. *J. R Stat. Soc. Ser. B.* **57,** 289–300 (1995).
77. Diggins, K.E. *et al.* Characterizing cell subsets using marker enrichment modeling. *Nat. Methods.* **14,** 275–278 (2017).
78. Hodges, J.L. & Lehmann, E.L. Estimates of Location Based on Rank Tests. *Ann. Math. Statist.* **34**, 598–611 (1963).
79. Rousseeuw, P. & Croux, C. *Explicit Scale Estimators with High Breakdown point* (1992).
80. Aghaeepour, N. et al. Early immunologic correlates of HIV protection can be identified from computational analysis of complex multivariate T-cell flow cytometry assays. *Bioinformatics*. **28,** 1009–1016 (2012).
81. Aghaeepour, N. *et al.* RchyOptimyx: cellular hierarchy optimization for flow cytometry. *Cytometry A.* **81,** 1022–1030 (2012).

Chapter 4

Exploring translocator 18kDa protein as a marker for measuring microglial immune activation in schizophrenia

Marjolein A.M. Sneeboer[1,2], Thalia van der Doef[1], Manja Litjens[1,2], NBB-PSY[3], J. Melief[1], Elly M. Hol[2,4], René S. Kahn[1,2,5] and Lot D. de Witte[1,5]

[1] Department of Psychiatry, Brain Center Rudolf Magnus, University Medical Center Utrecht, Utrecht University (BCRM-UMCU-UU), 3584 CG Utrecht, The Netherlands
[2] Department of Translational Neuroscience (BCRM-UMCU-UU), 3584 CG Utrecht, The Netherlands
[3] Netherlands Brain Bank for Psychiatry, Meibergdreef 47, 1105 BA Amsterdam, The Netherlands
[4] Neuroimmunology, Netherlands Institute for Neuroscience, An institute of the royal academy of arts and sciences, 1105 BA, Amsterdam, The Netherlands
[5] Department of Psychiatry, Icahn School of Medicine, New York, United States of America.

Manuscript in preparation

Abstract

It has been hypothesized that microglial activation may play an important role in the pathophysiology of schizophrenia. Various studies have therefore examined microglial activation in schizophrenia using positron emission tomography (PET) with radioligands that bind to the translocator 18kDa protein (TSPO) receptor. However, the results of these studies are heterogeneous and the exact link between TSPO expression and microglial activation in schizophrenia is debated. The aim of this study was to explore whether TSPO expression is a marker for microglial activation in patients with schizophrenia. We therefore investigated TSPO mRNA and protein expression in post-mortem brain tissue of patients with schizophrenia and controls. In addition, we studied the regulation of TSPO expression in human activated microglia and monocyte-derived macrophages *in vitro*. Similar expression of *TSPO* was found in patients and controls. In both groups a correlation between *TSPO* mRNA and the expression of microglial activation markers was absent. Furthermore, TSPO protein expression in schizophrenia, determined with immunohistochemistry, was not restricted to microglia, but also expressed in endothelial cells and astrocytes. Besides, *TSPO* expression was not elevated in activated human primary microglia and monocyte-derived macrophages. Our data are in line with previous studies showing that TSPO expression is not increased and is not a specific marker for activated microglia in schizophrenia.

Introduction

Genetic and epidemiological studies have shown an association between schizophrenia and the immune system[1,2]. It has therefore been hypothesized that activated microglia, the immune cells of the brain, are involved in schizophrenia pathogenesis and could be a target for novel therapies[3]. Various studies applied positron emission tomography (PET) with radioligands for the translocator 18kDa protein (TSPO) receptor to measure microglial immune activation in patients with schizophrenia *in vivo*. Several research reports found increased binding of TSPO tracers in schizophrenia in whole brain grey matter and specifically in frontal and temporal regions[4–7]. In contrast, other studies showed equal or decreased binding[8–15]. These results not only raise questions about the occurrence of microglial immune activation in schizophrenia, but also about the sensitivity and specificity of this method for detecting microglia activation in diseases, such as schizophrenia[8–10,16].

TSPO is a mitochondrial protein that is involved in a range of cellular functions, including steroidogenesis, proliferation and apoptosis[17]. TSPO is expressed among various species[18–21] and in many cell types, including myeloid immune cells, such as microglia and macrophages[22]. In rodents, it has been shown that microglial activation leads to increased expression of TSPO and binding of TSPO PET ligands[8,19,23–25]. For example, in a rat model for ischemia, more binding of 3H-PK11195 TSPO in hippocampal CA1 was found to overlap with increased microglial OX-42 expression and astrocytic GFAP immunoreactivity[26]. In humans, binding of TSPO tracers is increased in neuropathological conditions in which neuroinflammation and microglial activation is described, such as Alzheimer's disease[27–29], multiple sclerosis[30–32], epilepsy[33], stroke[34,35] and traumatic brain injury[36]. Also in healthy humans, increased binding potential of TSPO was found 180 minutes after injection with LPS and this was accompanied with increased peripheral cytokine levels and sickness symptoms[37]. In addition, it was shown using autoradiography that the tracers bind primarily to activated microglia or macrophages in these diseases[27,29,32,33]. PET imaging using TSPO tracers has therefore widely been used to measure neuroinflammation, or more specifically to detect microglial activation *in vivo*. However, several papers have shown that TSPO expression in the central nervous system (CNS) is not restricted to microglia, since astrocytes, neurons and endothelial cells also express *TSPO*[8,16,22,38]. Additionally, *in vitro* experiments on TSPO regulation of human myeloid cells show heterogeneous results. One study showed that TSPO expression and binding of TSPO ligands was not increased in activated human macrophages and cultured primary microglia[39], which is in contrast to rodents cells[39]. On the contrary, administration of LPS and IFNγ resulted in increased *TSPO* expression in adult microglia isolated from

post-mortem material of multiple sclerosis patients[40]. Together these studies question whether TSPO can be used as a marker to measure microglial immune activation.

The aim of this study was to explore whether TSPO expression is altered in schizophrenia and can be used as a valid marker to measure human microglial activation in this disease. In post-mortem brain tissue of patients with schizophrenia and controls we analyzed the expression of TSPO and the relation with microglia, inflammatory and astrocytic markers. Previous studies on the regulation of TSPO on activated human myeloid cells were performed on cultured microglia[8,39–41]. However, culturing microglia drastically changes the phenotype of microglia and might influence their ability to regulate TSPO expression upon inflammatory conditions[42]. Therefore, we also investigated the regulation of *TSPO* expression on acutely isolated human primary microglia that were challenged with different pro- and anti-inflammatory compounds and compared this with monocyte-derived macrophages (mo-Mϕ).

Material and methods

Human brain tissue

For this study we selected the medial frontal gyrus (MFG) as region of interest (ROI), since this region has frequently been associated with schizophrenia pathology[43,44]. Snap frozen and paraffin post-mortem tissue of the MFG from patients with schizophrenia (snap frozen N=8, paraffin embedded N=5) and controls (snap frozen N=10; paraffin embedded N=7), defined as subjects without a diagnosis of a psychiatric or neurologic disorder, was provided by the Netherlands Brain Bank (NBB; www.hersenbank.nl). For the isolation of microglia, fresh post-mortem brain tissue of the MFG and corpus callosum (CC) from controls as well as donors with a neurological disorder (N=provided by the NBB. We selected these regions because we and others previously showed that microglia in cortical and subcortical regions are phenotypically different and respond differently to inflammatory stimuli[45–47]. Informed consent was obtained by the NBB for brain autopsy and donation and the usage of clinical information for research purposes (Table 1 and Supplementary table 1 for clinicopathological information). In addition, we extracted expression data from a previously published microarray study[48] on post-mortem tissue of the dorsolateral prefrontal cortex from 34 patients with schizophrenia and 33 unaffected controls of the Stanley Medical Research Institute, Rockville, MD, USA (http://www.stanleyresearch.org). The clinical information of both cohorts are described in table 1.

Table 1: Summary of clinical information and post-mortem variables of the study

		Control (N=10)	Schizophrenia (N=8)
mRNA expression	Age (years)*	80.8 ± 12.2	64.0 ± 7.4
NBB cohort	Sex (M:F)	6:4	5:3
	PMD (minutes)	467 ± 231	614 ± 283
	pH	6.58 ± 0.31	6.70 ± 0.64
		Control (N=33)	**Schizophrenia (N=34)**
mRNA expression	Age years (range)	44.1 (31-59)	42.6 (19-59)
Stanley cohort	Sex M:F	26:9	26:9
	PMD minutes (range)	1764 (540-3480)	1878 (540 - 4800)
	pH (range)	6.60 (6.0-7.0)	6.50 (5.9-6.9)
		Control (N=7)	**Schizophrenia (N=5)**
Immunofluorescent microscopy	Age (years)	69.6 ± 11.1	68.6 ± 10.0
NBB cohort	Sex (M:F)	5:2	3:2
	PMD (minutes)	628 ± 478	1226 ± 1541
	pH	6.60 ± 0.17	6.55 ± 0.35
		Control (N=7)	
Human microglia	Age (years)	81.3 ± 12.5	
NBB cohort	Sex (M:F)	4:3	
	PMD (minutes)	429 ± 61.4	
	pH	6.67 ± 0.08	

Summary of the clinical information (age and sex) and post-mortem variables (post-mortem delay (PMD) and pH) of donors used in the study. Information is separated per experimental category. Numbers in the NBB cohort represent mean ± standard deviation, numbers in the Stanley cohort represent mean (range). M = males, F = females. *significantly different between controls and patients with schizophrenia.

Table 2: Correlation between mRNA expression of *TSPO* and several microglial genes

		Stanley Foundation				Netherlands Brain Bank			
		Control (N=33)		Schizophrenia (N=34)		Control (N=10)		Schizophrenia (N=8)	
	Marker	*rho*	*p*	*rho*	*p*	*rho*	*p*	*rho*	*p*
Microglia general	*AIF1*	-0.378	0.030	-0.221	0.208	0.042	0.918	0.036	0.964
	CX3CR1	-0.188	0.278	0.048	0.795	-0.370	0.296	0.107	0.840
	ITGAM	0.290	0.096	0.155	0.396	0.714	0.058	-1.000	0.083
Microglia activation	*CD163*	-0.093	0.608	-0.056	0.751	-0.310	0.462	-0.100	0.950
	HLA-DRA	0.185	0.302	-0.244	0.165	-0.273	0.448	0.607	0.167
	IL1B	0.262	0.140	-0.149	0.400	-0.261	0.470	0.179	0.713

Spearman's rank coefficients and *p*-values for the correlation between *TSPO* and general microglial genes (*AIF1*, *CX3CR1*, *ITGAM*) and microglial immune activation genes (*CD163*, *HLA-DRA*, *IL1B*) in middle frontal cortex (MFG) of two different cohorts (Stanley foundation and Netherlands Brain Bank).

Gene expression analysis

Frozen brain tissue of the MFG was sectioned (50 µM), grey and white matter was separated manually at the cryostat and lysed with TRIzol reagent (Invitrogen, Carlsbad, CA, USA). RNA extraction and cDNA production for brain tissue samples, primary microglia and mo-Mϕ were performed as described before[49]. Quantitative real-time polymerase chain reaction (qPCR) was performed on a QuantStudio™ 6 Flex Real-Time PCR System (Life Technologies Corporation, NY, USA). Per reaction, 3.5ng input of cDNA was mixed with Milli-Q water, 5µL SYBRgreen PCR Master Mix (Roche; Life Technologies Corporation, Grand Island, NY, USA), and 1µL primer mix (2 pmol/mL; supplementary table 2) until a final volume of 11µL. All primers were intron-spanning and designed with the online tool of NCBI. The following cycle conditions were used: 50°C for 2 minutes, 95°C for 10 minutes, 40 cycles at 95°C of 15 seconds and at 60°C for 60 seconds. Gene expression was normalized to reference genes that were most stable in brain tissue (Glyceraldehyde 3-phosphate dehydrogenase (*GAPDH)*, β-actin *(ACTB)* and Succinate dehydrogenase complex, subunit A (*SDHA*)), primary microglia (*GAPDH*) and mo-Mϕ (*GAPDH*). Normalization was performed according to the ΔΔCT method[50]. Non-detectable values (ND) were incorporated in the analysis as a CT value of 40 and shown in the graphs. The *TSPO* response after stimulation was calculated as fold change by dividing the normalized gene expression of the stimulated sample by the normalized gene expression of the unstimulated sample.

Immunofluorescence microscopy

Paraffin embedded tissue of the MFG of 5 patients with schizophrenia and 7 controls was sectioned (7µm) on a microtome (Leica Microsystems) and mounted on glass slides. Sections were deparaffinized via a standard xylene and alcohol series and washed in phosphate-buffered saline (PBS) with 0.05% Tween (Sigma-Aldrich, the Netherlands) before blocking of endogenous peroxidase activity with PBS, 1% H_2O_2 (Sigma-Aldrich, the Netherlands) for 10 minutes. Antigen retrieval was promoted by heating the sections in 0.01mM citrate buffer (Merck, Darmstadt, Germany) with 0.05% Tween-20 (Sigma-Aldrich, the Netherlands), pH 6.0 for 15 minutes. Subsequently, non-specific binding was blocked with PBS with 10% normal horse serum (NHS, Thermo Fisher Scientific, Massachusetts, USA), 0.1% BSA, 0.2% Triton (Sigma-Aldrich, the Netherlands). Polyclonal rabbit anti-human TSPO (1:100, OriGene) was combined with polyclonal goat anti-human ionized calcium-binding adapter molecule-1 (IBA1; 1:1000) Ab5076, Abcam) or monoclonal mouse anti-human glial fibrillary acidic protein (GFAP; 1:8000, G3893, Abcam) for microglia and astrocytes respectively. All antibodies were diluted in PBS, 10% NHS, 0.2% Triton, 0.1% BSA and incubated at 4°C overnight. Next day, the goat-anti-rabbit biotin (1:700, Jackson ImmunoResearch Laboratories Inc.) and 488 labeled streptavidin (1:700, Jackson ImmunoResearch Laboratories Inc.) were coupled to the TSPO antibody, whereas secondary donkey-anti-goat and donkey-anti-mouse Cy3 (1:700, Jackson ImmunoResearch Laboratories Inc.) antibodies were used for IBA1 and GFAP (RT for 45 minutes). Hoechst (1:1000, Thermo Fisher Scientific, Massachusetts, USA) was used as nuclear reagent. After staining procedure, the sections were mounted in Mowiol, visualized under a Zeiss AxioScope A1 and analyzed with open source program ImageJ.

Isolation of human primary microglia

Human primary microglia (primary) were isolated from the MFG (N=7) and the CC (N=6) of control donors (Supplementary table 1). The isolation was started within 2 to 24 hours after autopsy. 2-10 grams of frontal tissue was first mechanically dissociated through a metal sieve in a glucose- potassium-sodium buffer (GKN-BSA; 8g/L NaCl, 0.4g/L KCl, 1.77g/L Na2HPO4.2H2O, 0.69 g/L NaH2PO4.H2O, 2 g/L D-(1)- glucose, 0.3% bovine serum albumin (BSA, Sigma-Aldrich, Zwijndrecht, the Netherlands); pH 7.4) and supplemented with collagenase Type I (3700 units/ mL; Worthington, Lakewood, NJ, USA) and DNase I (200 µg/mL; Roche Diagnostics GmbH) at 37°C for 60 minutes while shaking. White matter corpus callosum tissue was incubated with 0.2% Trypsin (Sigma-Aldrich, Zwijndrecht, the Netherlands) for 30 minutes and 10 mg/mL DNase I for an additional 10 minutes while shaking. Fetal calf serum (FCS; Gibco Life technologies, Massachusetts) was finally supplemented to inactivate Trypsin. Suspension was put over a 100µM cell strainer and washed with GKN-BSA buffer (1800 rpm, 4°C, brake 4, 10 minutes) before the pellet was resuspended in 20mL GKN-BSA buffer. 10mL of Percoll (Amersham, GE Healthcare) was added drop wise and tissue was centrifuged at 4°C, 4000 rpm with fast acceleration and brake 4 for 30 minutes. Three different layers were observed: upper layer containing myelin, a lower erythrocyte layer and the middle layer containing different cell types including microglia. The middle layer was carefully taken out without disturbing the other layers and washed first with GKN-BSA buffer, followed by a magnetic-activated cell sorting (MACS) buffer (PBS, 1% heat-inactivated FCS; 2mM EDTA; 1500 rpm, 10°C, 10 minutes). Microglia were positively selected with CD11b conjugated magnetic microbeads (Miltenyi Biotec GmbH, Bergisch Gladbach, Germany) according to manufacturer's protocol, which resulted in a 99% pure microglia population as analyzed by flow cytometry. Microglia were lysed in TRIzol reagent or cultured in a poly-L-lysine coated 96-wells flat bottom plate (Greiner Bio-One) at a density of 1.0 x 10^5 cells in in a total volume of 200 µL Rosswell-Park-Memorial-Institute medium (RPMI; Gibco Life technologies, Massachusetts) supplemented with 10% FCS, 2mM L-glutamine (Gibco Life technologies, Massachusetts), 1% penicillin-streptomycin (p/s; Gibco Life technologies, Massachusetts) and 100ng/ml interleukin-34 (IL-34; Miltenyi Biotech, Bergisch Gladbach, Germany).

Monocyte cell isolation and mo-Mϕ differentiation

Primary microglia are mildly activated upon isolation and only a limited number of cells can be retrieved from post-mortem brain tissue, thereby restricting the number of functional experiments. In addition to primary microglia, we therefore also studied the regulation of TSPO on monocyte-derived macrophages (mo-Mϕ), a cell type from the same myeloid family that shows many resemblances with microglia[46]. Peripheral blood mononuclear cells (PBMCs) of 11 controls were isolated as previously described[49]. In short, PBMCs were subtracted from buffy coats (Sanquin, the Netherlands) by Ficoll density gradient separation (Ficoll Paque plus, GE Healthcare). After subtracting monocytes by magnetic CD14 microbeads separation (Miltenyi Biotech, Bergisch Gladbach, Germany), the cells were plated in a 48-wells flat bottom plate (Corning, New York, NY) in RPMI medium containing 1% p/s, 2mM L-glutamine and 10% human AB serum (Sanquin, the Netherlands) for 7 days to differentiate these cells towards a macrophage phenotype.

Stimulation of primary microglia and mo-Mϕ

To study the regulation of *TSPO* mRNA expression upon stimulation with different kinds of inflammatory stimuli we exposed primary microglia isolated from the MFG (N=7) and CC (N=6) and mo-Mϕ (n=11) to 100 ng/mL lipopolysaccharide (LPS) from *Eschericia coli* 0111:B4 (Sigma-Aldrich, Zwijndrecht, the Netherlands) for 6 hours or 1 μM dexamethasone (Sigma-Aldrich, Zwijndrecht, the Netherlands) and 40 ng/mL interleukin-4 (IL-4; Peprotech, London, UK) for 72 hours. Cells were lysed in TRIzol reagent. TSPO protein expression was studied by stimulating mo-Mϕ with 100 ng/mL LPS, 1 μM dexamethasone or 40 ng/mL IL-4 for 24 and 72 hours. After stimulation cells were harvested and used for flow cytometry.

Flow cytometry

Stimulated mo-Mϕ were fixed and permeabilized using the Cytofix/Cytoperm kit according to manufacturer's protocol (BD bioscience). The cells were stained with rabbit anti-human TSPO (ab109497, Abcam, Cambridge, UK) or purified rabbit IgG isotype (SAB4600055, Sigma-Aldrich, Zwijndrecht, the Netherlands), followed by Alexa 488 secondary antibody. The stimulated mo-Mϕ were processed on a BD FACS Calibur (Becton Dickinson). Relative geometric mean fluorescence intensity (MFI) was calculated by subtracting geoMFI of the $TSPO^+$ staining from the geoMFI of the isotype antigen staining. For fold change the MFI of stimulated cells was divided by the MFI of unstimulated cells.

Statistics

Statistical analysis was performed with GraphPad Prism software (version 5) and IBM SPSS Statistics (version 23). Spearman's rho was calculated to study correlations, whereas a Mann-Whitney U test was used to test differences in mRNA expression profiles. Bonferroni test was used to correct for Type I error and p-values <0.05 were considered as statistically significant.

Results

TSPO expression not increased in post-mortem brain tissue

The mRNA expression of *TSPO* was measured in grey and white matter post-mortem brain tissue of the MFG of 8 patients with schizophrenia and 10 controls. We found a similar expression of *TSPO* mRNA in patients with schizophrenia compared to controls, irrespective of grey (SCZ mean = 0.0021; CTRL mean = 0.0022) or white matter (SCZ mean = 0.0030, control mean = 0.004) (Figure 1). To study if confounder effects could explain the absence of different *TSPO* expression in schizophrenia, we looked into the correlation between *TSPO* and the variables age, sex, PMD and pH in the NBB cohort. None of the variables correlated with the mRNA expression of *TSPO* (Supplementary table 3). Therefore no correction for these confounders was applied in further analysis. Additionally, we investigated *TSPO* expression in a previously published microarray data of the Stanley Medical Research Institute on the dorsolateral prefrontal cortex from 34 patients with schizophrenia and 33 controls. Also in this cohort *TSPO* expression was not changed between patients with schizophrenia (mean = 7.87) and controls (mean = 7.75)[51].

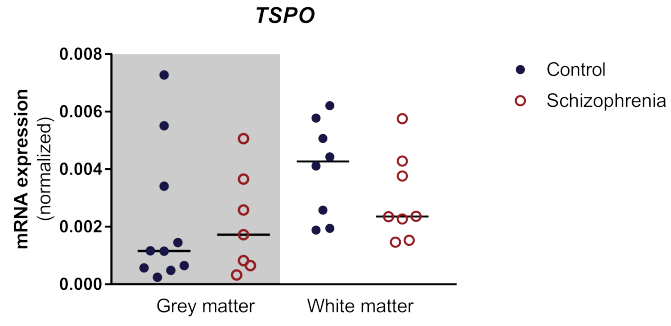

Figure 1: Expression of *TSPO* mRNA in post-mortem brain tissue of patients with schizophrenia. mRNA expression of *TSPO* was measured in grey and white matter from the middle frontal gyrus (MFG) in patients with schizophrenia (N=8, red circles) and controls (N=10, blue dots) by qPCR. *TSPO* gene expression was normalized to reference genes *ACTB*, *GAPDH* and *SDHA* with the ΔΔCT method[50].

TSPO expression does not correlate with expression of microglia genes

We then assessed whether *TSPO* expression was related to expression of general microglia genes (*AIF1, CX3CR1, ITGAM)* and genes upregulated in different types of activated microglia *(CD163, HLA-DRA, IL1B)*. These are common known genes in myeloid cell biology, defining both general microglial genes and genes involved in activation of the cells. The mRNA expression of the different microglial immune activation markers was not significantly different between patients and controls (figure 2a), as well as the expression of general microglial markers (Figure 2b). In addition, in the NBB cohort as well as the previously published dataset of the Stanley Medical Research Institute, no positive correlations were found between *TSPO* expression and expression of any of the microglial genes in either patients or controls (Table 2). In the microarray dataset the only significant association was a negative correlation between *AIF1* and *TSPO* in controls. However, when correcting for multiple testing, significance was not preserved.

TSPO expression is expressed on microglia and astrocytes in schizophrenia

Subsequently, we assessed the expression of TSPO on various cell types in the MFG of patients with schizophrenia (N=5) and controls (N= 7) by staining paraffin embedded tissue sections with antibodies recognizing TSPO, microglial marker IBA1 and astrocytic marker GFAP. For both patients and controls we found TSPO expression in IBA1$^+$ cells, defining microglia (Figure 3a, closed arrow) and GFAP$^+$ cells, defining astrocytes (Figure 3b, closed arrow). Furthermore, TSPO positivity was present in the vasculature of the brain tissue (Figure 3a, open arrow). TSPO$^+$/IBA1$^+$ cells had both ramified (immature) and amoeboid morphologies in patients with schizophrenia and controls. No difference in the distribution of TSPO expression was found between patients and controls.

TSPO expression is not affected by inflammatory activation

Finally, we assessed whether *TSPO* is upregulated when we stimulate human primary microglia that were acutely isolated from post-mortem brain tissue from the MFG and the CC, as well as mo-Mϕ. Human microglia and mo-Mϕ were challenged with LPS (24 hours), dexamethasone and IL-4 (72 hours) to induce different types of microglial/macrophage immune activation as confirmed by the upregulation of *TNF, CD163* and *CD200R1* respectively (Figure 4a-c, grey lines). LPS activates myeloid cells via toll like receptor 4 (TLR4) and stimulates the secretion of pro-inflammatory cytokines, such as interleukin-6 and TNFα. On the other hand, dexamethasone and IL-4 induce a more anti-inflammatory profile, supporting cell survival and dampening inflammation. Stimulation with these three compounds did not result in the upregulation or downregulation of *TSPO* mRNA expression in microglia of both MFG and CC or in mo-Mϕ (Figure 4a-c black lines). Additionally, we analyzed *TSPO* protein expression in mo-Mϕ after stimulation by flow cytometry. TSPO was not upregulated after 24 hours (Figure 4d) and 72 hours (data not shown) of stimulation.

a

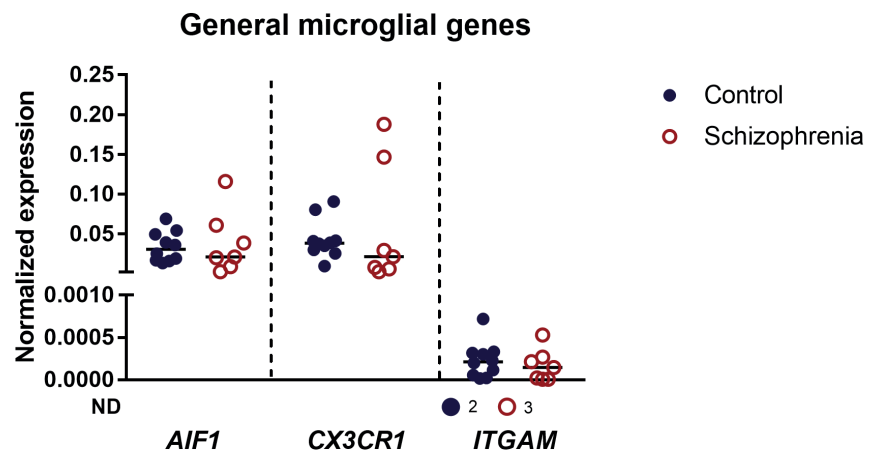

b

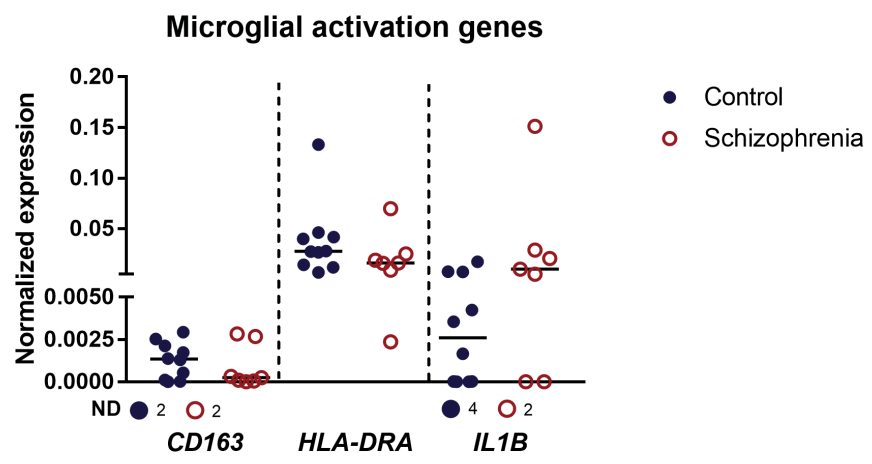

Figure 2: mRNA expression of microglial genes in the MFG of patients with schizophrenia and controls.

mRNA expression of microglial genes was determined in brain tissue of the MFG of patients with schizophrenia (N=8, red circles) and controls (N=10, blue dots) by qPCR. a) mRNA expression of general microglial markers *AIF1*, *CX3CR1*, and *ITGAM*. b) mRNA expression of genes involved in microglial immune activation (*CD163*, *HLA-DRA,* and *IL1B*). mRNA expression was normalized to reference genes *GAPDH*, *ACTB,* and *SDHA*. ND = non-detectable values.

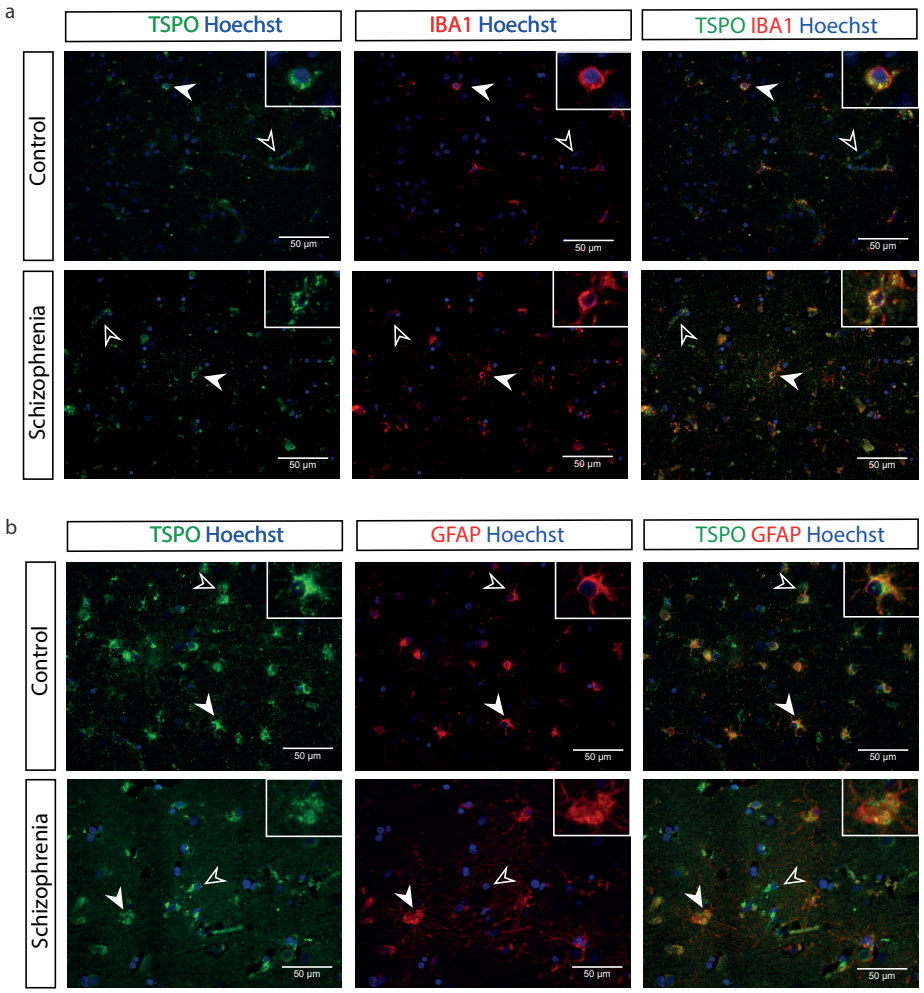

Figure 3: TSPO protein expression in microglia (A) and astrocytes (B) in controls and patients with schizophrenia.
Immunohistochemistry staining of TSPO with IBA1 (N=5; a) or GFAP (N=5; a) in paraffin embedded tissue of the medial frontal gyrus (MFG) of controls and patients with schizophrenia. Closed arrowheads and enlargement represent double positive cells for TSPO and IBA1 ($TSPO^+/IBA1^+$, a) or TSPO and GFAP ($TSPO^+/GFAP^+$, b), whereas open arrowheads depict single $TSPO^+$ cells without $IBA1^+$ ($TSPO^+/IBA^-$) or $TSPO^+$ without $GFAP^+$ ($TSPO^+/GFAP^-$) staining.

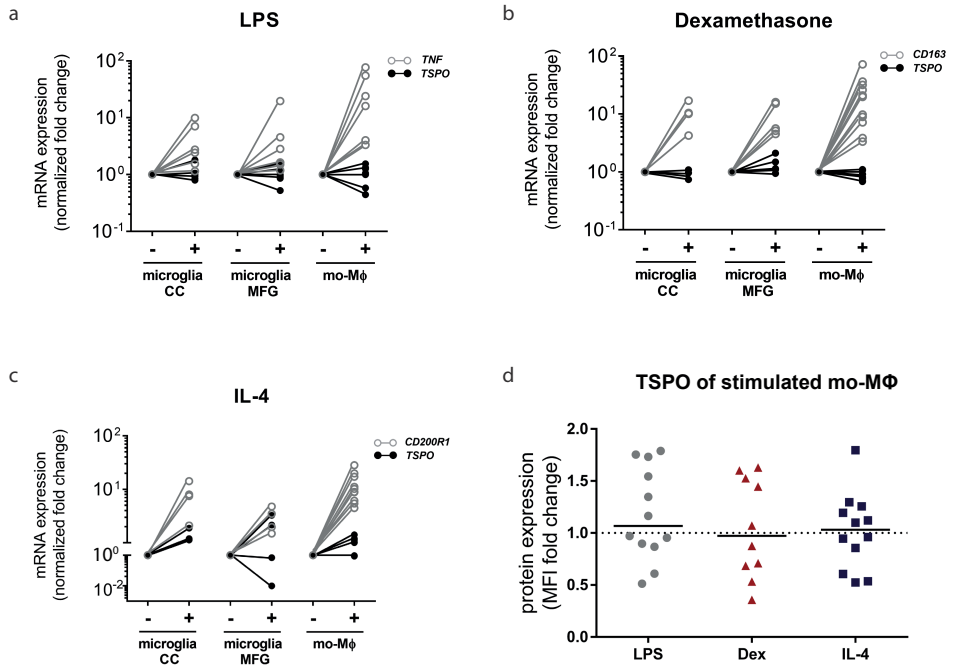

Figure 4: TSPO expression in primary microglia and mo-Mϕ after stimulation.
TSPO mRNA expression was measured in control microglia of corpus callosum (CC; N=6) and middle frontal gyrus (MFG; N=7) and mo-Mϕ (N=11) after stimulation with LPS (a), dexamethasone (b) and IL-4 (c). mRNA expression of the positive control of the stimulation is depicted in light grey, whereas *TSPO* is depicted in black. mRNA expression was normalized to *GAPDH* as reference gene. d) TSPO protein expression in mo-Mϕ by flow cytometry analysis after stimulation with LPS (grey dots; N=12), dexamethasone (red triangles; N=10) and IL-4 (blue squares; N=12).

Discussion

The aim of this study was to assess whether TSPO expression is elevated in schizophrenia, as was suggested in some of the published PET studies. We found that mRNA levels of *TSPO* are similar expressed in the MFG of patients with schizophrenia and controls and that *TSPO* expression does not correlate with the expression of general microglial markers and microglial activation markers. In addition, we showed that TSPO protein expression is not only expressed on microglia, but also on astrocytes and the vasculature in schizophrenia and controls. Furthermore, *TSPO* mRNA expression is not increased in immune challenged acutely isolated human primary microglia from the MFG and CC and mo-Mϕ of controls.

Our *TSPO* expression data in post-mortem brain tissue are consistent with the more recent TSPO PET studies that showed a lack of increased binding of TSPO PET tracers in schizophrenia[8–15]. They are also supported by an older ^{3}H-PK11195 binding study on post-mortem brain tissue of 13 patients with schizophrenia and 10 controls that showed no change in binding in various brain regions, including the prefrontal cortex[52]. Furthermore, also in a large RNA sequencing study performed on dorsolateral prefrontal cortex (144 patients and 196 controls) and hippocampus (83 patients and 187 controls) *TSPO* expression was not increased in schizophrenia[53].

The lack of an association between the expression of *TSPO* and microglial genes related to inflammatory processes (*CD163, HLA-DRA* and *IL1B*) indicates that microglial immune activation is not directly linked to *TSPO* expression in patients or controls. This is further substantiated by our results on immune activated acutely isolated human primary microglia and mo-Mϕ. After inducing an inflammatory phenotype, *TSPO* expression remained unchanged, irrespective of cortical or white matter microglia. Comparable results for human microglia and mo-Mϕ have been found by Owen et al. and Narayan et al., showing that expression of TSPO and binding of TSPO ligands is increased upon activation of rodent microglia, but not human microglia and macrophages[39,41]. In contrary, stimulation of human microglia with IFNγ increased TSPO expression five fold[40]. Beckers et al. recently reported that TSPO only highlights pro-inflammatory rodent microglia and is not induced by anti-inflammatory stimuli[54]. However, other groups have proposed an anti-inflammatory role for *TSPO*[23,41]. An important difference between these studies and our data is the fact that the microglia in the earlier mentioned studies have been in culture for 5-7 days before supplementing the inflammatory compounds. This is in contrast with our culture conditions, in which we use acutely isolated microglia that were stimulated directly the next day after isolation. It is known that microglia change phenotype rapidly in culture conditions. Key microglial genes, like P2RY12 and CX3CR1, and genes involved in immune regulation showed decreased expression after 7 days of culture[42]. This could indicate that the induction of the inflammatory phenotype was less efficient in cultured microglia compared to our acutely isolated microglia. Furthermore, there is a clear difference between the regulation of TSPO between rodent and human microglia. Several reasons could account for these differences. For example, the expression of TLR4 is more abundant in rodent microglia compared to human cells[55]. It might therefore be possible that the LPS stimulation in rodent microglia is more effective in inducing *TSPO* expression *in vitro* and *in vivo*.

Our results demonstrating the expression of *TSPO* in a variety of cell types in the CNS in both patients and controls are consistent with the study of Notter et al. and several

other studies[8,22]. These studies showed that *TSPO* expression and binding of TSPO tracers is not restricted to microglia, but is also present in astrocytes and endothelial cells in the vasculature. In post-mortem brain tissue of patients with schizophrenia and controls we found expression of TSPO on microglia as well as astrocytes and the vasculature. Our results in schizophrenia and controls are in contrast to findings on post-mortem studies of other neuropathological conditions[56]. For multiple sclerosis, Alzheimer's disease and ischemic stroke, it has been shown that *TSPO* is mainly expressed in microglia or macrophages[38,57–59]. In addition, in neurodegenerative disorders a positive correlation has been found between TSPO binding and elevated peripheral cytokine levels, which has not been established in psychiatric disorders[14,16]. These data suggest that TSPO expression is increased in microglia and macrophages in CNS disorders with a clear neuroinflammatory component, but not in conditions with subtle or absence of inflammation, including controls and patients with schizophrenia.

Although data from our post-mortem study is valuable for the discussion about the interpretation of PET studies with TSPO ligands, it is important to mention some crucial differences between the two approaches. TSPO PET studies have mainly been conducted on early stage patients with schizophrenia, generally have more information on potential confounder factors and the patient and control groups were more homogeneous in terms of age, sex and comorbidity. Postmortem studies generally include patients at later stages of the disease, are influenced by many pre- and post-mortem confounders and information on diagnosis, symptom severity and potential confounding factors is often absent or unclear. Directly comparing the results from post-mortem and PET studies is therefore difficult. Therefore, performing a TSPO PET study on patients at the end stage of disease would be informative to compare post-mortem outcomes with PET study data.

All together our results suggest that TSPO is not a specific marker for microglial immune activation and that PET binding data with TSPO ligands should be interpreted with care. This is particularly pertinent when using PET imaging in psychiatric and neurologic disorders without excessive microglial activation and subtle or sporadic neuroinflammation, as is thought of schizophrenia. To better interpret the findings of PET imaging with tracers binding to TSPO in schizophrenia, we propose a more detailed study of the underlying cellular mechanisms of TSPO regulation and alterations in other TSPO-expressing cells, such as astrocytes and endothelial cells. Further, more research is needed into the function of TSPO in the human brain, both physiological and pathological. As indicated, increased TSPO expression does not necessarily indicate inflammatory processes, since TSPO is also related to oxidative

stress, apoptosis and energy production[16]. Moreover, a combination of TSPO and other neuroinflammatory markers would be helpful to elucidate the origin of the TSPO binding in schizophrenia *in vivo*. Given the differences in TSPO expression between human and animal model studies, we recommend greater use of human tissue to elucidate cellular mechanisms. Regarding the hypothesis of the presence of neuroinflammation and microglial activation in schizophrenia, we propose to study the density and morphology of microglial cells and phenotypical characteristics of human isolated microglia with RNAseq. In addition, these studies emphasize the need for the development of specific tracers to study human microglial activation *in vivo,* preferably PET tracers that are able to distinguish between different inflammatory subpopulations.

Acknowledgements

This study is supported by a 2014 NARSAD Young Investigator Grant from the Brain & Behavior Research Foundation and by the Virgo Consortium, funded by the Dutch government project number FES0908. Furthermore, this study was supported by the psychiatric donor program of the Netherlands Brain Bank (NBB-Psy), which is supported by the Netherlands Organization for Scientific Research (NWO). The authors thank the team of the Netherlands Brain Bank for their excellent services (www.brainbank.nl).

Conflict of interest

The authors declare that they have no conflict of interest.

References

1. Ripke, S. *et al.* Biological insights from 108 schizophrenia-associated genetic loci. *Nature* **511,** 421–427 (2014).
2. Benros, M. E., Mortensen, P. B. & Eaton, W. W. Autoimmune diseases and infections as risk factors for schizophrenia. *Ann. N. Y. Acad. Sci.* **1262,** 56–66 (2012).
3. Howes, O. D. & McCutcheon, R. Inflammation and the neural diathesis-stress hypothesis of schizophrenia: a reconceptualization. *Transl. Psychiatry* **7,** e1024 (2017).
4. Doorduin, J. *et al.* Neuroinflammation in schizophrenia-related psychosis: a PET study. *J. Nucl. Med.* **50,** 1801–7 (2009).
5. van Berckel, B. N. *et al.* Microglia Activation in Recent-Onset Schizophrenia: A Quantitative (R)-[11C]PK11195 Positron Emission Tomography Study. *Biol. Psychiatry* **64,** 820–822 (2008).
6. Bloomfield, P. S. *et al.* Microglial Activity in People at Ultra High Risk of Psychosis and in Schizophrenia: An [11 C]PBR28 PET Brain Imaging Study. *Am. J. Psychiatry* **173,** 44–52 (2016).
7. Holmes, S. E. *et al.* In vivo imaging of brain microglial activity in antipsychotic-free and medicated schizophrenia: A [11C](R)-PK11195 positron emission tomography study. *Mol. Psychiatry* **21,** 1672–1679 (2016).
8. Notter, T. *et al.* Translational evaluation of translocator protein as a marker of neuroinflammation in schizophrenia. *Mol. Psychiatry* **23,** 323–334 (2018).
9. Collste, K. *et al.* Lower levels of the glial cell marker TSPO in drug-naive first-episode psychosis patients as measured using PET and [11C]PBR28. *Mol. Psychiatry* **22,** 850–856 (2017).
10. Hafizi, S. *et al.* Imaging Microglial Activation in Untreated First-Episode Psychosis: A PET Study With [18 F]FEPPA. *Am. J. Psychiatry* **174,** 118–124 (2017).
11. van der Doef, T. F. *et al.* In vivo (R)-[11C]PK11195 PET imaging of 18kDa translocator protein in recent onset psychosis. *npj Schizophr.* **2,** 16031 (2016).
12. Takano, A. *et al.* Peripheral benzodiazepine receptors in patients with chronic schizophrenia: a PET study with [11C]DAA1106. *Int. J. Neuropsychopharmacol.* **13,** 943–950 (2010).
13. Kenk, M. *et al.* Imaging neuroinflammation in gray and white matter in schizophrenia: An in-vivo PET study with [18 F]-FEPPA. *Schizophr. Bull.* **41,** 85–93 (2015).
14. Coughlin, J. M. *et al.* In vivo markers of inflammatory response in recent-onset schizophrenia: a combined study using [(11)C]DPA-713 PET and analysis of CSF and plasma. *Transl. Psychiatry* **6,** e777 (2016).
15. Di Biase, M. A. *et al.* PET imaging of putative microglial activation in individuals at ultra-high risk for psychosis, recently diagnosed and chronically ill with schizophrenia. *Transl. Psychiatry* **7,** e1225 (2017).
16. Notter, T., Coughlin, J. M., Sawa, A. & Meyer, U. Reconceptualization of translocator protein as a biomarker of neuroinflammation in psychiatry. *Mol. Psychiatry* **23,** 36–47 (2018).
17. Gut, P., Zweckstetter, M. & Banati, R. B. Lost in translocation: the functions of the 18-kD translocator protein. *Trends Endocrinol. Metab.* **26,** 349–356 (2015).
18. Shao, X. *et al.* Imaging of carrageenan-induced local inflammation and adjuvant-induced systemic arthritis with [(11)C]PBR28 PET. *Nucl. Med. Biol.* **40,** 906–11 (2013).
19. Ory, D. *et al.* PET imaging of TSPO in a rat model of local neuroinflammation induced by intracerebral injection of lipopolysaccharide. *Nucl. Med. Biol.* **42,** 753–61 (2015).
20. Dickens, A. M. *et al.* Detection of microglial activation in an acute model of neuroinflammation using PET and radiotracers 11C-(R)-PK11195 and 18F-GE-180. *J. Nucl. Med.* **55,** 466–72 (2014).
21. Hannestad, J. *et al.* Endotoxin-induced systemic inflammation activates microglia: [11C]PBR28 positron emission tomography in nonhuman primates. *Neuroimage* **63,** 232–239 (2012).
22. Woods, M. J. & Williams, D. C. Multiple forms and locations for the peripheral-type benzodiazepine receptor. *Biochem. Pharmacol.* **52,** 1805–1814 (1996).

23. Bae, K.-R., Shim, H.-J., Balu, D., Kim, S. R. & Yu, S.-W. Translocator protein 18 kDa negatively regulates inflammation in microglia. *J. Neuroimmune Pharmacol.* **9,** 424–37 (2014).
24. Zhao, Y.-Y. *et al.* TSPO-specific ligand vinpocetine exerts a neuroprotective effect by suppressing microglial inflammation. *Neuron Glia Biol.* **7,** 187–97 (2011).
25. Karlstetter, M. *et al.* Translocator protein (18 kDa) (TSPO) is expressed in reactive retinal microglia and modulates microglial inflammation and phagocytosis. *J. Neuroinflammation* **11,** 3 (2014).
26. Stephenson, D. T. *et al.* Peripheral benzodiazepine receptors are colocalized with activated microglia following transient global forebrain ischemia in the rat. *J. Neurosci.* **15,** 5263–74 (1995).
27. Cagnin, A. *et al.* In-vivo measurement of activated microglia in dementia. *Lancet (London, England)* **358,** 461–7 (2001).
28. Kreisl, W. C. *et al.* In vivo radioligand binding to translocator protein correlates with severity of Alzheimer's disease. *Brain* **136,** 2228–38 (2013).
29. Gulyás, B. *et al.* A comparative autoradiography study in post mortem whole hemisphere human brain slices taken from Alzheimer patients and age-matched controls using two radiolabelled DAA1106 analogues with high affinity to the peripheral benzodiazepine receptor (PBR) syst. *Neurochem. Int.* **54,** 28–36 (2009).
30. Colasanti, A. *et al.* Hippocampal Neuroinflammation, Functional Connectivity, and Depressive Symptoms in Multiple Sclerosis. *Biol. Psychiatry* **80,** 62–72 (2016).
31. Herranz, E. *et al.* Neuroinflammatory component of gray matter pathology in multiple sclerosis. *Ann. Neurol.* **80,** 776–790 (2016).
32. Banati, R. B. *et al.* The peripheral benzodiazepine binding site in the brain in multiple sclerosis: quantitative in vivo imaging of microglia as a measure of disease activity. *Brain* **123 (Pt 1,** 2321–37 (2000).
33. Brackhan, M. *et al.* Serial Quantitative TSPO-Targeted PET Reveals Peak Microglial Activation up to 2 Weeks After an Epileptogenic Brain Insult. *J. Nucl. Med.* **57,** 1302–1308 (2016).
34. Price, C. J. S. *et al.* Intrinsic activated microglia map to the peri-infarct zone in the subacute phase of ischemic stroke. *Stroke* **37,** 1749–53 (2006).
35. Thiel, A. *et al.* The temporal dynamics of poststroke neuroinflammation: a longitudinal diffusion tensor imaging-guided PET study with 11C-PK11195 in acute subcortical stroke. *J. Nucl. Med.* **51,** 1404–12 (2010).
36. Coughlin, J. M. *et al.* Neuroinflammation and brain atrophy in former NFL players: An in vivo multimodal imaging pilot study. *Neurobiol. Dis.* **74,** 58–65 (2015).
37. Sandiego, C. M. *et al.* Imaging robust microglial activation after lipopolysaccharide administration in humans with PET. *Proc. Natl. Acad. Sci.* **112,** 12468–12473 (2015).
38. Cosenza-Nashat, M. *et al.* Expression of the translocator protein of 18 kDa by microglia, macrophages and astrocytes based on immunohistochemical localization in abnormal human brain. *Neuropathol Appl Neurobiol* **35,** 306–328 (2009).
39. Owen, D. R. *et al.* Pro-inflammatory activation of primary microglia and macrophages increases 18 kDa translocator protein expression in rodents but not humans. *J. Cereb. Blood Flow Metab.* **37,** 2679–2690 (2017).
40. Beaino, W. *et al.* Purinergic receptors P2Y12R and P2X7R: potential targets for PET imaging of microglia phenotypes in multiple sclerosis. *J. Neuroinflammation* **14,** 259 (2017).
41. Narayan, N. *et al.* The macrophage marker translocator protein (TSPO) is down-regulated on pro-inflammatory 'M1' human macrophages. *PLoS One* **12,** 1–19 (2017).
42. Gosselin, D. *et al.* An environment-dependent transcriptional network specifies human microglia identity. *Science* **356,** (2017).
43. Smieskova, R. *et al.* Neuroimaging predictors of transition to psychosis--a systematic review and meta-analysis. *Neurosci. Biobehav. Rev.* **34,** 1207–22 (2010).

44. Fusar-Poli, P. *et al.* Neuroanatomy of vulnerability to psychosis: a voxel-based meta-analysis. *Neurosci. Biobehav. Rev.* **35,** 1175–85 (2011).
45. Grabert, K. *et al.* Microglial brain region-dependent diversity and selective regional sensitivities to aging. *Nat. Neurosci.* **19,** 504–16 (2016).
46. Melief, J. *et al.* Phenotyping primary human microglia: Tight regulation of LPS responsiveness. *Glia* **60,** 1506–1517 (2012).
47. De Biase, L. M. & Bonci, A. Region-Specific Phenotypes of Microglia: The Role of Local Regulatory Cues. *Neurosci.* 107385841880099 (2018). doi:10.1177/1073858418800996
48. Prabakaran, S. *et al.* Mitochondrial dysfunction in schizophrenia: evidence for compromised brain metabolism and oxidative stress. *Mol. Psychiatry* **9,** 684–697 (2004).
49. Melief, J. *et al.* Characterizing primary human microglia: a comparative study with myeloid subsets and culture models. *Glia* 1–12 (2016). doi:10.1002/glia.23023
50. Livak, K. J. & Schmittgen, T. D. Analysis of Relative Gene Expression Data Using Real-Time Quantitative PCR and the 2−ΔΔCT Method. *Methods* **25,** 402–408 (2001).
51. Harris, L. W. *et al.* Comparison of peripheral and central schizophrenia biomarker profiles. *PLoS One* **7,** e46368 (2012).
52. Kurumaji, A., Wakai, T. & Toru, M. Decreases in peripheral-type benzodiazepine receptors in postmortem brains of chronic schizophrenics. *J. Neural Transm.* **104,** 1361–70 (1997).
53. Birnbaum, R. *et al.* Investigating the neuroimmunogenic architecture of schizophrenia. *Mol. Psychiatry* (2017). doi:10.1038/mp.2017.89
54. Beckers, L. *et al.* Increased Expression of Translocator Protein (TSPO) Marks Pro-inflammatory Microglia but Does Not Predict Neurodegeneration. *Mol. Imaging Biol.* **20,** 94–102 (2018).
55. Smith, A. M. & Dragunow, M. The human side of microglia. *Trends Neurosci.* **37,** 125–135 (2014).
56. Venneti, S., Lopresti, B. J. & Wiley, C. A. Molecular imaging of microglia/macrophages in the brain. *Glia* **61,** 10–23 (2013).
57. Venneti, S. *et al.* PK11195 labels activated microglia in Alzheimer's disease and in vivo in a mouse model using PET. *Neurobiol. Aging* **30,** 1217–1226 (2009).
58. Venneti, S., Wang, G., Nguyen, J. & Wiley, C. A. The Positron Emission Tomography Ligand DAA1106 Binds With High Affinity to Activated Microglia in Human Neurological Disorders. *J. Neuropathol. Exp. Neurol.* **67,** 1001–1010 (2008).
59. Mirzaei, N. *et al.* In vivo imaging of microglial activation by positron emission tomography with [11 C]PBR28 in the 5XFAD model of Alzheimer's disease. *Glia* **64,** n/a-n/a (2016).

Supplementary table 1: clinicopathological information

Donor	Diagnosis	Sex	Age (years)	PMD (minutes)	pH	Cause of death	Used for
93-274	SCZ	F	68	620	6.5	Pneumonia and ileus	1
94-098	SCZ	M	58	755	7.9	Aspiration pneumonia with acute respiratory distress	1
96-238	CON	F	87	480	6.9	Cardiac failure	1
96-251	CON	M	84	540	6.2	Heart failure by uremia	1
99-144	CON	F	59	250	6.7	Ileus, induced by opiates and hypothyroidism	2
99-182	SCZ	M	67	3900	NA	Cardio-respiratory insufficiency	2
00-067	CON	M	73	1485	NA	NA	2
03-009	CON	M	51	464	NA	Bronchopneumonia	2
04-081	CON	M	67	1115	6.7	Myocardial infarct (presumably)	2
05-161	SCZ	F	66	670	7.2	Pancreas carcinoma	1
09-039	CON	M	78	1060	6.5	Natural death, probably cardiac cause	1
09-286	SCZ	M	78	200	NA	Cardiac distress	2
09-300	CON	F	71	430	6.3	Renal insufficiency by hypertensive nephropathy	1
09-301	CON	M	92	502	6.1	Heart failure	1
10-049	SCZ	M	59	750	5.9	Cardiac arrest	1
10-158	SCZ	M	64	1155	7.0	Pulmonary embolism	1,2
10-360	SCZ	F	79	285	6.3	Heart failure and heart fibrillation	1,2
11-028	CON	F	81	265	6.7	Intestinal ischemia	1
11-039	CON	F	91	255	6.5	Heart infarction	1
11-044	CON	M	51	465	7.1	Starvation by refusing food and water	1
12-001	CON	F	89	340	6.8	Ischemia	1
12-005	CON	F	84	335	6.7	Ischemia	1
12-031	SCZ	F	55	590	6.8	Euthanasia*	1,2
12-101	CON	M	80	265	6.6	Euthanasia*	2
12-104	CON	M	79	390	6.7	Euthanasia*	2
13-006	SCZ	F	63	300	6.5	Metastatic breast cancer	1
13-056	CON	M	95	435	6.6	Heart failure	3
14-005	CON	M	67	540	6.5	Aortic aneurysm, asystole	3
14-015	CON	M	70	380	6.6	Pneumonia with cardiogenic shock	3
14-029	CON	F	78	430	6.3	Euthanasia*	2
15-089	CON	F	92	465	6.7	Euthanasia*	3
16-038	CON	F	85	425	6.5	Bilateral pneumonia and heart failure	3
16-046	CON	F	92	411	6.6	Kidney failure and respiratory insufficiency	3
16-056	CON	M	68	350	6.5	Metastasized carcinoid	3

CON = Control; **SCZ** = Schizophrenia; **M** = male; **F** = female; PMD = post-mortem delay; **used for:** 1 = mRNA expression; 2 = immunohistochemistry; 3= microglia isolation and stimulation; **NA** = not applicable; *euthanasia is legal according to Dutch law

Supplementary table 2: primer sequence for qPCR analysis

Primer	Forward sequence	Reverse sequence
AIF1	AGACGTTCAGCTACCCTGACTT	GGCCTGTTGGCTTTTCCTTTTCTC
ACTB	GTGGACATCCGCAAAGACCT	TCTGCATCCTGTCGGCAAT
CD163	TTTGTCAACTTGAGTCCCTTCAC	TCCCGCTACACTTGTTTTCAC
CD200R1	GAGCAATGGCACAGTGACTGTT	GTGGCAGGTCACGGTAGACA
CX3CR1	TTGGCCTGGTGGGAAATTTGT	AGGAGGTAAATGTCGGTGACACT
GAPDH	TGCACCACCAACTGCTTAGC	GGCATGGACTGTGGTCATGA
HLA-DRA	CCCAGGGAAGACCACCTTT	CACCCTGCAGTCGTAAACGT
IL1B	TTTGAGTCTGCCCAGTTCCC	TCAGTTATATCCTGGCCGCC
IL6	TGCAATAACCACCCCTGACC	TGCGCAGAATGAGATGAGTTG
ITGAM	TGCTTCCTGTTTGGATCCAACCTA	AGAAGGCAATGTCACTATCCTCTTGA
SDHA	GAAGCCCTTTGAGGAGCACT	GTTTTGTCGATCACGGGTCT
TNF	TGGAGAAGGGTGACCGACTC	TCACAGGGCAATGATCCCAA
TSPO	TACCGTGGCCTGGTACCA	TCCCGCCATACGCAGTAGTT

Supplementary table 3: Correlation between TSPO mRNA expression of *TSPO* and various covariates.

Spearman's rank coefficients and p-values for the correlation between *TSPO* mRNA expression and the covariates age, PMD and pH.

	Control (N= 10)				Schizophrenia (N= 8)			
	Grey matter		White matter		Grey matter		White matter	
	rho	*p*	*rho*	*p*	*rho*	*p*	*rho*	*p*
Age	-0.207	0.567	-0.012	0.978	-0.643	0.119	-0.381	0.352
PMD	-0.212	0.556	0.762[a]	0.028[a]	0.464	0.294	-0.071	0.867
pH	-0.006	0.987	-0.311	0.453	-0.288	0.531	-0.383	0.349

PMD = post mortem delay; rho = Spearman's rho rank coefficient; *p* = *p*-value without Bonferroni correction; [a] non significant after Bonferroni correction

Chapter 5

Post-mortem analysis of the four hallmarks of neuroinflammation in schizophrenia: microglial activation, lymphocytic infiltrates, and gliosis

Marjolein A.M. Sneeboer[1,2], Hans van Mierlo[1], Evi Stotijn[2], Ninouk Akkerman[2], Psychiatric donor program of the Netherlands Brain Bank (NBB-Psy)[3], Donald J. MacIntyre[4], Colin Smith[4], René S. Kahn[1,5], Elly M. Hol[2,6], Lot D. de Witte[1,5]

[1] Department of Psychiatry, Brain Center Rudolf Magnus, University Medical Center Utrecht, Utrecht University (BCRM-UMCU -UU), 3584 CG Utrecht The Netherlands

[2] Department of Translational Neuroscience (BCRM-UMCU-UU), 3584 CG Utrecht, The Netherlands

[3] Psychiatric donor program of the Netherlands Brain Bank (NBB-Psy), Meibergdreef 47, 1105 BA Amsterdam, the Netherlands

[4] Division of Psychiatry, Centre for Clinical Brain Sciences, University of Edinburgh, Edinburgh, United Kingdom

[5] Department of Psychiatry, Icahn School of Medicine, New York, United States of America

[6] Neuroimmunology, Netherlands Institute for Neuroscience, An institute of the royal academy of arts and sciences, 1105 BA, Amsterdam, The Netherlands.

Manuscript in preparation

Abstract

Since many years the immune system has been suggested to play a role in the pathogenesis of schizophrenia (SCZ) and is under investigation as a potential novel target for treatment. How the immune system is involved is not clear yet. Neuroinflammation is hypothesized, but the concept of neuroinflammation is complex and misinterpreted over the years. The aim of this study is to evaluate the presence of neuroinflammation in SCZ based on the four classical hallmarks: 1) microglial activation; 2) increased cytokine levels; 3) lymphocyte recruitment and infiltration; and 4) gliosis and local tissue damage. We analysed these hallmarks in post-mortem tissue of the superior temporal gyrus of patients with SCZ and controls with immunochemistry and qPCR. We found no differences in microglial density, morphology, and in the expression of *ITGAM*, *AIF1*, *HLA-DRA,* and *IL1B*. Interestingly, we observed a decrease in *CX3CR1* mRNA in SCZ. There were no $CD3^+$ and $CD20^+$ infiltrates in SCZ, but we observed more single $CD3^+$ T-lymphocytes in the parenchyma of patients with SCZ. The number of $CD3^+$ T-lymphocytes did not correlate with microglia numbers and activation. The neuropathological reports did not indicate blood brain barrier disruption or tissue damage. In conclusion, SCZ is not a neuroinflammatory disorder since the four criteria of classic neuroinflammation are not met.

Introduction

Schizophrenia (SCZ) has been associated with activation of the immune system for many years. Therefore targeting the immune system is under investigation as a potential novel treatment for SCZ. A potential causal role for the immune system in SCZ has emerged from epidemiological and genetic studies. Birth cohort studies showed an increased risk for developing SCZ after perinatal and childhood infection[1,2] and for children born at the end of the winter/early spring season[3]. In addition, the prevalence of autoimmune and atopic disorders is increased in SCZ[1,2]. Large genetic studies identified genome wide significant single nucleotide polymorphisms in immune system related genes associated with SCZ[4,5]. Further analysis of these genetic data revealed involvement of immunological pathways in the pathogenesis of SCZ[6]. Moreover, altered levels of chemokines and cytokines, such as interleukin 1 beta (IL-1β), interleukin 6 (IL-6), and tumour necrosis factor alpha (TNFα) are found in serum and cerebrospinal fluid of SCZ patients[7–10]. Together, these studies suggest a role for the immune system in the pathogenesis of SCZ. However, how the immune system is involved, is yet unknown.

The general hypothesis in the field is that patients with SCZ display some degree of neuroinflammation and that these inflammatory processes contribute to development and persistence of neuronal abnormalities underlying the disease[11–13]. However, classic neuroinflammation contains several aspects and the clarity of this concept has diminished over the years[14,15]. As a result many neurological and psychiatric diseases are nowadays referred to as neuroinflammatory disorders, even if just a slight alteration in one of the characteristics of inflammation is observed. It is becoming evident that immune molecules also have non-immune functions (e.g. involvement in neurodevelopment and brain homeostasis). Therefore, Estes and McAllister (2014) emphasized to reserve the term 'neuroinflammation' when the following four criteria of pathological neuroinflammation are met: 1) activation of microglia; 2) increased cytokine levels; 3) lymphocyte recruitment and infiltrates; and 4) gliosis and local tissue damage[14]. Clarifying the presence of neuroinflammation in schizophrenia is of importance to decide whether anti-inflammatory drugs might be beneficial to reduce schizophrenic symptoms.

The aim of this study is therefore to evaluate the presence of neuroinflammation in post-mortem brain tissue of patients with SCZ based on these classical hallmarks. We analysed the presence of the four hallmarks of neuroinflammation in the superior temporal gyrus (STG) provided by the Netherlands and Scotland brain bank. We quantitatively investigated microglial density and morphology, mRNA expression of

cytokines and microglial-related genes, and the density of T- ($CD3^+$) and B- ($CD20^+$) lymphocytes. Additionally, we explored neuropathology reports on schizophrenia for their notification of neuroinflammation, gliosis, or local tissue damage, examined blood-brain barrier (BBB) intactness and the presence of tissue damage. Our study is the first that systematically analysed the four hallmarks of neuroinflammation in SCZ.

Material and methods

Human brain tissue

Paraffin embedded (SCZ N=16; control N=18) and snap frozen (SCZ: N=10; control: N=14) post-mortem tissue of the superior temporal gyrus (STG) was provided by the Netherlands Brain Bank (www.brainbank.nl) and the Scotland Brain Bank (Edinburgh). The STG was chosen as region of interest since it has been associated with schizophrenia before[16–18]. Paraffin tissue was processed for immunochemistry, whereas snap frozen tissue was used for both immunochemistry and mRNA expression analysis. Informed consent for brain autopsy and the usage of brain tissue and accompanied clinical information for research purposes was obtained ante-mortem. Clinical characteristics of the donors are listed in table 1 and supplementary table 1. Donors with different stages of Alzheimer pathology (Braak, amyloid) were included in the study. Although microglia are immune activated in Alzheimer's disease[19], pathology was present in both patients and controls and further correction was not applied. The donors of which tissue quality was sufficient varied from experiment to experiment. Thus, the number of included donors in the analyses is different per experiment. Patients and controls did not differ on the confounder variables age, sex, post-mortem delay (PMD), and pH (Table 1) for microglial density and morphology and expression analysis. PMD was significantly different between patients and controls for T-lymphocyte density. However, ANCOVA analysis showed no significant interaction effect of PMD and CD3 density. Correction for PMD is therefore not applied for further analysis.

Haematoxylin Eosin (HE) staining

Pre-stained HE brain sections of the STG of patients with SCZ (N=13) were provided by the Netherlands Brain Bank. Paraffin sections of patients with SCZ that were provided by the Scotland Brain bank (N=3) were deparaffinised through a xylene and alcohol series and stained with Mayer's haematoxylin (Carl Roth, Karlsruhe Germany) for 8 minutes. Sections were rinsed with tap water for 8 minutes and stained with eosin (pH 5.0, Carl Roth, Karlsruhe Germany) for 2 minutes. After staining, the sections were dehydrated through an alcohol series and mounted in Entellan (Merck, Darmstadt, Germany).

Table 1: Summary of clinical information and post-mortem variables of the study

		Control (N=18)	SCZ (N=16)
Paraffin tissue	Age (years)	70.1 ± 13.6	67.6 ± 13.8
	Sex (M:F)	13:6	10:6
	PMD (minutes)	1302 ± 1762	2039 ± 1703
	pH	6.55 ± 0.30	6.57 ± 0.37
		Control (N=14)	**SCZ (N=10)**
Frozen tissue	Age (years)	73.1 ± 17.0	64.0 ± 13.9
	Sex (M:F)	8:6	4:6
	PMD (minutes)	1713 ± 2093	1197 ± 1348
	pH	6.53 ± 0.37	6.51 ± 0.40

Summary of the clinical information (age and sex) and post-mortem variables (post mortem delay (PMD) and pH) of donors used in the study. Numbers represent mean ± standard deviation. M = male; F = female, Control = control donor; SCZ = schizophrenia.

Immunochemistry for microglia and lymphocytes

Paraffin tissue of the STG of patients with SCZ (N=16) and controls (N=18) was sectioned (7 µm) on the microtome (Leica Microsystems) and mounted on glass slides. Paraffin sections of the Scotland Brain Bank were already mounted upon arrival. Sections were deparaffinised via a standard xylene and alcohol series before blocking endogenous peroxidase activity with 1% H_2O_2 (Merck, Darmstadt, Germany) in phosphate-buffered saline (PBS) for 10 minutes. For antigen retrieval, sections were heated in 0.01 mM citrate (Merck, Darmstadt, Germany), 0.05% Tween-20 (Merck, Darmstadt, Germany) for 15 minutes. Aspecific binding was blocked in PBS supplemented with 1% normal horse serum (NHS, Thermo Fisher Scientific, Massachusetts, USA), 0.1% bovine serum albumin (BSA, Merck, Darmstadt, Germany), 0.2% TritonX (Merck, Darmstadt, Germany) at room temperature (RT) for 30 minutes. Polyclonal rabbit-anti-human ionized calcium-binding adapter molecule 1 (Iba1; 1:2000, FUJIFILM Wako Chemicals, USA); polyclonal rabbit-anti-human CD3 (1:100, DAKO, Glostrup, Denmark) and monoclonal mouse-anti-human CD20 (1:100, DAKO, Glostrup, Denmark) antibodies for microglia, T-lymphocytes and B-lymphocytes respectively, were diluted in PBS with 0.1% BSA and incubated at 4°C overnight. The specificity of these antibodies has been demonstrated previously[20,21]. Primary antibodies were detected using the Avidin-Biotin Complex method. Biotinylated goat-anti-rabbit antibody (1:400, Jackson ImmunoResearch Laboratories, Inc.) and biotinylated horse-anti-mouse (1:400, Jackson Immunoresearch, USA) were diluted in PBS, 1% BSA, 1% NHS and incubated at RT for 45 minutes, followed by an incubation with avidin-biotin-peroxidase (AB) complex (A: 1:800, B: 1:800, Vector Laboratories) at RT for 30 minutes. 3,3-Diaminobenzidine (DAB, Merck, Darmstadt, Germany) was used to visualize microglial immunoreactivity. For CD3/CD20 staining, cell nuclei were counterstained with haematoxylin for 6 minutes, followed by a rinse in tap water for 4 minutes. The sections were dehydrated through an alcohol series and mounted in Entellan (Merck, Darmstadt, Germany).

Microglia were also immunofluorescently stained with Iba1 to quantify microglia density relative to total cell number. Above described protocol was applied with small adaptations. Instead of using Avidin-Biotin-DAB complex, tissue sections were counterstained with secondary goat-anti-rabbit Alexa 488 (1:700, Jackson ImmunoResearch Laboratories, Inc.) and Hoechst (1:1000) at RT for 45 minutes. Sections were mounted in Mowiol.

Immunochemistry for blood-brain-barrier intactness

Snap frozen tissue of the STG of patients with SCZ (N=6) and controls (N=8) was sectioned (20 µm) at the cryostat and mounted on glass slides. Sections were air dried and incubated in 4% paraformaldehyde-PBS solution for 10 minutes. Tissue sections were blocked with PBS supplemented with 10% normal goat serum (NGS, Thermo Fisher Scientific, Massachusetts, USA) and 0.4% TritonX100? at RT for 1 hour, followed by incubation of primary rabbit anti-human IgG (1:2000, Merck, Germany) and mouse anti-human VE-Cadherin (1:100, Bioscience) in PBS with 3% NGS and 0.4% TritonX100? at RT overnight. Next day, tissue sections were washed in PBS and incubated with secondary goat anti-mouse 568 (1:650, Life technology, Carlsbad, USA) in PBS with 1% NGS at RT for 2 hours. After washing the sections were incubated with DAPI (Thermo Fisher Scientific, Massachusetts, USA), washed and embedded with FluorSave (Merck, Darmstadt, Germany).

Microscopy and quantification

Iba1, CD3, and CD20 DAB-immunostainings were visualized with a ZEISS Imager M2 light microscope, whereas a Zeiss AxioScope A1 microscope was used for Iba1, IgG and VE-Cadherin fluorescent stainings. Microglial density and morphology was determined in six randomly taken pictures in both grey and white matter to incorporate microglial heterogeneity[22], the experimenter was blinded for diagnosis. Open-source software ImageJ was used to quantify microglial cell numbers, their morphology and $Iba1^+$-area covered. A particle analysis macro-script was used to count microglial density. Microglia density relative to total cell numbers was calculated by dividing the number of double positive nuclei ($Iba1^+Hoechst^+$), determined with the RG2B co-localisation plugin, by the total number of $Hoechst^+$ nuclei. For morphology, the cell body-to-size-ratio was calculated[23]. The cell body and total perimeter of the cell was determined with an automated particle analysis and radius mask macro. Cell body-to-size ratio close to one is associated with more amoeboid microglia, whereas ramified microglia have a ratio closer to zero. IgG and VE-Cadherin stainings were visually screened on IgG presence and BBB disruption.

The HE sections were systematically screened at 10x magnification for the presence of infiltrates. According to neuropathological standards, an infiltrate was defined as an accumulation of cells in the brain parenchyma, often seen near a vessel or in the perivascular space (supplementary figure 1a). Additionally, we manually counted single $CD3^+$ and $CD20^+$ cells in whole tissue sections and the experimenter was blinded for diagnosis. A distinction was made between $CD3^+$ T-lymphocytes in the parenchyma, considered as infiltrated, and $CD3^+$ cells in the vessel wall (supplementary figure 1b). Density of $CD3^+$ and $CD20^+$ cells was visualized by showing the number of cells per mm^2.

Gene expression analysis

Grey and white matter of snap frozen brain tissue of the STG (SCZ: N=9; control N=14) was dissected manually and lysed in TRIzol reagent (Thermo Fisher Scientific, Massachusetts, USA) to study mRNA expression of microglial general genes and immune-activation genes. RNA extraction and cDNA production for frozen brain tissue samples was performed as described before[24]. Quantitative real-time polymerase chain reaction (qPCR) was performed on a QuantStudio™ 6 Flex Real-Time PCR System (Life Technologies Corporation, NY, USA). Per reaction, 3.5 ng input of cDNA was mixed with Milli-Q water, 5 µL SYBRgreen PCR Master Mix (Roche; Life Technologies Corporation, Grand Island, NY, USA), and 1 µL primer mix (2 pmol/mL; supplementary table 2) until a final volume of 11 µL. All primers were intron-spanning and designed with the online tool of NCBI. The following cycle conditions were used: 50°C for 2 minutes, 95°C for 10 minutes, 40 cycles at 95°C of 15 seconds and at 60°C for 60 seconds. Gene expression was normalized to reference genes stable for brain tissue (Glyceraldehyde 3-phosphate dehydrogenase (*GAPDH)*, β-actin (*ACTB*), and Succinate Dehydrogenase Complex Flavoprotein Subunit A (*SDHA)*) according to the ΔΔCT method[25]. Non-detectable values (ND) were incorporated in the analysis as a CT value of 40 and shown in the graphs.

Statistics

Statistical analysis ware performed with Graphpad software (version 7) and SPSS IBM 23. We used an ANCOVA analysis to study interaction effects of confounders on outcome variables. Non-parametric Mann-Whitney U test was performed to analyse differences in microglial density and morphology, lymphocyte numbers, and mRNA expression differences between patients with SCZ and controls. Spearman ranks correlation was calculated to determine the relation between microglia and cytokine gene expression and microglial and lymphocyte density. Bonferroni correction for multiple testing was applied for each experiment.

Results

Hallmark 1: microglial density and activation

For the assessment of microglia density and morphology we used an Iba1 staining. Figure 1a and b show representative pictures of the Iba1 DAB- (Figure 1a) and fluorescent-stainings (Figure 1b) in a control donor and a patient with SCZ. In total, three different parameters were included in the study, all analysed with automated methods. The total Iba1$^+$ area covered was not changed between SCZ and controls in both grey and white matter (Figure 1c). When counting the number of microglial cells per mm^2 (Figure 1d) and the percentage Iba1$^+$cells over total cell number (Figure 1e), we determined that microglial density in SCZ was not different from controls. To study changes in microglial morphology we analysed the perimeter of the cell and the cell body-to-cell-size-ratio in grey matter of the STG (Figure 1 f-g). Activated microglia are characterized by a small perimeter and large cell body-to-cell-size-ratio. We did not find a difference in the cell perimeter (Figure 1f) and the cell body-to-size-ratio (Figure 1g) between patients and controls. Additionally, mRNA expression of general microglial genes (*AIF1*, *CX3CR1*, and *ITGAM*, Figure 1h) was quantified in grey and white matter of the STG of patients and controls. None of these markers were increased in SCZ. Interestingly, *CX3CR1* expression was significantly decreased in the grey matter of patients with SCZ. Linear regression analysis showed a positive association between AIF1 expression and CX3CR1, indicating that within each donor AIF1 expression is correlated with CX3CR1 expression (Figure 1i).

Figure 1

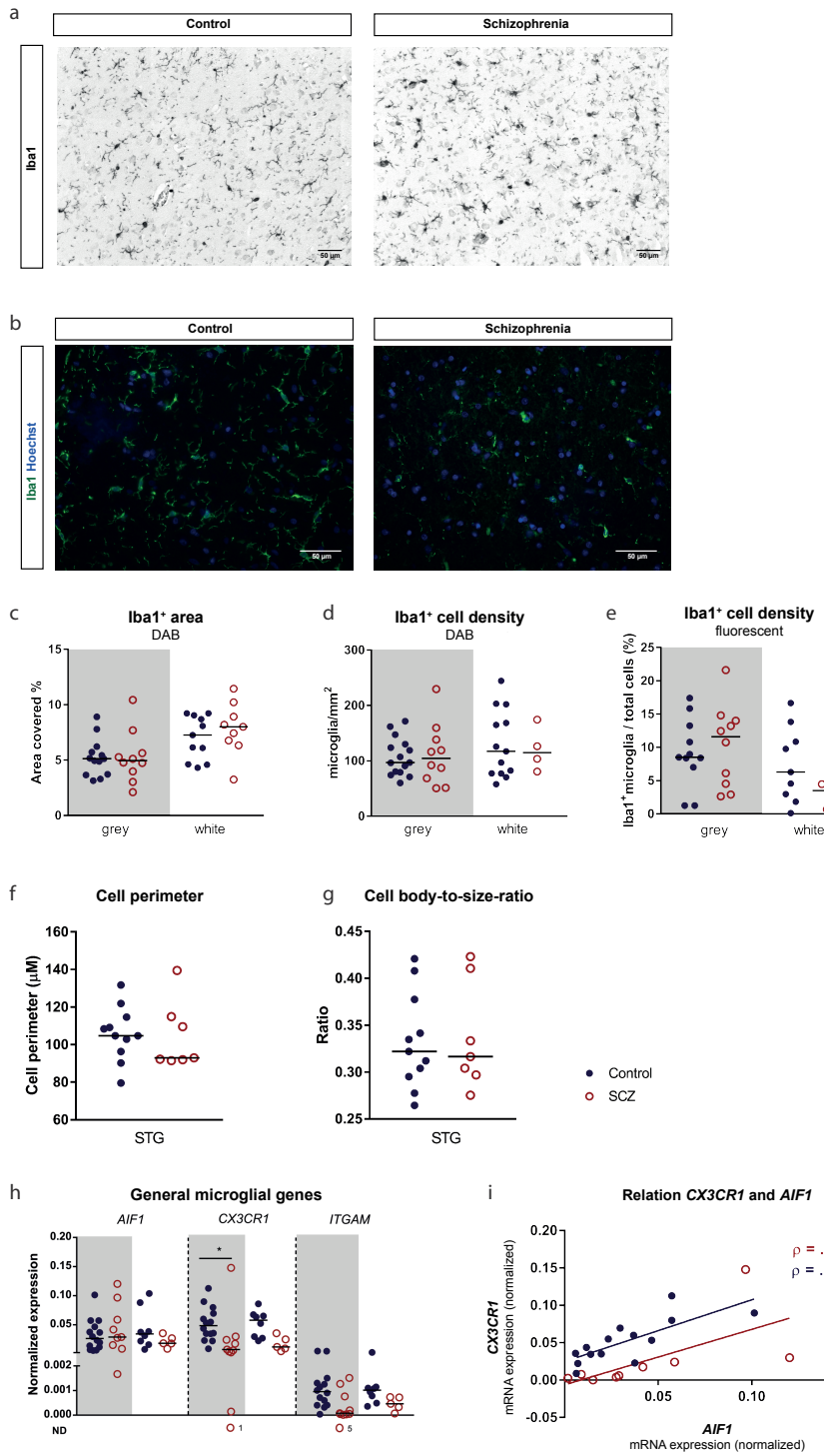

> Figure 1: Quantification of microglial density and morphology.
Microglial density and morphology was determined in the superior temporal gyrus (STG) of patients with schizophrenia (SCZ, N=10, red circles) and controls (N=15, blue dots) with Iba1 immunohistochemistry. a) Representative pictures of Iba1 immunostaining with DAB in controls and patients with SCZ. b) Fluorescent immunochemistry with Iba1-Alexa-488 (green) and Hoechst (blue) in controls and patients with SCZ. c) Percentage of Iba1$^+$ area in both grey and white matter in patients and controls. Cell density was determined with DAB (d) and fluorescent staining (e) in grey and white matter. Density of fluorescent stained microglia is represented as the number of Iba1$^+$ cells divided by the total cell number. Microglia morphology was determined in grey matter of the STG in patients and controls with the cell perimeter (f) and cell body-to-size-ratio (g). h) mRNA expression of general microglial genes (*AIF1*, *CX3CR1*, *ITGAM)* in grey and white matter of the superior temporal gyrus (STG) of patients with schizophrenia (SCZ, N=10, red circles) and controls (N=14, blue dots). i) Linear regression analysis of mRNA expression of *CX3CR1* and *AIF1* in patients with SCZ (red line) and controls (blue line). Spearman's rho correlation is given per linear regression. Gene expression was normalized to Glyceraldehyde 3-phosphate dehydrogenase (*GAPDH)*, β-actin (*ACTB*), and Succinate Dehydrogenase Complex Flavoprotein Subunit A (*SDHA)* using the ΔΔCT method[25]. Horizontal lines represents median and ND are non-detectable values. Bonferroni correction for multiple testing was applied. * $p < 0.05$, ** $p < 0.01$, *** $p < 0.001$.

Hallmark 2: increased cytokine levels

To determine the mRNA expression of microglial activation genes and cytokines (*HLA-DRA*, *IL1B* and *IL6*, Figure 2a), we performed a qPCR analysis on mRNA isolated from grey and white matter of snap frozen brain tissue of the STG of patients and controls. mRNA expression of microglial immune activation genes HLA-DRA and *IL1B* was not different between patients and controls. We found a significant increase of *IL6* in the grey matter of patients with SCZ (Figure 2a), mainly driven by one donor with high *IL6* expression. After outlier removal, no significant increase of *IL6* was found. To look specifically if microglial activation genes correlate with *AIF1* expression, we performed a linear regression analysis. HLA-DRA was positively correlated to AIF1 expression in patients and controls (Figure 2b). IL1B showed a positive correlation with AIF1 in controls (Figure 2c), whereas IL1B in patients and IL6 in both groups did not correlate with AIF1 (Figure 2c-d).

Hallmark 3: lymphocyte recruitment and infiltrates

As a first screening for infiltrates, defined as an accumulation of lymphocytes, we explored the pathology reports of all SCZ cases of the Netherlands Brain Bank (N=13). An experienced neuropathologist examined HE stainings of the frontal, temporal, parietal, and occipital cortex, pre- and post-central gyrus, thalamus, pituitary gland, hippocampus, substantia nigra, red nucleus, cingulate gyrus, caudate nucleus, putamen, insula, amygdala, locus coeruleus, pons, and medulla oblongata. Ischemic changes were reported in one patient, but they were related to the cause of death. Perivascular lymphocytic infiltrates around a few vessels were described in the putamen and caudate nucleus of one schizophrenia subject with comorbid rheumatoid arthritis. For this case, lymphocytic in the parenchyma were described. Neuroinflammatory changes in other cases were not described.

The screening of neuropathological reports was based on HE sections, and single infiltrating T- and B-lymphocytes would be missed with this method. Thus, we separately analysed the presence of lymphocytic infiltrates in paraffin embedded sections of the STG that were stained with CD3 or CD20 for T- and B-lymphocytes respectively. Figure 3 shows a representative picture of a CD3 staining in a control donor (Figure 3a) and a patient with SCZ (Figure 3b). As a positive control for lymphocyte infiltration we additionally stained a patient diagnosed with both SCZ and MS (Figure 3c). Only several individual $CD3^+$ cells were found in the parenchyma of patients and controls, whereas the positive control donor showed many lymphocytes and large infiltrations. For quantification of the number of T-lymphocytes, a distinction was made between $CD3^+$ lymphocytes in the vessel wall and in the parenchyma. No differences were found in the number of $CD3^+$ cells in the vessel wall between patients and controls (Figure 3d). In contrast, a significant increase in the number of $CD3^+$ cells was detected in the parenchyma of patients with SCZ. For the B-lymphocytes, only a few $CD20^+$ cells were detected in total brain sections of patients and controls (data not shown) and were not further quantified.

To determine the relation between the number of microglia ($Iba1^+$) and infiltrated $CD3^+$ lymphocytes we performed a linear regression analysis (Figure 4). The cell density of $Iba1^+$ cells per mm^2 was correlated with the number of $CD3^+$ cells per mm^2 in the vessel wall (Figure 4a), and in the parenchyma (Figure 4b). Although a positive correlation was found in the vessel wall and the parenchyma between Iba1 and CD3 density in patients and controls, there was no significant difference between the groups.

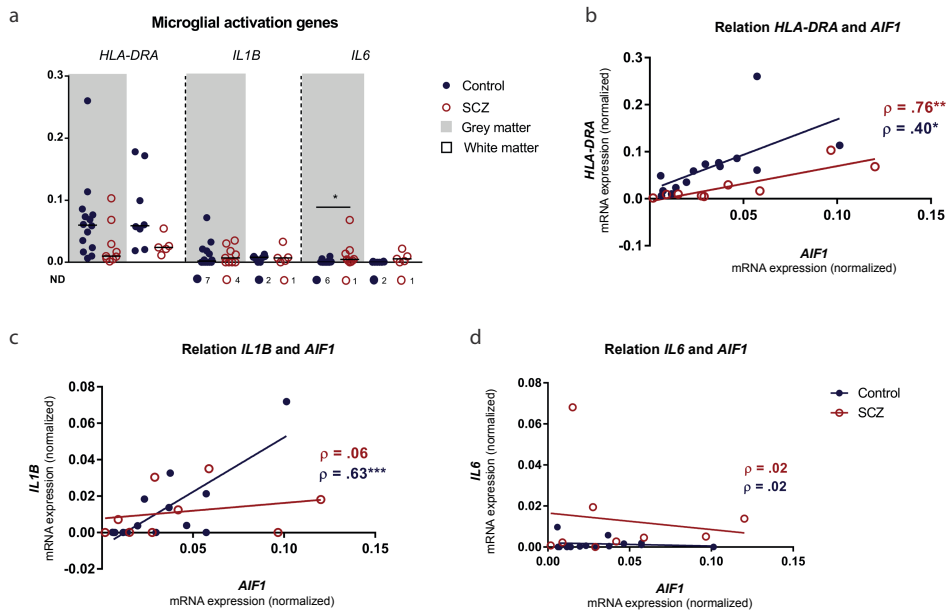

Figure 2: mRNA expression and correlations of general and microglial activation genes.
a) mRNA expression of microglial activation genes (*HLA-DRA, IL1B, IL6*) in grey and white matter of the superior temporal gyrus (STG) of patients with schizophrenia (SCZ, N=10, red circles) and controls (N=14, blue dots). Linear regression analysis was performed on *AIF1* mRNA expression and mRNA expression of *HLA-DRA* (b), *IL1B* (c), and *IL6* (d) in patients with SCZ (red line) and controls (blue line). Spearman's rho correlation is given per linear regression. Horizontal lines represents median. ND = non-detectable values. Bonferroni correction for multiple testing was applied. * $p < 0.05$, ** $p < 0.01$, *** $p < 0.001$.

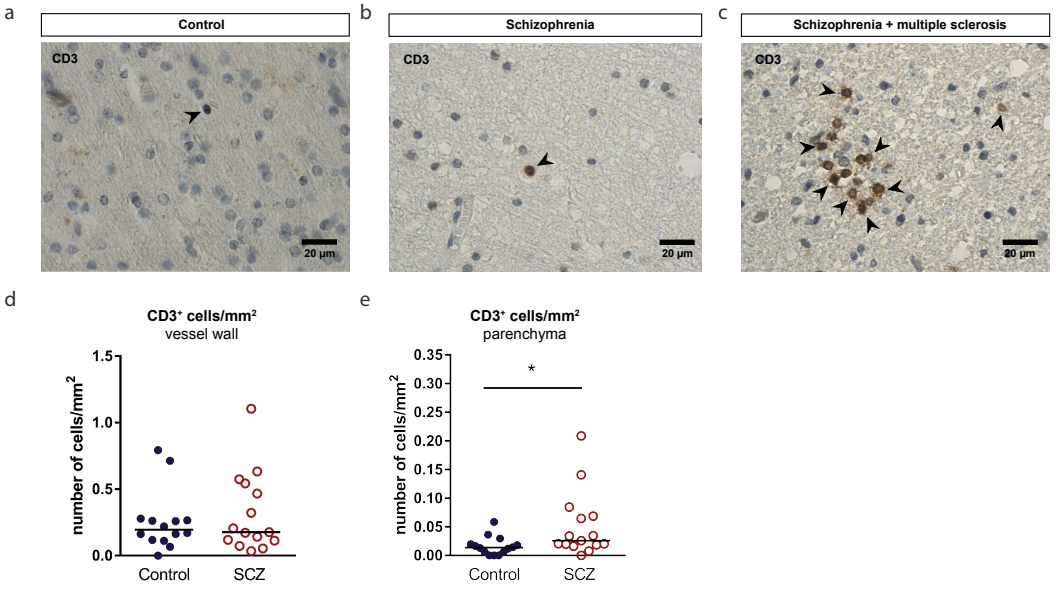

Figure 3: Quantification of lymphocytic infiltration and recruitment.
CD3 staining and quantification in post-mortem brain tissue of the superior temporal gyrus (STG) in patients with schizophrenia (SCZ) and controls. a-c) Representative CD3 stainings in a control donor (a), patient with SCZ (b), and patient with SCZ and multiple sclerosis (c) as positive control for lymphocyte infiltration. Black arrows represent $CD3^+$ cells. Quantification of CD3 density in the vessel wall (d) and the parenchyma (e) in controls (N=14, blue dots) and patients with SCZ (N=15, red circles). Horizontal lines represents median. Bonferroni correction for multiple testing was applied. $*p < 0.05$.

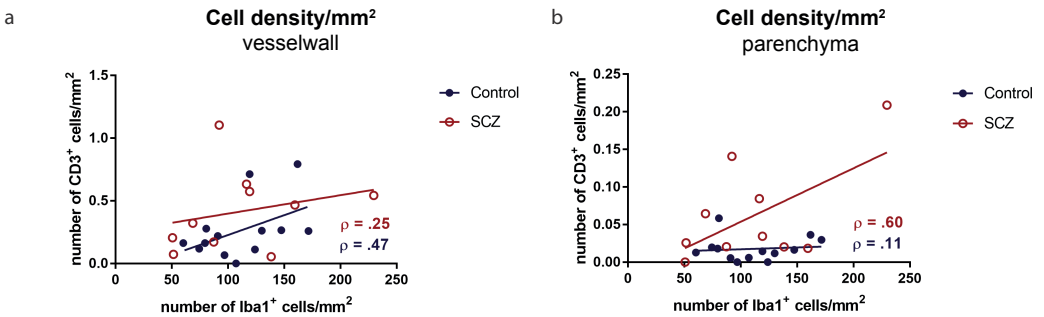

Figure 4: Linear regression of microglial density and $CD3^+$ lymphocytes.
Linear regression analysis was performed on microglial density (number of $Iba1^+$ cells per mm^2) and CD3 density in the superior temporal gyrus (STG) of patients with schizophrenia (SCZ, red line) and controls (blue line). Distinction was made between density in the vessel wall (a) and parenchyma (b). Spearman's rho correlation was given per linear regression.

Hallmark 4: gliosis and local tissue damage

The presence of local tissue damage was established by visually screening H&E stained tissue sections of the Netherlands and Scotland brain bank. We could not find signs of local tissue damage in patients and controls (data not shown). Since blood brain barrier intactness is often lost in neuroinflammatory disorders, we stained snap frozen tissue sections of patients with SCZ and controls with IgG and VE-Cadherin (Figure 5). Leakage of the BBB would result in IgG staining outside the VE-Cadherin$^+$ vessels. VE-Cadherin was equally expressed in patients and controls and co-localized with IgG^+ staining, indicating no leakage of IgG into the parenchyma and intactness of the BBB.

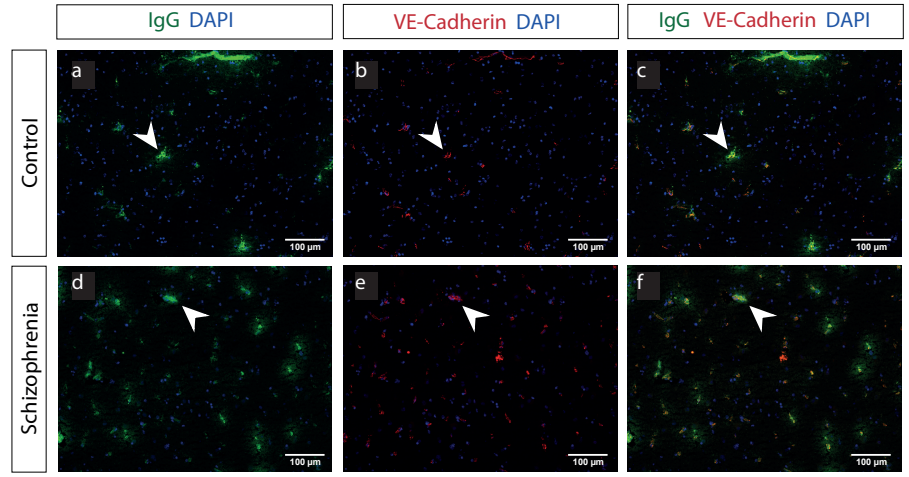

Figure 5: IgG and VE-Cadherin staining for blood-brain-barrier intactness.
Frozen sections of the superior temporal gyrus (STG) of patients with schizophrenia (SCZ, N=6, **a-c**) and controls (N=6, d-f) were stained for IgG (a, d, green) and VE-Cadherin (b, e, red). Co-localization of IgG and VE-Cadherin showed blood-brain-barrier intactness in patients (c) and controls (f). White arrows show positive staining for IgG and VE-Cadherin.

Discussion

In this study we investigated the four hallmarks of neuroinflammation in post-mortem brain tissue of the STG: 1) activation of microglia; 2) increased cytokine levels; 3) lymphocyte recruitment and infiltrates; and 4) gliosis and local tissue damage[14]. We found no differences in microglial density and activation state. qPCR analysis revealed decreased expression of *CX3CR1* in SCZ, but equal expression of *ITGAM* and *AIF1*. Regarding microglial activation and cytokine levels, similar expression of

HLA-DRA and *IL1B* were detected. $CD3^+$ and $CD20^+$ infiltrates were not found in SCZ, but slightly more single $CD3^+$ T-lymphocytes were detected in the parenchyma of patients with SCZ. Staining of the BBB and analysis of the neuropathological reports did not indicate BBB disruption, gliosis or tissue damage.

The absence of microglial density and activation has been described in previous studies. Trépanier et al. reviewed in total 21 studies, of which 15 studies performed immunochemistry to quantify microglial numbers in SCZ[9]. Most of the studies reported a lack of overall differences in microglial density, which is in line with our data. However, when other methods were included in the analysis (western blot, qPCR), 10/21 studies reported an increased of microglial markers. A meta-analysis with the same studies found an increased density of microglia[26]. However, one of the included studies that reported the largest differences between patients and controls, the study of Rao et al. (2013), was retracted. In total four studies assessed microglial morphology in SCZ as reflection of their activation state. Similar as in our study, two studies reported no differences in microglial morphology in the raphe nucleus[27,28]. Others found more amoeboid microglia in the temporal lobe, but only in the deeper cortical layers[29]. Additionally, they reported microglia with changed morphology, including cytoplasmic shrinkage and thinning, shortening, and fragmentation of microglial processes[30].

The heterogeneous findings on microglial density and morphological alterations cannot be explained by the various brain regions investigated, since studies analysing the same region also reported contradicting findings. One remarkable difference is that the studies with the most significant results were all using antibodies to recognize HLA-DP/DQ/DR, in contrast to studies staining with Iba1. It is known that HLA is more expressed on activated microglia and that the overlap between Iba1 and HLA-DR is limited[31]. Besides, Iba1 has higher specificity since it only stains ramified and amoeboid microglia, whereas HLA-DR also visualizes macrophages[31]. The density of $Iba1^+$ microglia was not different between patients and controls, as was shown here and by others[28,32]. Thus, HLA-DR might stain a specific microglia population that is increased in SCZ and need to be studied further. In our study we found a significant decrease of *CX3CR1* mRNA in SCZ. CX3CR1 is expressed on microglia and reacts on the CX3C Ligand 1 (CX3CL1) on neurons. CX3CR1-CX3CL1 signalling is highly important for neuron-microglia interaction and this directly influence on neurogenesis and social interactions in adulthood[33,34]. Lower expression of *CX3CR1* could indicate a disturbance in the neuron-microglia communication in SCZ, but need to be studied in more detail.

Another reason for the variety of results could be differences in disease severity or disease characteristics. For example, higher microglial numbers or changed morphology is reported for individual patients or in association with suicide[28,35–37]. Also without suicidal comorbidity, microglial alterations have been found in a subset of the patients. Hercher et al. observed numerous activated microglia in 15% of the patients, whereas Comte at al. found MHC II immunoreactivity in both patients and controls[28,35]. Furthermore, increased microglial density was observed in patients with paranoid SCZ compared to residual SCZ and controls[21].

With qPCR we determined gene expression of microglial activation genes. No increased *HLA-DRA* expression was found in SCZ in our cohort. This is in line with others who found equal[38,39] or even decreased[40,41] mRNA expression, but our data is in contrast to another study that reported higher mRNA and protein levels[42]. Two large RNA sequencing studies of the dorsolateral prefrontal cortex and the hippocampus confirmed the absence of changes in mRNA expression of several HLA subtypes[43,44]. This would indicate that mRNA levels of HLA-related genes are not differently expressed in SCZ. The lack of an inflammatory profile in SCZ is further supported by the lack of differences between patients and controls in the expression of *IL1B, IL6, TNF*, and *CD68*[43,44]. In our first analysis we found increased expression of *IL6* in SCZ, but this was driven by one patient. Fillman et al. reported similar individual pro-inflammatory profiles in 14/37 patients with significant upregulation of *IL6*, *IL8* and *IL1B*[42]. Together, these studies indicate that expression of pro-inflammatory cytokines may be present in a subgroup of patients and is not present in SCZ in general.

In SCZ there is an absence of infiltrates (accumulation of lymphocytes), gliosis, and signs of neurodegeneration as was also reported by others[16,21,45–47]. Especially the absence of gliosis, an indication for previous neuroinflammation, suggests no neuroinflammation in SCZ[47]. $CD3^+$ and, to a lesser extend, $CD20^+$ lymphocytes are not only present in SCZ tissue, but single cells are also randomly distributed throughout the tissue. Interestingly, we observed more single $CD3^+$ T-lymphocytes in the parenchyma of SCZ patients. This is in line with other reports that described the number of T-lymphocytes in SCZ. Busse et al. found more T- lymphocytes outside the vessels in the hippocampus of patients with residual SCZ compared to patients with paranoid SCZ and controls[21]. No increase in microglial density was reported in the same tissue, corresponding with our findings and the correlations between microglial and lymphocytic density. Although no discrimination was made between cells the vessel wall or parenchyma, Bogerts et al. detected more T-lymphocytes in the thalamus, cortex, cingulate gyrus and hippocampus in 15-40% of the patients with SCZ[45].

Why more T-lymphocytes are present in brain tissue of patients with SCZ is not clear yet. Higher densities of T-lymphocytes in the CNS are often associated with BBB disruption. However, our results suggest that the BBB is still intact and this is in line with earlier reports in which the presence of vascular impairments in SCZ is debated[21,4849]. Nicotine smoking is related to increased cell proliferation of T-lymphocytes in blood[50]. We observed that nicotine abuse is more common in our patient group and that the donors with the highest CD3+ density in our cohort have comorbidity with smoking, what could account for the difference. It is known that T-lymphocytes play a role in the crosstalk between the immune system and neurons. They can influence neuronal functioning and react to circulating neurotransmitters (e.g. dopamine) by increasing their proliferation and migration[48]. Besides, T-lymphocytes can be detrimental for neuronal function via the induction of neurotoxicity and neuronal damage[48]. Since each type of T-lymphocyte has its own function, more specific immunostainings with CD4 and CD8 for T helper and cytotoxic T-cells respectively are needed to interpret which role they might play in the CNS of patients with SCZ. Additionally, it is informative to stain for IFNγ, which is secreted by T-lymphocytes and regulates T-cell homeostasis, in post-mortem tissue of patients with SCZ.

Previous described literature on each of the four hallmarks of neuroinflammation showed that there is much divergence. Several reasons may account for the heterogeneity. A variety of markers was applied on various brain tissues and quantification was performed with manual counting, which is highly sensitive for bias. Another important factor is the effect of pre- and post-mortem variables. Many studies, including our study, corrected for age, sex, and PMD. It is however likely that other confounders have an impact on the data, such as the cause of death, pH, and comorbidity (e.g. smoking). For example, only two studies looked into the effect of smoking on *HLA-DRA* expression and reported opposite findings[51,52]. Furthermore, it is suggested that there is a role for suicide in microglial density and activation and maybe other hallmarks as well, as was already shown for major depressive disorder[27]. Medication is one of the most challenging confounding factors in post-mortem analysis. Patients with SCZ use a variety of antipsychotic medications, which are known to have anti-inflammatory properties[53,54]. Unfortunately, post-mortem brain tissue of unmedicated patients is not available to study the effect of antipsychotics on microglial activation and lymphocytic recruitment. Additionally, it needs to be noted that with post-mortem brain tissue conclusions are based on patients that are suffering from SCZ for multiple years. It might be possible that neuroinflammation can play a role in the earlier stages of the disorder, for example trigger the onset of SCZ or evoke a new psychotic episode[53].

Our data and current literature confirms the absence of classic neuroinflammation in SCZ in post-mortem brain tissue. However, certain aspects of neuroinflammation were present in a subset of the patients, as was shown with increased *IL6* and $CD3^+$ cells in the parenchyma of individual patients. Also other studies have found hallmarks of neuroinflammation in a small percentage of the patients. SCZ is a very heterogeneous disorder with various subtypes (residual, paranoid, catatonic, disorganized) and a broad range of symptoms. Individual patients with SCZ can express one of the four hallmarks of a classic neuroinflammatory disorder. In these patients' elevated cytokine levels, microglial activation or more lymphocytic recruitment is observed, as is seen in our study and by others. It would be interesting to study why certain patients display hallmarks of neuroinflammation and unravel the underlying mechanism. This will provide useful information for therapeutic strategies for individual patients with signs of neuroinflammation, since these patients might benefit from anti-inflammatory medication, such as Natalizumab[55].

In summary, SCZ cannot be seen as a classical neuroinflammatory disorder since not all four criteria are met. Therefore, we suggest using the term 'neuroinflammation' only for true neuroinflammatory disorders, like MS.

Acknowledgements

This study is supported by a 2014 NARSAD Young Investigator Grant from the Brain & Behavior Research Foundation and by the Virgo Consortium, funded by the Dutch government project number FES0908. DJM acknowledges the financial support of NHS Research Scotland, through NHS Lothian. Furthermore, this study was supported by the psychiatric donor program of the Netherlands Brain Bank (NBB-Psy), which is supported by the Netherlands Organization for Scientific Research (NWO). The authors thank the team of the Netherlands Brain Bank for their excellent services (www.brainbank.nl).

References

1. Benros, M. E., Mortensen, P. B. & Eaton, W. W. Autoimmune diseases and infections as risk factors for schizophrenia. *Ann. N. Y. Acad. Sci.* **1262,** 56–66 (2012).
2. Pedersen, M. S., Benros, M. E., Agerbo, E., Børglum, A. D. & Mortensen, P. B. Schizophrenia in patients with atopic disorders with particular emphasis on asthma: a Danish population-based study. *Schizophr. Res.* **138,** 58–62 (2012).
3. Davies, G., Welham, J., Chant, D., Torrey, E. F. & McGrath, J. A systematic review and meta-analysis of Northern Hemisphere season of birth studies in schizophrenia. *Schizophr. Bull.* **29,** 587–93 (2003).
4. Ripke, S. *et al.* Biological insights from 108 schizophrenia-associated genetic loci. *Nature* **511,** 421–427 (2014).
5. Sekar, A. *et al.* Schizophrenia risk from complex variation of complement component 4. *Nature* **530,** 177–183 (2016).
6. Network and Pathway Analysis Subgroup of Psychiatric Genomics Consortium. Psychiatric genome-wide association study analyses implicate neuronal, immune and histone pathways. *Nat. Neurosci.* **18,** 199–209 (2015).
7. Goldsmith, D. R., Rapaport, M. H. & Miller, B. J. A meta-analysis of blood cytokine network alterations in psychiatric patients: comparisons between schizophrenia, bipolar disorder and depression. *Mol. Psychiatry* **21,** 1696–1709 (2016).
8. Pandey, G. N., Rizavi, H. S., Zhang, H. & Ren, X. Abnormal gene and protein expression of inflammatory cytokines in the postmortem brain of schizophrenia patients. *Schizophr. Res.* **192,** 247–254 (2018).
9. Trépanier, M. O., Hopperton, K. E., Mizrahi, R., Mechawar, N. & Bazinet, R. P. Postmortem evidence of cerebral inflammation in schizophrenia: a systematic review. *Mol. Psychiatry* **21,** 1009–1026 (2016).
10. Mansur, R. B. *et al.* Cytokines in schizophrenia: Possible role of anti-inflammatory medications in clinical and preclinical stages. *Psychiatry Clin. Neurosci.* **66,** 247–260 (2012).
11. Meyer, U. Developmental neuroinflammation and schizophrenia. *Prog. Neuropsychopharmacol. Biol. Psychiatry* **42,** 20–34 (2013).
12. Monji, A. *et al.* Neuroinflammation in schizophrenia especially focused on the role of microglia. *Prog. Neuro-Psychopharmacology Biol. Psychiatry* **42,** 115–121 (2013).
13. Barron, H., Hafizi, S., Andreazza, A. C. & Mizrahi, R. Neuroinflammation and Oxidative Stress in Psychosis and Psychosis Risk. *Int. J. Mol. Sci.* **18,** (2017).
14. Estes, M. L. & McAllister, A. K. Alterations in immune cells and mediators in the brain: it's not always neuroinflammation! *Brain Pathol.* **24,** 623–30 (2014).
15. Carson, M. *et al.* A rose by any other name? The potential consequences of microglial heterogeneity during CNS health and disease. *Neurotherapeutics* **4,** 571–9 (2007).
16. Radewicz, K., Garey, L. J., Gentleman, S. M. & Reynolds, R. Increase in HLA-DR immunoreactive microglia in frontal and temporal cortex of chronic schizophrenics. *J. Neuropathol. Exp. Neurol.* **59,** 137–50 (2000).
17. Smieskova, R. *et al.* Neuroimaging predictors of transition to psychosis--a systematic review and meta-analysis. *Neurosci. Biobehav. Rev.* **34,** 1207–22 (2010).
18. Fusar-Poli, P. *et al.* Neuroanatomy of vulnerability to psychosis: a voxel-based meta-analysis. *Neurosci. Biobehav. Rev.* **35,** 1175–85 (2011).
19. Sarlus, H. & Heneka, M. T. Microglia in Alzheimer's disease. *J. Clin. Invest.* **127,** 3240–3249 (2017).
20. Anthony, I. C., Crawford, D. H. & Bell, J. E. B lymphocytes in the normal brain: contrasts with HIV-associated lymphoid infiltrates and lymphomas. *Brain* **126,** 1058–1067 (2003).
21. Busse, S. *et al.* Different distribution patterns of lymphocytes and microglia in the hippocampus of patients with residual versus paranoid schizophrenia: further evidence for disease course-related immune alterations? *Brain. Behav. Immun.* **26,** 1273–9 (2012).
22. Torres-Platas, S. G. *et al.* Morphometric characterization of microglial phenotypes in human cerebral cortex. *J. Neuroinflammation* **11,** 12 (2014).
23. Hovens, I., Nyakas, C. & Schoemaker, R. A novel method for evaluating microglial activation using ionized calcium-binding adaptor protein-1 staining: cell body to cell size ratio. *Neuroimmunol. Neuroinflammation* **1,** 82 (2014).
24. Melief, J. *et al.* Characterizing primary human microglia: a comparative study with myeloid subsets and culture models. *Glia* 1–12 (2016). doi:10.1002/glia.23023
25. Livak, K. J. & Schmittgen, T. D. Analysis of Relative Gene Expression Data Using Real-Time Quantitative PCR and the 2−ΔΔCT Method. *Methods* **25,** 402–408 (2001).
26. van Kesteren, C. F. M. G. *et al.* Immune involvement in the pathogenesis of schizophrenia: a meta-analysis on postmortem brain studies. *Transl. Psychiatry* **7,** e1075 (2017).
27. Brisch, R. *et al.* Microglia in the dorsal raphe nucleus plays a potential role in both suicide facilitation and prevention in affective disorders. *Eur. Arch. Psychiatry Clin. Neurosci.* **267,** 403–415 (2017).
28. Hercher, C., Chopra, V. & Beasley, C. L. Evidence for morphological alterations in prefrontal white matter glia in schizophrenia and bipolar disorder. *J. Psychiatry Neurosci.* **39,** 376–385 (2014).
29. Wierzba-Bobrowicz, T., Lewandowska, E., Lechowicz, W., Stepień, T. & Pasennik, E. Quantitative analysis of activated microglia, ramified and damage of processes in the frontal and temporal lobes of chronic schizophrenics. *Folia Neuropathol.* **43,** 81–9 (2005).
30. Wierzba-Bobrowicz, T. *et al.* Degeneration of microglial cells in frontal and temporal lobes of chronic schizophrenics. *Folia Neuropathol.* **42,** 157–65 (2004).
31. Hendrickx, D. A. E., van Eden, C. G., Schuurman, K. G., Hamann, J. & Huitinga, I. Staining of HLA-DR, Iba1 and CD68 in human microglia reveals partially overlapping expression depending on cellular morphology and pathology. *J. Neuroimmunol.* **309,** 12–22 (2017).
32. Connor, C. M., Guo, Y. & Akbarian, S. Cingulate White Matter Neurons in Schizophrenia and Bipolar Disorder. *Biol. Psychiatry* **66,** 486–493 (2009).
33. Zhan, Y. *et al.* Deficient neuron-microglia signaling results in impaired functional brain connectivity and social behavior. *Nat. Neurosci.* **17,** 400–406 (2014).
34. Paolicelli, R. C. *et al.* Synaptic pruning by microglia is necessary for normal brain development. *Science* **333,** 1456–1458 (2011).
35. Comte, I., Kotagiri, P. & Szele, F. G. Regional differences in human ependymal and subventricular zone cytoarchitecture are unchanged in neuropsychiatric disease. *Dev. Neurosci.* **34,** 299–309 (2012).
36. Steiner, J. *et al.* Immunological aspects in the neurobiology of suicide: Elevated microglial density in schizophrenia and depression is associated with suicide. *J. Psychiatr. Res.* **42,** 151–157 (2008).
37. Steiner, J. *et al.* Distribution of HLA-DR-positive microglia in schizophrenia reflects impaired cerebral lateralization. *Acta Neuropathol.* **112,** 305–316 (2006).
38. Nakatani, N. *et al.* Genome-wide expression analysis detects eight genes with robust alterations specific to bipolar I disorder: relevance to neuronal network perturbation. *Hum. Mol. Genet.* **15,** 1949–62 (2006).
39. Saetre, P. *et al.* Inflammation-related genes up-regulated in schizophrenia brains. *BMC Psychiatry* **7,** 46 (2007).
40. Schmitt, A. *et al.* Regulation of immune-modulatory genes in left superior temporal cortex of schizophrenia patients: a genome-wide microarray study. *World J. Biol. Psychiatry* **12,** 201–15 (2011).

41. Durrenberger, P. F. *et al.* Common mechanisms in neurodegeneration and neuroinflammation: a BrainNet Europe gene expression microarray study. *J. Neural Transm.* **122,** 1055–68 (2015).
42. Fillman, S. G. *et al.* Increased inflammatory markers identified in the dorsolateral prefrontal cortex of individuals with schizophrenia. *Mol. Psychiatry* **18,** 206–214 (2013).
43. Fromer, M. *et al.* Gene expression elucidates functional impact of polygenic risk for schizophrenia. *Nat. Neurosci.* **19,** 1442–1453 (2016).
44. Birnbaum, R. *et al.* Investigating the neuroimmunogenic architecture of schizophrenia. *Mol. Psychiatry* (2017). doi:10.1038/mp.2017.89
45. Bogerts, B. *et al.* Evidence of neuroinflammation in subgroups of schizophrenia and mood disorder patients: A semiquantitative postmortem study of CD3 and CD20 immunoreactive lymphocytes in several brain regions. *Neurol. Psychiatry Brain Res.* **23,** 2–9 (2017).
46. Powchik, P. *et al. Postmortem Studies in Schizophrenia*.
47. Harrison, P. J. Postmortem studies in schizophrenia. *Dialogues Clin. Neurosci.* **2,** 349–57 (2000).
48. Debnath, M. Adaptive Immunity in Schizophrenia: Functional Implications of T Cells in the Etiology, Course and Treatment. *J. Neuroimmune Pharmacol.* **10,** 610–619 (2015).
49. Kealy, J., Greene, C. & Campbell, M. Blood-brain barrier regulation in psychiatric disorders. *Neurosci. Lett.* (2018). doi:10.1016/j.neulet.2018.06.033
50. Herberth, M. *et al.* Differential effects on T-cell function following exposure to serum from schizophrenia smokers. *Mol. Psychiatry* **15,** 364–71 (2010).
51. Kano, S. *et al.* Altered MHC class I expression in dorsolateral prefrontal cortex of nonsmoker patients with schizophrenia. *Neurosci. Res.* **71,** 289–293 (2011).
52. Sinkus, M. L., Adams, C. E., Logel, J., Freedman, R. & Leonard, S. Expression of immune genes on chromosome 6p21.3-22.1 in schizophrenia. *Brain. Behav. Immun.* **32,** 51–62 (2013).
53. Obuchowicz, E., Bielecka-Wajdman, A. M., Paul-Samojedny, M. & Nowacka, M. Different influence of antipsychotics on the balance between pro- and anti-inflammatory cytokines depends on glia activation: An in vitro study. *Cytokine* **94,** 37–44 (2017).
54. Al-Amin, M. M., Nasir Uddin, M. M. & Mahmud Reza, H. Effects of antipsychotics on the inflammatory response system of patients with schizophrenia in peripheral blood mononuclear cell cultures. *Clin. Psychopharmacol. Neurosci.* **11,** 144–51 (2013).
55. Khademi, M. *et al.* The effects of natalizumab on inflammatory mediators in multiple sclerosis: prospects for treatment-sensitive biomarkers. *Eur. J. Neurol.* **16,** 528–36 (2009).

Supplementary table 1: clinicopathological information

Donor	Diagnosis	Sex	Age (years)	Braak	Amyloid	PMD (minutes)	pH	Somatic comorbidity	Cause of death	Used for
93/274	SCZ	F	68	1	-	620	6.45	2	1, 9	1b, 1c, 1d, 2a, 2b
96/238	Control	F	87	2	-	480	6.91	5	2	2a, 2b
96/251	Control	M	84	1	-	540	6.20	3	2	2a, 2b
96/373	Control	M	70	0	0	450	6.40	-	3	1a
98/127	SCZ	F	85	0	-	540	NA	5	2	1a, 1c, 1d
98/229	SCZ	M	76	NA	NA	5340	NA	3, 5, 6	2	1c, 1d
98/329	SCZ	M	48	NA	NA	2460	NA	6	5	1c, 1d
99/144	Control	F	59	1	0	250	6.67	NA	9	1a, 1b, 1c, 1d
99/182	SCZ	M	67	1	A	3900	NA	-	2	1a, 1b, 1c, 1d
99/209	SCZ	M	74	1	0	3120	NA	4, 5	1	1a, 1b, 1c, 1d
99/262	SCZ	M	95	3	C	3600	NA	5	2	1a, 1b, 1c, 1d
00/067	Control	M	73	0	0	1485	NA	-	NA	1a, 1b, 1c, 1d
01/158	Control	F	69	1	A	345	6.97	3	4	1a, 1b, 1c, 1d
03/009	Control	M	51	0	-	464	NA	5	NA	2a, 2b
04/019	Control	M	91	1	0	2360	6.61	-	NA	1a, 1c, 1d
04/021	SCZ	F	92	3	0	455	6.30	5	NA	2b
04/081	Control	M	67	1	B	1115	6.70	2	2	1a, 1b, 1c, 1d
05/019	Control	M	74	3	C	300	6.70	-	NA	1a, 1b, 1c, 1d
05/073	Control	F	87	3	A	365	6.96	-	NA	1a, 1c, 1d
05/161	SCZ	F	66	0	0	670	7.24	3, 5	3	1a, 1c, 1d, 2a, 2b
09/003	Control	M	62	1	0	440	6.36	-	NA	1a, 1b, 1c, 1d
09/039	Control	M	78	1	-	1060	6.52	5	2	2a, 2b
09/286	SCZ	M	78	1	B	200	NA	5, 6	2, 4e	1a, 1b, 1c, 1d
09/300	Control	F	71	1	A	4210	6.31	4d, 5	9	2a
09/301	Control	M	92	4	A	505	6.14	5	2	2a, 2b
10/049	SCZ	M	59	NA	NA	750	5.93	-	2	2a, 2b
10/158	SCZ	M	64	1	A	1155	7.00	-	2	1a, 1b, 1c, 1d, 2a, 2b
10/360	SCZ	F	79	1	NA	285	6.34	5	2	1a, 1b, 1c, 1d, 2a, 2b
11/028	Control	F	81	1	-	265	6.67	2, 5	9	2a, 2b
11/039	Control	F	91	1	B	255	6.50	4d, 5	2	2a, 2b
11/044	Control	M	51	0	-	465	7.05	-	5	2a, 2b
11/069	Control	M	49	0	0	375	6.23	-	NA	1a, 1b, 1c, 1d
11/096	Control	F	70	2	A	375	6.55	5	3	1a, 1b, 1c, 1d
12/001	Control	F	89	2	B	340	6.75	-	8a	2a
12/005	Control	F	84	2	A	336	6.68	3	8a	2a

Supplementary table 1: Continued

12/031	SCZ	F	55	NA	NA	590	6.82	2, 5, 6	4	1b, 1c, 1d, 2a
12/052	Control	F	64	0	A	340	6.35	3	NA	1a, 1c, 1d
12/101	Control	M	80	2	C	265	6.59	3	4	1d
12/104	Control	M	79	2	A	390	6.71	-	NA	1a, 1b, 1c, 1d
13/006	SCZ	F	63	NA	NA	300	6.50	3	3	1a, 1b, 1c, 1d, 2a
13/056	Control	M	95	2	B	435	6.56	-	NA	1a, 1b, 1c, 1d
14/029	Control	F	78	1	A	430	6.32	3, 5	4	1b, 1c, 1d
SD015/12	Control	M	70	NA	NA	4400	6.90	-	2	1a, 1b, 1d, 2a
SD017/06	SCZ	M	44	NA	NA	2640	6.40	5	2	1a, 1b, 1c, 1d, 2a
SD019/15	Control	M	50	NA	NA	6180	5.70	-	2	1a, 1d, 2a
SD022/13	Control	M	45	NA	NA	4440	6.60	-	2	1b, 1d, 2a
SD033/07#	SCZ	M	70	NA	NA	2700	6.28	2, 5	2	1c, 1d
SD035/08	SCZ	M	50	NA	NA	4500	6.10	5, 6	2	1c, 1d, 2a

Control = control donor; **SCZ** = donor with schizophrenia; **M** = male; **F** = female; **NA** = not applicable; **-** = absent; **PMD** = post-mortem delay; **somatic comorbidity**: 1 = infection < 2 weeks prior to death; 2 = auto-immune disease; 3 = cancer (in history); 4 = neuropathology; 5 = cardiovascular (hypertension, infarct); 6 = substance abuse (alcohol, cigarettes); a = Dementia; b = Parkinson; c = ischemia/infarction; d = bleeding (CVA, TIA); e = encephalopathy; **cause of death**: 1 = infection/inflammatory; 2 = cardiorespiratory; 3 = cancer; 4 = euthanasia/palliative sedation*; 5 = suicide; 6 = trauma; 7 = cachexia/dehydration; 8 = brain; a = ischemia/infarction; b = bleeding (CVA, TIA); 9 = other (ileus, organ failure); **used for:** 1 = paraffin tissue; 1a = Iba1 DAB; 1b = Iba1 immunofluorescent; 1c = CD3/CD20 immunochemistry; 1d = Haematoxylin Eosin staining; 2 = frozen tissue; 2a = mRNA expression; 2b = BBB immunochemistry; # positive control (SCZ + multiple sclerosis); * euthanasia is legal according to Dutch law

Supplementary table 2: Primer sequences

Primer	Forward sequence	Reverse sequence
AIF1	AGACGTTCAGCTACCCTGACTT	GGCCTGTTGGCTTTTCCTTTTCTC
ACTB	GTGGACATCCGCAAAGACCT	TCTGCATCCTGTCGGCAAT
CX3CR1	CTTACGATGGCACCCAGTGA	CAAGGCAGTCCAGGAGAGTT
HLA-DRA	CCCAGGGAAGACCACCTTT	CACCCTGCAGTCGTAAACGT
IL6	TGCAATAACCACCCCTGACC	TGCGCAGAATGAGATGAGTTG
IL1B	TTTGAGTCTGCCCAGTTCCC	TCAGTTATATCCTGGCCGCC
ITGAM	TGCTTCCTGTTTGGATCCAACCTA	AGAAGGCAATGTCACTATCCTCTTGA
GAPDH	TGCACCACCAACTGCTTAGC	GGCATGGACTGTGGTCATGA
SDHA	GAAGCCCTTTGAGGAGCACT	GTTTTGTCGATCACGGGTCT

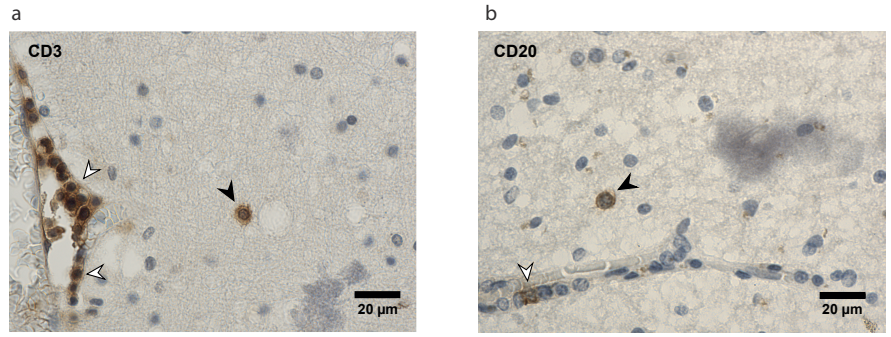

Supplementary figure 1: Lymphocyte staining in the vessel wall and parenchyma.
Representative pictures of $CD3^+$ (a) and $CD20^+$ (b) stainings in the superior temporal gyrus (STG). White arrows represent positive cells in the vessel wall; black arrows show positive cells in the parenchyma.

Chapter 6

Microglia in post-mortem brain tissue of patients with bipolar disorder are not immune activated

Marjolein A.M. Sneeboer[1,2*], Gijsje J.L.J. Snijders[1,2*], Woutje M. Berdowski[2], Alba Fernández-Andreu[2], Psychiatric donor program of the Netherlands Brain Bank (NBB-Psy)[3], Hans C. van Mierlo[1,2], Amber Berdenis van Berlekom[1,2], Manja Litjens[1,2], René S. Kahn[1,4], Elly M. Hol[2,5], Lot D. de Witte[1,2,4]

* These authors share first authorship

[1] Department of Psychiatry, Brain Center Rudolf Magnus, University Medical Center Utrecht, Utrecht University (BCRM-UMCU-UU), 3584 CG Utrecht, The Netherlands
[2] Department of Translational Neuroscience, Brain Center Rudolf Magnus, University Medical Center Utrecht, Utrecht University (BCRM-UMCU-UU), 3584 CG Utrecht, The Netherlands
[3] Psychiatric donor program of the Netherlands Brain Bank (NBB-Psy), Meibergdreef 47, 1105 BA Amsterdam, the Netherlands
[4] Department of Psychiatry, Icahn School of Medicine at Mount Sinai, New York, United States of America
[5] Neuroimmunology, Netherlands Institute for Neuroscience, an institute of the royal academy of arts and sciences, 1105 BA, Amsterdam, The Netherlands.

Manuscript under review: Translational psychiatry

Abstract

Genetic, epidemiological, and biomarker studies suggest that the immune system is involved in the pathogenesis of bipolar disorder (BD). It has therefore been hypothesized that immune activation of microglia, the resident immune cells of the brain, is associated with the disease. Only a few studies have addressed the involvement of microglia in BD so far and a more detailed immune profiling of microglial activation is lacking. Here, we applied a multi-level approach to determine the activation state of microglia in BD post-mortem brain tissue. We did not find differences in microglial density, morphology, and mRNA expression of microglial markers in the medial frontal gyrus (MFG) of patients with BD. Furthermore, we performed in depth characterization of human primary microglia isolated from fresh brain tissue of the MFG, superior temporal gyrus (STG), and thalamus (THA). Similarly, these *ex vivo* isolated microglia did not show elevated expression of inflammatory markers. Finally, challenging the isolated microglia with LPS did not result in an increased immune response in patients with BD compared to controls. Interestingly, we observed a trend towards a decreased expression of CX3CR1, consistent across brain tissues in total brain tissue and in acutely isolated human microglia. In conclusion, our study shows that microglia in post-mortem brain tissue of patients with BD are not immune activated. The results on CX3CR1 suggest that other key functions of microglia might play a role in the disease, which should be investigated in further studies.

Introduction

The aetiology of bipolar disorder (BD) is still largely unknown. Several lines of evidence suggest that the immune system is involved in the pathogenesis of BD. Epidemiological studies on large birth cohorts have shown an association between BD and autoimmune diseases, atopic disorders, and severe childhood infections[1–3]. Additionally, genetic studies found that several genes associated with BD cluster in immune pathways[4]. Furthermore, many research groups have reported alterations in peripheral immune markers in BD, with increased levels of C-reactive protein (CRP) and several cytokines, such as IL1β, IL6, and TNFα, in blood and cerebrospinal fluid of patients with BD[3,5–7]. Besides, a decreased percentage of T-regulatory cells[8–10] and an altered gene expression profile of circulating monocytes in the blood have been described[8,11].

It is not yet understood how these immune associations are involved in the pathogenesis of BD, but activation of microglia, the immune cells that reside in the brain parenchyma, has been hypothesized to play a central role[12–15]. Microglia are part of the innate immune system and have an important function in initiating and controlling neuroinflammation in the CNS via the secretion of pro- and anti-inflammatory cytokines. In addition, these cells are involved in neurodevelopment and neuronal functioning in adulthood via promoting synaptogenesis and synaptic pruning[16,17]. Besides, microglia are involved in the regulation and production of serotonin of which an imbalance has been implicated in BD[13]. In homeostatic conditions microglia have a ramified morphology with highly motile protrusions that scan the environment for possible danger signals, such as pathogens or cell debris. Upon detection, microglia become immune activated. They migrate to the site of injury, and change their expression profile and shape to a more rounded or so-called 'amoeboid' morphology. This process is necessary to adequately respond to the insult via the secretion of cytokines and chemokines, antigen presentation of the microglia, and apoptosis of the injured cell[18–20]. Although microglial immune activation is crucial to minimize the effects of the injury, prolonged activation will lead to release of reactive oxygen species, which are toxic to neurons and other neighbouring cells[21]. In BD it has been hypothesized that microglia are immune activated, possibly induced by circulating peripheral immune factors, and result in CNS damage and abnormalities[22,23].

However, evidence for immune activation of microglia in BD is still lacking. Five post-mortem studies investigated the density of microglia or the expression of microglia markers in BD. The samples sizes ranged from 9-20 patients, different microglial

markers were used, and multiple brain regions were studied. None of the studies found an increased microglial density or elevated expression of microglial markers[24–27]. One study even found decreased mRNA expression of the microglial markers *ITGAM* (CD11b) and *CD68* in the anterior cingulate cortex and prefrontal cortex[28]. Moreover, in a positron emission tomography study with the [(11)C]-(R)-PK11195 tracer, there was no sign for microglia activation in most regions of the brain in BD, except for the hippocampus[29]. A drawback of these studies was that most used one methodological approach (i.e. number of microglia, microglial mRNA expression or protein level), non-automated analysis and focussed on immunostainings that only give limited information about the diversity of microglial phenotype and function. To conclude, an in depth microglial immune profile examining more specific signs of microglial activation is still missing in BD.

Therefore, the aim of this study was to determine whether microglia in post-mortem brain tissue of patients with BD are immune activated. We applied a multi-level approach and characterized microglial density, morphology, phenotype, and inflammatory functions in the medial frontal gyrus (MFG) of patients with BD. To further profile the microglia and examine their inflammatory function, we isolated human primary microglia from fresh post-mortem brain tissue of the MFG, superior temporal gyrus and thalamus. This allows us to characterize microglia outside the brain and assess their functions more extensively[30–33]. This exclusive approach has been used to profile microglia in neurologic disorders, such as multiple sclerosis and Alzheimer's disease[34–36], but has not yet been applied to psychiatric disorders. To our knowledge the present study is the first investigating microglial immune activation in *ex vivo* isolated human microglia in combination with immunohistochemistry and mRNA profiling.

Materials & Methods

Donors

Paraffin (control N=12; BD N=16), snap frozen (control N=16; BD N=15), and fresh post-mortem brain tissue (control N=20; BD N=11) of patients with BD and controls was obtained from the Netherlands Brain Bank (www.brainbank.nl). An overview of the clinical characteristics and donors used per experiment is summarized in Table 1 and Supplementary table 1. We selected the medial frontal gyrus (MFG) as the main region of interest (ROI). For fresh post-mortem brain tissue we also selected the superior temporal gyrus (STG) and thalamus (THA). All three regions have been associated with BD[20,37,38]. Permission for brain autopsy and the usage of brain tissue

and accompanied clinical information for research purposes was obtained per donor ante-mortem. Due to insufficient quality of the tissue or limited number of viable microglia after isolation, we could not include every donor for all downstream analyses. There was no significant difference between controls and patients with BD in age, post-mortem delay (PMD), and pH (Table 1). Only in frozen tissue, sex was significantly different in both grey (p = 0.004) and white matter (p = 0.008) between patients with BD and controls.

Table 1: Summary of clinical information and post-mortem variables of the study

		Control (N=12)	BD (N=16)
	Age (years)	75.6 ± 11.8	72.0 ± 10.4
Immunohistochemistry	Sex (M:F)	7:5	12:4
(paraffin tissue)	PMD (minutes)	566 ± 376	429 ± 176
	pH	6.53 ± 0.18	6.45 ± 0.18
		Control (N=16)	BD (N=15)
	Age (years)	75.06 ± 13.02	74.73 ± 8.04
mRNA expression	Sex (M:F)	5:11*	12:3*
(frozen tissue)	PMD (minutes)	429 ± 189	430 ± 183
	pH	6.52 ± 0.29	6.42 ± 0.23
		Control (N=16)	BD (N=11)
	Age (years)	79.69 ± 11.97	74.27 ± 17.78
mRNA expression	Sex (M:F)	5:11	5:6
(isolated microglia)	PMD (minutes)	447 ± 128	456 ± 116
	pH	6.75 ± 0.32	6.67 ± 0.49
		Control (N=17)	BD (N=7)
	Age (years)	80.94 ± 12.15	72.14 ± 19.57
Protein expression	Sex (M:F)	5:12	2:5
(isolated microglia)	PMD (minutes)	443 ± 120	428 ± 117
	pH	6.74 ± 0.30	6.71 ± 0.54
		Control (N=20)	BD (N=8)
	Age (years)	80.4 ± 12.0	71.38 ± 19.71
LPS response	Sex (M:F)	7:13	2:6
(isolated microglia)	PMD (minutes)	455 ± 142	476 ± 127
	pH	6.71 ± 0.30	6.80 ± 0.57

Summary of the clinical information (age and sex) and post-mortem variables (post-mortem delay (PMD) and pH) of donors used in the study. Information is separated per experimental category. Numbers represent mean ± standard deviation. M = males, F = females, BD = bipolar disorder. *significantly different between patients with BD and controls in grey (p = 0.004) and white matter (p = 0.008).

Immunostaining and image analysis

Paraffin-embedded tissue of the MFG of patients with BD and controls was sectioned at 7µm. The sections were deparaffinised using a standard xylene and alcohol series, followed by blocking of endogenous peroxidase with PBS, 1% H_2O_2 (Merck, Germany). For antigen retrieval, sections were heated in 0.01mM citrate buffer

(Merck, Darmstadt, Germany), 0.05% Tween-20 (Merck, Darmstadt, Germany), pH = 6.0 for 15 minutes. Subsequently, aspecific binding was blocked in PBS with 1% normal horse serum (NHS, Thermo Fisher Scientific, Massachusetts, USA), 0.1% bovine serum albumin (BSA, Merck, Darmstadt, Germany), 0.2% Triton X (Merck, Darmstadt, Germany). Sections were incubated with a rabbit polyclonal anti-Iba1 antibody (Wako Pure Chemical Industries, Ltd., 1:1000) at 4°C. Next day, secondary goat-anti-rabbit biotin (Jackson ImmunoResearch Laboratories, Inc., 1:400) was added, followed by avidin-biotin-peroxidase (AB) complex (Vector Laboratories, USA). To visualize the microglia, the sections were incubated with a 3,3' diaminobenzidine (DAB) substrate (DAKO, USA). Finally, tissue sections were dehydrated using an alcohol and xylene series and embedded in Entellan (Merck, Darmstadt, Germany). Per tissue section, six pictures were taken randomly and blinded for diagnosis from grey matter and white matter. Microscopic images were analysed automatically using open source software ImageJ. Microglial cell density was calculated with a particle analysis macro-script, by dividing the cell numbers by the measured area (microglia/mm^2). To quantify microglial morphology we analysed the cell-body-to-size-ratio[39]. The size of the cell body and cell perimeter was determined with an automated particle outline analysis and radius circular mask macro. A cell-body-to-size-ratio close to zero is associated with a more ramified state, while amoeboid microglia have a cell-body-to-size-ratio close to one.

Human primary microglia isolation

Human primary microglia (pMG) were isolated from fresh post-mortem brain tissue of the different ROIs based on an earlier established protocol[30]. Brain tissue was first mechanically dissociated through a metal sieve in a glucose- potassium-sodium buffer (GKN-BSA; 8.0g/L NaCl, 0.4g/L KCl, 1.77g/L $Na_2HPO_4.2H_2O$, 0.69g/L $NaH_2PO_4.H_2O$, 2.0g/L D-(1)- glucose, 0.3% bovine serum albumin (BSA, Merck, Darmstadt, Germany); pH 7.4) and supplemented with collagenase Type I (3700 units/mL; Worthington, USA) and DNase I (200µg/mL; Roche, Switzerland) at 37°C for 30 minutes (THA) or 60 minutes (MFG, STG) while shaking. The suspension was put over a 100µM cell strainer and washed with GKN-BSA buffer in the centrifuge (1800 rpm, slow brake, 4°C, 10 minutes) before the pellet was resuspended in 20mL GKN-BSA buffer. 10mL of Percoll (Merck, Darmstadt, Germany) was added drop wise and the tissue homogenate was centrifuged at 4000 rpm (fast acceleration, slow brake at 4°C, 30 minutes). The middle layer was collected and washed with GKN-BSA buffer, followed by resuspension and centrifuging in a magnetic-activated cell sorting (MACS) buffer (PBS, 1% heat-inactivated fetal cow serum (FCS), 2mM EDTA; 1500 rpm, 10°C, 10 minutes). Microglia were positively selected with CD11b conjugated magnetic microbeads (Miltenyi Biotec, Germany) according to manufacturer's protocol. Microglia were lysed in TRIzol

reagent (Invitrogen, USA), stained for flow cytometry or cultured in a poly-L-lysine (PLL; Merck, Germany) coated 96-wells flat bottom plate (Greiner Bio-One, Austria) at a density of 1.0 x 10^5 cells in a total volume of 200µL Rosswell-Park-Memorial-Institute medium (RPMI; Gibco Life technologies, USA) supplemented with 10% FCS, 2mM L-glutamine (Gibco Life technologies, USA), 1% penicillin-streptomycin (Gibco Life technologies, USA) and 100ng/ml IL-34 (Miltenyi Biotech, Germany). After overnight incubation, pMG were stimulated with 100ng/mL lipopolysaccharide (LPS) from Escherichia coli 0111:B4 (Merck, Germany) for 6 hours. The cells were harvested with TRIzol reagent and stored at -80°C for further analysis of mRNA expression.

Gene expression analysis

Grey and white matter were manually separated from a 50µM section of frozen brain tissue at the cryostat and lysed with TRIzol reagent. RNA extraction, cDNA synthesis, and qPCR on these brain tissue samples and pMG were performed as described before[30]. Primer sequences are listed in Supplementary table 2. Absolute expression was calculated using the ΔΔCT method[40]. Expression Suite software 1.0.4 was used to select the most stable genes across ROIs, diagnosis, grey/white matter tissue and different donors for normalization. 18S ribosomal RNA (*18S*) and glyceraldehyde 3-phosphate dehydrogenase (*GAPDH*) were most stable for whole brain tissue and β-Actin (*ACTB*) and *GAPDH* for directly isolated pMG. LPS stimulated pMG were normalized with *GAPDH* and a combination of *ACTB* and Protein Phosphatase 1 Catalytic Subunit Alpha (*PP1A*). Undetermined values were set to maximum CT value of 40 to compare median levels of relative expression between BD and controls.

Flow cytometry of human primary microglia

12-20 x 10^4 human primary microglia were stained in a v-bottom 96-wells plate (Greiner Bio-One, Austria) directly after isolation. pMG were washed with 100µL PBS with 0.5% BSA (PBA) and incubated in 25µL PBA with specific monoclonal or isotype control antibodies (supplementary table 3). After staining, the cells were washed with PBA, fixated with 4% paraformaldehyde (Riedel-de Haën, Germany) in PBS at room temperature and stored in the fridge for flow cytometry analysis the next day. All microglia samples were processed on a FACS Canto (BD Bioscience) with calibrated settings and similar voltage for the fluorescent channels. The geomean fluorescence intensity (MFI) was determined by subtracting the MFI of the isotype control from the MFI of the positive antigen staining.

Statistical Analysis

Statistical analysis was done with GraphPad Prism software (version 7) and SPSS IBM 23. Chi-square tests and independent t-tests were used to test for sex, age, PMD, and pH difference. Non-parametric Mann-Whitney test was performed to analyse differences in microglia density, cell-body-to-cell-size ratio, gene expression, and protein levels between BD and controls. Bonferroni correction for multiple testing was used for the qPCR and flow cytometry experiments, since more than one marker was analysed per region in the same experiment. For all outcome measures in this study, a spearman ranks correlation was performed to assess whether sex, age, PMD or pH were associated with the outcome. In case we found a significant association (Supplementary table 4), an ANCOVA was applied to correct for possible confounding effects.

Results

Microglial density and morphology, and expression of microglial markers in total brain tissue

We analysed microglial density with immunohistochemistry using microglial marker ionized calcium-binding adapter molecule 1 (Iba1). Figure 1a shows four representative pictures of DAB-Iba1^{+} microglia in the grey (I, III) and white matter (II, IV) in the MFG of a control donor (I-II) and patient with BD (III-IV). Automated counting with ImageJ resulted in a similar microglial density between patients with BD and controls (Figure 1b). Results were validated with immunofluorescent staining, showing no differences in microglial number relative to total cell number in BD compared to controls (Supplementary figure 1a, b). A more specific sign of microglial immune activation is a change in morphology, which we analysed using the cell-body-to-cell-size ratio (Supplementary figure 1c). The cell-body-to-cell-size-ratio was similar for patients with BD and controls in the grey (p = 0.63) and white (p = 0.72) matter of the MFG (Figure 1c). Furthermore, we assessed whether the expression of a panel of microglial-related genes is changed in both grey and white matter of the MFG in BD. We defined three gene categories: 1) microglial-associated (*AIF1*, *P2Y12* and *TMEM119*), 2) expressed on all myeloid cells (*CD68* and *ITGAM*), and 3) microglial immune activation (*HLA-DRA, IL1B* and *IL6)* (Table 2 and Figure 1d-g). We did not find differences in expression between patients and controls for any of these genes.

Phenotype and function of isolated microglia

Isolation of human primary microglia provided us with the opportunity to profile and characterize microglia as a pure cell population more extensively. We found no differences in the expression of genes involved in pro-inflammatory signalling (*IL1B* and *IL6*; Figure 2a,b), genes related to anti-inflammatory functioning (*CD163* and *MRC1*; Figure 2c,d), and *TMEM119*, a microglial specific gene known for its homeostatic properties[33,41] in the MFG (Figure 2e), STG, and THA (Supplementary figure 2). We analysed the expression of a panel of proteins by flow cytometry, including more general markers for microglia and myeloid cells (CD11b, CD11c, CD45, CD14, CD16, CD32, CD40, CD64, CX3CR1) and markers related to immune activation of the cells (CD163, CD172α, CD200R, CD206, HLA-DR, CD83, CD86) (Figure 2f-h, Supplementary table 5). We found a slightly, but not significantly, increased expression of HLA-DR (Figure 2H). Similarly, we did not find differences in protein expression, including HLA-DR, between controls and BD in the STG and THA (supplementary figure 4).

Table 2: mRNA expression of microglial genes in the medial frontal gyrus

	Control		BD			Control		BD		
Gene	**Median**	**IQR**	**Median**	**IQR**	***p*-value**	**Median**	**IQR**	**Median**	**IQR**	***p*-value**
AIF1	3.05	6.35	2.19	4.75	0.68	4.78	6.81	3.28	5.88	0.43
P2Y12	0.86	3.08	0.74	1.64	0.50	1.22	2.95	1.48	1.78	0.85
TMEM119	0.27	0.73	0.23	0.38	0.78	0.39	0.75	0.19	0.48	0.43
CD68	1.31	2.89	0.58	1.44	0.30	2.88	3.69	1.25	1.69	0.10
ITGAM	0.06	0.14	0.06	0.09	0.47	0.08	0.19	0.11	0.13	0.85
IL1B	0.05	0.34	0.06	0.20	0.71	0.18	0.38	0.22	0.31	1.00
IL6	0.04	0.16	0.05	0.17	0.45	0.05	0.12	0.15	0.33	0.52
HLA-DRA	3.97	7.71	1.74	2.73	0.20	6.25	11.03	3.81	5.28	0.06

mRNA expression was determined in grey (left) and white matter (right) of the medial frontal gyrus in patients with bipolar disorder (BD, N=15) and controls (N=16) by qPCR. Median, interquartile range (IQR; 25–75%) and *p*-value is shown for microglial-associated genes (*AIF1*, *P2RY12*, *TMEM119*), genes expressed on all myeloid cells (*CD68*, *ITGAM*) and genes involved in microglial immune activation (*IL1B*, *IL6*, *HLA-DRA*).

To determine inflammatory responsiveness, we challenged the isolated human microglia with LPS and determined the mRNA expression levels of cytokines. Elevated expression of these markers in BD relative to controls would suggest increased (primed) immune activity of the cells. In contrast, less expression could indicate 'silenced' microglia in which sustained immune activation results in a blunted inflammatory response. We found that microglia from BD and controls both responded to LPS with increased expression of *IL1B*, *IL6,* and *TNF* (Figure 2i). The effect was not significantly different between microglia of patients with BD and controls. The same was observed in microglia from the STG and THA (Supplementary figure 4).

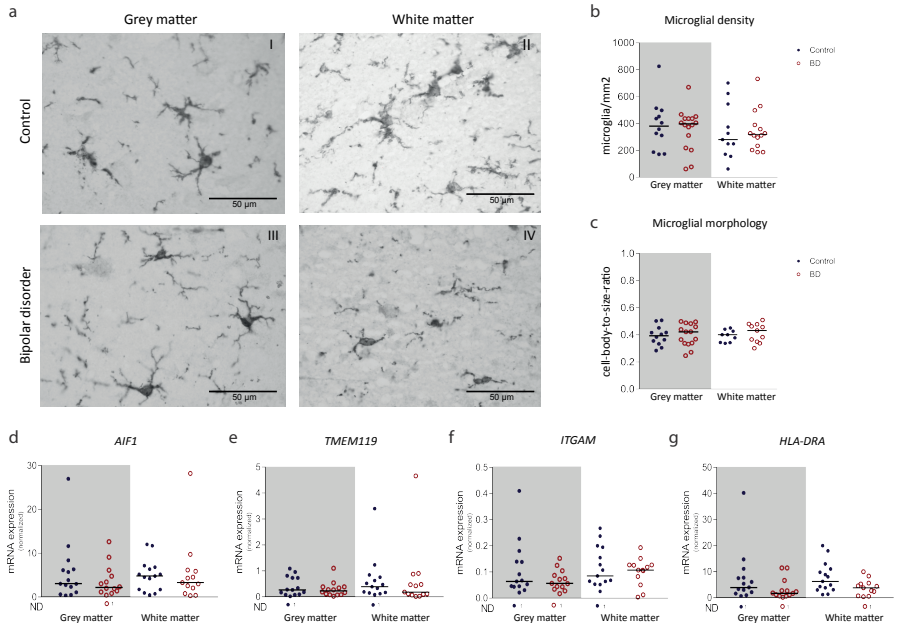

Figure 1: Microglial density and morphology, and expression of microglial markers in total brain tissue.

(a-c) The medial frontal gyrus of patients with bipolar disorder (BD) and controls was stained for microglial marker ionized calcium-binding adapter molecule (Iba1) to analyse microglial density and morphology. a) Representative pictures are shown of microglia in grey (I, III) and white (II, IV) matter of controls (I-II) and patients with BD (III-IV). b) The number of microglia (microglia/mm^2) was quantified in grey and white matter in controls (N=12, blue dots) and patients with BD (N=16, red circles). c) Quantification of microglial morphology shown as the cell-body-to-size-ratio of microglia in patients with BD (N=16) and controls (N=12). (d-g) mRNA expression of microglial markers *AIF1* and *TMEM119*, myeloid marker *ITGAM* and *HLA-DRA* in patients with BD (N=15) and controls (N=16) was determined using qPCR. Gene expression was normalized to 18S ribosomal RNA (*18S*) and glyceraldehyde 3-phosphate dehydrogenase (*GAPDH*) using the ΔΔCT method. Graphs show median expression levels and non-parametric testing with Bonferroni correction for multiple testing was performed. ND = number of non-detected samples.

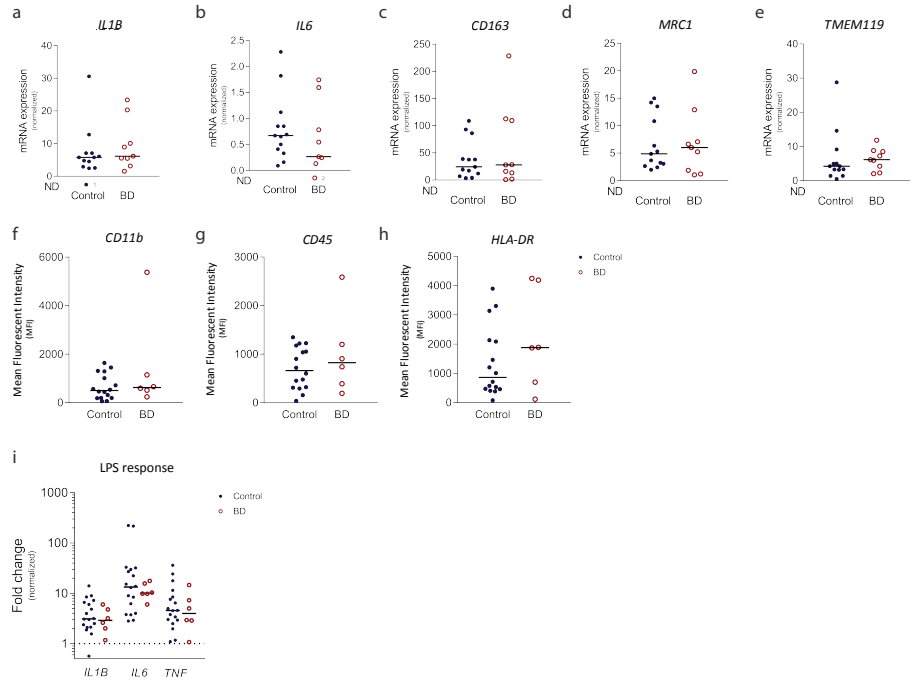

Figure 2: Phenotype and function of isolated microglia.

Human microglia were isolated from the medial frontal gyrus of controls (N=13, blue dots) and patients with bipolar disorder (BD, N=9, red circles). a-e) After isolation mRNA expression of pro-inflammatory genes (*IL1B* (a) and *IL6* (b)), anti-inflammatory genes (*CD163* (c) and *MRC1* (d)), and the microglial specific gene *TMEM119* (e) was determined in patients with BD and controls using qPCR. Gene expression was normalized to β-Actin (*ACTB*) and glyceraldehyde 3-phosphate dehydrogenase (*GAPDH*) using the ΔΔCT method. ND = number of non-detected samples. f-h) Protein expression of isolated microglia from controls (N=16) and patients with BD (N=6) was characterized by flow cytometry. The mean fluorescent intensity (MFI) is determined for CD11b (f), CD45 (g) and HLA-DR (h). i) Inflammatory response of isolated microglia from controls (N=18) and patients with BD (N=6) after 6 hours of stimulation with lipopolysaccharide (LPS) was determined by measuring mRNA expression of *IL1B, IL6* and *TNF*. The fold change was calculated by dividing mRNA expression of the LPS stimulated sample by mRNA expression of the non-stimulated sample of the same subject. The dotted line represents baseline mRNA expression of non-stimulated cells. Graphs show median expression levels and non-parametric testing with Bonferroni correction for multiple testing was performed.

Expression of CX3CR1 in total brain tissue and isolated microglia

The chemokine receptor CX3CR1 showed a non-significant but consistent disease-related effect in different experiments and ROIs. In total brain tissue we found small decreases of *CX3CR1* mRNA expression (Figure 3a), especially in the white matter. In microglia isolated from post-mortem brain tissue these changes were more abundant (Figure 3b-d). The decreased expression was not only present in the MFG (Figure 3b), but also seen in human microglia isolated from the STG (Figure 3c) and THA (Figure 3d). Besides, CX3CR1 protein levels were also lower in the STG and THA (Figure 3f-g).

Discussion

The aim of this study was to elucidate whether microglia are immune activated in patients with BD, as is hypothesised by many studies[12–15,22,23]. We performed the most extensive, multi-level study to date in characterizing microglial inflammation in BD. We did not find any support for microglial immune activation, since we did not find differences in microglial density, morphology, and the expression of mRNA levels genes related to microglial function in fixed and frozen brain tissue. The absence of an immune activated phenotype of microglia in BD was confirmed by the lack of upregulation of inflammatory markers in *ex vivo* isolated human microglia on mRNA and protein level. Moreover, challenging human microglia of patients with BD with LPS did not result in an altered immune phenotype compared to control microglia. Altogether, the results of post-mortem studies, including ours, are consistent and do not support the hypothesis that microglia are immune activated in BD.

Our findings are in line with previous post-mortem studies that investigated microglial immune activation in BD by quantifying microglial cell numbers[24–27]. The results are also in agreement with four recent post-mortem RNA sequencing studies on different brain regions in BD[42–45]. The largest study, including 34 patients with BD and 35 controls, reported no difference in mRNA and cytokine expression of several immune markers in BD[46]. In two smaller studies several microglial immune activation markers were downregulated, albeit not significant after correction for multiple testing[43,44]. Only one study reported enrichment of several immune pathways[45]. However, none of the activation markers that were examined in our present study were significantly different between BD and controls in that study.

The hypothesis of immune activation as driving force in BD was mainly based on studies that have described immune alterations in the periphery[5–7]. This is in contrast to our results showing no microglial activation in the CNS, but could be explained

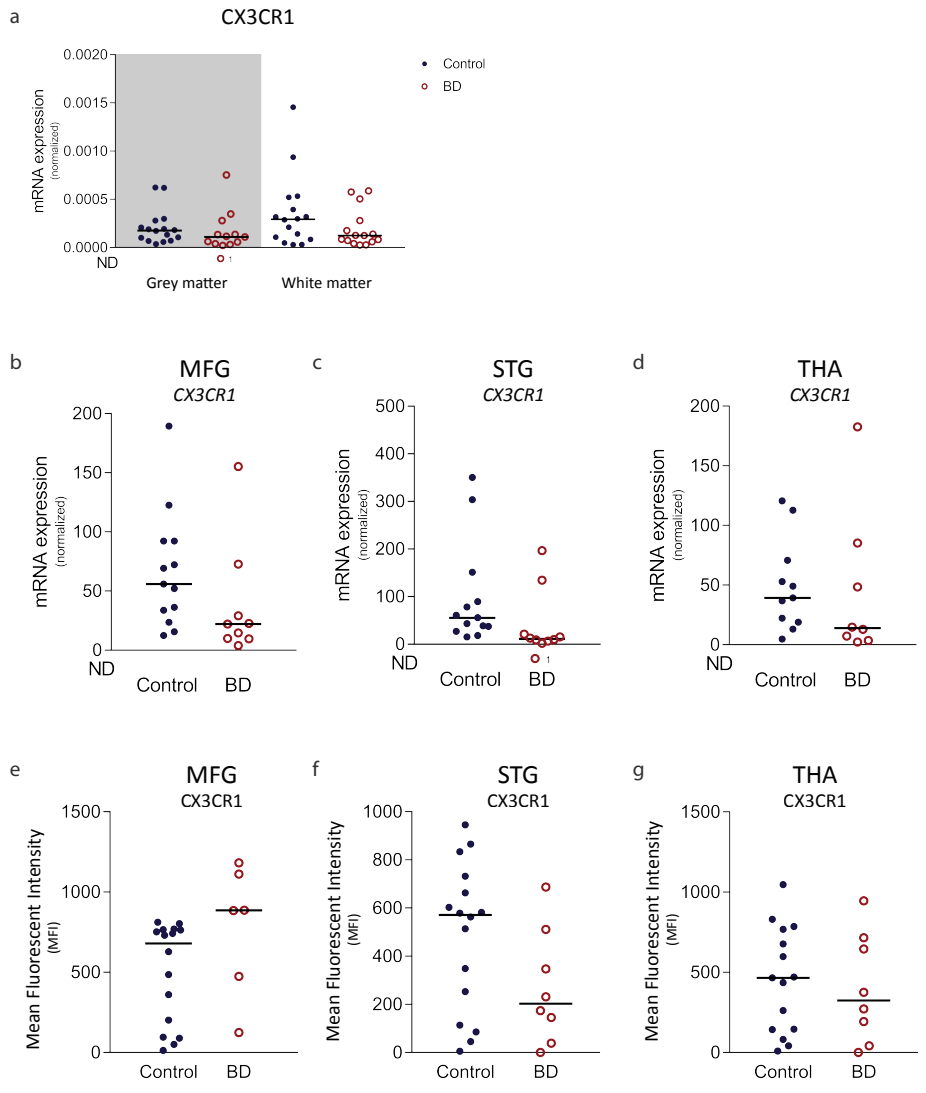

Figure 3: Expression of CX3CR1 in total brain tissue and isolated microglia.
a) mRNA expression of *CX3CR1* was determined in grey and white matter of the medial frontal gyrus in controls (N=16) blue dots) and patients with bipolar disorder (BD, N=15, red circles) by qPCR. Gene expression was normalized to 18S ribosomal RNA (*18S*) and glyceraldehyde 3-phosphate dehydrogenase (*GAPDH*) using the ΔΔCT method. ND = number of not-detected samples. b-d) Gene expression of *CX3CR1* in microglia isolated from the medial frontal gyrus (MFG; b), superior temporal gyrus (STG; **c**) and thalamus (THA; d) from controls (N=14) and patients with BD (N=10). Gene expression was normalized to β-Actin (*ACTB*) and succinate dehydrogenase complex flavoprotein subunit A (*SDHA*) using the ΔΔCT method. ND = number of non-detected samples. e-g) Mean fluorescent intensity (MFI) of CX3CR1 is quantified in the medial frontal gyrus (MFG; e), superior temporal gyrus (STG; f) and thalamus (THA; g) from controls (N=16) and patients with BD (N=8) by flow cytometry. Graphs show median expression levels and non-parametric testing with Bonferroni correction for multiple testing was performed.

in several ways. An important point is the difference in age between the patients in post-mortem studies and peripheral studies, with lower mean age in the latter. Therefore we are only able to draw conclusions on microglial immune activation in the late phases of the disease. To further understand the relationship between peripheral immune alterations in BD and microglial activation an interesting follow-up study would be to analyse peripheral markers in serum and relate this to markers for microglial activation in the same post-mortem brain donors. At the same time, it is important to look at other explanations for the observed peripheral immune alterations in BD. Immune biomarkers in blood are very sensitive to changes in life-style, such as smoking, BMI, diet, stress and sleep problems[47,48]. We should therefore include the possibility that the peripheral changes actually reflect behavioural consequences and not the cause of the disease. On the other hand, this does not explain the increased prevalence of immune-related disorders in BD. Other immune-mediated mechanisms should therefore be investigated, such as autoimmunity and the role of non-inflammatory immune pathways in the brain that are for instance involved in glia-neuron communication[49].

It is becoming more evident that microglia have many more functions than controlling inflammation. Microglia are for example actively participating in modifying synapses in the brain[50,51]. Several molecules have been described to be important for the communication between neurons and microglia, including fractalkine (CX3CL1), which is expressed by neurons and its receptor (CX3CR1) by microglia[52]. CX3CR1 is important for microglial migration, the motility of microglial processes, immune activation, synaptic plasticity, and controlling synaptic transmission in physiological conditions[50,51,53,54]. In our study we found a consistent trend across brain tissues towards decreased expression of CX3CR1 in microglia isolated from patients with BD, similar as found in one of the RNA sequencing studies[43]. Evidence showed that CX3CR1 is involved in non-immune related mechanisms that are also affected in BD[55]. These CX3CR1 regulated mechanisms are, for example, inhibition of glutamate in the hippocampus, increasing GABA activity at serotonergic neurons and regulation of synaptic plasticity. Furthermore, in an animal model for depression it was shown that prenatal stress leads to decreased expression of CX3CR1 in the brain[56]. Furthermore, $CX3CR1^{-/-}$ mice show alterations in brain connectivity and behaviour, elevated cytokine and corticosterone levels, and more HPA-axis activity[57–59]. In addition, it was shown that hormonal, metabolic and behavioural responses to chronic and acute stress were affected in these mice[60,61]. Since all of these biological systems have been associated with BD[62], we speculate that a lower CX3CR1 expression in BD, could play an important role in the pathogenesis of this disease.

The multi-level approach used in this study contributed to a more detailed understanding of microglial activation in BD. Microglial heterogeneity was taken into account by making a distinction between microglia in grey and white matter brain tissue and by analysing isolated microglia from three brain regions. We applied different techniques to frozen, paraffin, and acutely isolated microglia to elucidate whether microglial immune activation is present. Additionally, we used scripted and automated analyses in our study, which is more accurate and unbiased compared to visual analysis or manual counting. A drawback of this study is the limited sample size per experiment (minimal six donors per condition). The availability of fresh post-mortem brain tissue is sparse, especially for psychiatric disorders. Moreover, the heterogeneity of the BD donors in our cohort and pre- and post-mortem confounders may have influenced our results. For some of our outcome measures, we found a significant correlation with one of the confounders age, sex, pH or PMD. However, correction for these factors resulted in similar findings. Controlling for medication was very difficult, due to the high variability of medication received by the donors. We did study the effect of corticosteroids on mRNA and protein expression and could not find a correlation (data not shown). No information was available about state of the disease ((hypo)mania or depression) during time of death of the donor. This might be an important factor, since monocyte-induced-microglia generated from patients with BD during a manic or depressed stated have been shown to express a different immune profile[63].

In summary, the present study provides an overview of the immune state of microglia in BD. By using a multi-level approach, microglia were extensively profiled in post-mortem brain tissue of the MFG. Microglia in BD did not display any characteristics indicating immune activation. The data on CX3CR1 expression suggest that other microglial functions important for BD pathogenesis, such as the response to stress and their role in synaptic plasticity, could be affected.

Acknowledgements

This project is financially supported by a 2014 NARSAD Young Investigator Grant provided by the Brain & Behaviour Research Foundation. This study was further supported by the psychiatric donor program of the Netherlands Brain Bank (NBB-Psy), which is supported by the Netherlands Organization for Scientific Research (NWO). The authors thank the team of the Netherlands Brain Bank for their services and P.R. Ormel and Y. He for their help with the microglial isolations and LPS response experiments.

Conflict of interest

The authors declare no conflict of interest.

References

1 Benros ME, Waltoft BL, Nordentoft M, Ostergaard SD, Eaton WW, Krogh J *et al.* Autoimmune diseases and severe infections as risk factors for mood disorders: a nationwide study. *JAMA psychiatry* 2013; **70**: 812–20.

2 Cremaschi L, Kardell M, Johansson V, Isgren A, Sellgren CM, Altamura AC *et al.* Prevalences of autoimmune diseases in schizophrenia, bipolar I and II disorder, and controls. *Psychiatry Res* 2017; **258**: 9–14.

3 Wang L-Y, Chiang J-H, Chen S-F, Shen Y-C. Systemic autoimmune diseases are associated with an increased risk of bipolar disorder: A nationwide population-based cohort study. *J Affect Disord* 2018; **227**: 31–37.

4 Network and Pathway Analysis Subgroup of Psychiatric Genomics Consortium. Psychiatric genome-wide association study analyses implicate neuronal, immune and histone pathways. *Nat Neurosci* 2015; **18**: 199–209.

5 Fernandes BS, Steiner J, Molendijk ML, Dodd S, Nardin P, Gonçalves C-A *et al.* C-reactive protein concentrations across the mood spectrum in bipolar disorder: a systematic review and meta-analysis. *The Lancet Psychiatry* 2016; **3**: 1147–1156.

6 Goldsmith DR, Rapaport MH, Miller BJ. A meta-analysis of blood cytokine network alterations in psychiatric patients: comparisons between schizophrenia, bipolar disorder and depression. *Mol Psychiatry* 2016; **21**: 1696–1709.

7 Munkholm K, Braüner JV, Kessing LV, Vinberg M. Cytokines in bipolar disorder vs. healthy control subjects: A systematic review and meta-analysis. *J Psychiatr Res* 2013; **47**: 1119–1133.

8 Vogels RJ, Koenders MA, van Rossum EFC, Spijker AT, Drexhage HA. T Cell Deficits and Overexpression of Hepatocyte Growth Factor in Anti-inflammatory Circulating Monocytes of Middle-Aged Patients with Bipolar Disorder Characterized by a High Prevalence of the Metabolic Syndrome. *Front psychiatry* 2017; **8**: 34.

9 Snijders G, Schiweck C, Mesman E, Grosse L, De Wit H, Nolen WA *et al.* A dynamic course of T cell defects in individuals at risk for mood disorders. *Brain Behav Immun* 2016; **58**: 11–17.

10 do Prado CH, Rizzo LB, Wieck A, Lopes RP, Teixeira AL, Grassi-Oliveira R *et al.* Reduced regulatory T cells are associated with higher levels of Th1/TH17 cytokines and activated MAPK in type 1 bipolar disorder. *Psychoneuroendocrinology* 2013; **38**: 667–76.

11 Becking K, Haarman BCM, van der Lek RFR, Grosse L, Nolen WA, Claes S *et al.* Inflammatory monocyte gene expression: trait or state marker in bipolar disorder? *Int J bipolar Disord* 2015; **3**: 20.

12 Keshavarz M. Glial cells as key elements in the pathophysiology and treatment of bipolar disorder. *Acta Neuropsychiatr* 2017; **29**: 140–152.

13 Watkins CC, Sawa A, Pomper MG. Glia and immune cell signaling in bipolar disorder: insights from neuropharmacology and molecular imaging to clinical application. *Transl Psychiatry* 2014; **4**: e350–e350.

14 Réus GZZ, Fries GRR, Stertz L, Badawy M, Passos ICC, Barichello T *et al.* The role of inflammation and microglial activation in the pathophysiology of psychiatric disorders. *Neuroscience* 2015; **300**: 141–154.

15 Naaldijk YM, Bittencourt MC, Sack U, Ulrich H. Kinins and microglial responses in bipolar disorder: a neuroinflammation hypothesis. *Biol Chem* 2016; **397**: 283–96.

16 Kettenmann H, Kirchhoff F, Verkhratsky A. Microglia: New Roles for the Synaptic Stripper. *Neuron* 2013; **77**: 10–18.

17 Schafer DP, Stevens B. Microglia Function in Central Nervous System Development and Plasticity. *Cold Spring Harb Perspect Biol* 2015; **7**: a020545.

18 Sklar P, Smoller JW, Fan J, Ferreira MAR, Perlis RH, Chambert K *et al.* Whole-genome association study of bipolar disorder. *Mol Psychiatry* 2008; **13**: 558–69.

19 Kettenmann H, Hanisch U-K, Noda M, Verkhratsky A. Physiology of microglia. *Physiol Rev* 2011; **91**: 461–553.

20 Maletic V, Raison C. Integrated neurobiology of bipolar disorder. *Front Psychiatry* 2014; **5**: 98.

21 Takeuchi H. Neurotoxicity by microglia: Mechanisms and potential therapeutic strategy. *Clin Exp Neuroimmunol* 2010; **1**: 12–21.

22 Rosenblat JD, McIntyre RS. Bipolar Disorder and Immune Dysfunction: Epidemiological Findings, Proposed Pathophysiology and Clinical Implications. *Brain Sci* 2017; **7**. doi:10.3390/brainsci7110144.

23 Beumer W, Gibney SM, Drexhage RC, Pont-Lezica L, Doorduin J, Klein HC *et al.* The immune theory of psychiatric diseases: a key role for activated microglia and circulating monocytes. *J Leukoc Biol* 2012; **92**: 959–975.

24 Hercher C, Chopra V, Beasley CL. Evidence for morphological alterations in prefrontal white matter glia in schizophrenia and bipolar disorder. *J Psychiatry Neurosci* 2014; **39**: 376–385.

25 Brisch R, Steiner J, Mawrin C, Krzyżanowska M, Jankowski Z, Gos T. Microglia in the dorsal raphe nucleus plays a potential role in both suicide facilitation and prevention in affective disorders. *Eur Arch Psychiatry Clin Neurosci* 2017; **267**: 403–415.

26 Hamidi M, Drevets WC, Price JL. Glial reduction in amygdala in major depressive disorder is due to oligodendrocytes. *Biol Psychiatry* 2004; **55**: 563–569.

27 Dean B, Gibbons AS, Tawadros N, Brooks L, Everall IP, Scarr E. Different changes in cortical tumor necrosis factor-α-related pathways in schizophrenia and mood disorders. *Mol Psychiatry* 2013; **18**: 767–773.

28 Seredenina T, Sorce S, Herrmann FR, Ma Mulone X-J, Plastre O, Aguzzi A *et al.* Decreased NOX2 expression in the brain of patients with bipolar disorder: association with valproic acid prescription and substance abuse. *Transl Psychiatry* 2017; **7**: e1206.

29 Haarman BCM (Benno), Riemersma-Van der Lek RF, de Groot JC, Ruhé HG (Eric), Klein HC, Zandstra TE *et al.* Neuroinflammation in bipolar disorder – A [11C]-(R)-PK11195 positron emission tomography study. *Brain Behav Immun* 2014; **40**: 219–225.

30 Melief J, Sneeboer MAM, Litjens M, Ormel PR, Palmen SJMC, Huitinga I *et al.* Characterizing primary human microglia: a comparative study with myeloid subsets and culture models. *Glia* 2016; : 1–12.

31 Melief J, Koning N, Schuurman KGK, Van De Garde MMDB, Smolders J, Hoek RRM *et al.* Phenotyping primary human microglia: Tight regulation of LPS responsiveness. *Glia* 2012; **60**: 1506–1517.

32 Mizee MR, Miedema SSM, van der Poel M, Adelia, Schuurman KG, van Strien ME *et al.* Isolation of primary microglia from the human post-mortem brain: effects of ante- and post-mortem variables. *Acta Neuropathol Commun* 2017; **5**: 16.

33 Olah M, Patrick E, Villani A-C, Xu J, White CC, Ryan KJ *et al.* A transcriptomic atlas of aged human microglia. *Nat Commun* 2018; **9**: 539.

34 de Haas AH, Boddeke HWGM, Brouwer N, Biber K. Optimized isolation enables ex vivo analysis of microglia from various central nervous system regions. *Glia* 2007; **55**: 1374–84.

35 Moore CS, Ase AR, Kinsara A, Rao VTS, Michell-Robinson M, Leong SY *et al.* P2Y12 expression and function in alternatively activated human microglia. *Neurol Neuroimmunol neuroinflammation* 2015; **2**: e80.

36 Keren-Shaul H, Spinrad A, Weiner A, Matcovitch-Natan O, Dvir-Szternfeld R, Ulland TK *et al.* A Unique Microglia Type Associated with Restricting Development of Alzheimer's Disease. *Cell* 2017; **169**: 1276–1290.e17.

37 Emsell L, McDonald C. The structural neuroimaging of bipolar disorder. *Int Rev Psychiatry* 2009; **21**: 297–313.

38 Price JL, Drevets WC. Neurocircuitry of mood disorders. *Neuropsychopharmacology* 2010; **35**: 192–216.

39 Hovens I, Nyakas C, Schoemaker R. A novel method for evaluating microglial activation using ionized calcium-binding adaptor protein-1 staining: cell body to cell size ratio. *Neuroimmunol Neuroinflammation* 2014; **1**: 82.

40 Livak KJ, Schmittgen TD. Analysis of Relative Gene Expression Data Using Real-Time Quantitative PCR and the 2−ΔΔCT Method. *Methods* 2001; **25**: 402–408.

41 Satoh J ichi, Kino Y, Asahina N, Takitani M, Miyoshi J, Ishida T *et al.* TMEM119 marks a subset of microglia in the human brain. *Neuropathology* 2016; **36**: 39–49.

42 Darby MM, Yolken RH, Sabunciyan S. Consistently altered expression of gene sets in postmortem brains of individuals with major psychiatric disorders. *Transl Psychiatry* 2016; **6**: e890.

43 Akula N, Barb J, Jiang X, Wendland JR, Choi KH, Sen SK *et al.* RNA-sequencing of the brain transcriptome implicates dysregulation of neuroplasticity, circadian rhythms and GTPase binding in bipolar disorder. *Mol Psychiatry* 2014; **19**: 1179–85.

44 Cruceanu C, Tan PPC, Rogic S, Lopez JP, Torres-Platas SG, Gigek CO *et al.* Transcriptome Sequencing of the Anterior Cingulate in Bipolar Disorder: Dysregulation of G Protein-Coupled Receptors. *Am J Psychiatry* 2015; **172**: 1131–1140.

45 Pacifico R, Davis RL. Transcriptome sequencing implicates dorsal striatum-specific gene network, immune response and energy metabolism pathways in bipolar disorder. *Mol Psychiatry* 2017; **22**: 441–449.

46 Fillman SG, Sinclair D, Fung SJ, Webster MJ, Shannon Weickert C. Markers of inflammation and stress distinguish subsets of individuals with schizophrenia and bipolar disorder. *Transl Psychiatry* 2014; **4**: e365.

47 Duivis HE, Vogelzangs N, Kupper N, de Jonge P, Penninx BWJH. Differential association of somatic and cognitive symptoms of depression and anxiety with inflammation: findings from the Netherlands Study of Depression and Anxiety (NESDA). *Psychoneuroendocrinology* 2013; **38**: 1573–85.

48 Lamers F, Milaneschi Y, de Jonge P, Giltay EJ, Penninx BWJH. Metabolic and inflammatory markers: associations with individual depressive symptoms. *Psychol Med* 2018; **48**: 1102–1110.

49 Suzumura A. Neuron-microglia interaction in neuroinflammation. *Curr Protein Pept Sci* 2013; **14**: 16–20.

50 Wake H, Moorhouse AJ, Jinno S, Kohsaka S, Nabekura J. Resting microglia directly monitor the functional state of synapses in vivo and determine the fate of ischemic terminals. *J Neurosci* 2009; **29**: 3974–80.

51 Tremblay M-È, Lowery RL, Majewska AK. Microglial Interactions with Synapses Are Modulated by Visual Experience. *PLoS Biol* 2010; **8**: e1000527.

52 Wolf Y, Yona S, Kim K-W, Jung S. Microglia, seen from the CX3CR1 angle. *Front Cell Neurosci* 2013; **7**: 26.

53 Arnoux I, Audinat E. Fractalkine Signaling and Microglia Functions in the Developing Brain. *Neural Plast* 2015; **2015**: 689404.

54 Paolicelli RC, Bolasco G, Pagani F, Maggi L, Scianni M, Panzanelli P *et al.* Synaptic pruning by microglia is necessary for normal brain development. *Science* 2011; **333**: 1456–1458.

55 Rogers JTJT, Morganti JMJM, Bachstetter AD, Hudson CECE, Peters MMM, Grimmig BAB *et al.* CX3CR1 deficiency leads to impairment of hippocampal cognitive function and synaptic plasticity. *J Neurosci* 2011; **31**: 16241–50.

56 Trojan E, Ślusarczyk J, Chamera K, Kotarska K, Głombik K, Kubera M *et al.* The Modulatory Properties of Chronic Antidepressant Drugs Treatment on the Brain Chemokine - Chemokine Receptor Network: A Molecular Study in an Animal Model of Depression. *Front Pharmacol* 2017; **8**: 779.

57 Zhan Y, Paolicelli RC, Sforazzini F, Weinhard L, Bolasco G, Pagani F *et al.* Deficient neuron-microglia signaling results in impaired functional brain connectivity and social behavior. *Nat Neurosci* 2014; **17**: 400–406.

58 Corona AW, Huang Y, O'Connor JC, Dantzer R, Kelley KW, Popovich PG *et al.* Fractalkine receptor (CX3CR1) deficiency sensitizes mice to the behavioral changes induced by lipopolysaccharide. *J Neuroinflammation* 2010; **7**: 93.

59 Winkler Z, Kuti D, Ferenczi S, Gulyás K, Polyák Á, Kovács KJ. Impaired microglia fractalkine signaling affects stress reaction and coping style in mice. *Behav Brain Res* 2017; **334**: 119–128.

60 Winkler Z, Kuti D, Ferenczi S, Gulyás K, Polyák Á, Kovács KJ. Impaired microglia fractalkine signaling affects stress reaction and coping style in mice. *Behav Brain Res* 2017; **334**: 119–128.

61 Rimmerman N, Schottlender N, Reshef R, Dan-Goor N, Yirmiya R. The hippocampal transcriptomic signature of stress resilience in mice with microglial fractalkine receptor (CX3CR1) deficiency. *Brain Behav Immun* 2017; **61**: 184–196.

62 Maletic V, Raison C. Integrated neurobiology of bipolar disorder. *Front Psychiatry* 2014; **5**: 98.

63 Ohgidani M, Kato TA, Haraguchi Y, Matsushima T, Mizoguchi Y, Murakawa-Hirachi T *et al.* Microglial CD206 Gene Has Potential as a State Marker of Bipolar Disorder. *Front Immunol* 2016; **7**: 676.

Supplementary table 1: clinicopathological information of donors included in the study (1 of 3)

NBB number	Diagnosis	Sex	Age (years)	Braak	Amyloid	PMD (minutes)	pH	Medication 24h	Medication 3 months	Medication ever used	Somatic comorbidity	Cause of death	Used for
96/067	Control	F	70	1	NA	NA	NA				NA	NA	1
96/238	Control	F	87	2	0	480	6.91	NA			NA	2	2
96/251	Control	M	84	1	NA	540	6.20				3	2	2
96/373	Control	M	70	0	0	450	6.4	NA	AI		3	3	1
97/171	BD	F	90	3	B	390	NA	AD		MS	NA	2	1, 2
99/258	BD	M	68	1	A	355	6.82	NA		AD, MS	4c	2	1, 2
00/182	BD	M	73	2	B	315	6.38	NA	AP	AC, AD, MS	4, 4c	7	2
00/142	Control	M	73	0	0	1485	NA	NA	NA	NA	NA	2	1
00/244	BD	M	70	1	0	290	6.26	NA	NA	AC, AP, MS	4	2, 9	1, 2
01/144	Control	F	81	3	C	425	6.30	NA		AP, AD,	1, 4a, 4c	1	1, 2
02/031	BD	M	68	1	0	NA	6.64	NA		AP, AD, MS	4c	8b	1, 2
04/081	Control	M	67	1	B	1115	6.70	NA			NA	2	1
05/106	Control	M	67	5	C	250	6.4	B, 0	AP, AI		4a	7	1
06/061	BD	M	70	3	C	383	6.53	B, 0	AD, AP, MS		1	6	1
06/235	BD	F	80	1	B	570	6.33	AB, AC, AD	AI	MS	2	2	1, 2
08/270	BD	M	71	1	0	385	6.49	NA	AD	MS	3, 4b	3	1
09/039	Control	M	78	1	0	1060	6.52	AC, B		AD	4d	2	2
09/300	Control	F	71	1	A	430	6.31	0			4c	9	2
11/028	Control	F	81	1	0	265	6.67	B, 0	AI		2	9	2
11/039	Control	F	91	1	B	255	6.50			NA	4c	2	2
11/044	Control	M	51	0	0	465	7.05	NA	NA		NA	5, 7	1, 2
11/069	Control	M	49	0	0	375	6.23	AI	AI	AI	1,3	4	2
11/072	Control	F	76	2	0	435	6.87	B, 0	AI		2, 3	3, 9	2
11/096	Control	F	70	2	A	375	6.55	AP, B, 0	AD, AI		3	1, 2, 7	1
12/001	Control	F	89	2	B	340	6.75	B, 0			1	1, 2	2
12/002	Control	M	55	0	B	435	NA	B, 0			NA	9	2
12/005	Control	F	84	2	A	336	6.68	AP, B, 0	AC		3, 4c	2	1,2
12/048	BD	M	81	NA	NA	400	6.70		AC, AD, AI, MS		1, 3, 4b	4	1, 2
12/049	Control	F	70	2	A	455	6.03	NA	AC		3	3, 7	2
12/059	Control	F	78	2	A	275	6.41	B, 0			3	1	2
12/101	Control	M	80	2	C	265	6.59	0			3	4	1
12/104	Control	M	79	2	A	390	6.71				NA	4	1

Supplementary table 1: clinicopathological information of donors included in the study (2 of 3)

12/110	BD	M	87	3	0	195	6.39	B, 0	AC		4c	1	1, 2
12/127	BD	M	68	5	C	295	6.47	B, 0	AC, AD, AP, MS		4	7	1, 2
13/038	BD	M	72	1	A	275	6.40	AP, B, 0	AD, MS		NA	8, 9	1, 2
13/056	Control	M	95	2	B	435	6.56	0			3	2	1, 5
14/005	Control	M	67	NA	NA	540	6.48	NA	NA		NA	NA	5
14/020	Control	F	93	3	0	395	6.12	B, 0			NA	2	1
14/029	Control	F	78	1	A	430	6.32	AD, B, 0	NA	NA	3, 4c	4	1
14/041	BD	F	79	2	B	480	6.31	B, 0	AC, AI, AP, MS		2	9	1, 2
14/069	Control	M	73	NA	NA	265	7.00	NA	NA		NA	NA	5
14/070	BD	M	66	1	B	455	5.83	AP, B, 0	AD, MS	AC	3	3	2
15/027	Control	F	76	2	NA	285	6.40	AP, B, 0			2, 3	3	2
15/031	BD	F	51	0	NA	270	6.23	B, 0	AP, MS	MS	3	8b	1
15/044	BD	M	83	1	A	925	6.50	NA	AD		4c	5	1, 2
15/069	BD	M	64	0	0	485	6.37	AB, AP, B	AC	MS	1, 4c	1, 7	1, 2
15/075	BD	M	58	NA	NA	555	NA	AD	AD	AD	NA	1, 2	1, 3, 5
15/077	BD	M	72	1	A	595	6.47	NA	AC, AD	AI, MS	NA	1, 2	1, 2, 3
15/087	Control	F	75	NA	NA	550	6.57				NA	4	3, 4, 5
15/089	Control	F	92	NA	NA	465	6.71				NA	4	4, 5
15/101	BD	F	92	NA	NA	NA	NA			AP, AD	4a, 4d	2	3, 5
15/107	BD	F	77	NA	NA	NA	NA	AP, B, 0		AD, MS	2	9	3, 4, 5
16/024	BD	F	88	NA	NA	600	6.26	AP, B, 0	AD		3	7	3, 4, 5
16/027	Control	M	70	NA	NA	525	6.35	NA	NA	NA	NA	3	3, 4, 5
16/033	BD	M	85	NA	NA	525	6.28	AD, MS				4	3, 4
16/038	Control	F	85	NA	NA	425	6.52	NA	NA	NA		1	3, 4, 5
16/046	Control	F	92	NA	NA	411	6.60					9	3, 4, 5
16/056	Control	M	68	NA	NA	350	6.50	AP, B, 0				3	3, 4, 5
16/065	BD	F	93	NA	NA	310	7.55	AP		MS	2, 3	2	3, 4, 5
16/067	Control	M	89	NA	NA	492	6.59	NA	NA	NA		2	4
16/078	Control	F	84	NA	NA	460	7.50	NA	NA	NA		9	3, 4, 5
16/080	Control	M	83	NA	NA	305	7.12			AI	3	4	3, 4, 5
16/116	Control	F	81	NA	NA	315	NA					8a	3, 4, 5
16/137	Control	M	77	NA	NA	765	6.46				3	2	3, 4, 5
17/003	Control	F	96	NA	NA	315	6.71	0			4a	7	3, 4, 5
17/004	BD	F	45	NA	NA	450	6.93			AP		NA	3, 4, 5
17/005	Control	F	60	NA	NA	330	7.07		AD	AI		4	3, 4, 5

Supplementary table 1: clinicopathological information of donors included in the study (2 of 3)

17/009	BD	F	46	NA	NA	345	NA	AB, AC, MS		AD		4	3, 4, 5
17/043	Control	M	80	NA	NA	570	NA				4a	9	3
17/078	Control	F	88	NA	NA	600	6.66				2, 4b, 4d	2	3, 4, 5
17/097	Control	F	83	NA	NA	410	6.75		AI	AI	2	4	3, 4, 5
17/102	Control	F	98	NA	NA	365	6.92		AP			4	3, 4, 5
17/124	Control	F	55	NA	NA	450	NA		AC, AD			4	3, 5
17/128	BD	M	90	NA	NA	380	NA			AI, MS	4a, 4d	9	3
17/148	BD	M	71	NA	NA	340	6.54			AC, AP, MS	4a	4	3, 4, 5

NBB = Netherlands brain bank. **Control =** control donor; **BD =** donor with bipolar disorder; **M** = male; **F** = female; **NA** = not applicable; **PMD** = post-mortem delay; **medication**: If medication was used 24 hours prior to death, it has not been reported again at 3 months or ever used. If medication is used 3 months prior to death, it has not been reported again at ever used. AB = antibiotics (only reported at 24h); AC = anticonvulsants; AD = antidepressants; AI = anti-inflammatory (corticosteroids); AP = antipsychotics; B = benzodiazepines (only reported at 24h); MS = mood stabilizers; O = opiates (only reported at 24h); **somatic comorbidity**: 1 = infection < 2 weeks prior to death; 2 = auto-immune disease; 3 = cancer (in history); 4 = neuropathology; a = Dementia; b = Parkinson; c = ischemia/infarction; d = bleeding (CVA, TIA); **cause of death**: 1 = infection/inflammatory; 2 = cardiorespiratory; 3 = cancer; 4 = euthanasia/palliative sedation*; 5 = suicide; 6 = trauma; 7 = cachexia/dehydration; 8 = brain; a = ischemia/infarction; b = bleeding (CVA, TIA); 9 = other (ileus, organ failure); **used for**: 1 = immunochemistry (paraffin tissue); 2 = mRNA expression (frozen tissue); 3 = mRNA expression (isolated microglia); 4 = protein expression (isolated microglia); 5 = LPS response (isolated microglia); * euthanasia is legal according to Dutch law.

Supplementary table 2: primer sequence for qPCR analysis

Primer	Forward sequence	Reverse sequence
18S	TAGTCGCCGTGCCTACCAT	CCTGCTGCCTTCCTTGGA
ACTB	GTGGACATCCGCAAAGACCT	TCTGCATCCTGTCGGCAAT
AIF1	AGACGTTCAGCTACCCTGACTT	GGCCTGTTGGCTTTTCCTTTTCTC
CD68	CTTCTCTCATTCCCCTATGGACA	GAAGGACACATTGTACTCCACC
CD163	TTTGTCAACTTGAGTCCCTTCAC	TCCCGCTACACTTGTTTTCAC
CX3CR1	CTTACGATGGCACCCAGTGA	CAAGGCAGTCCAGGAGAGTT
GAPDH	TGCACCACCAACTGCTTAGC	GGCATGGACTGTGGTCATGA
HLA-DRA	CCCAGGGAAGACCACCTTT	CACCCTGCAGTCGTAAACGT
IL1B	TTTGAGTCTGCCCAGTTCCC	TCAGTTATATCCTGGCCGCC
IL6	TGCAATAACCACCCCTGACC	TGCGCAGAATGAGATGAGTTG
ITGAM	TGCTTCCTGTTTGGATCCAACCTA	AGAAGGCAATGTCACTATCCTCTTGA
MRC1	TGCAGAAGCAAACCAAACCTGTAA	CAGGCCTTAAGCCAACGAAACT
P2RY12	TTTGTGTGTCAAGTTACCTCCG	CTGGTGGTCTTCTGGTAGCG
SDHA	GAAGCCCTTTGAGGAGCACT	GTTTTGTCGATCACGGGTCT
TMEM119	CTTCCTGGATGGGATAGTGGAC	GCACAGACGATGAACATCAGC

Supplementary table 3: flow cytometry antibodies and isotype controls

Antibody	Label	Clone	Species	Manufacturer
CD11c	FITC	3.9	mouse	Thermo Fisher Scientific
CD16	FITC	LNK16	mouse	BIO RAD
CD32	FITC	6C4	mouse	Thermo Fisher Scientific
CD45	FITC	2D1	mouse	Thermo Fisher Scientific
CD200R	FITC	OX108	mouse	BIO RAD
CD11b	PE	ICRF44	mouse	Thermo Fisher Scientific
CD40	PE	5C3	mouse	Thermo Fisher Scientific
CD83	PE	HB15e	mouse	Thermo Fisher Scientific
CD86	PE	IT2.2	mouse	Thermo Fisher Scientific
CD163	PE	eBioGHI/61	mouse	Thermo Fisher Scientific
CD14	APC	61D3	mouse	Thermo Fisher Scientific
CD64	APC	10.1	mouse	Thermo Fisher Scientific
CD172α	APC	15-414	mouse	Thermo Fisher Scientific
CD206	APC	19.2	mouse	BD biosciences
CX3CR1	APC	2A9-1	rat	Thermo Fisher Scientific
HLA-DR	APC	LN3	mouse	Thermo Fisher Scientific
IgG1	FITC		mouse	Thermo Fisher Scientific
IgG1	APC		mouse	Thermo Fisher Scientific
IgG2a	APC		mouse	Thermo Fisher Scientific
IgG2b	APC		rat	Thermo Fisher Scientific
IgG2b	PE		mouse	Biolegend
IgG1	PE		mouse	Biolegend
IgG2b	APC		mouse	Biolegend

Thermo Fisher Scientific, Massachusetts, USA; BIO RAD, California, USA; BD biosciences, New Jersey, USA; Biolegend, California, USA.

Supplementary table 4: Spearman rho correlations of confounding variables gender, age, PMD and pH (1 of 2)

			Gender		Age		PMD		pH	
			Spearman rho	N	Spearman rho	N	Spearman rho	N	Spearman rho	N
Immunohistochemistry (paraffin tissue)	medial frontal gyrus	**microglial density**	-.317*	53	0.170	53	0.021	51	-0.189	49
		microglial morphology	0.248	49	0.301	49	0.222	47	0.170	45
mRNA expression (frozen tissue)	medial frontal gyrus	***AIF1***	-0.262	57	0.114	57	-0.222	55	0.258	54
		P2Y12	0.084	57	0.070	57	-0.065	55	0.292	54
		TMEM119	-0.155	57	0.099	57	-0.281	55	0.293	54
		CD68	-0.260	57	0.232	57	-0.217	55	0.326	54
		ITGAM	-0.213	57	0.177	57	-0.336	55	0.288	54
		IL1B	-0.299	57	0.181	57	-0.251	55	.376*	54
		IL6	-0.348	57	0.238	57	-0.092	55	0.044	54
		HLA-DRA	-0.301	57	0.153	57	-0.100	55	0.363	54
		CX3CR1	-0.020	60	0.057	60	-0.132	58	.467**	57
mRNA expression (isolated microglia)	medial frontal gyrus	***IL1B***	-0.007	22	0.152	22	0.506	20	0.400	15
		IL6	0.197	22	-0.022	22	0.312	22	0.397	20
		CD163	0.007	22	0.223	22	.578*	20	0.407	15
		MRC1	-0.095	22	-0.092	22	0.342	20	-0.421	15
		TMEM119	-0.182	22	-0.265	22	-0.193	20	-0.293	15
		CX3CR1	-0.197	22	-0.115	22	-0.209	20	-0.207	15
	superior temporal gyrus	***IL1B***	0.138	22	-0.044	22	.550*	22	0.257	17
		IL6	-0.444	22	-0.168	22	0.285	22	0.191	17
		CD163	0.342	22	0.142	22	.643**	22	-0.037	17
		MRC1	0.095	22	-0.287	22	0.199	22	-0.363	17
		TMEM119	-0.153	22	0.032	22	-0.410	22	0.007	17
		CX3CR1	-0.309	23	-0.266	23	-0.081	22	-0.147	17
	thalamus	***IL1B***	-0.464	20	-0.008	20	0.365	19	0.107	15
		IL6	-0.060	19	-0.382	19	0.528	18	0.253	14
		CD163	0.300	20	0.434	20	0.341	19	-0.386	15
		MRC1	-0.080	19	-0.257	19	0.353	18	-0.323	14
		TMEM119	0.000	19	-0.112	19	-0.347	18	-0.248	14
		CX3CR1	-0.259	19	-0.457	19	-0.091	18	0.218	14

Supplementary table 4: Spearman rho correlations of confounding variables gender, age, PMD and pH (2 of 2)

			Gender		Age		PMD		pH	
			Spearman rho	N	Spearman rho	N	Spearman rho	N	Spearman rho	N
protein expression (isolated microglia)	medial frontal gyrus	**CD11b**	0.208	22	0.084	22	-0.119	21	0.451	19
		CD45	0.392	22	-0.089	22	0.248	21	-0.028	19
		HLA-DR	0.254	22	0.180	22	0.198	21	0.447	19
		CX3CR1	0.115	22	-0.024	22	0.205	21	0.353	19
	superior temporal gyrus	**CD11b**	0.026	24	0.061	24	-0.270	23	0.182	21
		CD45	0.370	24	0.134	24	0.204	23	-0.013	21
		HLA-DR	0.230	24	0.292	24	-0.010	23	0.247	21
		CX3CR1	0.217	24	0.138	24	0.044	23	-0.009	21
	thalamus	**CD11b**	0.157	23	-0.048	23	-0.338	22	0.147	20
		CD45	0.157	23	0.273	23	-0.079	22	-0.127	20
		HLA-DR	-0.043	23	0.064	23	0.001	22	0.190	20
		CX3CR1	0.128	23	-0.061	23	0.023	22	0.344	20
LPS response (isolated microglia)	medial frontal gyrus	***IL1B***	0.030	23	-0.083	23	-.708**	21	0.389	17
		IL6	0.269	23	-0.317	23	-0.474	21	0.396	17
		TNF	-0.090	23	0.039	23	-.543*	21	0.482	17
	superior temporal gyrus	***IL1B***	0.194	12	0.063	12	-0.500	11	0.213	10
		IL6	0.075	11	-0.410	11	-0.100	11	0.067	10
		TNF	0.324	12	-0.359	12	-0.218	11	-0.006	10
	thalamus	***IL1B***	-0.315	17	0.304	17	-0.263	15	0.509	13
		IL6	-0.063	17	0.122	17	-0.465	15	0.619	13
		TNF	0.031	17	0.133	17	-0.395	15	0.503	13

Spearman rho correlations, *p*-values and number of donors included (N) of the four confounding variables (gender, age, post-mortem delay (PMD) and pH) on different experiments in the study. Significant values after Bonferroni correction for multiple testing are highlighted in red. In case of significant associations, ANCOVA was applied for further analysis to correct the confounding effect.
* $p<0.05$; ** $p<0.01$

Supplementary table 5: mean fluorescent intensity (MFI) of isolated microglia

	Medial frontal gyrus (MFG)			Superior temporal gyrus (STG)			Thalamus (THA)		
Marker	**Control (N=16)**	**BD (N=6)**	***p*-value**	**Control (N=16)**	**BD (N=8)**	***p*-value**	**Control (N=15)**	**BD (N=8)**	***p*-value**
CD11b	500.5 ± 131.1	628.5 ± 799.5	0.37	620.5 ± 120.7	442.5 ± 179.3	0.98	429.0 ± 163.3	847.5 ± 324.2	0.64
CD11c	327.0 ± 46.6	212.5 ± 113.1	0.18	299.5 ± 60.9	291.0 ± 185.4	0.78	359.0 ± 51.1	372.0 ± 99.7	0.69
CD14	178.5 ± 70.1	178.0 ± 309.5	0.96	113.0 ± 70.4	89.5 ± 66.3	0.66	165.9 ± 70.8	241.0 ± 143.1	0.38
CD16	55.5 ± 33.7	0.0 ± 40.0	0.08	86.5 ± 38.8	19.0 ± 34.6	0.11	82.0 ± 45.3	41.0 ± 55.0	0.60
CD32	407.0 ± 152.9	654.0 ± 1120.0	0.36	368.5 ± 156.4	179.5 ± 1212.0	0.70	474.0 ± 216.2	515.9 ± 951.8	0.55
CD40	0.0 ± 5.6	0.0 ± 1.7	0.34	0.0 ± 12.5	0.0 ± 4.0	0.98	0.0 ± 5.6	0.0 ± 8.2	0.67
CD45	661.5 ± 107.9	823.5 ± 348.9	0.64	718.5 ± 136.6	852 ± 245.4	0.70	847 ± 85.9	882.5 ± 237.4	0.64
CD64	1781.0 ± 498.2	1532.0 ± 106.2	0.64	1460.0 ± 355.7	1251.0 ± 473.7	0.47	2135.0 ± 382.5	1115.0 ± 781.0	0.50
CD83	0.0 ± 33.9	0.0 ± 0.8	0.34	0.0 ± 47.4	0.0 ± 6.7	0.33	0.0 ± 67.5	0.5 ± 2.3	0.89
CD86	59.5 ± 18.8	103.5 ± 68.3	0.41	86.0 ± 19.2	68.5 ± 55.9	0.87	80.0 ± 28.2	116.0 ± 51.15	0.68
CD163	0.0 ± 0.7	0.0 ± 2.8	0.69	0.0 ± 0.7	0.0 ± 2.5	0.77	0.0 ± 2.9	0.0 ± 1.4	>0.99
CD172α	634.0 ± 89.4	551.0 ± 115.3	0.56	511.0 ± 94.3	286.0 ± 125.4	0.45	893.0 ± 155.8	603.0 ± 179.6	0.86
CD200R	211.5 ± 166.0	150.0 ± 205.2	0.58	230.0 ± 223.0	453.5 ± 579.5	0.32	133.0 ± 166.5	296.0 ± 208.1	0.73
CD206	0.0 ± 56.3	1.5 ± 3.5	>0.99	0.0 ± 6.9	0.0 ± 4.1	0.81	0.0 ± 12.7	0.0 ± 20.1	0.93
CX3CR1	679.0 ± 78.3	885.5 ± 165.1	0.06	571.0 ± 76.5	202.5 ± 83.5	0.09	466.0 ± 84.8	324.0 ± 120.0	0.69
HLA-DR	863.5 ± 299.2	1883.0 ± 705.2	0.33	738.0 ± 319.2	1151.0 ± 253	0.88	1389.0 ± 283.2	1158.0 ± 417.9	0.97

Protein expression of isolated microglia from the medial frontal gyrus, superior temporal gyrus and thalamus from controls and patients with bipolar disorder (BD), determined by flow cytometry. Mean fluorescent intensity is visualized as mean ± standard error of the mean. Non-parametric testing was used to test differences between controls and patients with BD.

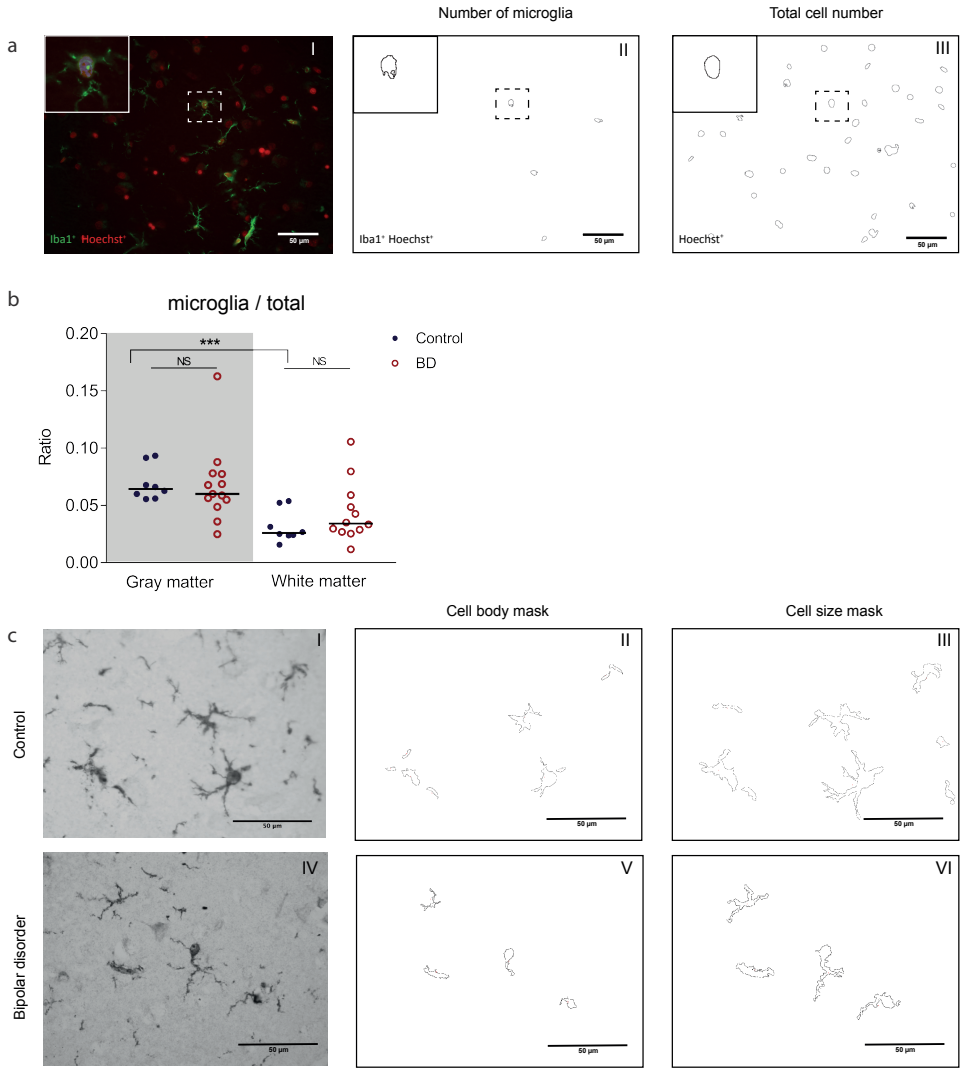

Supplementary figure 1: Microglial density and morphological analysis.
Microglial density and morphological analysis in the medial frontal gyrus of patients with bipolar disorder (BD) and controls in both grey and white matter. a) Immunofluorescent staining was performed additionally to determine the number of microglia relative to total cell number (I). Staining procedure was highly similar as for DAB-immunostained microglia, with the usage of donkey anti-rabbit Alexa 488 (1:700) and Hoechst (1:1000) as secondary antibody. An automated macro script was used to quantify the number of microglia (Iba1⁺Hoechst⁺; II) or total cell number (Hoechst⁺; III). Square shows zoom-in of a single cell. b) Quantification of the number of microglia relative to total cell number in grey and white matter of patients with BD (red circles) and controls (blue dots), displayed as the ratio of microglia divided by the total cell number. **c)** Visual representation of the automated analysis with ImageJ to determine microglial morphology in controls (I-III) and patients with BD (IV-VI). The threshold was adjusted to generate a cell body mask (II, V) and a cell size mask (III, VI), representing the cell body and cell size respectively.

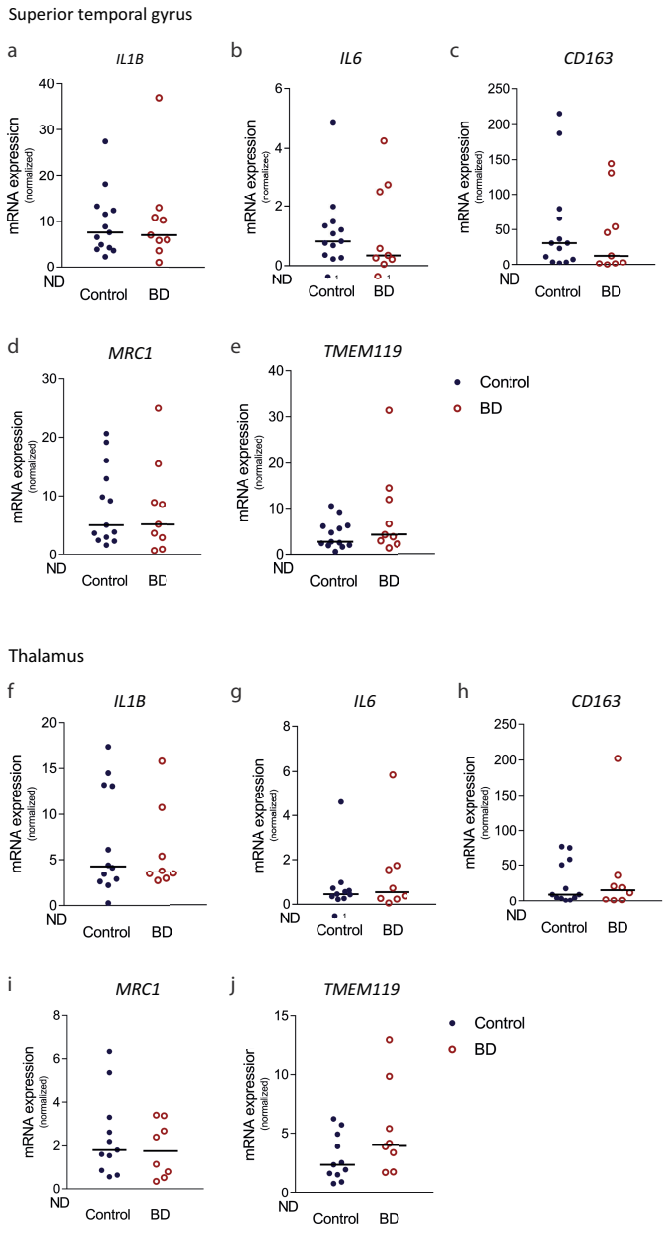

Supplementary figure 2: mRNA expression profile of isolated microglia from superior temporal gyrus and thalamus. mRNA expression was determined in microglia isolated microglia from the superior temporal gyrus (a-e) and thalamus (f-j) in patients with bipolar disorder (BD, red circles) and controls (blue dots). mRNA expression of *IL1B* (a, f), *IL6* (b, g), *CD163* (c, h), *MRC1* (d, i) and *TMEM119* (e, j) by qPCR. Distinction was made between pro-inflammatory genes *IL1B* (a, f) and *IL6* (b, g), anti-inflammatory genes *CD163* (c, h) and *MRC1* (d, i), and the microglial specific gene TMEM119 (e, j). mRNA expression was normalized to β-Actin (*ACTB*) and glyceraldehyde 3-phosphate dehydrogenase (*GAPDH*) using the ΔΔCT method. ND = number of non-detected samples.

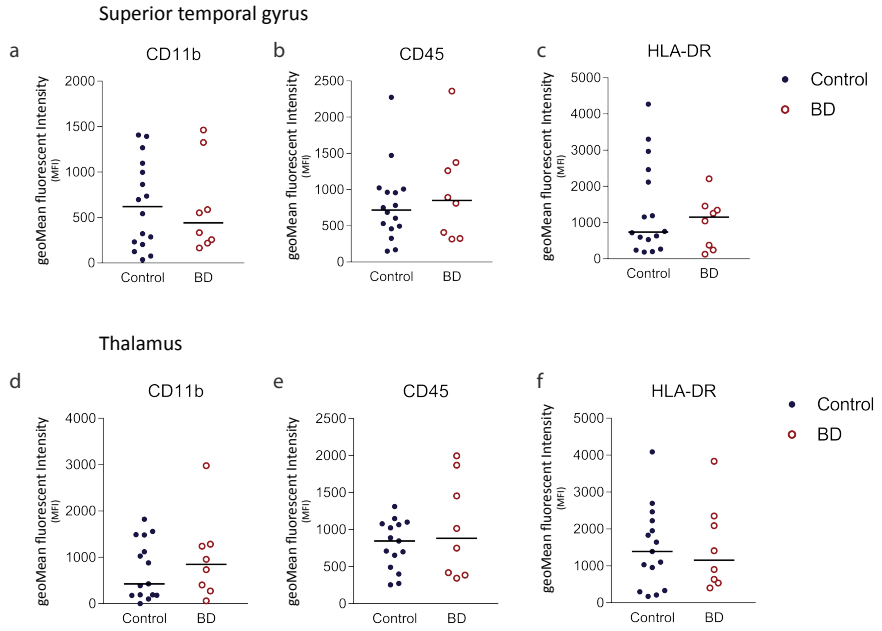

Supplementary figure 3: Protein expression profile of isolated microglia from superior temporal gyrus and thalamus.
Protein expression, determined by flow cytometry, of microglia isolated from the superior temporal gyrus (a-c) and thalamus (d-f) from controls (N=16, blue dots) and patients with bipolar disorder (BD, N=8, red circles). Mean fluorescent intensity (MFI) is shown for CD11b (a, d), CD45 (b, e) and HLA-DR (c, f).

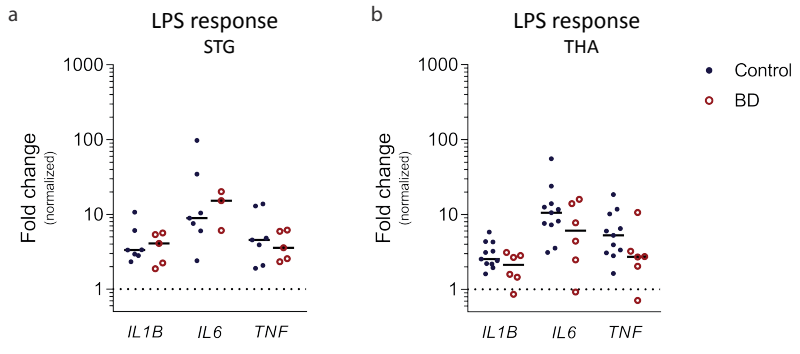

Supplementary figure 4: LPS response of isolated microglia from superior temporal gyrus and thalamus.
LPS response of human primary microglia isolated from the superior temporal gyrus (STG; a) and thalamus (THA; b) in controls (blue dots) and patients with bipolar disorder (BD, red circles). mRNA expression of *IL1B*, *IL6* and *TNF* expression is determined with qPCR. The fold change was calculated by dividing mRNA expression of the LPS stimulated sample by mRNA expression of the non-stimulated sample of the same subject. The dotted line represents baseline mRNA expression of non-stimulated cells.

Chapter 7

Ex vivo profiling of microglia in major depressive disorder

Marjolein A.M. Sneeboer[1,2*], Gijsje J.L.J. Snijders[1,2*], Alba Fernández-Andreu[2], Evan Udine[3], Psychiatric donor program of the Netherlands Brain Bank (NBB-Psy)[4], Paul R. Ormel[1,2], Amber Berdenis van Berlekom[1,2], Hans C. van Mierlo[1,2], Manja Litjens[1,2], Towfique Raj[3], René S. Kahn[1,5], Elly M. Hol[2,6], Lot D. de Witte[1,2,5]

* These authors share first authorship

[1] Department of Psychiatry, Brain Center Rudolf Magnus, University Medical Center Utrecht, Utrecht University (BCRM-UMCU-UU), 3584 CG Utrecht, The Netherlands
[2] Department of Translational Neuroscience, Brain Center Rudolf Magnus, University Medical Center Utrecht, Utrecht University (BCRM-UMCU-UU), 3584 CG Utrecht, The Netherlands
[3] Department of Neuroscience, Icahn School of Medicine at Mount Sinai, New York, New York, USA
[4] Psychiatric donor program of the Netherlands Brain Bank (NBB-Psy), Meibergdreef 47, 1105 BA Amsterdam, the Netherlands
[5] Department of Psychiatry, Icahn School of Medicine at Mount Sinai, New York, United States of America
[6] Neuroimmunology, Netherlands Institute for Neuroscience, an institute of the royal academy of arts and sciences, 1105 BA, Amsterdam, The Netherlands.

Manuscript in preparation

Abstract

Genetic, epidemiological, and post-mortem studies suggest a role for microglia in the pathogenesis of major depressive disorder (MDD). However, studies assessing microglia involvement in the disorder are inconsistent and an in depth profile of microglia in MDD is lacking. Here, we studied the phenotype and functionality of microglia directly isolated from post-mortem tissue of patients with MDD and control donors. Four regions were included: medial frontal gyrus (MFG), superior temporal gyrus (STG), thalamus (THA), and subventricular zone (SVZ). Protein expression of a panel of 14 myeloid markers was assessed by flow cytometry. Decreased expression of CD14 and CD32 was found in the MFG and SVZ respectively. Microglial immune responses were determined by culturing microglia with pro- and anti-inflammatory compounds. The response of microglia was largely similar between patients and controls. We only found increased expression of *MRC1* after dexamethasone treatment of microglia isolated from the MFG. Additionally, we performed a transcriptomic analysis of MDD and control microglia. 194 differentially expressed genes were detected. 188 genes were downregulated and 6 genes upregulated. Pathway analyses showed an associated with pathways involved in cell cycle and cell division, which were significantly downregulated in MDD. Together our data indicate that microglia in MDD are not immune activated, but that the phenotype of microglia in MDD is changed. The functional consequences of these changes in phenotype need to be further elucidated in future studies.

Introduction

Major depressive disorder (MDD) is a common and severe mental disorder affecting 300 million people worldwide[1]. MDD is characterized by periods of depressed mood, anhedonia, loss of energy, change in appetite, sleep disturbances, depressive thoughts that can include thoughts of death or suicide, and cognitive problems (lack of attention and indecisiveness)[2]. Females are twice as often diagnosed with MDD compared to males and their episodes are more reoccurring[3]. Several genetic and environmental risk factors have been identified for MDD. Environmental factors and psychosocial stressors, such as smoking, drug abuse, and traumatic experiences are very common. Disturbances of neurotransmitter systems, including the monoamines, glutamate, and GABA, are related to MDD[2]. Current successful pharmacotherapy focuses on restoring these neurotransmitter imbalances. Furthermore, the hypothalamic–pituitary–adrenal (HPA) axis, the neuroendocrine system important for the regulation of stress and the immune system, is dysregulated in MDD and is suggested to contribute to MDD pathogenesis. Additionally, reduced volume and neuronal atrophy are observed in the prefrontal cortex (PFC) and the hippocampus[4]. How genetic and environmental factors lead to neurotransmitter dysregulation and why a subgroup of patients is not responsive is still largely unknown.

The immune system has been proposed to be an important contributor to MDD pathology. Clinical indications include the high comorbidity of MDD with chronic inflammatory diseases, like diabetes and cardiovascular diseases[4]. Additionally, viral infections (e.g. influenza) can induce sickness behaviour that overlap with depressive symptoms, such as social withdrawal, decreased food intake, and anhedonia. Moreover, pronounced depressive and cognitive symptoms, similar as observed in MDD, can be induced by the administration of interferon alpha (IFNα) and glucocorticoids[5–8]. In patients with MDD, alterations are found in leukocytes, with increased expression of immune-related genes in monocytes, defective T-cell functioning, decreased numbers of $CD4^+$ T-helper (Th) cells, and impaired maturation of natural killer cells, Th2 cells, and Th17 cells[9–11]. In blood and cerebrospinal fluid (CSF) of patient with MDD altered levels of cytokines and chemokines, such as interleukin 1 beta (IL-1β), interleukin 6 (IL-6), and TNFα are found[12,13]. Moreover, both increased and decreased mRNA expression and protein levels (e.g. IL1B, IL6, IFN) are found in post-mortem brain tissue of the PFC and ACC[14–17]. Besides, RNA sequencing on the PFC of 22 MDD suicide patients and 9 non-suicidal MDD patients shows downregulation of immune related pathways and microglial cellular functions[18]. Furthermore, genome wide association studies (GWAS) reported an association between MDD and single nucleotide polymorphisms in several immune-related genes, including

tumour necrosis factor-alpha (*TNF)* and interferon regulatory factor 1 (*IRF1*)[19–22]. The most recent and largest GWAS found 44 loci associated with MDD, including loci in the major histocompatibility complex, a region that contains important genes for the regulation of the immune system. The associated genes grouped together in a pathway related to cytokine and immune response[22].

How the immune system is involved in MDD at the mechanistic level is still unknown. A role for microglia, the immune cells of the brain, is suggested. Microglia are highly dynamic cells and fulfil various functions in the brain[23,24]. They are most known for their role in the regulation of central nervous system (CNS) immunity. Microglia scan the environment for pathogens and other cellular debris that can be harmful for the brain. In case of threat, microglia become immune activated, release inflammatory cytokines such as IL-6, IL-1β, IFNγ, and TNFα, and eliminate the pathogen via phagocytosis. Besides immune control, microglia are important in surveillance and shaping brain networks via their close connection with neurons. They support neurogenesis, axon growth, and neuronal survival. Besides, microglia eliminate dysfunctional synapses during neurodevelopment and later in life[25,26]. In MDD it is thought that microglia may get immune activated. This activation can be induced in several ways, for example due to the hyperactivation of the HPA-axis, changes in the CNS, or the elevated levels of inflammatory cytokines. It is proven that prolonged secretion of these cytokines causes damage to astrocytes, oligodendrocytes, and neurons. The cytokines stimulate excessive glutamate release and decrease the synthesis of brain derived neurotrophic factor (BDNF), which is involved in neuronal repair[27]. Additionally, microglial immune activation promotes the metabolism of kynurenine from tryptophan, thereby directly hindering the synthesis of serotonin in the brain[28]. All these processes induce stress and will disturb the neurotransmitter balance in the brain, thereby possibly inducing depressive symptoms.

So far, microglial alterations in MDD have been studied using post-mortem brain tissue and positron emission tomography (PET) imaging. PET studies found an elevation of the total translocator protein (TSPO) distribution volume in several brain regions in MDD, suggesting increased microglial density[4,29,30]. With immunohistochemistry, a higher density of HLA-DR$^+$ or QUIN$^+$ microglia was also found in the hippocampus, anterior cingulate cortex (ACC), dorsolateral PFC, and the thalamus of post-mortem brain tissue of patients with MDD[31–33]. Additionally, increased density of Iba1$^+$ cells is reported around the blood vessels of patients with MDD, indicating specific microglial activation around the vasculature[34,35]. When focussing on microglial morphology as a reflection of their activation state, one study found more primed microglia (early stage of activation) in de ACC[34], whereas no differences in the number of homeostatic or immune activated microglia are found in the dorsolateral PFC[35]. Interestingly, the previous reported differences in microglial numbers and reactivity are only found in cohorts that included patients with MDD that committed suicide. Studies that included non-suicidal MDD patients could not find differences in microglial density[36,37] or showed a decreased density of HLA-DR$^+$ microglia[37]. This might suggest a specific role for microglia in suicide or more severe subtypes of MDD. Besides human studies, animal work supports the contribution of microglia in depression. Especially in the social defeat model, which induces stress and leads to depressive- and anxiety related behaviour in the animals, increased Iba1 immunoreactivity and elevated mRNA expression of *IL1B*, *IL6,* and *TNF* have been found[38].

In summary, previous post-mortem and PET studies suggest that microglia are changed in MDD, even though the results are heterogeneous. However, these types of studies are not informative about the way the phenotype and immune function of microglia is altered in MDD. In addition, most studies have been performed on only one brain region and used a single technique and microglial marker. So far, an in depth profiling of microglia in MDD across different brain regions is lacking. Here, we studied the phenotype and functionality of microglia directly isolated from four different brain regions post-mortem. The microglial immune phenotype was investigated by analysing the protein levels of general and immune-related markers of microglia isolated from patients with MDD and controls. Additionally, the immune responsiveness of MDD microglia in relation to several stressors was tested. Finally, an in-depth transcriptomic analysis was performed on microglia isolated from two brain regions of patients with MDD and controls.

Material and Methods

Donors

Fresh post-mortem brain tissue of MDD patients and controls was obtained from the Netherlands Brain Bank (www.hersenbank.nl). We selected the medial frontal gyrus (MFG), superior temporal gyrus (STG), thalamus (THA), and subventricular zone (SVZ) as regions of interest (ROI). Impaired cognitive functioning observed in MDD is associated with the frontal and temporal cortex[39–41]. Subcortical limbic areas, including the thalamus, have been implicated in MDD before[41]. Additionally, we included the SVZ due to its close proximity to the lateral ventricle, which is in close contact with the CSF[42]. Informed consent of each donor was obtained during life. Clinical characteristics of the included donors are summarized per experiment in Table 1 and more extensively in Supplementary table 1. Age was significant different

between patients and controls for all three experiments. Correction for age was therefore applied in all analyses.

Table 1: summary of clinical information and post-mortem variables of the study

		Control (N=17)	MDD (N=18)
Flow cytometry	Age (years)**	83.11 ± 10.40	62.78 ± 21.75
	Sex (M:F)	6:11	7:11
	PMD (minutes)	448 ± 122	499 ± 191
	pH	6.75 ± 0.29	6.55 ± 0.41
		Control (N=21)	**MDD (N=17)**
***ex vivo* responsiveness**	Age (years)**	79.90 ± 11.12	61.59 ± 22.86
	Sex (M:F)	8 : 13	7:10
	PMD (minutes)	440 ± 120	496 ± 189
	pH	6.72 ± 0.29	6.60 ± 0.36
		Control (N=12)	**MDD (N=10)**
RNA sequencing	Age (years)**	79.58 ± 13.14	54,20 ± 18.91
	Sex (M:F)	4:8	5:5
	PMD (minutes)	452 ± 141	559 ± 220
	pH	6.72 ± 0.25	6.59 ± 0.40

Summary of the clinical information (age and sex) and post-mortem variables (post-mortem delay (PMD) and pH) of donors used in the study. Information is separated per experimental category. Numbers represent mean ± standard deviation. M = males, F = female, MDD = major depressive disorder. **significant different ($p<0.01$) between controls and patients with MDD.

Human primary microglia isolation

Human primary microglia (pMG) were isolated from fresh post-mortem brain tissue of the medial frontal gyrus (MFG), superior temporal gyrus (STG), thalamus (THA), and subventricular zone (SVZ) of MDD patients and controls according to an earlier described protocol (Bötcher et al. 2018, in press). In short, fresh post-mortem brain tissue of these four brain regions was mechanically and enzymatically dissociated with collagenase and DNase (MFG, STG (60 minutes), THA (30 minutes)) or 0.2% trypsin and 30 mg DNase (SVZ, 30 and 10 minutes respectively) at 37°C. After dissociation, 0.2% fetal calf serum (FCS) was added to the SVZ only. A Percoll (Amersham, Merck, Germany) gradient was generated to separate the microglia from myelin and cellular debris. The middle layer enriched for microglia was washed twice and microglia were pulled down with CD11b conjugated magnetic beads (Miltenyi Biotec, Germany). Microglia were directly lysed with 500 µl TRIzol reagent (Invitrogen, USA) for characterization with quantitative polymerase chain reaction (PCR) or with 200 µl RLT buffer (Qiagen, Germany) for RNA sequencing analysis. Additionally, microglia were stained for flow cytometry analysis and cultured to study microglia ex vivo responsiveness.

Flow cytometry

12-20 x 10^4 human pMG were stained for flow cytometry in a v-bottom 96-wells plate directly after isolation. Microglia were washed with 100 µl PBA (PBS supplemented with 0,5% bovine serum albumin (Merck, Germany)) and stained in 25 µl PBA with monoclonal antibodies and isotype controls (Supplementary table 2) for 30 minutes. Cells were washed twice with 100 µl PBA and fixated with 4% paraformaldehyde (Riedel-de-Haën, Germany). The samples were processed on a FACS Canto (BD Bioscience) with calibrated settings and similar voltage for the fluorescent channels. Protein levels are represented as geomean fluorescence intensity (geoMFI) in which the geoMFI of the isotype control was subtracted from the geoMFI of the positive antigen staining.

Microglia *ex vivo* responsiveness

Human pMG were cultured at a density of 10 x 10^4 cells in 200 µL Rosswell-Park-Memorial-Institute medium (RPMI; Gibco Life technologies, USA) with 10% FCS, 2 mM L-glutamine (Gibco Life technologies, USA), 1% penicillin-streptomycin (Gibco Life technologies, USA), and 100 ng/ml IL-34 (Miltenyi Biotech, Germany) in a 96-wells flat bottom plate (Greiner Bio-One) coated with poly-L-lysine (PLL; Merck, Germany). After overnight incubation, microglial medium was supplemented with 100 ng/mL lipopolysaccharide (LPS) from Escherichia coli 0111:B4 (Merck, Germany) for 6 hours or with 1 µM dexamethasone (Merck, USA for 72 hours. Microglia were lysed with 500 µl TRIzol reagent and stored at -80 until further usage.

Gene expression analysis

For RNA extraction, 100 µl chloroform was added to 500 µl TRIzol and centrifuged at 12000 rcf at 7°C for 15 minutes. Upper aqueous phase was equally mixed with isopropanol, 1 µl glycogen as carrier was added and centrifuged (maximum speed at 4°C for 60 minutes). The cell pellet was washed twice with 75% ethanol and dissolved in 8 µl RNase-free water. NanoDrop 2000 (Thermo Scientific, USA) was used to measure the RNA concentration. 40 ng RNA was reverse transcribed with the QuantiTect Reverse Transcription kit (Qiagen, Germany) according to manufacturers protocol. For qPCR analysis, an input of 3.5 ng cDNA was supplemented with water, 5 µl SYBRgreen PCR mix, and 1 µl primer mix (2 pmol/mL; Supplementary table 3) to a volume of 11 µl. A QuantStudio 6 Flex Real-Time PCR system (Applied Biosystems, USA) was used with the following cycle conditions: 50°C for 2 minutes, 95°C for 10

minutes, 40 cycles at 95°C for 15 seconds, and 60°C for 60 seconds. Absolute gene expression was calculated with the ΔΔCT method[43]. The most stable genes across ROIs, diagnosis, and different donors for normalization was determined with Expression Suite software 1.0.4. Glyceraldehyde 3-phosphate dehydrogenase (*GAPDH*) was used to normalize stimulated pMG. The fold change of stimulated microglia was calculated by dividing mRNA expression of the stimulated sample by the mRNA expression of the non-stimulated sample.

RNA sequencing

Total RNA of directly isolated pMG of MFG and STG of patients with MDD (N=10) and controls (N=12) were extracted with a RNeasy mini kit (Qiagen, Germany) in combination with a RNase-Free DNase Set (Qiagen, Germany) for additional DNA removal, according to manufacturers protocol. RNA integrity numbers (RIN) were determined with a RNA 6000 Pico Kit (Agilent Technologies, USA) on a BioAnalyzer (Agilent Technologies, USA). Samples with RIN ≥6.5 were included in the study. 10 ng of RNA was reversed transcribed with poly-A enrichment and amplified with the SMART-Seq® v4 Ultra® Low Input RNA Kit for sequencing (Takara Bio, USA), according to manufacturers protocol. To generate cDNA fragments of 200–500 base pair size, samples were sheared with the following conditions: peak power 175, duty 10%, and burst cycle 200 for 5 minutes. Size selection was performed with SPRIselect reagent (Beckman Coulter, USA) with a ratio of 0.5:1 SPRI beads to amplified cDNA, followed by 1:1 ratio purification with the Agencourt AMPure XP Kit (Beckman Coulter, USA). Quality control (QC) of the samples resulted in an elimination of six samples due to low quality and concentration. RNA sequencing libraries were generated of the remaining 34 samples according to the Low Input Library Prep Kit v2 (Takara Bio, USA) with 7 amplification cycles. Samples were purified and pooled for sequencing. Sequencing was performed with a depth of 30 million reads per sample on an illumina platform (illumina, USA).

Differential expression and pathway analysis

For automatic read alignment, QC, and quantitative analysis of the sequencing gene expression, the RAPiD pipeline was applied. STAR aligner53 version 2.5 was used to align the sequences along the ensemble hg38 reference genome. Aligned files were analysed with RNA-seQC in order to evaluate the quality of the data. For quantification, featureCounts54 was applied. Additionally, kallisto was run as an alternate to the STAR – featureCounts combination. Exonic and intergenic rate was normal, mapped reads ranged from 20-70 million reads per sample, and ribosomal rate was below 0.05% (Supplementary figure 3a-d). Due to low mapped reads, two samples were excluded. The mapped reads of the remaining 32 samples were normalized for each gene by the total number of counts across all genes and gene length, resulting in transcripts per kilobase million (TPM) for analyses. Principal component analyses (PCA) on both kallisto and featureCounts data were performed to identify potential outliers and understand confounding variables. To further assess variance, the R package variancePartition, which utilizes a linear mixed model, was applied to give insight in contribution of the various covariates. For differential expression analyses, we corrected for age, sex, batch, post-mortem delay (PMD), and pH. Since DESeq2 is specifically designed for small sample sizes, this package was used to extract the differential expressed genes (DEGs) between MDD and controls. To gain power to find DEGs related to disease status, MFG and STG were pooled. Genes were selected with the following cut-off: p<0.001 (FDR<0.05) and 2LogFoldChange -1/+1. Gene Ontology (GO) pathway analysis was performed with the online available Gene Set Enrichment Analysis (GSEA) tool of the BROAD institute (http://software.broadinstitute.org/gsea/index.jsp).

Statistical analysis

Statistical analysis was performed with SPSS IBM 23 and Graphpad software (version 7). Confounder effects on microglial protein expression and functionality were analysed with an ANCOVA. ANOVA was performed to study region specific protein expression differences. Non-parametric Mann-Whitney U test was used to analyse differences in protein expression and inflammatory functionality between patients with MDD and controls. Microglial inflammatory response per sample was analysed with a Wilcoxon matched-pairs signed rank test. For each experiment Bonferroni correction for multiple testing was applied.

Results

Protein expression in primary microglia

First, we determined the protein expression of primary microglia isolated from patients with MDD (N=18) and controls (N=17) of four brain regions (MFG, STG, THA, and SVZ; Figure 1). We investigated a panel of 14 myeloid markers. Based on the FSC-SSC plot, the microglia were separated from the cell debris (Figure 1a I) and discriminated from autofluorescent cells (Figure 1a II). CD11b (Figure 1b) and CD45 (Figure 1c) expression was not different between patients with MDD and controls, irrespective of brain region. Microglial activation markers, such as HLA-DR and CD200R, were equal expressed between patients and controls (Supplementary table 4). For two markers we observed a significant decrease in protein expression in MDD. CD14 was lower expressed in the MFG (Figure 1d), whereas CD32 showed a decrease

Figure 1

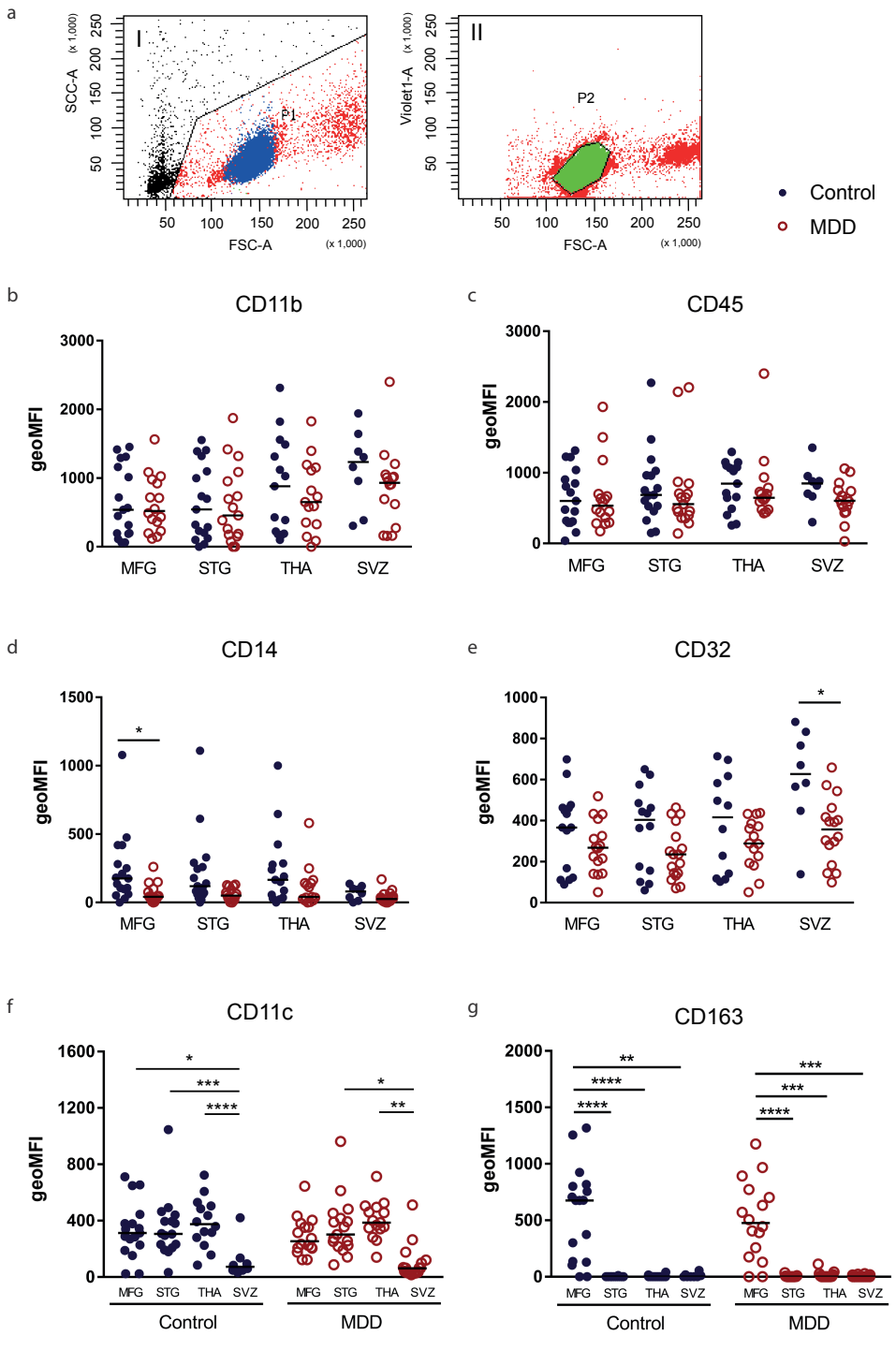

< Figure 1: protein profile of microglia in major depressive disorder.
Protein expression with flow cytometry was determined in microglia isolated from controls (blue dots, N=17) and patients with major depressive disorder (MDD, red circles, N=17) in four brain regions: medial frontal gyrus (MFG), superior temporal gyrus (STG), thalamus (THA), and subventricular zone (SVZ). a) Gating strategy for human microglia. Microglia are separated from death cells (I) and distinguished from high autofluorescent cells (II). Protein expression of CD11b (b), CD45 (c), CD14 (d), CD32 (e), CD11c (f), and CD163 (g) in patients with MDD and controls. Horizontal lines show median expression and non-parametric testing with Bonferroni correction was applied. *p< 0.05, **p<0.01, ***p<0.001, ****p<0.0001.

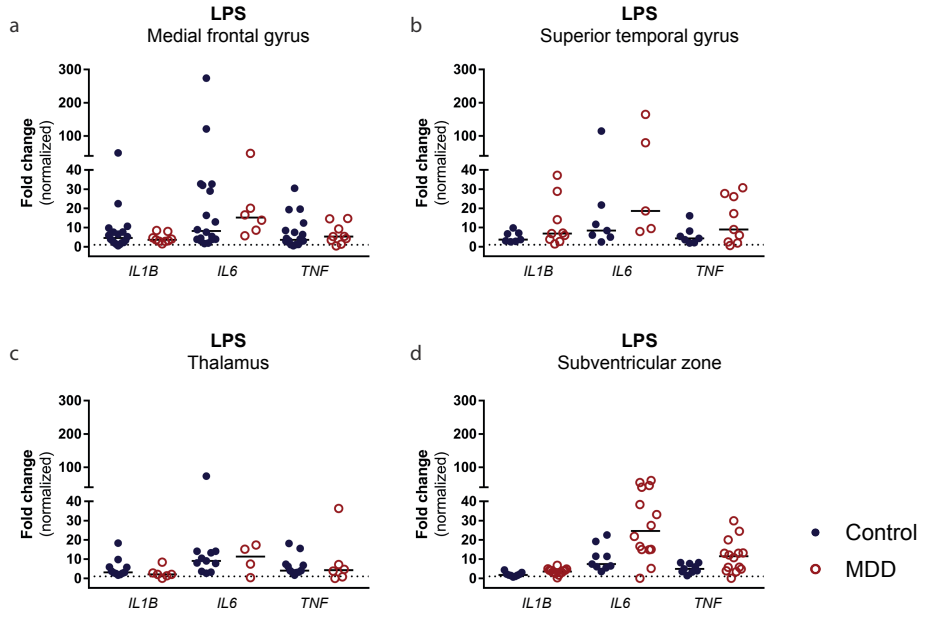

Figure 2: Microglial inflammatory response after treatment with LPS.
Microglia of controls (blue dots) and patients with major depressive disorder (MDD, red circles) were isolated from post-mortem brain tissue of four different regions: medial frontal gyrus (MFG, a), superior temporal gyrus (STG, b), thalamus (THA, c), and subventricular zone (SVZ, d). mRNA expression of *IL1B*, *IL6*, and *TNF* was determined by qPCR after 6 hours of stimulation with lipopolysaccharide (LPS). Gene expression was normalized to glyceraldehyde 3-phosphate dehydrogenase (*GAPDH*) with the ΔΔCT method. Fold change was calculated by dividing mRNA expression of the LPS stimulated sample by the mRNA expression of the non-stimulated sample of the same donor. Dotted line represents baseline mRNA expression of the non-stimulated samples. Horizontal lines show median expression and non-parametric testing with Bonferroni correction was applied.

in the SVZ (Figure 1e). Additionally, we found region-specific differences in both patients and controls. Significant lower expression of CD11c was noticed in the SVZ, whereas higher expression of CD163 was found in the MFG compared to the other brain regions.

Inflammatory response not altered in MDD microglia

Isolated microglia of patients with MDD (N=17) and controls (N=21) of the four brain regions were challenged with compounds to study their responsiveness. LPS mimics a bacterial infection and will induce inflammation via the toll like receptor 4 (TLR4)[44]. After culturing microglia with LPS for 6 hours we observed increased mRNA expression of *IL1B*, *IL6,* and *TNF*, indicating an inflammatory response (Supplementary figure 1). However, the fold change in mRNA expression of these genes was not different between patients with MDD and controls in the MFG (Figure 2a), STG (Figure 2b), THA (Figure 2c), and SVZ (Figure 2d).

Although MDD microglia displayed a normal pro-inflammatory phenotype, we were also interested if there is a difference in the induction of an anti-inflammatory response by glucocorticoids. Microglia were cultured with dexamethasone for 72 hours (Figure 3). Dexamethasone is known to dampen inflammation and decrease the production of inflammatory cytokines (e.g. TNFα and IL-6)[45]. As expected we found an increased expression of *CD163*, *CD200R1*, and *MRC1* upon stimulation (Supplementary figure 2). The fold change was not different between patients and controls (MFG, Figure 3a; STG, Figure 3b; THA, Figure 3c; SVZ, Figure 3d). After correction for age, *MRC1* was significantly upregulated in the MFG only (Figure 3a).

Transcriptomic profiling of MDD microglia

The similar expression of microglial activation proteins and microglial responsiveness to LPS and dexamethasone suggests the absence of an inflammatory profile in MDD. To provide a more in-depth phenotype of microglia we performed RNA sequencing on microglia isolated from the MFG and STG of patients with MDD (N=10) and controls (N=12). First, we checked for enrichment of classic microglial genes in our samples (Supplementary figure 4a). As expected we found high expression of microglial genes (e.g. *P2RY12*, *CX3CR1*, *SPI1*) and low expression of genes specific for oligodendrocytes (e.g. *OLIG2*, *MOG*) and neurons (*SST*, *RELN*). Although some samples show low express *GFAP*, characteristic for astrocytes, other astrocytic genes (*ALDH1L1*, *AQP4*) were barely expressed in the same samples. Moreover, the expression of GFAP was still negligible compared to the expression of microglial genes. pH, PMD, age, sex, and batch were selected as covariates based on the VariancePartition analysis and were included as covariates for further analyses (Supplementary figure 4b).

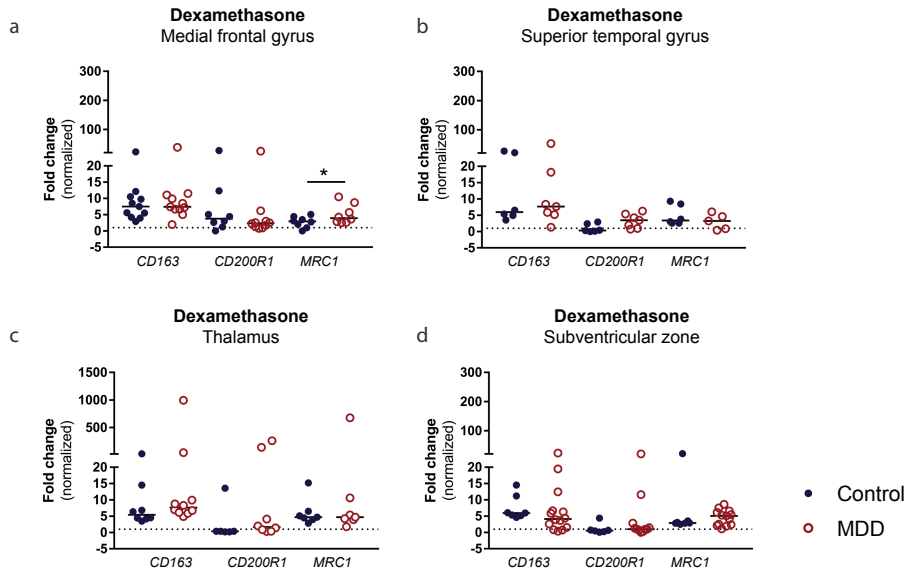

Figure 3: Microglial inflammatory response after treatment with dexamethasone.
Microglia of controls (blue dots) and patients with major depressive disorder (MDD, red circles) were isolated from post-mortem brain tissue of four different regions: medial frontal gyrus (MFG, a), superior temporal gyrus (STG, b), thalamus (THA, c), and subventricular zone (SVZ, d). mRNA expression of *CD163*, *CD200R*, and *MRC1* was determined by qPCR after 72 hours of stimulation with dexamethasone. Gene expression was normalized to glyceraldehyde 3-phosphate dehydrogenase (*GAPDH*) with the ΔΔCT method. Fold change was calculated by dividing mRNA expression of the LPS stimulated sample by the mRNA expression of the non-stimulated sample of the same donor. Dotted line represents baseline mRNA expression of the non-stimulated samples. Horizontal line shows median expression and non-parametric testing with Bonferroni correction was applied. *p<0.05.

To extract differential expressed genes (DEGs) between patients and controls we ran DESeq2 on the MFG and STG combined to gain power (global analysis). In total, we found 194 DEGs, with upregulation of six genes and downregulation of 188 genes in MDD (Figure 4a). Table 2 shows the most significant up- and downregulated genes. Upregulated genes are *FPR3*, *KCNAB1*, *RARG*, *GPNMB*, *CNTNAP2*, and *TMEM37*. The ten most downregulated genes are *C1orf162*, *PEAK3*, *HIST2H2BF*, *SLC11A1*, *SAPCD2*, *CKAP2L*, *KIF23*, *CDC20*, *TOP2A*, and *BCL2A1*. We plotted the TPMs for the three most significantly DEGs of the global analysis (Figure 4b-d) and MFG and STG separately (Figure 4e-g) to investigate region specific gene expression. *C1orf162*, (Figure 4b) *PEAK3* (Figure 4c), and *HIST2H2BF* (Figure 4d) were all significantly downregulated in MDD. Region specific analyses showed a downregulation of *C1orf162* in both MFG and STG (Figure 4e), whereas *PEAK3* was downregulated in the MFG specifically (Figure 4f). Although *HIST2H2BF* was significantly downregulated in the global analysis,

Figure 4

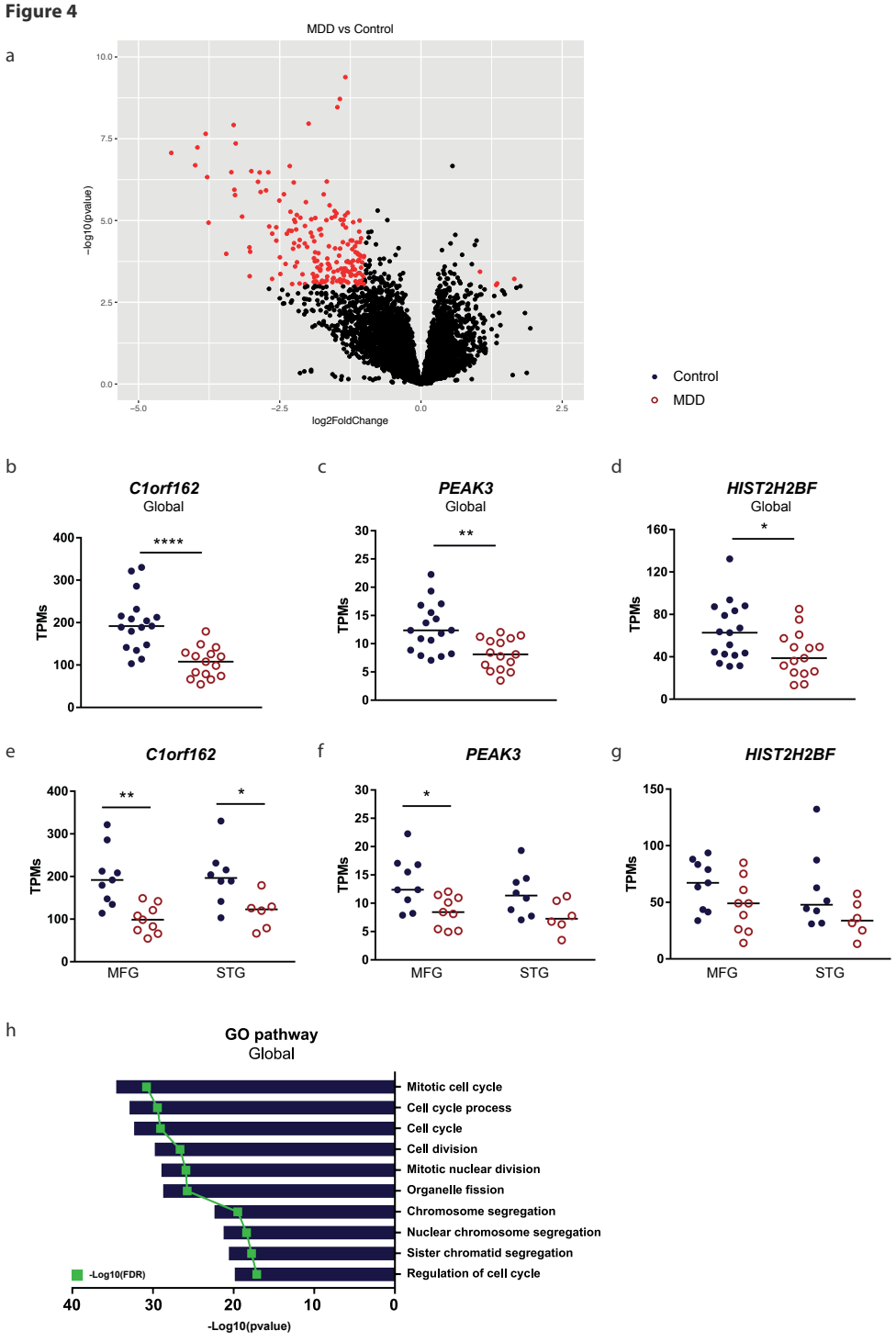

< Figure 4: Transcriptomic profiling of microglia in major depressive disorder.
RNA sequencing was performed on microglia isolated from post-mortem tissue of the medial frontal gyrus (MFG) and superior temporal gyrus (STG) of controls (N = 12) and patients with major depressive disorder (MDD, N = 10). a) Volcano plot of the 194 significant differential expressed genes (DEGs, red dots) between MDD and control microglia in the MFG and STG with FDR<0.05 and Log2FoldChange -1/+1. b-g) Dot plots of the three most significant DEGs in the global analysis (*C1orf162* (e), *PEAK3* (f), and *HIST2H2BF* (g)) and per brain region separately (g-i) in controls (blue dots) and patients with MDD (red circles). Horizontal lines represent median and non-parametric analysis with Bonferroni correction was applied. *p<0.05, **p<0.01, ***p<0.001. h) Gene Ontology (GO) pathway analysis of the ten most significant downregulated pathways. Bars show significance of the pathway as –log10(pvalue), were as the green squares represent the –Log10(FDR) significance of the pathway.

Table 2: Top 10 most significant differential expressed genes

	Gene	Ensembl ID	Log2FoldChange	p value	padj
Upregulated	*FPR3*	ENSG00000187474	1.045681	0.000368	0.028541
	KCNAB1	ENSG00000169282	1.651754	0.000611	0.036743
	RARG	ENSG00000172819	1.349352	0.000842	0.043125
	GPNMB	ENSG00000136235	1.330604	0.000934	0.045834
	CNTNAP2	ENSG00000174469	1.760360	0.001022	0.048165
	TMEM37	ENSG00000171227	1.053047	0.001056	0.048769
Downregulated	*C1orf162*	ENSG00000143110	-1.338210	4.14E-10	5.18E-06
	PEAK3	ENSG00000188305	-1.435680	1.93E-09	1.21E-05
	HIST2H2BF	ENSG00000203814	-1.479440	3.44E-09	1.44E-05
	SLC11A1	ENSG00000018280	-1.988480	1.09E-08	3.01E-05
	SAPCD2	ENSG00000186193	-3.315910	1.20E-08	3.01E-05
	CKAP2L	ENSG00000169607	-3.810800	2.24E-08	4.68E-05
	KIF23	ENSG00000137807	-3.278840	4.41E-08	7.88E-05
	CDC20	ENSG00000117399	-3.956750	5.84E-08	9.14E-05
	TOP2A	ENSG00000131747	-4.419630	8.58E-08	0.000119
	BCL2A1	ENSG00000140379	-2.321530	2.17E-07	0.000226

no differences were found in the region specific analyses (Figure 4g). Finally we performed a Gene Ontology (GO) pathway analysis. The most significantly associated pathways were cell cycle and cell division (Figure 4h).

Discussion

The aim of this study was to profile microglia isolated from four different brain regions of patients with MDD. We studied their protein expression, immune responsiveness, and transcriptomic signature. Upregulation of proteins related to immune activation was not found. Significant lower expression was observed for CD14 and CD32. Additionally, we found region specific differences in the expression of CD163 and CD11c, irrespective of diagnosis. The immune response of MDD microglia was not different from control microglia after culturing with LPS. *MRC1* was increased in the MFG in MDD after dexamethasone stimulation, but this was not consistent across brain areas. Transcriptomic analysis showed no change in immune-regulatory pathways, but a clear downregulation of pathways involved in cell cycle and cell division.

Flow cytometry analysis showed downregulation of CD14 and CD32 in the MFG and SVZ respectively. Also in our transcriptomic analysis of the MFG and STG both genes were downregulated, but did not reach significance. CD14 is normally upregulated directly after isolation, indicative of microglial activation[46], and regulates microglial responsiveness to LPS. For example, $CD14^-$ microglia are a 1000-fold more reactive to LPS compared to $CD14^+$ microglia[47]. The decreased CD14 expression in MDD microglia would suggest a higher sensitivity to LPS. However, we observed similar responsiveness of MDD microglia after culturing with LPS as control microglia. Additionally, we found a decreased protein expression of CD32. CD32 is a type II FC receptor which belongs to the immunoglobulin gene superfamily and is a marker that has been associated with pro-inflammatory activation of microglia[48]. We did not find a decrease of other markers related to this type of activation in the SVZ, such as the other FC markers CD16 and CD64. CD32 is most known as mediator of phagocytosis[49,50], but its role in microglia is still largely unknown. To further investigate alterations in microglial phagocytic activity, specific phagocytosis assays need to be performed.

Region-specific protein expression was observed in microglia isolated from post-mortem tissue. This is a reflection of the microglial heterogeneity in the brain, as was seen before in human (Bötcher et al. 2018, in press) and rodent microglia[51,52] with mass cytometry (CyTOF). In our study we found lower expression of CD11c in the SVZ and higher expression of CD163 in the MFG compared to the other regions. Currently, we are validating our region-specific expression of CD11c and CD163 with CyTOF data.

Our transcriptomic analysis of isolated microglia resulted in a total of 194 DEGs of which 188 genes were downregulated and only six genes upregulated in MDD microglia compared to controls. Only limited information is available of the top three most significant DEGs. Both *C1orf162* (Chromosome 1 Open Reading Frame 162) and *PEAK3* (PEAK Family Member 3) are associated with chromosome open reading frames, whereas *HIST2H2BF* (Histone Cluster 2 H2B Family Member F) is a histone gene involved in chromatin accessibility. A dysregulation of histone modification has been associated with MDD and depressive behaviour before[53–55]. Reduced acetylation of histone H3 and histone H4 were found in mice after stress exposure[55]. Moreover, increased histone methylation in the mouse forebrain resulted in less depressive behaviour, including reduced anhedonia, helplessness, and depressive-like behaviour[56]. Also, post-mortem studies found a link with altered histone acetylation in patients with MDD. For example, more accessibility of the *BDNF* promotor with the histone mark H3K27me3 was observed in patients with MDD that use antidepressant medication[55]. Our findings imply an altered phenotype of MDD microglia specifically in processes vulnerable to epigenetic factors, such as histone modification. Currently taken steps are the separate DEG analyses of the MFG and STG to identify brain region specific microglial transcriptomic profiles.

Gene ontology showed that pathways involved in cell cycle and cell division were significantly downregulated in MDD. Especially genes associated with mitotic cell cycle and sister chromatid segregation are lower expressed. Cyclins and cyclin-dependent protein kinases are highly important for successful cell division[57] and were significantly downregulated in our study. These data suggest that proliferation is impaired in microglia of patients with MDD. In microglia, proliferation and self-renewal are very dynamic processes that is normally in balance with apoptosis, as is shown before in mice[58]. More research is needed to study whether self-renewal is decreased in MDD microglia or that it is a reflection of earlier CNS pathology. To study cell proliferation more specifically, immunochemistry on post-mortem tissue of patients with MDD with Iba1 and Ki67 or PCNA, visualizing microglia and proliferating cells respectively, is needed. Besides, cell cycle can be studied more specifically in the *ex vivo* microglia with flow cytometry or CyTOF antibodies against proteins involved in different stages of cell division. This has been showed before and could give information about region-specific microglial profiles additionally (Bötcher et al. 2018, in press). Additionally, immunostainings with apoptotic markers, such as cleaved caspase-3, need to be performed, since decreased proliferation and self-renewal might be related to increased apoptosis of microglia[58].

Although the fourth most significant DEG (*SLC11A1*) is associated with the susceptibility to infectious and inflammatory diseases, such as tuberculosis and rheumatoid arthritis, no inflammatory pathways were differentially regulated between patients and controls. This is in contrast with a sequencing study on blood cells of MDD patients that found enrichment of IL-6 and natural killer cell activation pathways[59]. This might indicate that the peripheral immune system is upregulated, which is in line with the increased cytokine levels found by others[12,13], but that the CNS immune system is not altered in terms of inflammatory pathways.

Here, we provided an extensive profile of microglia isolated from post-mortem tissue of patients with MDD. Whereas microglia in MDD have mainly been studied with immunochemistry, we used a multi-level approach that contained various techniques. We assessed microglial protein expression, immune responsiveness upon stimulatory treatment, and their transcriptomic profile. Besides, we studied microglia isolated from four different brain regions of the human brain. This provided us with the opportunity to investigate the general phenotype of microglia in MDD, but also their heterogeneity across the brain.

Limitations of this study include the potential contribution of confounders. In this study we corrected for several confounding factors (age, sex, PMD, and pH). However, many other covariates could be of importance. For example, medication could have an impact on microglial phenotype and suppress their immune activity[60]. Also smoking is known to be associated with inflammation, with both immunosuppressive as immunostimulatory effects. Since the patients with MDD used a wide range of different antidepressants and smoking was often not reported, correction for these variables was not possible. In addition, we observed substantial variation in the clinical phenotyping of patients with MDD. Whereas MDD is for some donors the main diagnosis, others had major psychiatric comorbidities. Also there was variability in the disease phase of the patients. To study the effect of microglia on prolonged depressive episodes, more donors need to be included with MDD as main diagnosis. A role for suicide in relation to microglial density was proposed by Schnieder et al., who found more Iba1$^+$ cells in the white matter of the prefrontal cortex of patients with MDD who committed suicide[35]. In our cohort we include one patient with suicide. This donor did not display a different microglial profile in comparison to other MDD microglia.

Acknowledgements

This project is financially supported by a 2014 NARSAD Young Investigator Grant provided by the Brain & Behaviour Research Foundation. This study was further supported by the psychiatric donor program of the Netherlands Brain Bank (NBB-Psy), which is supported by the Netherlands Organization for Scientific Research (NWO). The authors thank the team of the Netherlands Brain Bank for their services and R.D. van Dijk and Y. He for their help with the microglial isolations and immune response experiments.

References

1 Depression. http://www.who.int/news-room/fact-sheets/detail/depression (accessed 21 Sep2018).

2 Otte C, Gold SM, Penninx BW, Pariante CM, Etkin A, Fava M *et al.* Major depressive disorder. *Nat Rev Dis Prim* 2016; **2**: 16065.

3 Seedat S, Scott KM, Angermeyer MC, Berglund P, Bromet EJ, Brugha TS *et al.* Cross-National Associations Between Gender and Mental Disorders in the World Health Organization World Mental Health Surveys. *Arch Gen Psychiatry* 2009; **66**: 785.

4 Wohleb ES, Franklin T, Iwata M, Duman RS. Integrating neuroimmune systems in the neurobiology of depression. *Nat Rev Neurosci* 2016; **17**: 497–511.

5 Capuron L, Miller AH. Cytokines and psychopathology: Lessons from interferon-α. *Biol Psychiatry* 2004; **56**: 819–824.

6 Malaguarnera M, Di Fazio I, Restuccia S, Pistone G, Ferlito L, Rampello L. Interferon Alpha-Induced Depression in Chronic Hepatitis C Patients: Comparison between Different Types of Interferon Alpha. *Neuropsychobiology* 1998; **37**: 93–97.

7 Lotrich FE. Major depression during interferon-alpha treatment: vulnerability and prevention. *Dialogues Clin Neurosci* 2009; **11**: 417–25.

8 Brown ES, Chandler PA. Mood and Cognitive Changes During Systemic Corticosteroid Therapy. *Prim Care Companion J Clin Psychiatry* 2001; **3**: 17–21.

9 Becking K, Haarman BCM, Grosse L, Nolen WA, Claes S, Arolt V *et al.* The circulating levels of CD4+ t helper cells are higher in bipolar disorder as compared to major depressive disorder. *J Neuroimmunol* 2018; **319**: 28–36.

10 Toben C, Baune BT. An Act of Balance Between Adaptive and Maladaptive Immunity in Depression: a Role for T Lymphocytes. *J Neuroimmune Pharmacol* 2015; **10**: 595–609.

11 Grosse L, Hoogenboezem T, Ambrée O, Bellingrath S, Jörgens S, de Wit HJ *et al.* Deficiencies of the T and natural killer cell system in major depressive disorder: T regulatory cell defects are associated with inflammatory monocyte activation. *Brain Behav Immun* 2016; **54**: 38–44.

12 Dowlati Y, Herrmann N, Swardfager W, Liu H, Sham L, Reim EK *et al.* A Meta-Analysis of Cytokines in Major Depression. *Biol Psychiatry* 2010; **67**: 446–57.

13 Young JJ, Bruno D, Pomara N. A review of the relationship between proinflammatory cytokines and major depressive disorder. *J Affect Disord* 2014; **169**: 15–20.

14 Dean B, Gibbons AS, Tawadros N, Brooks L, Everall IP, Scarr E. Different changes in cortical tumor necrosis factor-α-related pathways in schizophrenia and mood disorders. *Mol Psychiatry* 2013; **18**: 767–773.

15 Dean B, Tawadros N, Scarr E, Gibbons AS. Regionally-specific changes in levels of tumour necrosis factor in the dorsolateral prefrontal cortex obtained postmortem from subjects with major depressive disorder. *J Affect Disord* 2010; **120**: 245–248.

16 Clark SM, Pocivavsek A, Nicholson JD, Notarangelo FM, Langenberg P, McMahon RP *et al.* Reduced kynurenine pathway metabolism and cytokine expression in the prefrontal cortex of depressed individuals. *J Psychiatry Neurosci* 2016; **41**: 386–394.

17 Pandey GN. Inflammatory and Innate Immune Markers of Neuroprogression in Depressed and Teenage Suicide Brain. In: *Modern trends in pharmacopsychiatry*. 2017, pp 79–95.

18 Pantazatos SP, Huang Y-Y, Rosoklija GB, Dwork AJ, Arango V, Mann JJ. Whole-transcriptome brain expression and exon-usage profiling in major depression and suicide: evidence for altered glial, endothelial and ATPase activity. *Mol Psychiatry* 2017; **22**: 760–773.

19 Bosker FJ, Hartman CA, Nolte IM, Prins BP, Terpstra P, Posthuma D *et al.* Poor replication of candidate genes for major depressive disorder using genome-wide association data. *Mol Psychiatry* 2011; **16**: 516–532.

20 Song GG, Kim J-H, Lee YH. Genome-Wide Pathway Analysis in Major Depressive Disorder. *J Mol Neurosci* 2013; **51**: 428–436.

21 Okbay A, Baselmans BML, De Neve J-E, Turley P, Nivard MG, Fontana MA *et al.* Genetic variants associated with subjective well-being, depressive symptoms and neuroticism identified through genome-wide analyses. *Nat Genet* 2016; **48**: 624–633.

22 Wray NR, Ripke S, Mattheisen M, Trzaskowski M, Byrne EM, Abdellaoui A *et al.* Genome-wide association analyses identify 44 risk variants and refine the genetic architecture of major depression. *Nat Genet* 2018; **50**: 668–681.

23 Sklar P, Smoller JW, Fan J, Ferreira MAR, Perlis RH, Chambert K *et al.* Whole-genome association study of bipolar disorder. *Mol Psychiatry* 2008; **13**: 558–69.

24 Kettenmann H, Hanisch U-K, Noda M, Verkhratsky A. Physiology of microglia. *Physiol Rev* 2011; **91**: 461–553.

25 Tremblay M-È, Lowery RL, Majewska AK. Microglial Interactions with Synapses Are Modulated by Visual Experience. *PLoS Biol* 2010; **8**: e1000527.

26 Sierra A, Encinas JM, Deudero JJP, Chancey JH, Enikolopov G, Overstreet-Wadiche LS *et al.* Microglia shape adult hippocampal neurogenesis through apoptosis-coupled phagocytosis. *Cell Stem Cell* 2010; **7**: 483–95.

27 Leonard BE. The concept of depression as a dysfunction of the immune system. *Curr Immunol Rev* 2010; **6**: 205–212.

28 Singhal G, Baune BT. Microglia: An Interface between the Loss of Neuroplasticity and Depression. *Front Cell Neurosci* 2017; **11**: 270.

29 Li H, Sagar AP, Kéri S. Microglial markers in the frontal cortex are related to cognitive dysfunctions in major depressive disorder. *J Affect Disord* 2018; **241**: 305–310.

30 Setiawan E, Wilson AA, Mizrahi R, Rusjan PM, Miler L, Rajkowska G *et al.* Role of translocator protein density, a marker of neuroinflammation, in the brain during major depressive episodes. *JAMA psychiatry* 2015; **72**: 268–75.

31 Bayer TA, Buslei R, Havas L, Falkai P. Evidence for activation of microglia in patients with psychiatric illnesses. *Neurosci Lett* 1999; **271**: 126–8.

32 Steiner J, Bielau H, Brisch R, Danos P, Ullrich O, Mawrin C *et al.* Immunological aspects in the neurobiology of suicide: Elevated microglial density in schizophrenia and depression is associated with suicide. *J Psychiatr Res* 2008; **42**: 151–157.

33 Steiner J, Walter M, Gos T, Guillemin GJ, Bernstein H-G, Sarnyai Z *et al.* Severe depression is associated with increased microglial quinolinic acid in subregions of the anterior cingulate gyrus: evidence for an immune-modulated glutamatergic neurotransmission? *J Neuroinflammation* 2011; **8**: 94.

34 Torres-Platas SG, Cruceanu C, Chen GG, Turecki G, Mechawar N. Evidence for increased microglial priming and macrophage recruitment in the dorsal anterior cingulate white matter of depressed suicides. *Brain Behav Immun* 2014; **42**: 50–9.

35 Schnieder TP, Trencevska I, Rosoklija G, Stankov A, Mann JJ, Smiley J *et al.* Microglia of prefrontal white matter in suicide. *J Neuropathol Exp Neurol* 2014; **73**: 880–90.

36 Hamidi M, Drevets WC, Price JL. Glial reduction in amygdala in major depressive disorder is due to oligodendrocytes. *Biol Psychiatry* 2004; **55**: 563–569.

37 Brisch R, Steiner J, Mawrin C, Krzyżanowska M, Jankowski Z, Gos T. Microglia in the dorsal raphe nucleus plays a potential role in both suicide facilitation and prevention in affective disorders. *Eur Arch Psychiatry Clin Neurosci* 2017; **267**: 403–415.

38 Stein DJ, Vasconcelos MF, Albrechet-Souza L, Ceresér KMM, de Almeida RMM. Microglial Over-Activation by Social Defeat Stress Contributes to Anxiety- and Depressive-Like Behaviors. *Front Behav Neurosci* 2017; **11**: 207.

39 Peng W, Chen Z, Yin L, Jia Z, Gong Q. Essential brain structural alterations in major depressive disorder: A voxel-wise meta-analysis on first episode, medication-naive patients. *J Affect Disord* 2016; **199**: 114–123.

40 Harrison NA. Brain Structures Implicated in Inflammation-Associated Depression. 2016, pp 221–248.

41 Pandya M, Altinay M, Malone DA, Anand A, Anand A. Where in the brain is depression? *Curr Psychiatry Rep* 2012; **14**: 634–42.

42 Quiñones-Hinojosa A, Sanai N, Soriano-Navarro M, Gonzalez-Perez O, Mirzadeh Z, Gil-Perotin S *et al.* Cellular composition and cytoarchitecture of the adult human subventricular zone: a niche of neural stem cells. *J Comp Neurol* 2006; **494**: 415–34.

43 Livak KJ, Schmittgen TD. Analysis of Relative Gene Expression Data Using Real-Time Quantitative PCR and the 2−ΔΔCT Method. *Methods* 2001; **25**: 402–408.

44 Lu Y-C, Yeh W-C, Ohashi PS. LPS/TLR4 signal transduction pathway. *Cytokine* 2008; **42**: 145–151.

45 Chao CC, Hu S, Close K, Choi CS, Molitor TW, Novick WJ *et al.* Cytokine release from microglia: differential inhibition by pentoxifylline and dexamethasone. *J Infect Dis* 1992; **166**: 847–53.

46 Melief J, Sneeboer MAM, Litjens M, Ormel PR, Palmen SJMC, Huitinga I *et al.* Characterizing primary human microglia: a comparative study with myeloid subsets and culture models. *Glia* 2016; : 1–12.

47 Janova H, Böttcher C, Holtman IR, Regen T, van Rossum D, Götz A *et al.* CD14 is a key organizer of microglial responses to CNS infection and injury. *Glia* 2016; **64**: 635–649.

48 Bedi SS, Smith P, Hetz RA, Xue H, Cox CS. Immunomagnetic enrichment and flow cytometric characterization of mouse microglia. *J Neurosci Methods* 2013; **219**: 176–82.

49 Peress NS, Fleit HB, Perillo E, Kuljis R, Pezzullo C. Identification of FcγRI, II and III on normal human brain ramified microglia and on microglia in senile plaques in Alzheimer's disease. *J Neuroimmunol* 1993; **48**: 71–79.

50 Gessner JE, Heiken H, Tamm A, Schmidt RE. The IgG Fc receptor family. Springer-Verlag, 1998https://link.springer.com/content/pdf/10.1007/s002770050396.pdf (accessed 5 Dec2018).

51 Mrdjen D, Pavlovic A, Hartmann FJ, Schreiner B, Utz SG, Leung BP *et al.* High-Dimensional Single-Cell Mapping of Central Nervous System Immune Cells Reveals Distinct Myeloid Subsets in Health, Aging, and Disease. *Immunity* 2018; **48**: 380–395.e6.

52 Korin B, Ben-Shaanan TL, Schiller M, Dubovik T, Azulay-Debby H, Boshnak NT *et al.* High-dimensional, single-cell characterization of the brain's immune compartment. *Nat Neurosci* 2017; **20**: 1300–1309.

53 Saavedra K, Molina-Márquez AM, Saavedra N, Zambrano T, Salazar LA. Epigenetic Modifications of Major Depressive Disorder. *Int J Mol Sci* 2016; **17**: 124–37.

54 Saavedra K, Molina-Márquez AM, Saavedra N, Zambrano T, Salazar LA. Epigenetic Modifications of Major Depressive Disorder. *Int J Mol Sci* 2016; **17**. doi:10.3390/ijms17081279.

55 Deussing JM, Jakovcevski M. Histone Modifications in Major Depressive Disorder and Related Rodent Models. In: *Advances in experimental medicine and biology*. 2017, pp 169–183.

56 Jiang Y, Jakovcevski M, Bharadwaj R, Connor C, Schroeder FA, Lin CL *et al.* Setdb1 histone methyltransferase regulates mood-related behaviors and expression of the NMDA receptor subunit NR2B. *J Neurosci* 2010; **30**: 7152–67.

57 Nigg EA. Cyclin-dependent protein kinases: Key regulators of the eukaryotic cell cycle. *BioEssays* 1995; **17**: 471–480.

58 Askew K, Li K, Olmos-Alonso A, Garcia-Moreno F, Liang Y, Richardson P *et al.* Coupled Proliferation and Apoptosis Maintain the Rapid Turnover of Microglia in the Adult Brain. *Cell Rep* 2017; **18**: 391–405.

59 Jansen R, Penninx BWJH, Madar V, Xia K, Milaneschi Y, Hottenga JJ *et al.* Gene expression in major depressive disorder. *Mol Psychiatry* 2016; **21**: 339–347.

60 Ohgidani M, Kato TA, Mizoguchi Y, Horikawa H, Monji A, Kanba S. Antidepressants Modulate Microglia Beyond the Neurotransmitters Doctrine of Mood Disorders. In: *Melatonin, Neuroprotective Agents and Antidepressant Therapy*. Springer India: New Delhi, 2016, pp 611–620.

Supplementary table 1: Clinicopathological information of donors included in the study

Donor	Diagnosis	Sex	Age (years)	PMD (minutes)	pH	Medication <24 hours	Medication ever used	Somatic comorbidity	Cause of death	Used for
14/005	Control	M	67	540	6.48	NA	NA	NA	NA	2
14/069	Control	M	73	265	7.00	NA	NA	NA	NA	2
15/087	Control	F	75	550	6.57			5	4	1, 2, 3
15/089	Control	F	92	465	6.71				4	1, 2
16/027	Control	M	70	525	6.35	NA	NA	NA	3	1, 2, 3
16/028	MDD	F	94	475	6.19	O	AD, AP	4a, 5	4	1, 2
16/038	Control	F	85	425	6.52	NA	NA		1	2
16/046	Control	F	92	411	6.60			5	8	1, 2
16/049	MDD	M	47	355	6.67		AD, AP	5	4	1, 2, 3
16/056	Control	M	68	350	6.50	B, O, AP		5	3	1, 2
16/067	Control	M	89	492	6.59	NA	NA	5	2	1, 2, 3
16/078	Control	F	84	460	7.50	NA	NA	3	8	1, 2
16/080	Control	M	83	305	7.12			3, 5	4	1, 2, 3
16/082	MDD	F	68	385	6.30				NA	1, 2
16/110	MDD	F	69	970	6.28	AD, B		6	2	1, 2, 3
16/111	MDD	F	58	440	5.61	AP, B			8	1
16/112	MDD	F	77	520	6.77	AD, B, O	MS	5, 6	4	1, 2, 3
16/116	Control	F	81	315	NA			5	4a	1, 2, 3
16/117	MDD	M	50	580	6.80	B	AD, AP	1	4	1, 2, 3
16/118	MDD	M	38	375	6.79				4	1, 2, 3
16/137	Control	M	77	765	6.46			3, 5	2	1, 2, 3
17/003	Control	F	96	315	6.71	O		4a, 5	6	1, 2, 3
17/005	Control	F	60	330	7.07		AD		4	1, 2, 3
17/017	MDD	F	67	520	7.07	B	AD, AP	5	4	1, 2
17/029	MDD	F	23	515	NA		AD, AP	6	4	1, 2, 3
17/032	MDD	M	48	765	6.76				NA	1, 2, 3
17/043	Control	M	80	570	NA			4a, 5	8	2
17/074	MDD	F	85	270	6.93	AD, B		4d	4	1, 2, 3
17/078	Control	F	88	600	6.66			2, 5, b,4d	2	1, 2, 3
17/094	MDD	M	62	NA	5.71		AD	4a, 4c, 5, 6	7a	1, 2, 3
17/097	Control	F	83	410	6.75			2, 5	4	1, 2, 3
17/099	MDD	F	74	380	6.96		AD, AP	2, 6	4	1, 2
17/102	Control	F	98	365	6.92		AP	5	4	1, 2, 3
17/124	Control	F	55	450	NA		AC, AD		4	2, 3
17/136	MDD	F	43	680	NA				5	2, 3

Supplementary table 1: Continued

18/010	MDD	M	21	535	6.73			1, 2
18/018	Control	F	82	330	6.48		1	2
18/021	Control	M	92	530	6.89			1
18/023	MDD	F	68	785	6.66			1
18/074	MDD	F	90	235	6.62			1, 2
18/079	MDD	M	91	370	6.42			1, 2

Control = control donor; **MDD** = major depressive disorder donor; **M** = male; **F** = female; **PMD** = post-mortem delay; **medication**: A D = antidepressants (SSRI, MAO, TCA); AP = antipsychotic; B = benzodiazepines; AI = anti-inflammatory (dexamethasone, prednisolone); MS = mood stabilizer (lithium); AC = anticonvulsant; O = opiates; AB = antibiotics; CAN = cancer; **somatic comorbidity**: 1 = infection < 2 weeks; 2 = auto-immune disease; 3 = cancer history; 4 = neuropathology; 5 = cardiovascular (hypertension, infarct); 6 = substance abuse (smoking, drugs); a = dementia; b = Parkinson; c = ischemia/infarction; d = bleeding (CVA, TIA); **cause of death**: 1 = infection/ inflammatory; 2 = cardiorespiratory; 3 = cancer; 4 = euthanasia/palliative sedation*; 5 = suicide; 6 = cachexia/dehydration; 7 = brain; 8 = other (ileus, organ failure); a = ischemia/infarction; **used for**: 1 = protein expression (flow cytometry); 2 = microglia responsiveness (*ex vivo* microglia)); 3 = transcriptomic analysis (RNA sequencing); **NA** = not applicable; * euthanasia is legal according to Dutch law.

Supplementary table 2: flow cytometry antibodies and isotype controls

Antibody	Label	Clone	Species	Manufacturer
CD11c	FITC	3.9	mouse	Thermo Fisher Scientific
CD16	FITC	LNK16	mouse	BIO RAD
CD32	FITC	6C4	mouse	Thermo Fisher Scientific
CD45	FITC	2D1	mouse	Thermo Fisher Scientific
CD200R	FITC	OX108	mouse	BIO RAD
CD11b	PE	ICRF44	mouse	Thermo Fisher Scientific
CD40	PE	5C3	mouse	Thermo Fisher Scientific
CD83	PE	HB15e	mouse	Thermo Fisher Scientific
CD86	PE	IT2.2	mouse	Thermo Fisher Scientific
CD163	PE	eBioGHI/61	mouse	Thermo Fisher Scientific
CD14	APC	61D3	mouse	Thermo Fisher Scientific
CD64	APC	10.1	mouse	Thermo Fisher Scientific
CD172α	APC	15-414	mouse	Thermo Fisher Scientific
CD206	APC	19.2	mouse	BD biosciences
CX3CR1	APC	2A9-1	rat	Thermo Fisher Scientific
HLA-DR	APC	LN3	mouse	Thermo Fisher Scientific
IgG1	FITC		mouse	Thermo Fisher Scientific
IgG1	APC		mouse	Thermo Fisher Scientific
IgG2a	APC		mouse	Thermo Fisher Scientific
IgG2b	APC		rat	Thermo Fisher Scientific
IgG2b	PE		mouse	Biolegend
IgG1	PE		mouse	Biolegend
IgG2b	APC		mouse	Biolegend

Thermo Fisher Scientific, Massachusetts, USA; BIO RAD, California, USA; BD biosciences, New Jersey, USA; Biolegend, California, USA.

Supplementary table 3: primer sequence for qPCR analysis

Primer	Forward sequence	Reverse sequence
CD163	TTTGTCAACTTGAGTCCCTTCAC	TCCCGCTACACTTGTTTTCAC
CD200R1	GAGCAATGGCACAGTGACTGTT	GTGGCAGGTCACGGTAGACA
CX3CR1	CTTACGATGGCACCCAGTGA	CAAGGCAGTCCAGGAGAGTT
GAPDH	TGCACCACCAACTGCTTAGC	GGCATGGACTGTGGTCATGA
IL1B	TTTGAGTCTGCCCAGTTCCC	TCAGTTATATCCTGGCCGCC
IL6	TGCAATAACCACCCCTGACC	TGCGCAGAATGAGATGAGTTG
MRC1	TGCAGAAGCAAACCAAACCTGTAA	CAGGCCTTAAGCCAACGAAACT
TNF	TGGAGAAGGGTGACCGACTC	TCACAGGGCAATGATCCCAA

Supplementary table 4: geomean fluorescent intensity (MFI) of human isolated microglia

	Medial frontal gyrus				Superior temporal gyrus				Thalamus				Subventricular zone			
Marker	**Control (N=17)**	**MDD (N=16)**	***p*-value**		**Control (N=17)**	**MDD (N=16)**	***p*-value**		**Control (N=15)**	**MDD (N=15)**	***p*-value**		**Control (N=8)**	**MDD (N=16)**	***p*-value**	
CD11b	650.5 ± 125.0	621.1 ± 101.9	0.9495		649.9 ± 131.9	609 ± 134.6	0.7404		881.1 ± 182.3	731.1 ± 135.0	0.6236		1136.0 ± 201.7	866.5 ± 140.4	0.1358	
CD11c	333.5 ± 48.0	291.1 ± 33.7	0.5276		349.9 ± 55.6	353.6 ± 49.9	0.9784		387.2 ± 46.8	402.5 ± 34.5	0.8221		115.4 ± 45.0	101.9 ± 31.8	0.4896	
CD14	239.8 ± 62.7	64.5 ± 18.6	0.0028**		218.2 ± 66.8	57.25 ± 11.9	0.0147*		240.9 ± 70.5	112.5 ± 38.4	0.0872		71.4 ± 17.9	37.6 ± 11.0	0.1164	
CD16	90.8 ± 29.5	68.1 ± 21.0	0.8990		162.5 ± 44.6	70.29 ± 23.4	0.1070		135.4 ± 47.3	88.5 ± 25.7	0.7595		450.4 ± 271.8	168.6 ± 82.6	0.4077	
CD32	352.8 ± 50.0	272.1 ± 32.1	0.2354		356.9 ± 54.7	240 ± 31.3	0.1155		387.1 ± 68.9	288.5 ± 31.4	0.2937		610.8 ± 84.7	351.2 ± 40.5	0.0087**	
CD40	13.1 ± 5.3	18.6 ± 6.5	0.3236		9.875 ± 3.9	20.24 ± 7.0	0.4334		13.6 ± 6.0	18.7 ± 8.4	0.9345		19.0 ± 9.3	23.6 ± 8.6	>0.999	
CD45	648.6 ± 96.8	662.4 ± 120.1	0.7966		796.1 ± 125.0	721.9 ± 140.8	0.2897		809.0 ± 88.7	782.2 ± 126.0	0.4124		819.0 ± 105.0	605.6 ± 65.0	0.0702	
CD64	2051.0 ± 464.5	1284.0 ± 133.5	0.3193		2162 ± 369.3	1254 ± 173.4	0.0494*		2065.0 ± 392.9	1386.0 ± 156.6	0.3389		3765.0 ± 717.8	2067.0 ± 258.3	0.0382*	
CD86	85.0 ± 21.0	97.3 ± 11.6	0.3365		107.4 ± 25.6	105.8 ± 19.3	0.7525		110.2 ± 33.9	177.9 ± 65.7	0.3946		471.4 ± 161.2	213.3 ± 38.1	0.1901	
CD163	567.5 ± 100.0	501.1 ± 86.4	0.6628		0.75 ± 0.7	3.471 ± 2.0	0.0811		4.9 ± 3.0	14.1 ± 7.7	0.4313		10.6 ± 6.9	6.0 ± 2.4	0.8552	
CD172a	609.5 ± 83.8	616.7 ± 71.1	0.7624		612.2 ± 100.8	663.5 ± 71.0	0.4444		868.2 ± 152.2	906.3 ± 111.1	0.5722		197.8 ± 151.6	227.2 ± 102.0	0.7966	
CD200R	369.9 ± 146.5	235.4 ± 97.2	0.5992		465.5 ± 202.2	331.2 ± 131.5	0.6033		426.7 ± 163.2	271.9 ± 55.8	0.7130		339.5 ± 171.6	109.1 ± 26.0	0.3422	
CX3CR1	454.3 ± 88.6	573.6 ± 72.5	0.4636		482 ± 77.3	442.9 ± 63.5	0.4958		426.8 ± 89.5	370.5 ± 60.4	0.7510		1119.0 ± 225.2	795.0 ± 140.2	0.2144	
HLA-DR	1302.0 ± 278.9	1057.0 ± 181.2	0.8655		1339.0 ± 308.5	1234.0 ± 218.2	0.9188		1643.0 ± 358.3	1624.0 ± 307.4	0.8381		1819.0 ± 656.7	1611.0 ± 271.3	0.8340	

Protein expression of human isolated microglia from the medial frontal gyrus, superior temporal gyrus, thalamus and subventricular zone from controls and patients with major depressive disorder (MDD), determined by flow cytometry. geoMean fluorescent intensity is visualized as mean ± standard error of the mean. Non-parametric testing was used to test differences between controls and MDD. *$p < 0.05$; **$p < 0.01$ statistically significant, red p-values are significant after Bonferroni correction.

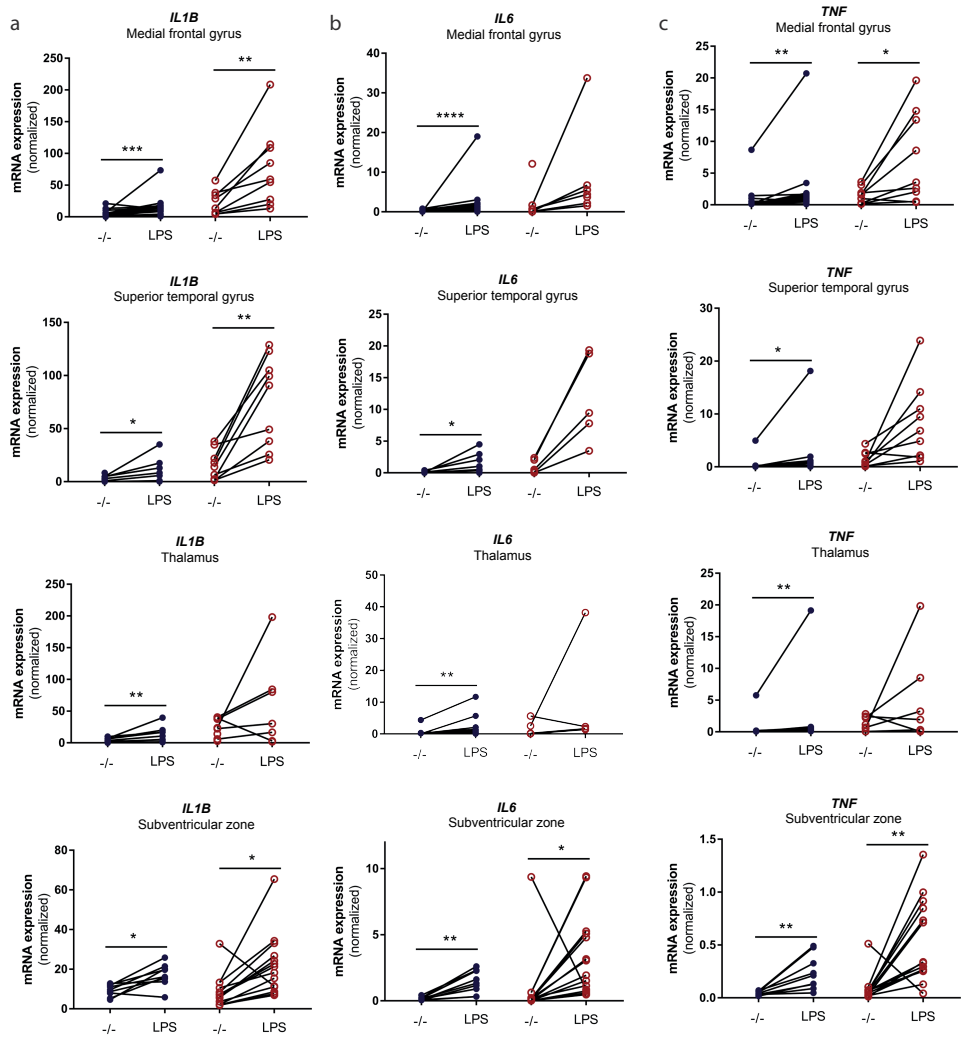

Supplementary figure 1: Microglial immune response after LPS treatment for individual samples.

Inflammatory responsiveness was studied in microglia isolated from the medial frontal gyrus, superior temporal gyrus, thalamus, and subventricular zone of controls (blue dots) and patients with major depressive disorder (MDD, red circles). mRNA expression of *IL1B* (a), *IL6* (b), and *TNF* (c) was determined in unstimulated (-/-) and 6 hour lipopolysaccharide (LPS) stimulated microglia. Gene expression was normalized to glyceraldehyde 3-phosphate dehydrogenase (*GAPDH*) with the ΔΔCT method. Wilcoxon matched-pairs signed rank test and Bonferroni correction were applied. *p<0.05, **p<0.01.

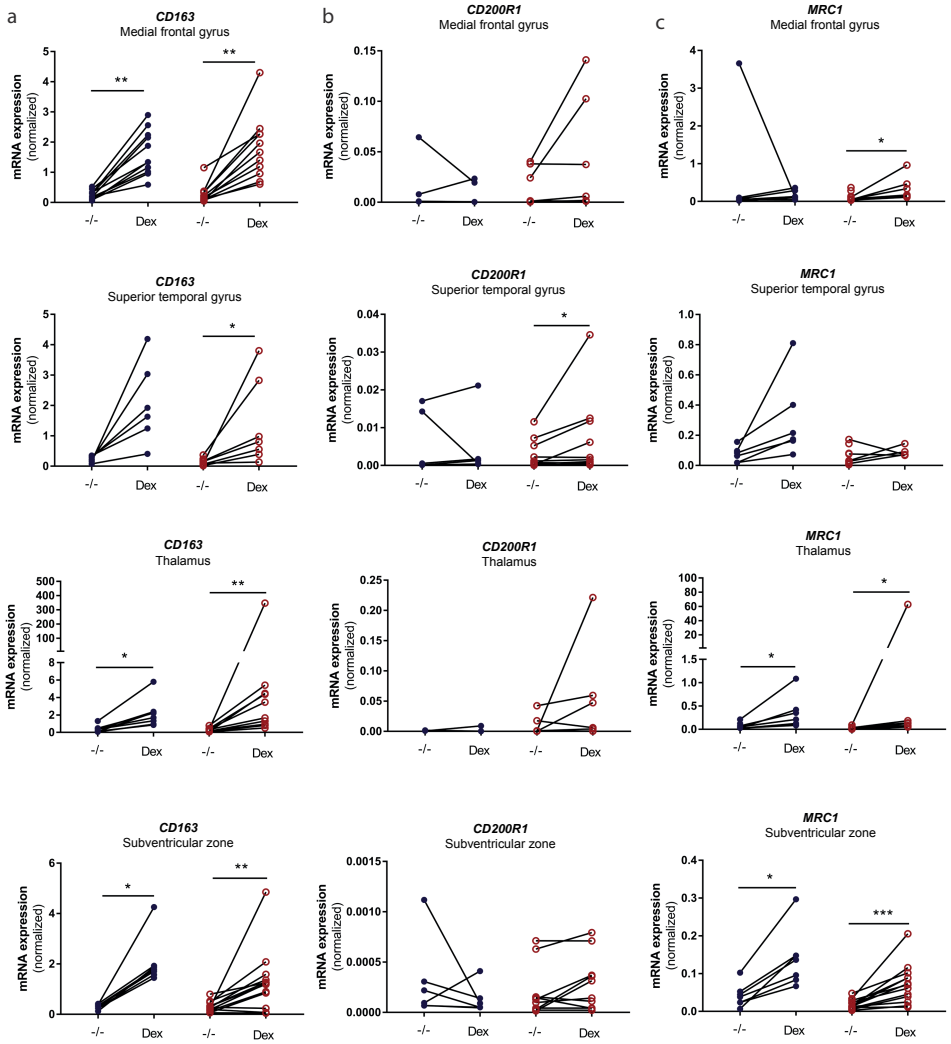

Supplementary figure 2: Microglial immune response after dexamethasone treatment for individual samples.

Inflammatory responsiveness was studied in microglia isolated from the medial frontal gyrus, superior temporal gyrus, thalamus, and subventricular zone of controls (blue dots) and patients with major depressive disorder (MDD, red circles). mRNA expression of *CD163* (a), *CD200R1* (b), and *MRC1* (c) was determined in unstimulated (-/-) and 72 hour dexamethasone (Dex) stimulated microglia. Gene expression was normalized to glyceraldehyde 3-phosphate dehydrogenase (*GAPDH*) with the ΔΔCT method. Wilcoxon matched-pairs signed rank test and Bonferroni correction were applied. *p<0.05, **p<0.01, ***p<0.001.

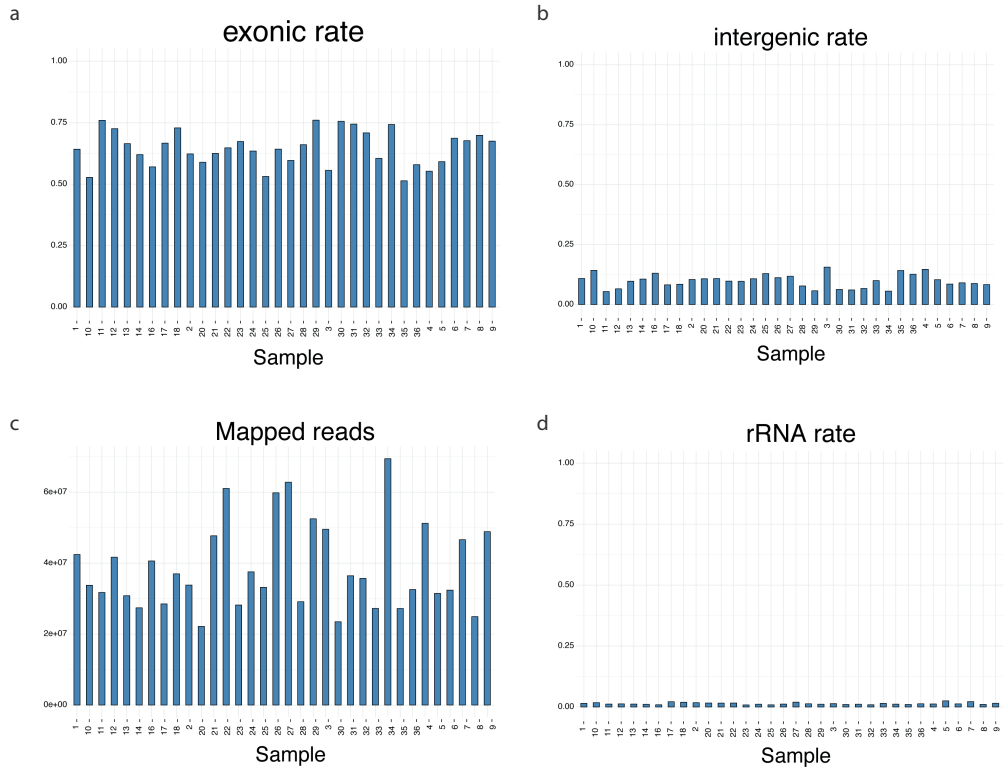

Supplementary figure 3: Quality control of sequenced microglial samples.

RNA sequencing was performed on microglia isolated from the medial frontal gyrus and superior temporal gyrus of controls (N=12) and patients with major depressive disorder (MDD, N=10). Quality control of the samples is displayed as exonic rate (a), intergenic rate (b), mapped reads (c), and ribosomal RNA rate (rRNA rate, d). Samples are organized horizontally.

a

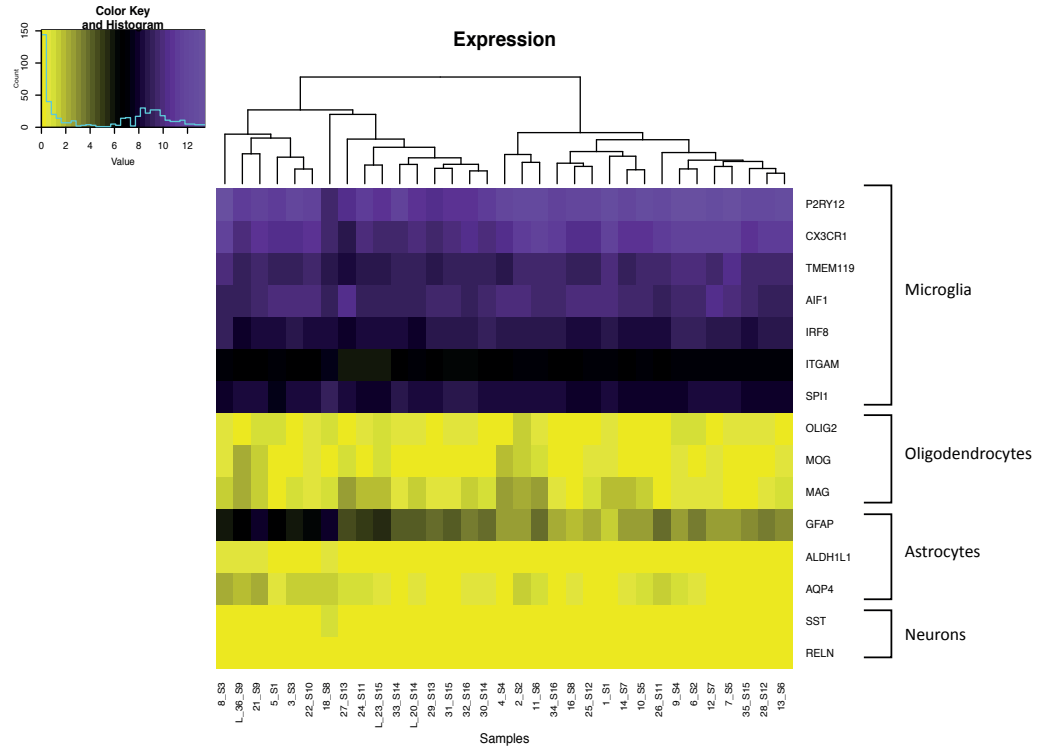

b

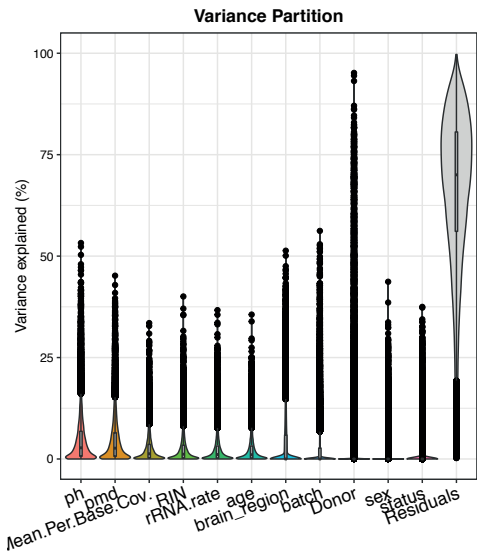

< Supplementary figure 4: Microglial enrichment and confounder analysis in sequenced microglia.

a) Heat plot of microglial, astrocytic, oligodendrocytic, and neuronal genes in the sequenced samples. Gene enrichment is displayed as purple, where as low gene expression is yellow. Samples are organized horizontally. b) VariancePartition plot to determine the influence of confounders on the sequencing analysis. Different confounders are aligned on the x-axis.

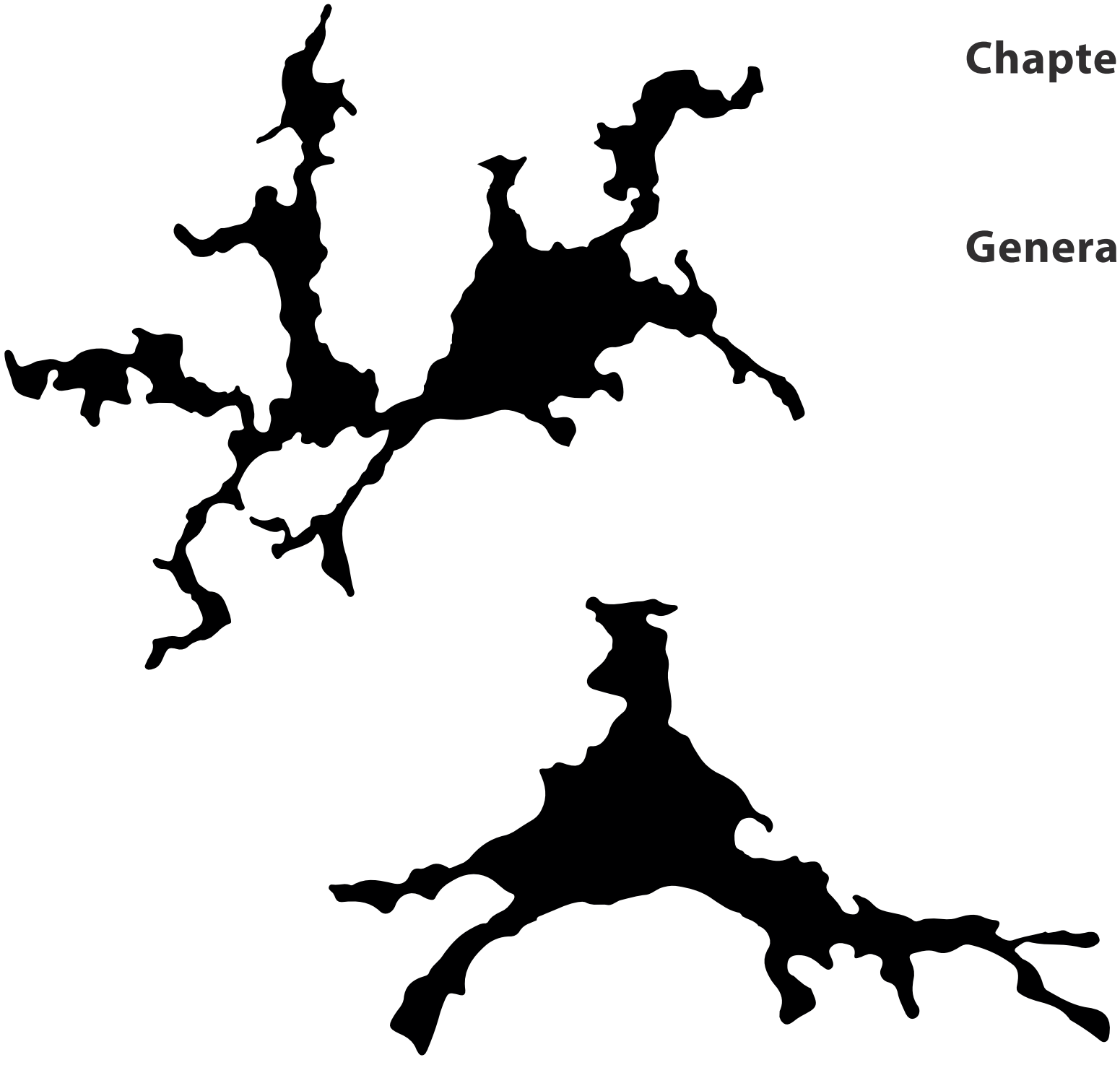

Chapter 8

General discussion

The involvement of the immune system has been implicated in the aetiology of schizophrenia (SCZ), bipolar disorder (BD), and major depressive disorder (MDD). Epidemiological, imaging, and genomic studies provided solid evidence for an association of immunology and psychiatry. Although previous research supports immune alterations in SCZ, BD, and MDD, less is known about how the immune system is involved in causing brain dysfunction in these disorders. Since microglia are the immune cells of the central nervous system (CNS), it is hypothesized that these cells contribute to the pathophysiology of SCZ, BD, and MDD. Therefore, the aim of this thesis was to elucidate the role of microglia, and more specifically their immune activating properties, in SCZ, BD, and MDD by using a multi-level approach.

8.1 Profiling isolated human microglia

To study microglia in psychiatric disorders, we established a protocol to isolate human microglia from post-mortem human brain tissue. This enabled us to study microglia of psychiatric patients, who donated their brain after death for research, *ex vivo* and define their immune activation signature and functionality with various experimental methods. In **chapter 2** we characterized the phenotype of the isolated microglia of donors without a psychiatric disorder. We compared these microglia with monocytes, monocyte-derived macrophages (mo-MΦ), monocyte-derived microglia-like cells, and microglial cell lines. We showed that the isolated human post-mortem microglia are a distinct and unique population, that differs in their gene expression and protein profile from monocytes, mo-MΦ, and monocyte-derived microglia-like cells. *In vitro*, these isolated microglia maintained their immune functions as they responded to external inflammatory compounds, such as lipopolysaccharide (LPS) and dexamethasone. An important finding was that *ex vivo* microglia are phenotypically very different from monocyte-derived microglia-like cells and cell lines. Several key microglial genes, such as *P2RY12*, *TREM2*, and *MERTK*, were low expressed in these cells, indicating important phenotypic differences. Our data emphasize the importance of using isolated human microglia in research and that validation of results from other microglia models with these primary cells is recommended.

To further characterize the isolated human microglia, a proteomic profile of these cells was generated with mass cytometry (CyTOF) (**chapter 3)**. We developed a specific cryopreservation protocol for microglia, which provided us with the opportunity to perform protein analysis from different donors at the same time. We showed that post-mortem isolated microglia can be distinguished from peripheral myeloid cells and from microglia isolated from biopsy material. With the multidimensional power of CyTOF, we were able to study microglial heterogeneity. Specific microglial phenotypic signatures were found in various brain regions. For example, microglia of cortical brain regions were very distinct of microglia from subcortical areas (thalamus and subventricular zone). This study confirmed the diversity in microglial signature across the human brain. Others already reported on microglial heterogeneity in the murine brain, but this was so far not shown in humans[1–3]. The brain consists of different brain regions, each with its own cell type composition and tasks that need to be executed. Our results suggest that microglia adopt different phenotypes to fulfil the demands of these specific brain areas. This information provides the opportunity to study phenotypic alterations in region-specific microglia region, since the core signature of these cells is now established. The next step would be to perform single cell RNA sequencing of similar brain regions and overlay this with CyTOF data of the same donors. With this approach, a map of microglial heterogeneity across the human brain can be generated, providing information about mRNA expression and protein markers for each microglial subset. Such an atlas would greatly enhance the interpretation of changes in microglial mRNA and protein expression profiles that are found in neurodegenerative and psychiatric disorders, thereby opening the possibility to localize specific molecular targets for therapeutic interventions.

8.2 TSPO as reflection of immune activation in schizophrenia

In vivo, microglia can only be visualised with positron emission tomography (PET) using radioligands that bind to the translocator 18kDa protein (TSPO). In SCZ this method has been applied often to investigate microglial activation. However, the results are very conflicting, with studies reporting both increased and decreased TSPO binding. Besides, it was shown that TSPO expression and binding is not restricted to microglia only[4–7]. Thus, we studied whether TSPO expression is altered in SCZ and whether it can be used as a valid marker to measure human microglial activation in SCZ (**chapter 4**). Quantitative PCR analysis revealed similar expression of *TSPO* mRNA, general microglial markers, and microglial activation genes in brain tissue of patients with SCZ and controls. This implies that microglia in SCZ are not immune activated. Immunochemistry confirmed the presence of TSPO on microglia, astrocytes and the vasculature of patients with SCZ. The expression of TSPO in PET studies is therefore not a reflection of solely microglia, but more a representation of TSPO binding to cells of the CNS in general. Although current PET analysis is taking endothelial binding into account, no correction method for astrocytic and neuronal binding is applied. Thus, it is not accurate of current PET studies to relate to microglial activation with TPSO binding as outcome measurement.

It was also unclear whether TSPO expression is changed under inflammatory circumstances. In our study, we did not find an upregulation of TSPO mRNA and protein expression after induction of an inflammatory phenotype in isolated

microglia and mo-Mϕ. This implies that TSPO expression is not reflecting the activation state of human microglia. Altered *TSPO* expression was found rodent microglia activated with LPS or in combination with other inflammatory compounds (IFNγ, IL-4, dexamethasone). However, mixed results were obtained for human microglia or other myeloid cell types[8–12]. It is important to note that the microglia in these studies were in culture for 5-7 days, which might account for difference in responsiveness. It is clear that human and rodent microglia are phenotypically different from each other[13]. Despite executing similar functions in the brain, they vary in their morphology and transcriptome. For example, the expression of membrane bound molecules to recognize pathogens (e.g. TLR4) is more abundant in rodents. Since LPS response is mediated via TLR4, rodent microglia might be more capable of increasing *TSPO* expression after LPS stimulation.

8.3 Lack of neuroinflammation in schizophrenia

Since the immune system is associated with SCZ, it has been hypothesized that neuroinflammation contributes to SCZ pathology. In current literature microglial activation is often used interchangeable with the term 'neuroinflammation'. In **chapter 5** we studied the presence of the four hallmarks of classical neuroinflammation in SCZ: activation of microglia; increased cytokine levels; lymphocyte recruitment and infiltrates; and gliosis and local tissue damage. In post-mortem brain tissue of the Netherlands Brain Bank we studied the occurrence of the four hallmarks of neuroinflammation. We concluded that SCZ does not fulfil the four criteria and thus is not a neuroinflammatory disorder. In contrast with other studies we did not find signs of increased microglial density or activation in SCZ[14–17]. These results are supported by RNA sequencing studies on large cohorts that did not find upregulation of genes related to microglial density and activation[18,19]. This is an important finding, since previous studies suggested that microglia are highly activated in SCZ[20,21]. Excessive microglial activation was thought to impair to neurogenesis and increase the elimination of spines, resulting in the decreased dendritic spine density observed in SCZ. Although we and others did not find microglial activation in SCZ[16,17,22–25], this does not mean that microglia do not contribute to SCZ pathogenesis. Our post-mortem analysis is a reflection of microglia in late-stages of the disease. In addition, it is not yet understand which microglial phenotypes are involved in synaptic pruning. It is possible that immune activation was present during development and could account for decreased spine density. Also, fewer spines might be generated during development or the spines could be less functional and might thus be removed or pruned in SCZ. However, this can never be studied in post-mortem tissues.

Even though the blood-brain barrier was still intact, we observed more $CD3^+$ T-lymphocytes in the parenchyma of patients with SCZ, which was also shown by others[25,26]. T-lymphocytes play a role in the crosstalk between neurons and the immune system and are able to induce neurotoxicity and neuronal damage[27]. This would suggest a role for T-lymphocytes in the neuronal loss in SCZ. However, nicotine smoking is known to influence T-lymphocyte proliferation in blood[28]. Since smoking is more common in our patient group compared to controls, this might account for the difference. Elevated cytokine expression, lymphocytic infiltrates, and tissue damage were not observed in SCZ.

Both in our own analysis of the tissue as well as in neuropathological reports no signs of neuroinflammation were found. This has important implications for the current clinical trials. Various studies are currently investigating anti-inflammatory medication as an add-on strategy in schizophrenia, with the aim of targeting an underlying neuroinflammatory process. Our data challenges this view and questions whether treatment with anti-inflammatory medication will be beneficial for patients with SCZ in general. It has to be noted that our group was too small to rule out the possibility that neuroinflammation is present in subgroups of patients with SCZ. If these would be present, these subgroups may benefit from anti-inflammatory treatment. Therefore it would be very informative to study the predisposition of certain patients with SCZ for neuroinflammation. This will make therapeutic interventions more personalized and effective.

8.4 Absence of microglial activation in bipolar disorder and major depressive disorder

In the final two chapters, microglia isolated form fresh post-mortem brain tissue of patients with BD (**chapter 6**) and MDD (**chapter 7)** were characterized regarding their inflammatory state. For both disorders we used a multi-level approach in which a combination of mRNA expression, protein profiling and *in vitro* functionality was applied. Besides, we included multiple brain regions to study microglial heterogeneity and functionality across brain areas. **Chapter 6** showed the lack of an inflammatory profile of microglia in BD: no increase in microglial density and change in morphology was observed. In addition, mRNA expression of general microglial genes was not changed and protein analyses confirmed the absence of an activation state in patients with BD. Since many studies found alterations in the peripheral immune system[29–31], we hypothesized that these cytokines could enter the CNS, activate microglia, and affect CNS functioning. The recent discovery of a meningeal lymphatic system in the brain[32], undermining the idea of the brain as an immune privileged organ, made this hypothesis more feasible. To our surprise,

we could not find changes in microglial immune activation. This questions whether cytokines can be exchanged freely between the brain and the periphery and to what extend they can influence microglial functioning in BD. We know that peripheral cytokines can interfere with CNS homeostasis and microglia functioning. However, this is often accompanied with leakage of the blood-brain barrier (BBB), as is seen in neuroinflammatory disorders[33,34]. Although disruption of the BBB is proposed in BD, no solid evidence is available yet[34]. From our data we can conclude that, irrespective of BBB intactness, microglia of patients with BD respond similar to inflammatory compounds as microglia of controls, indicating that peripheral cytokines do not affect them. Thus, microglia in BD are not primed or blunted regarding their inflammatory response and are still capable of executing their immune regulatory functions in the brain.

Finally, we performed a proteomic and transcriptomic analysis on microglia isolated from patients with MDD (**chapter 7**). The overall protein profile of MDD microglia was not deviant from control microglia, except for a decreased expression of CD14 and CD32. CD14 is normally upregulated directly after isolation, indicative of microglial activation[35]. Besides, CD14 is regulating microglial responsiveness to LPS. It was shown that $CD14^-$ microglia react more strongly to LPS compared to $CD14^+$ microglia[36]. This would suggest a higher sensitivity of MDD microglia after treatment with LPS. However, we observed similar responsiveness of MDD microglia compared to controls after LPS administration. This implies that the decreased expression of CD14 is not affecting LPS sensitivity. Additionally, we found a decreased expression of CD32. CD32 is a type II FC receptor and a known mediator of phagocytosis[37]. This would indicate that phagocytic activity by CD32 might be dampened in MDD. Phagocytic assays need to be performed to elucidate whether there is indeed a diminished phagocytosis in MDD. Besides differences between MDD and controls, we found region-specific protein expression, with lower expression of CD11c in the subventricular zone and higher expression of CD163 in the medial frontal gyrus compared to the other three tissues. More research with for example CyTOF is needed to elucidate the variation of protein expression across brain regions. Transcriptomic analysis revealed 194 differential expressed genes (DEGs) between microglia of patients with MDD and controls. 188 genes were downregulated genes and only six genes were upregulated. The top three significant DEGs were al downregulated in MDD and associated with histone modification and chromatin accessibility. Besides, pathway analyses showed decreased expression of pathways involved in cell cycle and cell division. This implies that microglia are not immune altered, but that they are still phenotypically changed in MDD. The next steps that we are currently performing are replication and validation of these results using immunostainings and quantitative PCR. Future steps will be to further understand how the changes in MDD microglial phenotypes related to changes in function.

8.5 Current perspective on microglial activation in psychiatric disorders

In the last decade many researchers studied the inflammatory role of microglia in psychiatric disorders. With PET-imaging microglia were studied *in vivo* with tracers binding to TSPO, cytokine levels were measured in blood and CSF, and post-mortem studies determined microglial density and morphology, mRNA and protein expression, and transcriptomic profiles. Despite all these efforts, there is still no consensus whether microglia are immune activated in SCZ, BD, and MDD. Where some of the earlier studies reported increased microglial densities, cytokine levels, and an inflammatory phenotype of the cells, more recent studies, including ours, could not support these findings. This thesis contributes to the discussion by providing information about the immune phenotype of microglia directly isolated from post-mortem tissue of psychiatric patients.

There are several reasons that could have contributed to the inconsistency of the results. First of all, the inclusion of many different brain regions that investigated in the different studies, including cortical (e.g. PFC, temporal cortex), limbic (e.g. hippocampus, amygdala), subcortical (e.g. thalamus), and white matter areas (e.g. SVZ). These regions fulfil divergent functions in the brain and different microglial phenotypes per brain area are determined in chapter 3. Increased microglial density in one brain region does not necessarily indicate that there is immune activation in the whole brain and vice versa. Until now there is no study available that investigated microglia in SCZ, BD, and MDD in a wide range of brain areas, which would provide a better overview of microglial immune activation in psychiatric disorders. Furthermore, there is diversity in the type of marker that is used to study microglia. In immunochemistry, microglia were visualized with multiple antibodies, for example HLA-DR, CD68, Iba1, and QUIN. It was shown that the specificity of these antibodies to stain microglia is different and that some markers only label a certain microglial population (e.g. CD68 for phagocytic microglia)[38]. The combination of different brain regions and a variety of markers makes it complicated to make assumptions from these earlier studies regarding microglial activation.

Transcriptomic analysis on post-mortem brain tissue provides a good alternative to investigate microglial activation in psychiatric disorders at a large scale. A drawback of transcriptomic studies is that the post-mortem brain tissue used for the analysis is not perfused and therefore also includes peripheral myeloid cells, such as monocytes,

lymphocytes, granulocytes, and dendritic cells. These peripheral cells express similar markers as microglia, including *ITGAM*, *CD14*, *HLA-DRA*, and *CD45*. When interpreting transcriptomic studies (e.g. RNA sequencing) of total brain tissue, it is therefore important to focus on differences in the expression of specific microglial genes (e.g. *P2RY12*, *PROS1*, *MERTK*[39]). Furthermore, the presence of T- and B-lymphocytes cannot be studied, since no distinction is made between lymphocytes in the vasculature and the parenchyma, as is observed in SCZ[16,25]. Currently, there are several RNA sequencing studies performed on post-mortem brain tissue of patients with SCZ, BD, and MDD. Whereas the sample sizes differed between the studies, with the largest cohorts for SCZ, none found alterations in the expression of genes involved in the immune system[18,19,48–52,40–47]. The data presented in this thesis is in line with the sequencing studies with lacking evidence of immune activated microglia. Although the sample size of our cohort is relatively small, we used a multi-level approach, which is more extensive compared to the already published studies. Besides, we are the first who isolated microglia directly from post-mortem brain tissue of patients with a psychiatric disorder. The microglia of these patients provided us with the unique opportunity to characterize them extensively as a single population. We determined microglial density and morphology, flow cytometry determined protein expression, mRNA expression, and microglial immune responsiveness in the same brain tissue. All these different methods failed in detecting immune activation of microglia in the three disorders.

PET imaging studies and post-mortem studies have a different approach to investigate microglia, each with its own strengths and limitations. TSPO PET studies could provide information on microglial functioning *in vivo,* including the early stages of disease, but the specificity of currently used TSPO PET tracers is under debate. On the other hand, post-mortem studies provide the possibility to assess microglia in much more detail. However, they are only able to study microglia at the end stage of the disorder. It is known that aging influences microglia in the brain[53,54]. It is possible that the microglial deficits in the disorder in our studies are now masked due to aging effects. Furthermore, microglia can play a role during the acute stages of the disorder, which can only be detected with PET. Post-mortem studies can provide information about the influence of chronic psychiatric disorders on microglia. In addition, many potential pre- and post-mortem confounders could affect the results from post-mortem studies. All together, this makes direct comparison of microglial activation in PET data and post-mortem data highly complicated. Development of more specific microglial PET tracers is needed to answer the question if microglia are altered *in vivo*, since in post-mortem tissue we and others did not find sigs of activation after many years of sickness.

Altogether, literature and our studies hint towards a non-immune activated phenotype of microglia in SCZ, BD, and MDD. However, it is still possible that the immune system still contributes to the disorder in individual patients. Increased microglial density[24,55,56], altered cell morphology[57,58], elevated cytokine levels (e.g. IL-6, IL-1β)[44], and more $CD3^+$ T-lymphocytes[16,25] were found in a subpopulation of the patients. Also suicide may be associated with changes in microglial density and morphology[16,56,59,60]. More research is needed to specifically investigate the role of microglia and inflammation in these patients.

8.6 Microglia in psychiatric disorders: the end?

In this thesis we conclude that microglial activation is absent in SCZ, BD, and MDD. We show that microglia in these disorders are not different in their density, morphology, gene expression, protein profile, and inflammatory responsiveness compared to control microglia (Figure 1). The suggested hypothesis (for figure, see chapter 1) that constantly activated microglia are the source of brain dysfunctioning and psychopathology in psychiatric diseases should therefore be adjusted. Although no aberrant inflammatory phenotype was detected in these disorders, this does not mean that microglia are fully homeostatic and do not contribute to the pathogenesis of SCZ, BD, and MDD. Microglia play a role in many more CNS processes than solely immune regulation. The next paragraphs will provide an overview of the aspects in which microglia can still contribute to the disorders.

8.6.1 Microglia interaction with other cells

During homeostasis, microglia are in constant contact with other cell types, including neurons. Both a loss of communication between microglia and neurons and a deficit from the neuronal side can induce homeostatic disturbances and neuronal stress. In this thesis we also studied the expression of general microglial markers, indicative for overall microglial functioning. We noticed some alterations in the phenotype of microglia, but not related to their immune response. The most pronounced finding was a decreased expression of the fractalkine receptor (CX3CR1) in SCZ and BD (Figure 1, number 6). Previous studies already reported lower levels of CX3CR1 in blood and brain tissue of patients with SCZ[61]. Furthermore, CX3CR1 was implicated as a potential risk gene in BD[62]. CX3CR1 is expressed in microglia, whereas neurons present the CX3CR1 ligand (CX3CL1) on their membrane[63]. In microglia, CX3CR1 is involved in the regulation of motility and migration of the processes. Moreover, it plays a role in synaptic plasticity and controlling synaptic transmission in physiological conditions[64–67]. CX3CR1-CX3CL1 functioning is highly important for accurate communication between microglia and neurons. In conditions without danger or pathology, CX3CR1-CX3CL1 interaction keeps microglia silent and reduces neuronal

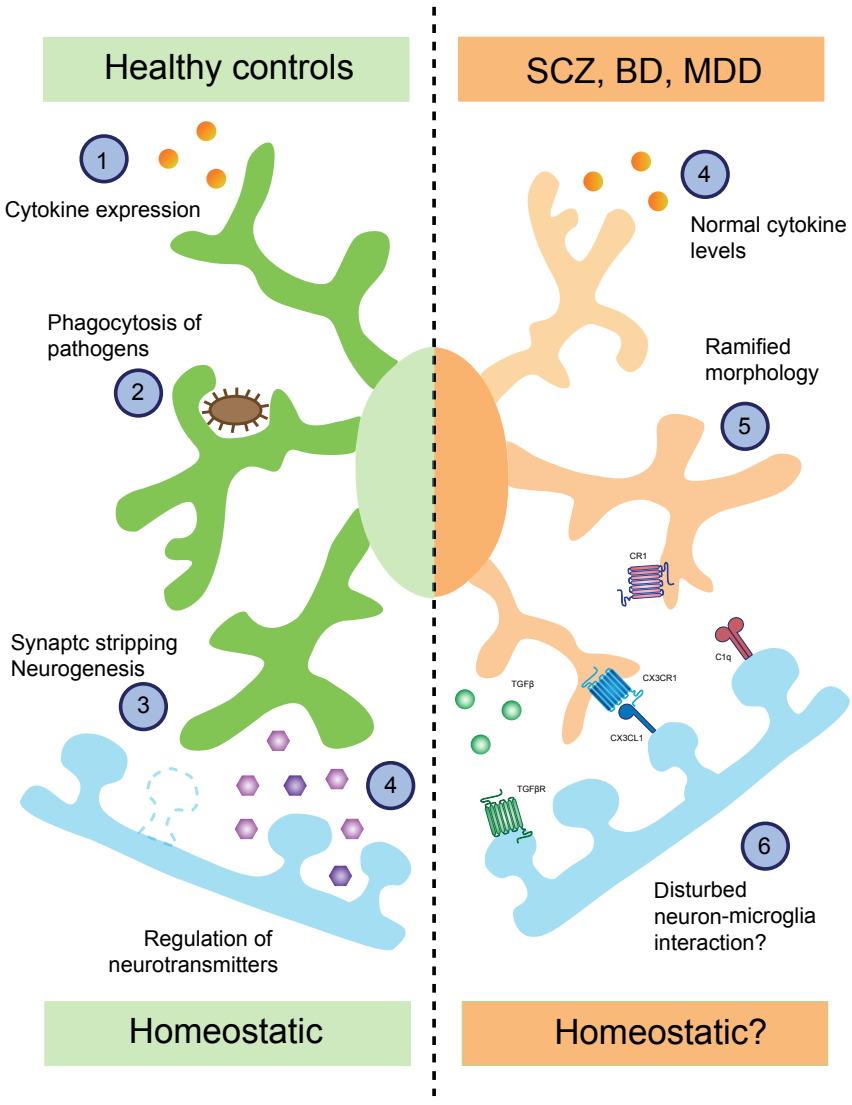

Figure 1: New view of microglia in psychiatric disorders. Microglia in healthy controls are homeostatic (left). They display a ramified morphology; regulate cytokine expression when needed (1), phagocytose pathogens, such as bacteria and death cells (2), are involved in neurogenesis and synaptic stripping (3), and regulate several neurotransmitter systems in the brain (4). Although immune activated microglia with excessive cytokine expression were expected, microglia in schizophrenia (SCZ), bipolar disorder (BD), and major depressive disorder (MDD) (right) were highly similar compared to microglia in healthy controls. They have normal cytokine expression (5) and their morphology is ramified (6). Our and other studies do suggest that neuron-microglia interaction might be disturbed in SCZ, BD, and MDD, which needs to be elucidated in future studies.

death[64,68]. With a loss of this signalling, microglia will become immune activated. Regarding to their morphology, microglia of CX3CR1$^{-/-}$ mice are unable to adopt a hyperramified phenotype under stress conditions, as was observed in wild type mice[69]. Interestingly, CX3CR1 deficiency resulted in less amyloid beta deposition in an Alzheimer's mouse model[70]. Patients with SCZ had similar levels of cortical amyloid beta compared to elderly controls. Compared to patients with Alzheimer's disease, even reduced amyloid levels were reported[71]. The same was observed in BD, with lower levels of soluble amyloid protein in the CSF of patients compared to controls. This suggests a protective function for CX3CR1 in amyloid deposition in SCZ and BD.

Besides morphological alterations of microglia, a deficiency of CX3CR1 or the ligand leads to increased production of pro-inflammatory cytokines, like IL-1β and reactive oxygen species. This will induce disturbances in brain homeostasis and lead to cell toxicity and excessive cell death[64,72]. Our data does not show a complete loss of CX3CR1. This is in line with the fact that we do not detect high levels of pro-inflammatory cytokines, as was reported in CX3CR1$^{-/-}$ mice. Besides immune regulatory and interaction functions, CX3CR1 is able to regulate neurotransmitter levels (e.g. glutamate, serotonin) via the inhibition or activation of specific neurons. This emphasizes that CX3CR1 alterations can directly influence the neurotransmitter system, resulting in neurotransmitter imbalances found in SCZ, BD, and MDD. We hypothesize that the decrease of factalkine-CX3CR1 interaction, as is observed in SCZ and BD, is not leading to microglial activation, but can disturb the neurotransmitter system and brain homeostasis.

8.6.2 Microglia and effect on neurogenesis

The promotion of neurogenesis and the role in synaptic pruning during development is one of the main functions of microglia. It is known that microglial immune activation during CNS development has direct consequences on neurogenesis. Alterations were found in the dopaminergic, serotonergic, GABAergic, and glutamatergic system in the offspring of animals in the maternal immune activation (MIA) model. More apoptosis of neurons and glia were observed in multiple brain regions and neurogenesis was impaired[73–75]. These CNS deficits highly resemble the pathology observed in psychiatric patients, with alterations in synaptic spine density and volume loss.

Our results and previous studies suggest that microglia in post-mortem studies are not immune activated, which challenges the view that overactivation of these cells is the cause of the spine loss. However, these results do not exclude the possibility that microglia activation during development contributes to neuronal abnormalities underlying SCZ, BD, and MDD. It is possible that these neuronal deficits are not

primarily be caused by microglia activation, but that microglia are still involved in the pathological process. For example, alterations in the complement system have been associated with SCZ. The complement system is involved in the opsonisation and clearance of pathogens and important for synaptic pruning. Increased copy numbers of complement factor 4 A (C4A) increase the risk for SCZ and increased expression of C4 is observed in post-mortem tissue of five brain regions of patients with SCZ[76]. It is thought that C4 contributes to the pruning of C1q opsonized synapses by complement receptors on the microglia. In this case, microglia just fulfil their job by eliminating tagged synapses. However, it is still unclear whether the diminished spine density in SCZ is a consequence of increased C4 expression or that microglial activation throughout life resulted in fewer spines.

8.7 Methodological considerations

All experimental work in this thesis has been performed with post-mortem brain tissue. Post-mortem material is currently the main strategy to study the cellular and molecular basis of psychiatric disorders. We used the tissue for multiple purposes: RNA extraction, protein analysis, and the isolation of primary microglia. There are various brain banks all over the world, collecting brain tissue of controls and patients with psychiatric and neurological disorders. However, the amount of available post-mortem samples is still limited for psychiatric disorders and many studies perform their experiments on the same tissue.

Most brain tissue studied in this thesis was provided by the Netherlands brain bank (NBB). Tissue of this brain bank was not evaluated for microglial changes or neuroinflammation yet. In 2012 the NBB started a novel program to recruit and phenotype donors with psychiatric disorders[77]. As a result of this program the number of registered donors with psychiatric disorders largely increased. This initiative enabled the studies using fresh post-mortem tissue described in chapter 5 and 6. In addition, a large benefit of the NBB is their pre-mortem donor registration program, which results in a relatively short post-mortem delay (PMD) and tissue can therefore be collected and distributed among researchers quickly. It was shown that various factors, including post-mortem delay, have a negative impact on RNA and protein quality of total brain tissue[78]. To study the quality of isolated microglia, analysis for the effect of ante- and post-mortem variables in 100 brains of the NBB revealed that PMD and time before starting the isolation did not influence microglial yields. No assumptions were made regarding RNA quality or protein integrity. On the other hand, pH negatively influenced microglia viability[79]. To limit the effect of PMD, donors with PMD over 12 hours were not included in our study and as soon as possible after autopsy. However, RNA and tissue quality remained a limiting factor in our studies and contributed to the fact that not all donors could be used for each experiment (e.g. immunostainings, mRNA analysis, microglial isolations).

Besides the influence of pH and PMD on the quality of the tissue and microglial numbers, many other confounding factors have been associated to affect post-mortem tissue and brain functioning. One of the external factors is substance abuse (e.g. smoking, alcohol, drugs). Substance abuse is very common among psychiatric patients and is related to increased suicide, earlier disease onset and more psychotic symptoms[80]. Furthermore, substance abuse has direct effect on brain functioning and neurobiology. For example, smoking will lead to thinning of the cortex and decreased brain volume[81,82]. Another confounder is medication. Psychiatric patients are using a wide range of different types of medicine, including antidepressants, mood stabilizers (e.g. lithium), antipsychotics, and cardiovascular medication. Although no correlation has been found between medication and changes in brain structure[83], studies suggest that they could have anti-inflammatory effects that might influenced microglial morphology and functioning[84]. Additionally, the cause of death, and especially suicide, might have a great impact on the brain and quality of the tissue. Lack of oxygen due to suffocation and medication overdose negatively influences cell viability and tissue quality. Since suicide is more common among psychiatric patients, this is an important confounder for microglial research. In our cohort we were able to include age, gender, PMD and pH as covariates. A confounder analysis was performed when significant differences between the groups were found. Unfortunately, type of medication, cause of death, and somatic comorbidity could not be included due to the large variability for these covariates. Our study was lacking power to take all these confounders into account. Suicide as cause of death was barely present in our cohort. Although we have a lot of donors with euthanasia, the impact on the brain of this event is likely different from suicide due to its more controlled manner. Moreover, the underlying neurobiology of a successful suicide attempt might be different from considered euthanasia.

To isolate microglia, the cells were positively selected with magnetic CD11b beads. This method is quick and efficient to extract microglia from fresh post-mortem brain tissue, but questions are raised regarding microglial purity. Besides microglia, other myeloid populations present in the CNS, like perivascular macrophages and resident monocytes, are also expressing CD11b[85]. With the use of CD11b beads, there is a possibility that both microglia and other myeloid cells are extracted from the tissue. To control for purity, all samples were screened with flow cytometry for the presence of other myeloid cells. These cells are $CD11b^{+}/CD45^{high}$, whereas microglia have a $CD11b^{+}/CD45^{low}$ profile. However, the possibility of resident or infiltrated

myeloid cells in our sample cannot be ruled out. A more pure microglia population can be achieved with flow cytometry cell sorting. A drawback of this technique is that the sorting will affect cell viability. Since cell death is already increased in culture conditions after isolation, this effect is even larger with sorted microglia. For time purposes and to increase microglial yield, we chose to use the magnetic beads over cell sorting.

8.8 Future directions

Although increased immune activation of microglia is not underlying psychiatric pathogenesis, other non-immune functions of microglia can still contribute to the disorders. Future studies to unravel the biological mechanism underlying SCZ, BD and MDD should focus more on microglia-neuron communication, the specific role of microglia in neurogenesis and synaptic pruning, and the effect of genetic and environmental factors on these cells.

To increase sample size and incorporate post-mortem tissue of multiple brain banks is one of the most important tasks for future researchers. Until now, microglial research in psychiatric disorders is performed with relatively small sample sizes, transcriptomic studies for SCZ excluded. Due to the large diversity among the patients, current sample sizes of post-mortem tissue are too small to cover the full range of the disorders and to adequately control for possible confounders. Only recently new initiatives were taken to collect more post-mortem tissue of psychiatric patients[77]. The benefit of the NBB is the recruitment of patients during life, which is in contrast to other brain banks. This resulted in better availability and quality of the clinical information of the donors included in the cohort. To increase the sample size of post-mortem tissue, better communication and exchange of brain tissue among brain banks worldwide should be established. Only when joining forces the cohorts will be diverse enough to investigate microglia in subpopulations of patients with SCZ, BD, and MDD on a larger scale.

Besides larger cohorts, better screening of the patients is necessary. SCZ, BD, and MDD are very heterogeneous disorders with a variety of symptoms. Clinical records are not always up to date and often self-diagnosis is present. For MDD specifically, we experienced that it was difficult to make a distinction between MDD comorbid depressive symptoms when evaluating the clinical post-mortem reports. Additionally, it is important to study microglia in relation to suicide. To make this possible, more clinical information is needed regarding suicidal thoughts and/or suicide attempts. With the availability of this information, subgroups among patients can be made.

Another interesting approach would be to look specifically at the overlapping factors of SCZ, BD, and MDD, instead of the diagnosis itself. For example, all three disorders display cognitive deficits; BD and MDD overlap in their depressive episodes, and SCZ and BD share the manic phases. With this approach microglial alterations can be directly related to symptomatology instead of overall pathology. This will provide more information about the direct influence of microglia in these disorders and hopefully result in more personalized and symptom specific medication.

The role of microglia in psychiatric disorders is only established recently. More knowledge about their functionality and phenotype of these cells is gained every day, but still a lot of questions remain. One of the most intriguing characteristics of microglia is their diversity across the brain. Even though microglial differences are proposed between cortical, subcortical, grey, and white matter areas, no clear profile of microglia for each brain region is available yet. Our CyTOF data showed that this is now feasible. Furthermore, we know that microglia can migrate to the site of injury. However, it needs to be elucidated if they stay in their own niche or will cross the border and adopt the phenotype of that specific brain area. To answer these questions, a large microglial characterization per brain region is needed. Thus, microglia should be isolated from multiple brain regions simultaneously and profiled on a transcriptomic and proteomic level with RNA sequencing and CyTOF.

There are many fundamental questions regarding the role of microglia in psychiatric disorders that are still not fully understood yet. For example, it is unclear to what extend microglia contribute to the diminished spine density observed in post-mortem tissue. Although some questions can be studied with post-mortem isolated microglia, it is impossible to investigate microglia in neurodevelopment and culture conditions will change their phenotype[86]. Cerebral organoids highly resemble the developing human brain and maintain the natural environment of the microglia[87,88]. SCZ, BD, and MDD have a strong genetic component, which makes these disorders suitable to create an *in vitro* model with patient derived cells. This model will provide us with the opportunity to study the contribution of genetics and epigenetics to the disorders, the communication of microglia with other cell types, and the influence of environmental factors on microglia, such as medication and nutrition.

Finally, it needs to be emphasized that post-mortem tissue is of high value to study psychiatric disorders. However, SCZ, BD, and MDD are very complex, with multiple risk factors and a broad range of symptoms. Animal models are only able to mimic a subset of the symptoms (e.g. depressive behaviour, cognitive problems) and cannot cover the complete psychiatric syndrome. The use of post-mortem brain tissue is

therefore unavoidable. The combination of *in vivo* PET imaging, *in vitro* cell models such as microglia-containing brain organoids, and post-mortem tissue will be the best approach to finally understand the role of microglia in SCZ, BD, and MDD.

References

1. Mrdjen, D. *et al.* High-Dimensional Single-Cell Mapping of Central Nervous System Immune Cells Reveals Distinct Myeloid Subsets in Health, Aging, and Disease. *Immunity* **48,** 380–395.e6 (2018).
2. Korin, B. *et al.* High-dimensional, single-cell characterization of the brain's immune compartment. *Nat. Neurosci.* **20,** 1300–1309 (2017).
3. Ajami, B. *et al.* Single-cell mass cytometry reveals distinct populations of brain myeloid cells in mouse neuroinflammation and neurodegeneration models. *Nat. Neurosci.* **21,** 541–551 (2018).
4. Notter, T. *et al.* Translational evaluation of translocator protein as a marker of neuroinflammation in schizophrenia. *Mol. Psychiatry* **23,** 323–334 (2018).
5. Notter, T., Coughlin, J. M., Sawa, A. & Meyer, U. Reconceptualization of translocator protein as a biomarker of neuroinflammation in psychiatry. *Mol. Psychiatry* **23,** 36–47 (2018).
6. Woods, M. J. & Williams, D. C. Multiple forms and locations for the peripheral-type benzodiazepine receptor. *Biochem. Pharmacol.* **52,** 1805–1814 (1996).
7. Cosenza-Nashat, M. *et al.* Expression of the translocator protein of 18 kDa by microglia, macrophages and astrocytes based on immunohistochemical localization in abnormal human brain. *Neuropathol Appl Neurobiol* **35,** 306–328 (2009).
8. Owen, D. R. *et al.* Pro-inflammatory activation of primary microglia and macrophages increases 18 kDa translocator protein expression in rodents but not humans. *J. Cereb. Blood Flow Metab.* **37,** 2679–2690 (2017).
9. Narayan, N. *et al.* The macrophage marker translocator protein (TSPO) is down-regulated on pro-inflammatory 'M1' human macrophages. *PLoS One* **12,** 1–19 (2017).
10. Bae, K.-R., Shim, H.-J., Balu, D., Kim, S. R. & Yu, S.-W. Translocator protein 18 kDa negatively regulates inflammation in microglia. *J. Neuroimmune Pharmacol.* **9,** 424–37 (2014).
11. Beckers, L. *et al.* Increased Expression of Translocator Protein (TSPO) Marks Pro-inflammatory Microglia but Does Not Predict Neurodegeneration. *Mol. Imaging Biol.* **20,** 94–102 (2018).
12. Beaino, W. *et al.* Purinergic receptors P2Y12R and P2X7R: potential targets for PET imaging of microglia phenotypes in multiple sclerosis. *J. Neuroinflammation* **14,** 259 (2017).
13. Smith, A. M. & Dragunow, M. The human side of microglia. *Trends Neurosci.* **37,** 125–135 (2014).
14. Trépanier, M. O., Hopperton, K. E., Mizrahi, R., Mechawar, N. & Bazinet, R. P. Postmortem evidence of cerebral inflammation in schizophrenia: a systematic review. *Mol. Psychiatry* **21,** 1009–1026 (2016).
15. van Kesteren, C. F. M. G. *et al.* Immune involvement in the pathogenesis of schizophrenia: a meta-analysis on postmortem brain studies. *Transl. Psychiatry* **7,** e1075 (2017).
16. Brisch, R. *et al.* Microglia in the dorsal raphe nucleus plays a potential role in both suicide facilitation and prevention in affective disorders. *Eur. Arch. Psychiatry Clin. Neurosci.* **267,** 403–415 (2017).
17. Hercher, C., Chopra, V. & Beasley, C. L. Evidence for morphological alterations in prefrontal white matter glia in schizophrenia and bipolar disorder. *J. Psychiatry Neurosci.* **39,** 376–385 (2014).
18. Fromer, M. *et al.* Gene expression elucidates functional impact of polygenic risk for schizophrenia. *Nat. Neurosci.* **19,** 1442–1453 (2016).
19. Birnbaum, R. *et al.* Investigating the neuroimmunogenic architecture of schizophrenia. *Mol. Psychiatry* (2017). doi:10.1038/mp.2017.89
20. Monji, A., Kato, T. & Kanba, S. Cytokines and schizophrenia: Microglia hypothesis of schizophrenia. *Psychiatry Clin. Neurosci.* **63,** 257–65 (2009).
21. Tay, T. L. *et al.* Microglia Gone Rogue: Impacts on Psychiatric Disorders across the Lifespan. *Front. Mol. Neurosci.* **10,** 421 (2017).

22. Connor, C. M., Guo, Y. & Akbarian, S. Cingulate White Matter Neurons in Schizophrenia and Bipolar Disorder. *Biol. Psychiatry* **66,** 486–493 (2009).
23. Arnold, S. E. *et al.* Absence of Neurodegeneration and Neural Injury in the Cerebral Cortex in a Sample of Elderly Patients With Schizophrenia. *Arch. Gen. Psychiatry* **55,** 225 (1998).
24. Steiner, J. *et al.* Distribution of HLA-DR-positive microglia in schizophrenia reflects impaired cerebral lateralization. *Acta Neuropathol.* **112,** 305–316 (2006).
25. Busse, S. *et al.* Different distribution patterns of lymphocytes and microglia in the hippocampus of patients with residual versus paranoid schizophrenia: further evidence for disease course-related immune alterations? *Brain. Behav. Immun.* **26,** 1273–9 (2012).
26. Bogerts, B. *et al.* Evidence of neuroinflammation in subgroups of schizophrenia and mood disorder patients: A semiquantitative postmortem study of CD3 and CD20 immunoreactive lymphocytes in several brain regions. *Neurol. Psychiatry Brain Res.* **23,** 2–9 (2017).
27. Debnath, M. Adaptive Immunity in Schizophrenia: Functional Implications of T Cells in the Etiology, Course and Treatment. *J. Neuroimmune Pharmacol.* **10,** 610–619 (2015).
28. Herberth, M. *et al.* Differential effects on T-cell function following exposure to serum from schizophrenia smokers. *Mol. Psychiatry* **15,** 364–71 (2010).
29. Fernandes, B. S. *et al.* C-reactive protein concentrations across the mood spectrum in bipolar disorder: a systematic review and meta-analysis. *The Lancet Psychiatry* **3,** 1147–1156 (2016).
30. Goldsmith, D. R., Rapaport, M. H. & Miller, B. J. A meta-analysis of blood cytokine network alterations in psychiatric patients: comparisons between schizophrenia, bipolar disorder and depression. *Mol. Psychiatry* **21,** 1696–1709 (2016).
31. Munkholm, K., Braüner, J. V., Kessing, L. V. & Vinberg, M. Cytokines in bipolar disorder vs. healthy control subjects: A systematic review and meta-analysis. *J. Psychiatr. Res.* **47,** 1119–1133 (2013).
32. Absinta, M. *et al.* Human and nonhuman primate meninges harbor lymphatic vessels that can be visualized noninvasively by MRI. *Elife* **6,** (2017).
33. da Fonseca, A. C. C. *et al.* The impact of microglial activation on blood-brain barrier in brain diseases. *Front. Cell. Neurosci.* **8,** 362 (2014).
34. Patel, J. P. & Frey, B. N. Disruption in the Blood-Brain Barrier: The Missing Link between Brain and Body Inflammation in Bipolar Disorder? *Neural Plast.* **2015,** 708306 (2015).
35. Melief, J. *et al.* Characterizing primary human microglia: a comparative study with myeloid subsets and culture models. *Glia* 1–12 (2016). doi:10.1002/glia.23023
36. Janova, H. *et al.* CD14 is a key organizer of microglial responses to CNS infection and injury. *Glia* **64,** 635–649 (2016).
37. Peress, N. S., Fleit, H. B., Perillo, E., Kuljis, R. & Pezzullo, C. Identification of FcγRI, II and III on normal human brain ramified microglia and on microglia in senile plaques in Alzheimer's disease. *J. Neuroimmunol.* **48,** 71–79 (1993).
38. Hendrickx, D. A. E., van Eden, C. G., Schuurman, K. G., Hamann, J. & Huitinga, I. Staining of HLA-DR, Iba1 and CD68 in human microglia reveals partially overlapping expression depending on cellular morphology and pathology. *J. Neuroimmunol.* **309,** 12–22 (2017).
39. Butovsky, O. *et al.* Identification of a unique TGF-β-dependent molecular and functional signature in microglia. *Nat. Neurosci.* **17,** 131–43 (2014).
40. Hwang, Y. *et al.* Gene expression profiling by mRNA sequencing reveals increased expression of immune/inflammation-related genes in the hippocampus of individuals with schizophrenia. *Transl. Psychiatry* **3,** e321 (2013).
41. Zhao, Z. *et al.* Transcriptome sequencing and genome-wide association analyses reveal lysosomal function and actin cytoskeleton remodeling in schizophrenia and bipolar disorder. *Mol. Psychiatry* **20,** 563–572 (2015).
42. Kohen, R., Dobra, A., Tracy, J. H. & Haugen, E. Transcriptome profiling of human hippocampus dentate gyrus granule cells in mental illness. *Transl. Psychiatry* **4,** e366 (2014).
43. Xiao, Y. *et al.* The DNA methylome and transcriptome of different brain regions in schizophrenia and bipolar disorder. *PLoS One* **9,** e95875 (2014).
44. Fillman, S. G. *et al.* Increased inflammatory markers identified in the dorsolateral prefrontal cortex of individuals with schizophrenia. *Mol. Psychiatry* **18,** 206–214 (2013).
45. Chang, X. *et al.* RNA-seq analysis of amygdala tissue reveals characteristic expression profiles in schizophrenia. *Transl. Psychiatry* **7,** e1203 (2017).
46. Ramaker, R. C. *et al.* Post-mortem molecular profiling of three psychiatric disorders. *Genome Med.* **9,** 72 (2017).
47. Voisey, J. *et al.* Clinically proven drug targets differentially expressed in the prefrontal cortex of schizophrenia patients. *Brain. Behav. Immun.* **61,** 259–265 (2017).
48. Wu, J. Q. *et al.* Transcriptome sequencing revealed significant alteration of cortical promoter usage and splicing in schizophrenia. *PLoS One* **7,** e36351 (2012).
49. Darby, M. M., Yolken, R. H. & Sabunciyan, S. Consistently altered expression of gene sets in postmortem brains of individuals with major psychiatric disorders. *Transl. Psychiatry* **6,** e890 (2016).
50. Akula, N. *et al.* RNA-sequencing of the brain transcriptome implicates dysregulation of neuroplasticity, circadian rhythms and GTPase binding in bipolar disorder. *Mol. Psychiatry* **19,** 1179–85 (2014).
51. Cruceanu, C. *et al.* Transcriptome Sequencing of the Anterior Cingulate in Bipolar Disorder: Dysregulation of G Protein-Coupled Receptors. *Am. J. Psychiatry* **172,** 1131–1140 (2015).
52. Pacifico, R. & Davis, R. L. Transcriptome sequencing implicates dorsal striatum-specific gene network, immune response and energy metabolism pathways in bipolar disorder. *Mol. Psychiatry* **22,** 441–449 (2017).
53. Keren-Shaul, H. *et al.* A Unique Microglia Type Associated with Restricting Development of Alzheimer's Disease. *Cell* **169,** 1276–1290.e17 (2017).
54. Galatro, T. F. *et al.* Transcriptomic analysis of purified human cortical microglia reveals age-associated changes. *Nat. Neurosci.* **20,** 1162–1171 (2017).
55. Comte, I., Kotagiri, P. & Szele, F. G. Regional differences in human ependymal and subventricular zone cytoarchitecture are unchanged in neuropsychiatric disease. *Dev. Neurosci.* **34,** 299–309 (2012).
56. Steiner, J. *et al.* Immunological aspects in the neurobiology of suicide: Elevated microglial density in schizophrenia and depression is associated with suicide. *J. Psychiatr. Res.* **42,** 151–157 (2008).
57. Wierzba-Bobrowicz, T. *et al.* Degeneration of microglial cells in frontal and temporal lobes of chronic schizophrenics. *Folia Neuropathol.* **42,** 157–65 (2004).
58. Wierzba-Bobrowicz, T., Lewandowska, E., Lechowicz, W., Stepień, T. & Pasennik, E. Quantitative analysis of activated microglia, ramified and damage of processes in the frontal and temporal lobes of chronic schizophrenics. *Folia Neuropathol.* **43,** 81–9 (2005).
59. Schnieder, T. P. *et al.* Microglia of prefrontal white matter in suicide. *J. Neuropathol. Exp. Neurol.* **73,** 880–90 (2014).
60. Torres-Platas, S. G., Cruceanu, C., Chen, G. G., Turecki, G. & Mechawar, N. Evidence for increased microglial priming and macrophage recruitment in the dorsal anterior cingulate white matter of depressed suicides. *Brain. Behav. Immun.* **42,** 50–9 (2014).
61. Bergon, A. *et al.* CX3CR1 is dysregulated in blood and brain from schizophrenia patients. *Schizophr. Res.* **168,** 434–443 (2015).
62. Jin, W., Chorath, A., Cao, S. & Disorder, B. Three Potential Risk Genes for Bipolar Disorder: MT1E, MT1X and CX3CR1. *J. Psychiatry Brain Sci.* **2017,** (2017).
63. Wolf, Y., Yona, S., Kim, K.-W. & Jung, S. Microglia, seen from the CX3CR1 angle. *Front. Cell. Neurosci.* **7,** 26 (2013).

64. Arnoux, I. & Audinat, E. Fractalkine Signaling and Microglia Functions in the Developing Brain. *Neural Plast.* **2015,** 689404 (2015).
65. Wake, H., Moorhouse, A. J., Jinno, S., Kohsaka, S. & Nabekura, J. Resting microglia directly monitor the functional state of synapses in vivo and determine the fate of ischemic terminals. *J. Neurosci.* **29,** 3974–80 (2009).
66. Tremblay, M.-È., Lowery, R. L. & Majewska, A. K. Microglial Interactions with Synapses Are Modulated by Visual Experience. *PLoS Biol.* **8,** e1000527 (2010).
67. Paolicelli, R. C. *et al.* Synaptic pruning by microglia is necessary for normal brain development. *Science* **333,** 1456–1458 (2011).
68. Biber, K., Neumann, H., Inoue, K. & Boddeke, H. W. G. M. Neuronal 'On' and 'Off' signals control microglia. *Trends Neurosci.* **30,** 596–602 (2007).
69. Hellwig, S. *et al.* Altered microglia morphology and higher resilience to stress-induced depression-like behavior in CX3CR1-deficient mice. *Brain. Behav. Immun.* **55,** 126–137 (2016).
70. Lee, S. *et al.* CX3CR1 Deficiency Alters Microglial Activation and Reduces Beta-Amyloid Deposition in Two Alzheimer's Disease Mouse Models. *Am. J. Pathol.* **177,** 2549–2562 (2010).
71. Chung, J. K. *et al.* B-Amyloid Burden is Not Associated with Cognitive Impairment in Schizophrenia: A Systematic Review. *Am. J. Geriatr. Psychiatry* **24,** 923–939 (2016).
72. Sheridan, G. K. & Murphy, K. J. Neuron-glia crosstalk in health and disease: fractalkine and CX3CR1 take centre stage. *Open Biol.* **3,** 130181 (2013).
73. Boksa, P. Effects of prenatal infection on brain development and behavior: A review of findings from animal models. *Brain. Behav. Immun.* **24,** 881–897 (2010).
74. Liu, Y.-H., Lai, W.-S., Tsay, H.-J., Wang, T.-W. & Yu, J.-Y. Effects of maternal immune activation on adult neurogenesis in the subventricular zone–olfactory bulb pathway and olfactory discrimination. *Schizophr. Res.* **151,** 1–11 (2013).
75. Smolders, S., Notter, T., Smolders, S. M. T., Rigo, J.-M. & Brône, B. Controversies and prospects about microglia in maternal immune activation models for neurodevelopmental disorders. *Brain. Behav. Immun.* **73,** 51–65 (2018).
76. Sekar, A. *et al.* Schizophrenia risk from complex variation of complement component 4. *Nature* **530,** 177–183 (2016).
77. de Lange, G. M., Rademaker, M., Boks, M. P. & Palmen, S. J. M. C. Brain donation in psychiatry: results of a Dutch prospective donor program among psychiatric cohort participants. *BMC Psychiatry* **17,** 347 (2017).
78. Ferrer, I., Martinez, A., Boluda, S., Parchi, P. & Barrachina, M. Brain banks: benefits, limitations and cautions concerning the use of post-mortem brain tissue for molecular studies. *Cell Tissue Bank.* **9,** 181–194 (2008).
79. Mizee, M. R. *et al.* Isolation of primary microglia from the human post-mortem brain: effects of ante- and post-mortem variables. *Acta Neuropathol. Commun.* **5,** 16 (2017).
80. Jakobsson, J. *et al.* Altered concentrations of amyloid precursor protein metabolites in the cerebrospinal fluid of patients with bipolar disorder. *Neuropsychopharmacology* **38,** 664–72 (2013).
81. Schneider, C. E. *et al.* Smoking status as a potential confounder in the study of brain structure in schizophrenia. *J. Psychiatr. Res.* **50,** 84–91 (2014).
82. Karama, S. *et al.* Cigarette smoking and thinning of the brain's cortex. *Mol. Psychiatry* **20,** 778–785 (2015).
83. Roiz-Santiañez, R., Suarez-Pinilla, P. & Crespo-Facorro, B. Brain Structural Effects of Antipsychotic Treatment in Schizophrenia: A Systematic Review. *Curr. Neuropharmacol.* **13,** 422–434 (2015).
84. Kato, T. A. *et al.* Anti-Inflammatory properties of antipsychotics via microglia modulations: are antipsychotics a 'fire extinguisher' in the brain of schizophrenia? *Mini Rev. Med. Chem.* **11,** 565–74 (2011).
85. Prinz, M., Priller, J., Sisodia, S. S. & Ransohoff, R. M. Heterogeneity of CNS myeloid cells and their roles in neurodegeneration. *Nat. Neurosci.* **14,** 1227–1235 (2011).
86. Gosselin, D. *et al.* An environment-dependent transcriptional network specifies human microglia identity. *Science* **356,** (2017).
87. Lancaster, M. a *et al.* Cerebral organoids model human brain development and microcephaly. *Nature* **501,** 373–9 (2013).
88. Ormel, P. R. *et al.* Microglia innately develop within cerebral organoids. *Nat. Commun.* **9,** 4167 (2018).

Appendices

Nederlandse samenvatting

Al meer dan een eeuw wordt er gesuggereerd dat het immuunsysteem betrokken is bij het ontstaan van schizofrenie (SCZ), bipolaire stoornis (BD) en depressie (MDD). Onderzoekers vonden veranderingen in belangrijke genen van het immuunsysteem en een verhoging van chemokines en cytokines, belangrijke immuunstoffen in het lichaam, in patiënten. Het is duidelijk dat het immuunsysteem een rol speelt bij deze drie stoornissen, maar niet exact op welke manier. Dit proefschrift is gefocust op microglia, de immuuncellen van het brein. Deze cellen zijn essentieel voor het bestrijden van ziekten en het opruimen van afval in het brein. Daarnaast zijn ze nauw betrokken bij de ontwikkeling van de hersenen, onder andere door het elimineren van foutieve of overbodige neuronen en het stimuleren van de groei van nieuwe neuronen. Tot nu toe is nog vrij weinig bekend in hoeverre zij bijdragen aan het ontstaan van SCZ, BD en MDD, maar er wordt gesuggereerd dat de microglia overactief zijn, resulterend in de psychische klachten.

Het belangrijkste doel was om de microglia in deze drie stoornissen zo goed mogelijk in kaart te brengen en te onderzoeken of deze cellen anders zijn in hersenweefsel van patiënten ten opzichte van controles, oftewel mensen zonder een psychiatrische stoornis. Voor dit proefschrift is gebruikt gemaakt van een bijzondere techniek, waarbij microglia uit het brein van overleden patiënten en controles werden gehaald waarna ze gekarakteriseerd konden worden. Wij hebben laten zien dat de geïsoleerde microglia verschillen van andere immuuncellen, zoals monocyten, en dat ze hun immuuneigenschappen behouden zodra ze uit het brein gehaald zijn (**hoofdstuk 2**). Ook ontwikkelden wij een methode waarbij de eiwitexpressie van de cellen direct na het isoleren bewaard bleef en later ontrafeld kon worden. Dit had als grote voordeel dat de samples eerst allemaal verzameld en later tegelijk geanalyseerd konden worden, waarbij technische variatie tussen de samples geminimaliseerd werd. Hierbij ontdekten wij onder andere dat de eiwitexpressie van microglia specifiek is voor het hersengebied waaruit ze geïsoleerd worden (**hoofdstuk 3**).

Microglia in levende mensen worden momenteel vooral gevisualiseerd met behulp van het eiwit TSPO. Echter, verschillende onafhankelijke onderzoeken rapporteerden verhoogde, verlaagde, of zelfs gelijke expressie van TSPO in patiënten met SCZ. In post-mortem weefsel vonden wij dat de expressie van TSPO vergelijkbaar was tussen patiënten met SCZ en controles (**hoofdstuk 4**). Ook bleek dat TSPO niet direct gerelateerd was aan immuunactivatie van microglia. Dit betekent dat TSPO mogelijk geen goede marker is om microglia te meten in het brein van patiënten met SCZ. Daarnaast ontkrachtten wij de hypothese dat SCZ een neuroinflammatoire ziekte is (**hoofdstuk 5**). Wij vonden geen verschil in het aantal microglia of tekenen van immuunactivatie in patiënten met SCZ. Echter, meer T-lymfocyten werden geobserveerd in het parenchym van patiënten, wat mogelijk gerelateerd is aan veranderingen in genen die betrokken zijn bij de interferon response, een belangrijke cytokine voor het immuunsysteem.

In zowel BD als MDD vonden wij geen aanwijzingen dat microglia een immuungeactiveerd profiel hadden. In BD was het aantal microglia in patiënten en controles gelijk, hadden ze geen geactiveerde morfologie, oftewel ronde vorm, en was de eiwit- en genexpressie vergelijkbaar (**hoofdstuk 6**). Een grote transcriptoomanalyse is uitgevoerd op microglia geïsoleerd uit het brein van patiënten met MDD en controles (**hoofdstuk 7**). In totaal kwamen 194 genen verschillend tot expressie in de patiënten ten opzichte van de controles. Hiervan was de expressie van 188 genen verminderd en zes genen verhoogd. De genen met het grootste expressieverschil tussen patiënten en controles spelen voornamelijk een rol bij celdeling en celcyclus, processen die allemaal verlaagd waren in MDD. In beide ziektebeelden bleek microglia activatie niet de grote boosdoener, maar dragen zij mogelijk op een andere manier bij aan BD en MDD.

Aan de hand van dit proefschrift werd geconcludeerd dat de microglia in SCZ, BD en MDD niet immuun geactiveerd zijn. Dit hoeft echter niet te betekenen dat deze cellen niet betrokken zijn bij de stoornissen. Naast immuunregulatie zijn microglia ook betrokken bij vele andere processen in het brein. Zo zijn er aanwijzingen dat de communicatie tussen neuronen en microglia verstoord is. Dit heeft mogelijk directe invloed op het behoud of de eliminatie van neuronen en de regulatie van neurotransmitters. Om de onderliggende biologie van SCZ, BD en MDD te ontrafelen zal toekomstig onderzoek zich moeten focussen op de communicatie tussen microglia en neuronen, hun specifieke rol in neuronale ontwikkeling en het effect van genetische- en omgevingsfactoren op de microglia.

List of publications

Böttcher, C.*, Schlickeiser, S.*, **Sneeboer, M.A.M.***, Kunkel, D., Knop, A., Paza, E. *et al.* Human microglia regional heterogeneity and phenotypes determined by multiplexed single-cell mass cytometry. *Nat. Neurosci.* **22,** 78–90 (2019).

Ormel, P.R., Vieira de Sá, R., van Bodegraven, E.J., Karst, H., Harschnitz, O., **Sneeboer, M.A.M.** *et al.* Microglia innately develop within cerebral organoids. *Nat. Commun.* **9,** 4167 (2018).

van Mierlo, H.C., Wichers, C.G.K., He, Y., **Sneeboer, M.A.M.**, Radstake, T.R.D.J., Kahn, R.S. *et al.* Telomere quantification in frontal and temporal brain tissue of patients with schizophrenia. *J. Psychiatr. Res.* **95,** 231–234 (2017).

Arkink, E.B., Schoonman, G.G., van Vliet, J.A., Bakels, H.S., **Sneeboer, M.A.M.**, Haan, J. *et al.* The cavernous sinus in cluster headache - a quantitative structural magnetic resonance imaging study. *Cephalalgia* **37,** 208–213 (2017).

Melief, J.*, **Sneeboer, M.A.M.***, Litjens, M., Ormel, P.R., Palmen, S.J.M.C., Huitinga, I. *et al.* Characterizing primary human microglia: a comparative study with myeloid subsets and culture models. *Glia* 1–12 (2016).

Kanski R, **Sneeboer, M.A.M.**, van Bodegraven, E.J., Sluijs, J.A., Kropff, W., Vermunt, M.W. *et al.* Histone acetylation in astrocytes suppresses GFAP and stimulates a reorganization of the intermediate filament network. *J. Cell Sci.* **127,** 4368–4380 (2014).

* These authors contributed equally

Acknowledgements

De afgelopen jaren stonden in het teken van hard werken, lachen, microglia, collega's, frustratie en succes, donoren, pipetteren, vriendschap en persoonlijke ontwikkeling. Vele mensen hebben deze tijd onvergetelijk gemaakt en wil ik graag bedanken.

Prof. dr. Kahn, beste **René**: bedankt voor de mogelijkheid om de afgelopen vier jaar aan dit onderzoek te werken en de kans om onze meetings drie maanden in New York te laten plaatsvinden.

Prof. dr. Hol, beste **Elly**: bedankt voor al je wetenschappelijke input en steun. Ik heb enorm veel van je geleerd en bewonder je manier van leidinggeven. Recht door zee, geen blad voor de mond, maar tegelijk supportive, stimulerend om het beste uit jezelf en het onderzoek te halen en altijd zin om een drankje mee te drinken. Jouw kritische blik zal mij tot op de dag van vandaag scherp houden.

Lot, jij leerde mij de wonderenwereld van microglia kennen. Je had een duidelijk beeld hoe het project eruit moest komen te zien, wat voor mij een ideaal startpunt was. Onder jouw supervisie kon ik mij ontwikkelen als zelfstandige onderzoeker. Ik heb genoten van onze drie maanden samen in New York, waarbij ik zelfs een paar dagen onderdeel was van jouw gezin. Bedankt voor alle adviezen, je vertrouwen in mij en het overdragen van je liefde voor microglia.

Saskia, als voormalig co-promotor was je nauw bij mijn traject betrokken. Maandelijks vertelde ik je waar ik mee bezig was en leerde ik om mijn eigen onderzoek op een begrijpelijke manier uit te leggen. Naast wetenschappelijke input waren je coachsessies meer dan zinvol om mijn promotie succesvol af te ronden. Bedankt voor al je tips en begeleiding.

Manja, lieve paranimf. Tijdens mijn sollicitatie vroeg je of ik van het organiseren en structuur ben. Ik beaamde dit, waarna jouw reactie was: 'mooi, ik ook'. Een vriendschap was meteen geboren. Van jou leerde ik de beginselen van het isoleren, de weg in het lab, en daarbij ook meteen het hele departement kennen. Want een sociaal dier ben je in hart en nieren. Met pijn in mijn hart moest ik afscheid van je nemen als collega, maar als vriendin bleef je. Met veel plezier kom ik bij jou en Michiel thuis, mee-eten en ravotten met de kids. Uren kunnen we op de bank kletsen, de theekoppen steeds bijvullend. Dankjewel dat je 12 maart aan mijn zijde wil staan. Ik had het niet anders gewild

Paul, mijn paramacho. Ik zie je nog zo binnenkomen tijdens mijn isolatie en jouw sollicitatie: gekleed in pak, maar direct geïnteresseerd. Volgens Elly was jij het tegengas wat ik nodig had en daar had ze gelijk in. Jij de chaoot, ik de organisatorische nerd. We hebben samen gelachen, gepipetteerd, gesport, gereisd (Berlijn, New York), gepresenteerd (het legendarische 'blue eyes' moment), bier gedronken, elkaar moed ingesproken en vele keren de Pasterkampers uitgedaagd. Dankjewel voor deze mooie herinneringen. En met jou als echte gangmaker aan mijn zijde weet ik zeker dat op 12 maart mijn zenuwen zullen verdwijnen als sneeuw voor de zon.

Bart, wat moest ik toch doen als je mijn kamer in kwam lopen, vaak zonder duidelijke reden. Door trial and error leerde ik dat ik je op de bank moest zetten en een kop koffie moest geven. Dan waren we beiden gelukkig. Ik heb genoten van onze maandelijkse koffieochtenden en de daarbij horende discussies over wetenschap en tegenslagen in ons onderzoek. Bedankt voor deze mooie momenten.

Emma, tijdens mijn masterstage bij Elly had iedereen het alleen maar over de vorige studente van Regina. Geen idee wie ze was, maar ze heette 'Emma', had lang blond haar, was een goede wetenschapper én ook een leuk mens. Toen we eindelijk echt collega's werden bleek alles waar te zijn. Ik heb enorm met je gelachen, het eerste Bergen Hollab uitje met je georganiseerd (inclusief speurtocht) en vele biertjes gedronken en oesters gegeten. Bedankt voor je grote passie voor GFAP, waar ik na één stage toch wel genoeg van had, en wens je heel veel succes in Parijs. Ik zal onze strijd om de labradio missen.

Amber, ik heb je vanaf dag één als mijn kleine labzusje beschouwd. Vooral omdat ik mezelf erg in je herkende: gedisciplineerd en een harde werker, maar ook een gezelligheidsmens en altijd in voor een goede grap. Ook al is jouw onderzoek vooral gericht op de astrocyten in het psychiatrische brein, ik hoop dat mijn liefde voor microglia toch een beetje op jou overgeslagen is. Bedankt voor al je vrolijkheid en opbeurende woorden wanneer het nodig was.

Sophietje, ik ken geen vrolijker en opgewekter persoon dan jij. Zelfs de zoveelste mislukte klonering kon je nog niet doen mopperen. Deze onophoudelijke positiviteit werkte aanstekelijk en het was een groot plezier om met je samen te werken. Bedankt voor alle goede adviezen en de leuke tijd. Ik wens je heel veel succes met je opleiding tot neurochirurg en ik blijf naar je zwaaien als ik voorbij loop.

Yujie, I am so proud of you. I have seen you growing in the past years, both personally as in your work. You are always happy and one of the most funniest girls I have ever met. Thank you so much for teaching me new 'words' (green tea bitch), showing me the Chinese symbol for mountain on the UMC wall (I cannot see it differently anymore), and invite me to your legendary hotpot and mahjong parties. I am looking forward to stand by your side at your defense.

Gijsje, mijn partner in crime als het gaat om het microglia onderzoek! Ik vond het ontzettend leuk om samen met jou de rol van microglia in psychiatrische ziekten te ontrafelen. Aan mij de taak jou de fijne kneepjes van het isolatie-vak te leren, waarna we het 'isolatie team' a.k.a. 'masters of microglia' waren. Samen wisten we in rap tempo miljoenen microglia te isoleren en een mooi paper over bipolaire stoornis te schrijven. Lieve Gijs, zet hem op in New York en bedankt voor het doorzetten van het microglia onderzoek.

Hans, wat een heerlijk nuchtere kerel ben jij. Je scherpe blik, gulle lach, het gemak waarmee je artikelen schrijft en de bizarre situaties die je gewoon overkomen zijn kenmerkend voor jou. Elke keer als we elkaar zagen had je weer een prachtig verhaal, waarna ik buikpijn had van het lachen. Bedankt voor de fijne tijd.

Tamar, tijdens het Hollab bowlinguitje leerde ik je kennen. Jij nog niet begonnen met je PhD, ik net drie weken bezig. Helaas vertegenwoordigde jij de Amsterdamse Hollab tak en zag ik je in het begin weinig. Gelukkig kwam je naar Utrecht en besloot je zelfs microglia te gaan isoleren. Hierna zouden we steeds vaker kennis uitwisselen, wat mij ook scherp hield en op nieuwe ideeën bracht. Bedankt.

Jacqueline, helaas hebben we nooit samen gewerkt aan een project, maar ik kon altijd bij jou terecht voor vragen. Of het nou ging om de selectie van de beste referentie genen voor qPCR of western blots die niet werkten, met altijd even veel geduld gaf je advies. Bedankt voor alle hulp en het lenen van je p2 die toch echt het fijnste was voor het pipeteren van primers.

Roland, de uren die wij samen doorgebracht hebben in de humane kweek zijn niet meer te tellen, inclusief onze nachtelijke isolatie. Allebei vrijgezel, dus ons liefdesleven werd uitgebreid besproken. Als 'terminator' leerde ik jou hoe je netjes een relatie hoort te beëindigen en als wederdienst kreeg ik inzicht in het mannelijk brein over vrouwen aan het lijntje houden. Special thanks to you, voor al deze belangrijke levenslessen die ik nooit meer zal vergeten en het delen van mijn grote liefde voor Qmusic het foute uur.

Dick, hoe bijzonder is het om op exact dezelfde dag ons promotietraject te beginnen en twee uur na elkaar te promoveren. We leerden elkaar kennen op onze eerste dag bij de UMC introductie, beiden promovendi, beiden bij de psychiatrie, beiden een kamer in Translational Neuroscience. Je kwam bij onze journal club met als eerste een artikel over genetica en de dikheid van de inwoners van Samoa. Ook hebben we samen in de borrelcommissie gezeten en waren we fervente aanhangers van de alternative borrel. Dankjewel voor deze leuke tijd.

Thanks to all the other Hollab members, current and former: **Miriam**, **Saskia**, **Jinte**, **Vanessa**, **Ketharini**, **Jessy**, **Christiaan**, **Lianne**, **Marloes**, and **Claudia**. Thank you for all the fun and good science. It was a pleasure to work with you.

Thanks to all the students who helped me in the past years with many experiments: **Lynn**, **Evi**, **Ninouk**, **Astrid**, **Alba**, and **Emma**. I really enjoyed being your supervisor and see the spark in your eyes when you discovered something new.

Thanks to the whole **department of Translational Neuroscience**. It was such a unique environment to work: inspiring, motivating, people helping each other and joined lunches in the coffee room where professor and student are sitting side by side. **Leo, Henk** en **Erwin**, bedankt voor de dagelijkse vrolijke ochtendgroet en praatjes in het lab. Thanks to the **Pasterkamp group** for the fun and competition throughout the years. Thanks to the **borrelcommittee** with whom I organised many amazing borrels.

Thanks to all the people I have collaborated with over the years. De **Nederlandse hersenbank**, met name Michiel Kooreman, voor het uitnemen van al het hersenweefsel van de afgelopen jaren. **Pien** en **Jeroen**, het was altijd een feest om uren bij jullie achter de Canto te zitten. Bedankt voor het meedenken met alle experimenten. Many thanks to **Chotima** and **Josef** for all the CyTOF experiments. **Towfique** and **Evan**, thanks for answering my many many RNAseq questions. Thanks to the **Merad group** for adopting me in their lab during my visit to New York.

Max, **Oliver**, **Jeroen**, **Jelle**, **Katherine** en **Katherina**, wat hebben jullie als kamergenoten een onvergetelijke bijdrage geleverd aan mijn promotietijd. Bedankt voor het vergroten van mijn voetbalkennis, Jennifer, het jaarlijks krijgen van de mooie mannen kalender, het eten van mijn vele taarten en cakes, de discobal, het bekritiseren van het design van mijn grafieken, de goede koffie, de gesprekken over wetenschap, de pan, de broodjes biba en het verzinnen van de meest bizarre bijnamen.

Martijn, **Lucie** en **Marjolein**, als mastervrienden nog steeds op de hoogte van elkaars leven. **Martijn**, bedankt voor de vele koffiemomenten en supportive woorden als het nodig was. **Lucie** en **Marjolein**, bedankt voor de etentjes en de vele die nog komen gaan.

Jackelien, **Sybren**, **Lizz**, **Inger**, **Jurrien** en **Robin**, vrienden sinds onze stage op het N.i.N. Ik vind het enorm waardevol dat we nog steeds zo vaak mogelijk proberen te eten en te borrelen. **Sybren**, bedankt voor onze uren ouwehoeren met een biertje en het legendarische ONWAR paard moment. **Lizz**, bedankt voor de tips voor wormenbestrijding in je keukenkasten. **Inger**, bedankt voor de smakelijke liefdesverhalen. **Jurrien**, bedankt voor de vrolijke telefoongesprekken als je namens de hersenbank mocht vertellen dat er een donor voor mij was. **Robin**, graag gedaan voor mijn studente ;) **Jackelien**, jouw vriendschap is zo waardevol. We begrijpen elkaar met een half woord, zowel privé als wetenschappelijk gezien. Jij snapt als geen ander hoe het voelt als de pipetpunten random uit de box zijn gehaald, een experiment mislukt of je juist die ene doorbraak hebt. Het maakt niet uit waar we zijn, samen op congres naar Edinburgh of op bezoek in New York, we hebben plezier samen. Bedankt voor al je steun en je geweldige vriendschap. LOLOLOLOLOL.

Mijn lieve **Club8^{+}-ers**, wat een heerlijk zooitje zijn we bij elkaar. Allemaal anders, maar wat klinkt het enorm goed. Regelmatig samen eten, borrelen bij de MaPo, schaatsen, schilderen in nieuwe huizen en als toppunt onze lustrumreis naar Lissabon. Bedankt voor de afleiding en de schrijf M&Ms.

Sanne, **Marieke** en **Annemarijn**, we zijn al jaren vriendinnen en kennen elkaar door dik en dun. **Sanne**, bijna buurvrouw waardoor aanwaaien zo makkelijk was. De spontane cappuccino momenten, gesprekken en kliekjes diners waren de ideale tegenhanger van het harde werk van de afgelopen jaren. **Marieke**, als mede moleculaire PhDer konden we veel ervaringen uitwisselen en elkaar steunen waar nodig. Je hebt mij vele malen moed ingesproken als het weer eens tegen zat. Nog een half jaar en dan ben je er ook! **Annemarijn**, wat een feest toen ik ook in Utrecht kwam wonen én we erachter kwamen dat het Julius centrum toch wel erg dichtbij Translational Neuroscience is. Onder het genot van een koffie van het Mii café praatten we regelmatig over ons onderzoek, banenjacht, kleine Stijn en wanneer we weer samen zouden eten. Meiden, samen zijn we opgegroeid tot de succesvolle vrouwen die we nu zijn. Bedankt dat jullie er voor mij zijn. Alles verandert, niks verdwijnt.

Rosanne en **Esther**, chica's. Zonder uitloting voor geneeskunde en een kapotte fiets hadden we elkaar nooit leren kennen. Een vriendschap ontstond, die sinds die dag alleen maar hechter is geworden. We hebben al zoveel mooie momenten gedeeld en het is niet voor niks dat ik jullie mijn gekozen familie noem. Ik vergeef het dan ook dat jullie mijn artikelen als de ideale slaaplectuur gebruiken. Meisjes, bedankt voor jullie liefde, steun en zoveel meer.

Lieve **Sebas**, als een vrolijke wind kwam je in mijn leven. Een stuiterbal boordevol liefde. Je bent open, onbevangen en door je klunzigheid rollen regelmatig de tranen van het lachen over mijn wangen. Jij bent mijn rustpunt in de dagelijkse hectiek. Bedankt voor je liefde, steun en zoveel meer.

Mijn lieve zusjes, **Jacqueline** en **Antoinette**. Wat ben ik ontzettend trots om jullie grote zus te zijn. Ondanks ons leeftijdsverschil vind ik het heel bijzonder hoe hecht we zijn. We hebben dezelfde humor, voorliefde voor sushi en snelheid van praten. Bedankt voor jullie liefde, steun en zoveel meer.

Lieve **papa** en **mama**, jullie zijn de basis in mijn leven. Mama, van jou heb ik mijn sociale antenne, gulle lach en voorliefde voor praten. Papa, jij zegende mij met je analytisch vermogen, klustalent en leergierigheid. Samen maakten jullie mij tot de zelfstandige zelfverzekerde vrouw die ik nu ben. Bedankt voor jullie liefde, steun en zoveel meer.

Liefs,
Marjolein